UNIVERSITY OF ALBERTA

AN INVERSE GAS CHROMATOGRAPHY (IGC) STUDY OF THE THERMODYNAMICS OF POLYOLEFIN BLENDS

By

Liyan Zhao

©

A thesis submitted to the Faculty of Graduate Studies and Research in partial fulfillment of the requirements for the degree of Doctor of Philosophy

in

Chemical Engineering

Department of Chemical and Materials Engineering

Edmonton, Alberta

Spring, 2002

Canada

<div align="center">

University of Alberta

Library Release Form

</div>

Name of Author: Liyan Zhao
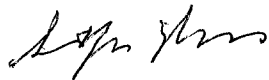
Title of Thesis: An inverse gas chromatography (IGC) study of the thermodynamics of polyolefin blends

Degree: Doctor of Philosophy

Year this Degree Granted: 2002

Permission is hereby granted to the University of Alberta to reproduce single copies of this thesis and to lend or sell such copies for private, scholarly or scientific research purposes only.

The author reserves all other publication and other rights in association with the copyright in the thesis, and except as herein before provided, neither the thesis nor any substantial portion thereof may be printed or otherwise reproduced in any material form whatever without the author's prior written permission.
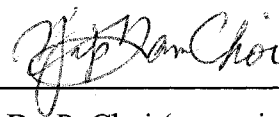
Liyan Zhao   *Mar. 14, 2002*

Liyan Zhao

449L Michener Park

Edmonton, AB

Canada T6H 4M5

UNIVERSITY OF ALBERTA

FACULTY OF GRADUATE STUDIES AND RESEARCH
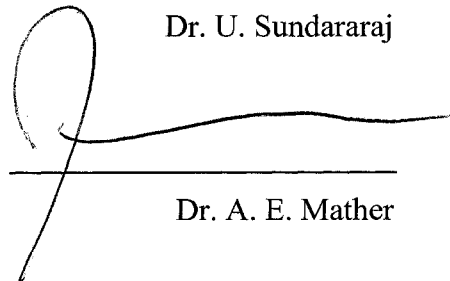
The undersigned certify that they have read and recommend to the faculty of Graduate Studies and Research for acceptance, a thesis entitled **An Inverse Gas Chromatography (IGC) Study of the Thermodynamics of Polyolefin Blends** submitted by Liyan Zhao in partial fulfillment of the requirements of the degree of **Doctor of Philosophy in Chemical Engineering**.

_____
Dr. P. Choi (supervisor)

_____
Dr. U. Sundararaj

_____
Dr. A. E. Mather

_____
Dr. L. Mcmullen

Mar. 8, 2002

Dr. D. Gardner (external examiner)

Abstract

Polyethylene blends have been widely used in packaging, piping and film industries due to their excellent processability and harmlessness to the human body. To optimize the design of such blends, a great deal of attention has been focused on developing techniques for characterizing the miscibility of these blends. In this thesis, an experimental method, based on inverse gas chromatography (IGC), has been developed to address the issues.

When IGC is used to measure the polymer-polymer interaction parameters, a common problem has been encountered: the interaction parameter is dependent on the nature of the solvent used in the experiment. Therefore, in the first part of the thesis, a new approach of data analysis was developed to obtain solvent independent interaction parameters. Interaction parameters for the HDPE/LDPE, HDPE/i-PP, HDPE/PS and HDPE/LLDPE blends were measured to check the validity of the approach. Interaction parameters obtained for the HDP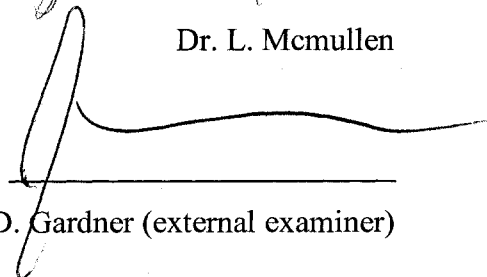E/LDPE blends were about one order of magnitude higher than those derived from small angle neutron scattering and molecular dynamics simulations. For the HDPE/i-PP and HDPE/PS blends, the measured interaction parameters were very comparable to those obtained from neutron reflectivity measurements. HDPE/LLDPE blends were studied to determine the effect of the branch content of LLDPE on its miscibility with HDPE. The results showed that increasing the branch content of LLDPE reduced miscibility and the cut-off value of branch content for inducing immiscibility was about 50 branches per 1,000 backbone carbons. This result was consistent with the findings of other researchers. Based on the present results, it seems that the proposed approach provides a simple and reliable alternative to study the

miscibility of polyolefin blends. The same IGC technique together with the proposed data analysis approach was also applied to the LLDPE/LDPE blends to investigate the effect of molecular characteristics of LLDPE on its miscibility with LDPE. It was found that the values of interaction parameters for all these blends were in the same order of magnitude and no obvious trends were identified. This was attributed to the narrow ranges of variation of the characteristics under study.

Acknowledgments

I would like to thank my supervisor Professor Phillip Choi for his encouragement, guidance and support during the course of my research and valuable advice he gave me during the ups and downs in my life.

I also thank Dr. Sundararaj and Dr. Mather for their valuable advice and suggestions.

I also thank the staff of the Department of Chemical and Materials Engineering who helped me in various situations: Mingqian, Andree, Walter, Richard, Jack and Bob.

The financial support provided by Nova Chemicals Corporation, the University of Alberta and the National Sciences and Engineering Council of Canada was highly appreciated.

I would like to thank my husband Zhiguo for his love and support. He showed a great deal of encouragement and understanding during the time of my study.

TABLE OF CONTENTS

HDPE/LLDPE blends

LIST OF TABLES

HDPE and 30% i-PP at 170, 190, 210 and 230 °C

210 and 230 °C

LIST OF FIGURES

NOMENCLATURE

A	Constant in Antoine equation
$A(T)$	Temperature coefficient in equation 6-2
B	Constant in Antoine equation
B_{11}	Second virial coefficient (L/mol)
$B(T)$	Temperature coefficient in equation 6-2
C	Constant in Antoine equation
F	Flowrate of the carrier gas (mL/min)
J	James-Martin correction factor
M_1	Molecular weight of solvent (g/mol)
M_n	Number average molecular weight of polymer (g/mol)
M_w	Weight average molecular weight of polymer (g/mol)
P_1^0	Vapor pressure of solvent (kPa)
P_c	Critical pressure (kPa)
P_i	Inlet pressure of the column (kPa)
P_o	Outlet pressure of the column (kPa)
R	Universal gas constant (L*Pa/mol/K)
T	Temperature (K)
T_c	Critical temperature (K)
T_r	Reduced temperature
V_0	Reference volume for the determination of lattice size (cm^3/mol)
V_1	Molar volume of solvent (L/mol)
V_g^0	Specific retention volume (cm^3/g)

$c_1{}^g$	Concentration of solvent in the gaseous phase (g/L)
$c_1{}^l$	Concentration of solvent in the liquid phase (g/L)
k	Boltzmann constant (J/K)
n_i	Molar number of the ith component (mol)
t_0	Retention time of marker (min)
t_n	Net retention time of solvent (min)
t_R	Retention time of solvent (min)
v_i	Specific volume of polymer i (L/g)
w	Mass of polymer (g)
w_i	Weight fraction of polymer i in the liquid phase
x	Number of repeating units in polymer molecule
z	Number of nearest neighbors in liquid lattice
ΔH_m	Enthalpy change on mixing (J)
ΔH_s	Heat of sorption (J)
ΔG_m	Gibbs free energy change on mixing (J)
ΔS_m	Entropy change on mixing (J/K)
ΔX_{br}	Fraction of the repeating units containing ethyl branches
Δg_m	Gibbs free energy change for the formation of a single solvent segment contact (J)
α_1	Activity of solvent
δ_i	Solubility parameter of polymer i (MPa$^{1/2}$)
$\mu_1{}^0$	Chemical potential of solvent at the standard state (J/mol)
$\mu_1{}^g$	Chemical potential of solvent in the gaseous phase (J/mol)
$\mu_1{}^l$	Chemical potential of solvent in the liquid phase (J/mol)

ρ Saturated liquid density of solvent (g/cm^3)

ϕ_i Volume fraction if the ith component

χ_{ij} Flory-Huggins interaction parameter between components i and j

ω Acentric factor

Chapter 1

Introduction

1.1 Introduction

Polyethylene is one of the most important polymeric materials owing to its excellent processability, light weight, superb chemical resistance, low cost, and harmlessness to the human body. About 50 million metric tons of polyethylenes are produced annually around the world. According to a new study of olefin derivatives compiled by CMAI in Houston, the demand for high-density polyethylene (HDPE) will grow an average of 4% per year worldwide over the next five years. The rates of growth of low-density polyethylene (LDPE) and linear low-density polyethylene (LLDPE) are estimated to be 6.4% and 7% per year worldwide over the same period, respectively.

Polyethylene was first discovered in 1933 by polymerizing ethylene under very high pressures (at least 120 MPa) at Imperial Chemical Industries, Ltd. In the 1950s, an organometallic type catalyst discovered by Ziegler and Natta caused a revolutionary change in the polyethylene industry. With this type of catalyst, linear polyethylene could be produced at atmospheric pressure and room temperature. With recent advances in polymerization technology using Ziegler-Natta and metallocene catalysts, polyethylene can be produced in a variety of molecular architectures with different processing properties and performance. Figure 1.1 depicts three major molecular structures of

1

polyethylene that are manufactured commercially: HDPE, LDPE, and LLDPE. Both HDPE and LDPE are homo-polymers made by polymerizing ethylene monomers while LLDPE is a co-polymer formed by co-polymerizing ethylene and α-olefin monomers. Depending on the type of α-olefin used in the co-polymerization reaction, LLDPE with different branch lengths can be made. The most commonly used α-olefins are 1-butene, 1-hexene, and 1-octene.

Since each type of polyethylene has its advantages and disadvantages, it is common practice in the polyethylene industry to blend these homo- and/or co-polymers to develop products with specific properties that would not have been obtained from the neat polymers. For example, for many film applications, LDPE and LLDPE are blended to create products with improved melt strength, transparency, flexibility, and toughness. To optimize the design of such blends to achieve the desired physical and mechanical properties, a great deal of attention has been focused on improving our understanding of the phase behavior of these polymers and on developing techniques to characterize and to predict the miscibility between the blend components (Olabisi *et al.* 1979 and Utracki 1989).

However, most of the studies reported in the literature have focused on determining the miscibility of such blends in the solid state or at temperatures slightly above the melting temperatures of the polyethylenes (105 °C to 167 °C). In my view, the results obtained from these studies cannot be applied to describe the phase behaviour of the blends at their processing temperatures that are generally in the range of 180 °C to 230 °C. In addition, most of the reported findings were obtained either by inference from

2

what was observed in the solid-state samples or with the use of very expensive equipment such as small angle neutron scattering (SANS). Therefore, it would be extremely valuable to develop an inexpensive experimental technique to study the miscibility of these blends at elevated temperatures. This is the major thrust of the present research project.

1.2 Interaction parameters

The Flory-Huggins interaction parameter (χ) is the key parameter to determine the miscibility of polymer blends. The interaction parameter is a dimensionless quantity that characterizes the inter-segmental interaction energy between two polymers. This concept was first introduced in concentrated small molecule mixtures. Later, Flory (1941) and Huggins (1941) independently extended the theory to polymer solutions. Scott and Tompa then extended the Flory-Huggins theory to polymer blends. According to this theory, the contribution of enthalpy to the Gibbs free energy dominates over the contribution of entropy (combinatorial). And the enthalpy change on mixing can be obtained from the interaction parameter. Therefore, determining the values of interaction parameters is very important for predicting the phase behavior of polymer blends.

Direct measurement of the thermodynamic energy associated with mixing two polymers is extremely difficult because of the high viscosities of polymer melts. Among the indirect techniques available, SANS is considered to be the most reliable technique for investigating the phase behavior of polymer blends. However, this technique is still

3

not widely used in the analysis of polymer blends because the equipment is very expensive to build and run. As a result, indirect approaches utilizing ternary systems, which usually require less expensive equipment, are often employed.

In general, such approaches involve the measurement of the interaction parameters between the blend and a solvent, as well as its corresponding pure polymers and the same solvent. The interaction parameter between two polymers is derived using a suitable polymer solution theory (e.g., the Flory-Huggins theory). Since different theories suffer from different inadequacies, the calculated interaction parameters from these approaches naturally inherit the weaknesses of the chosen theory. Among all the methods that require the use of a third solvent, inverse gas chromatography (IGC) has become a very common method to determine polymer-solvent, and polymer-polymer interaction parameters because the experimental procedure is simple and the gas chromatography (GC) equipment is readily available in many laboratories. Unfortunately, this technique suffers from a severe drawback, which is that the measured interaction parameters are dependent on the nature of solvents used. Therefore, much work is needed to improve this technique and this is one of the foci of this thesis.

1.3 Objectives of the thesis

One of the major objectives of the research is to develop an inexpensive technique based on IGC to characterize the miscibility of binary polymer blends with different compositions at elevated temperatures. Another objective is to apply such a technique to study the effects of factors such as molecular architecture, molecular weight average,

4

molecular weight distribution, branch content, branch length, and branch distribution on the thermodynamics of a series of selected binary polyolefin blends composed of HDPE and LDPE, HDPE and LLDPE, LDPE and LLDPE, HDPE and isotactic-polypropylene (i-PP), and HDPE and polystyrene (PS).

1.4 Structure of the thesis

The thesis consists of eight chapters. In Chapter 2, the literature relevant to the miscibility of polyolefin blends will be reviewed and discussed. First I will review miscibility studies of polyethylene blends using indirect methods; then, I will summarize the experimental and simulation methods used to measure interaction parameters of these blends in the melt state. For the HDPE/i-PP and HDPE/PS blends, it is well established in the literature that these blends are immiscible not only in the solid state but also in the melt state.

In Chapter 3, the IGC technique will be introduced; its advantages and drawbacks will be discussed. In particular, the "probe dependence" problem will be discussed and other researchers' attempts to solve the problem will be reviewed. In this chapter, experimental set-up and theories relevant to IGC measurements will be presented and my approach to resolve the probe dependence problem will be explained.

In the subsequent chapters (Chapters 4 to 7), I will show the application of the proposed method to four different polyolefin blends. In Chapter 4, I will present the experimental data for the HDPE/LDPE blends. I started on the HDPE/LDPE blends first

5

since the materials were readily available and have been studied extensively by other researchers.

To further investigate the applicability of the newly proposed IGC approach to other polyolefin blends, I studied HDPE/i-PP and HDPE/PS blends because these blends are known to be immiscible and χ values are available in the literature. Chapter 5 shows the results of HDPE/i-PP and HDPE/PS blends. It was found that χ values for these blends were comparable to those obtained from neutron reflectivity (NR) measurements.

In Chapter 6, I extend the method to a series of binary blends composed of HDPE and LLDPEs having different branch contents to check if the method can capture the effect of branch content on the miscibility. In this study, I found that χ values increased with increasing branch content of LLDPEs. This indicates that increase in the average number of branches of LLDPE reduces the miscibility of HDPE and LLDPE blends. This result is consistent with the findings from other techniques.

After the technique for the aforementioned polyolefin blends had been validated, I applied the technique to study the effects of molecular architecture, molecular weight average, molecular weight distribution, branch content, branch length, and branch distribution on the miscibility of a series of LDPE and LLDPE blends. The experimental data and results are shown in Chapter 7. In the last chapter, I conclude the major findings of this study and list some recommendations for further work.

6

1.5 References

Flory, P.J. (1941) Thermodynamics of High Polymer Solutions, *J. Chem. Phys.*, 9, 660.

Huggins, M.L. (1941) Solutions of Long Chain Compounds, *J. Chem. Phys.*, 9, 440.

Olabisi, O., L.M. Robeson and M.T. Shaw, (1979) Polymer-Polymer Miscibility, Academic Press, New York

Utracki, L.A. (1989) Polymer Alloys and Blends – Thermodynamics and Rheology, Academic Press, New York

Figure 1.1 Schematic diagrams of different molecular structures of polyethylene

produced under various reactor conditions and catalysts
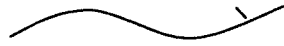
High-density
polyethylene

Low-density
polyethylene
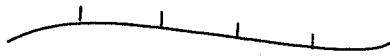
Linear low-density
polyethylene
(metallocene catalyst-
regularly distributed
branches)

Linear low-density
polyethylene (Ziegler-
Natta catalyst-
randomly distributed
branches)

8

Chapter 2

Literature Review

2.1 Miscibility of polyethylene blends

Polyethylene occupies an important position in the commodity plastics market. It is estimated that about 70% of polyethylene enters into the market as blends. Since the miscibility of the blend affects the processing properties and the product performance, the miscibility of polyethylene blends has been a prevalent research topic in the polymer community over the past two decades. Earlier studies mainly focused on the blend in the solid state (Datta and Birley 1982) simply because these blends are used in the solid state. However, over the years, researchers have come to recognize that the solid-state morphology and mechanical properties of the blends can be significantly affected by the melt miscibility. Therefore, recent research efforts have concentrated on the liquid state of these blends. In addition, since miscibility is a thermodynamics concept that it is only meaningful at the thermodynamic equilibrium state, studying miscibility in the liquid state is more appropriate than that in the solid state where kinetics also plays a role. The first part of this chapter presents a survey of the previous study on the miscibility of polyethylene blends both in the solid state and in the melt state.

An extensive review provided by Crist and Hill (1997) addressed the miscibility study of polyolefin blends, especially polyethylene blends, in the melt state. To date,

9

experimental methods available to study the miscibility of polyethylene blends are still restricted to a few indirect techniques, such as differential scanning calorimetry (DSC), X-ray diffraction (XD), dynamic mechanical analysis (DMA), scanning electron microscopy (SEM), transmission electron microscopy (TEM), and small angle neutron scattering (SANS).

In the literature, researchers have studied both model and real systems. Since model systems have uniform chemical structures and narrow molecular weight distribution, the corresponding data can provide valuable information for studying more complicated systems such as commercial polyethylene blends. In general, Crist and Hill (1997) concluded from the present situation of studies on miscibility of polyolefin blends that "there are abundant thermodynamic data for current and future theoretical approaches to the subtle interactions that control phase behavior in polyolefin blends. It is hoped that continued advances in model polymer synthesis, experimental techniques, and theory will lead to a reasonably quantitative description of binary and multicomponent mixtures of polyolefin chains."

2.1.1 Studies of polyethylene blends using indirect methods

The miscibility of different polyethylene blends in the solid state has been studied extensively in the literature. Those studies have two foci. One is simply on the crystalline phase while the other on the amorphous phase of the blends because of the semi-crystalline nature of polyethylene.

10

Datta and Birley (1982) was one of the first groups of researchers to study the compatibility of both HDPE/LDPE and HDPE/LLDPE blends in the solid state, particularly in the crystalline phase, using DSC, XD, and mechanical property testing. The branch contents of LDPE and LLDPE were not reported. In DSC measurements, they observed two distinct endothermic peaks for both fast and slowly cooled HDPE/LDPE blend samples, while HDPE/LLDPE blends had only one endothermic peak for both cooling conditions. Therefore, they suggested that HDPE and LLDPE are thermodynamically compatible in the crystalline phase, while HDPE and LDPE are not. X-ray analysis of the same samples showed that the unit cell dimensions for the HDPE/LLDPE blends are identical to those of pure HDPE samples, which further supported the hypothesis that HDPE/LLDPE blends are compatible. In their work, most of conclusions were drawn from DSC results. Unfortunately, the authors did not link the mechanical property testing results to DSC results.

Hu *et al.* studied HDPE/LLDPE (Hu, 1987) and LDPE/LLDPE (Kyu *et al.*, 1987, Ree *et al.* 1987) blend systems by DSC, wide-angle x-ray diffraction (WAXD), small angle x-ray scattering (SAXS), Raman longitudinal-acoustic-mode spectroscopy (LAM), and light scattering (LS). The branch contents of LDPE and LLDPE used were 26 and 18 branches per 1,000 backbone carbons. For the HDPE/LLDPE blend, their results from DSC measurements are similar to those of Datta *et al.* (1982). In their study, they also investigated the effect of the branches of the LLDPE on its crystallization behavior utilizing WAXD, SAXS, LAM, and LS. They found that branches are excluded from the polyethylene unit cell resulting in thinner lamellae. This finding has been recently observed by Doran and Choi (2001) using molecular dynamics (MD) simulations. For

11

the LDPE/LLDPE blend, they suggested that the blend is not miscible in the crystalline phase. Based on the information given by SAXS patterns, they proposed that when LDPE/LLDPE blends are cooled from the molten state, LLDPE crystallizes first and forms volume-filling spherulites, and is followed by a secondary crystallization of LDPE within the spherulites formed by LLDPE.

Tashiro et al. (1992, 1994) investigated the crystallization behavior of 50/50-wt% HDPE and LLDPE blends by DSC and Fourier transform infrared spectroscopy (FTIR). To study the effect of the branch content of LLDPE on its miscibility with HDPE, two LLDPE samples were used, one having 17 ethyl branches per 1,000 backbone carbons and the other 41. Since HDPE and LLDPE have similar chemical structure of carbon and hydrogen atoms, they used a deuterated HDPE (DHDPE) sample as one component. They found that even under slow cooling conditions, DHDPE and LLDPE co-crystallized over the whole composition range if the branch content of the LLDPE used was 17 ethyl branches /1000 backbone carbons. To the contrary, LLDPE with 41 ethyl branches/1000 backbone carbons was found to be immiscible with DHDPE. These results indicated that increase in the number of branches of LLDPE reduces the miscibility of HDPE/LLDPE blend. Similar results were also obtained in the melt state by SANS (Alamo et al., 1997), MD simulations (Fan, 2001), and IGC (see Chapter 6). It is believed that the foregoing described immiscibility is attributed to the differences in the interaction energies of CH_2, CH_3, and CH groups.

Lee et al. (1997) investigated the miscibility of HDPE/LDPE, HDPE/LLDPE, and LDPE/LLDPE blends not only in the crystalline phase but also in the amorphous phase using DSC and DMA. The branch contents of LDPE and LLDPE used in this work were

12

34 and 16 branches per 1,000 backbone carbons. The DSC measurements indicate that HDPE/LDPE and HDPE/LLDPE blends are miscible in the crystalline phase, which are consistent with Datta and Birley's (1982) findings. For LDPE/LLDPE blends, their DSC results are in agreement with Kyu's (Kyu *et al.*, 1987) results indicating that the constituent polymers form separate crystals. Moreover, the dynamic mechanical relaxation studies suggest that HDPE/LDPE, HDPE/LLDPE and LDPE/LLDPE blends are miscible in the amorphous phase.

The steady-state rheological, thermal and mechanical properties for binary blends consisting of a hexene-based LLDPE with narrow short chain branching distribution and an LDPE that had long chain branches, were investigated by Yamaguchi and his coworkers (1999 a, b) in both solid and melt states to reveal the relation between the miscibility in the melt state and the morphology in the solid state. The LLDPE was produced using a metallocene catalyst with a density lower than those of conventional LLDPEs polymerized using Ziegler-Natta catalyst, with 18.6 butyl branches per 1,000 backbone carbons. The LDPE had 9 short and 5 long branches per 1,000 backbone carbons. The number average molecular weight, M_n and the weight average molecular weight, M_w of LLDPE used were 3.7×10^5 and 6.9×10^5, respectively. For the LDPE, M_n and M_w were 7.0×10^4 and 6.6×10^5, respectively. According to the rheological measurements, the LLDPE is miscible with LDPE in the melt state. In their study, it was also found that the crystallization temperature of LDPE is higher than that of the LLDPE. Here, the LDPE acted as a nucleation agent for the crystallization of the LLDPE. Therefore, by adding a small amount of the LDPE to LLDPE, the degree of crystallinity, melting temperature, and hardness were enhanced. These findings conflict Kyu's results

13

(Kyu *et al.*, 1987). In particular, Kyu's results showed that the crystallization temperature of LLDPE is higher than that of LDPE. Consequently, LLDPE crystallizes first and forms spherulites and LDPE crystallizes inside these spherulites. It should be noted that the branch contents of the LLDPE and LDPE used by Kyu were 18 and 26 branches per 1,000 backbone carbons, respectively; compared to 18.6 and 14, used by Yamaguchi *et al.* It is possible that the difference of branch contents between the LDPEs used causes the discrepancy of the observed crystallization temperatures. It is well known that increasing the number of branches of polyethylene molecules reduces the thickness of lamella and reduces the melting temperature. In Kyu's work, the branch content of LDPE is higher than that of LLDPE, but in Yamaguchi's work, LLDPE has more branches than LDPE. An alternative explanation to Yamaguchi's results is that the presence of LDPE may allow the linear molecules to separate from the highly branched molecules, resulting in the crystallization of linear segments at a higher temperature than that of pure LLDPE (Drummond *et al.*, 2000).

Muller *et al.* (1994) studied the effect of different blending methods on the miscibility of LDPE (M_w=110,000) and octene-based LLDPE (M_w=130,000) blends by means of DSC. The samples were prepared by both melt blending and physical solid mixing. Melt blending is the method that the samples are melted and mixed together. Physical solid mixing, as the name implies, is simply to mix the polymers without melting them. In DSC measurements, two melting peaks were obtained for both the melt mixed and physically mixed samples. The authors contended that LDPE/LLDPE blends are immiscible in the solid state. This conclusion is similar to those of other researchers (Lee *et al.*, 1998, Kyu *et al.*, 1987). However, since the thermographs of the samples

14

prepared using different mixing methods differed considerably, they suggested that partial miscibility exists between the components prepared by melt blending.

The effect of the crystallization temperature on the morphology of binary blends composed of a low molecular weight linear polyethylene (M_w=2,500) and high molecular weight branched polyethylenes (M_w=65,000 to 166,000) were studied by Gedde and coworkers (Rego Lopez *et al.*, 1989, Iragorri *et al.*, 1992, Conde Brana *et al.*, 1992) using DSC, polarized light microscopy, and SAXS. The branch contents of the branched component used ranged from 2 to 8 branches per 1,000 backbone carbons. They found two different types of crystallization behaviour depending on the crystallization temperature. If the crystallization temperature was higher than 392.5 K, only the branched component crystallized and spherulitic crystals were obtained. If the crystallization temperature was lower than 392.5 K, the linear and branched molecules are co-crystallized and a microspherulitic morphology was found. These results imply that these two polymers are miscible in the solid state.

Kwag *et al.* (2000) investigated the miscibility of binary polyolefin blends, in which one of the components was a special type of polyethylene synthesized using a metallocene catalyst (metallocene polyethylene or MCPE) and the other component included HDPE, polypropylene or PP, poly(propylene-co-ethylene) or CoPP, and poly(propylene-co-ethylene-co-1-butylene) or TerPP, prepared using a Ziegler-Natta catalyst, using rheological, thermal, and morphological techniques in the solid and melt states. According to the thermal and mechanical behaviours, they reported that all of the blends are thermodynamically immiscible but mechanically compatible in the solid state. However, based upon the rheological results, they concluded that an HDPE/MCPE blend

15

is miscible in the melt state, but MCPE/PP, MCPE/CoPP and MCPE/TerPP blends are not. In terms of the phase morphology, the degree of compatibility is highest for the HDPE/MCPE blend compared to the other three blends in the solid state. However, the interfacial region between the matrix and the dispersed phase of those phase-separated systems was observed to have strong adhesion. It is possible that this is due to the similar chemical structure of the components.

Cho *et al.* (1997) studied the miscibility of blends of octene-based LLDPE and ethylene-propylene-butene-1 terpolymer (ter-PP) by means of DSC, DMA, SEM, and capillary rheometry. DSC and dynamic mechanical relaxation measurements indicate that the blends are not miscible in the crystalline and amorphous phases due to the weak interfacial adhesion between the two components. Measuring the melt viscosity of the blends, they found a strong negative deviation from the linear additive rule, which suggests that the blends are also immiscible in the melt state. However, they also found that by adding 20% of ter-PP into LLDPE can improve processability and mechanical properties dramatically. It should be noted that the determination of polymer blend miscibility based on their melt viscosity measurements is questionable due to the lack of a sound theoretical basis.

Rheological measurements were performed by Lee and Denn (2000) on different polyethylene blends at 160 °C. M_w and M_w/M_n of the HDPE, LLDPE, and LDPE used were 40,000 and 3.1, 68,300 and 3.2, and 388,440 and 10, respectively. The branch content of LLDPE used in their work was 10 branches per 1,000 backbone carbons. The dynamic mechanical data show that HDPE and LLDPE blends are miscible in the melt at all composition ranges. This is consistent with the results obtained from other techniques

16

(Alamo *et al.*, 1997, Fan 2001, Chapter 6). The dynamic mechanical data suggest that HDPE/LDPE and LDPE/LLDPE blends are partially miscible in the melt. In addition to the binary systems, they also studied an HDPE/LDPE/LLDPE ternary system and found that HDPE can be used as a compatibilizing agent for LDPE/LLDPE blends to form a fully miscible ternary blend. However, no explanations were given in their article. In practice, it is found that the processability of LDPE/LLDPE blend can be enhanced significantly by adding a small amount of HDPE.

Zhao *et al.* (1998) studied the miscibility of HDPE/LLDPE blends in the amorphous phase by excimer fluorescence. They did not report the branch content of the LLDPE used. The theoretical basis of this method is that one of the components of the blends is labeled by using a chromophore. The aromatic rings labeled on LLDPE chains cannot crystallize with other linear molecules. Detection of the change in excimer to monomer ratio allows the inter-penetration of chromophore labeled LLDPE with HDPE chains to be determined. Based upon their results, they concluded that chromophore labeled LLDPE is miscible with HDPE for samples quenched from 140 °C to room temperature. This is a novel approach to study the miscibility of polyethylene blends. Unfortunately, in their work, they did not discuss whether the chromophore label could influence the phase behavior of the blends. Further studies on this issue are needed.

Hill and coworkers did extensive studies on a variety of polyethylene blends using DSC and TEM. The basic assumption made in their research is that fast quenching of a liquid sample does not change the liquid morphology. Therefore, the morphology observed in the quenched samples reflects the morphology of the samples in the liquid state. It is worth pointing out that this assumption is controversial. This is because the

rate of the crystallization of pure polyethylene is higher than the rate of quenching normally used in such sample preparation procedures. Therefore, inferring miscibility of polyethylene blends in the melt state by examining the corresponding quenched samples is uncertain. Nonetheless, Hill and co-workers did a series of studies on HDPE/LDPE, HDPE/LLDPE, and LDPE/LLDPE systems with different molecular weight averages, molecular weight distribution, and branch contents over a temperature range of 130 $^{\circ}$C to 160 $^{\circ}$C and obtained the following results.

First, Barham and Hill (1988) studied miscibility of HDPE and LDPE blends at different concentrations. The weight average molecular weights of HDPE and LDPE were 98,000 and 208,100, respectively. The LDPE had 10 long branches and 16 short branches per 1,000 backbone carbons. The samples were prepared by the solution blending method. Their results show that at high HDPE concentrations (>50%), the blends are miscible in the melt. However, if the HDPE concentration was lower than 40% in the blends, they found phase separation. This observation was further supported by the type of morphology revealed by TEM. In particular, at high HDPE concentrations, the blends have a uniform "fine-grained texture" while at low HDPE concentrations, a circular spherulitic domain was observed. Accordingly, they concluded that HDPE and LDPE blends will phase segregate in the melt state if HDPE concentration is below 40%.

To map out the full phase diagram for the HDPE/LDPE blends, Hill et al. (Hill et al., 1991, Hill and Barham, 1992b) used two additional techniques: rheological measurements and hot stage electron microscopy. They constructed a closed loop phase diagram in an LDPE-rich region, which has both upper and lower critical solution temperatures at 200 and 130 $^{\circ}$C, respectively. Later, they used TEM to confirm the

18

conclusion that the phase diagram is in the shape of a closed loop at low HDPE concentrations. Based upon the observations that the phase segregation temperatures are not dependent on whether the blends are heated and cooled, they argued that the phase diagram displays an equilibrium phase boundary.

Hill *et al.* (Hill and Barham, 1995, Hill, Barham and Keller, 1992, Hill, 1991) also studied the effect of the branch content of LDPE and the molecular weight of HDPE on the phase behavior of an HDPE/LDPE system. They examined four HDPEs with different molecular weights (M_w) in the range of 2,550 to 2×10^6 and blended with two different LDPEs. It was found that liquid-liquid phase separation takes place in the LDPE-rich region and the size of phase separation region in the phase diagram decreases with decreasing molecular weight of HDPE. When the M_w of HDPE was 2,550, no phase separation region existed. Furthermore, they blended HDPEs with different molecular weights to determine if the phase separation observed in the HDPE/LDPE blends is induced by molecular weight differences in HDPE itself. They found that there is no observable phase separation, which means that the phase separation observed in HDPE and LDPE systems is not a result of molecular weight differences in HDPE. In terms of the branch content effect of LDPE, they used two LDPEs containing different number of branches, one with 26 and the other with 17 branches per 1,000 backbone carbons. They suggested that systems with lower branch contents of LDPE show greater miscibility, which is in agreement with other researchers' findings (Tashiro *et al.*, 1992, Fan 2001)

Hill *et al.* (1993) also studied HDPE/octene-based LLDPE blends and found that the blends with lower branch contents (10 to 40 branches per 1,000 backbone carbons) exhibit a closed loop phase diagram at low HDPE concentrations, which is similar to

19

what was observed for the HDPE/LDPE blends. Later, they examined blends composed of butene-based LLDPE and HDPE as well as hexene-based LLDPE with HDPE (Hill, Morgan and Barham, 1997), and found that the extent of phase separation is similar to that for blends of octene-based LLDPE and HDPE if the co-polymers have comparable branch contents. They concluded that the branch length is not the decisive factor to determine phase behavior, but the branch content is.

In addition to binary blend systems, Hill and coworkers also investigated ternary blends of polyethylenes using DSC and TEM (Thomas *et al.*, 1993, Hill and Barham, 1994, Morgan *et al.*, 1997). They first studied blends composed of one HDPE and two octene-based LLDPE with branch contents of 10 and 40 branches per 1,000 backbone carbons, respectively. They constructed the phase diagrams in which three phase separation regions were observed for blends with high branch content LLDPE. Later, they used a butene-based LLDPE to replace the octene-based LLDPE. Similar phase behavior was detected and they concluded that branch length is not as important as branch content for determining phase behavior of such polyethylene blends.

Most recently, using the same techniques, Hill's group investigated the phase behavior of LDPE/LLDPE blends (Hill and Puig, 1997). The LLDPE used had 15 branches and the LDPE had 25 (10 long and 15 short) branches per 1,000 backbone carbons. The results indicated that these blends also exhibit a closed loop phase behavior similar to those of the HDPE/LDPE and HDPE/LLDPE blends.

In summary, Hill and coworkers have done a substantial amount of work on the liquid-liquid phase separation in binary and ternary blends of different types of polyethylenes. The effects of molecular weight, degree of branching, branch length, and

20

blend composition were addressed. They found that increasing molecular weight of HDPE and branch contents of LDPE and LLDPE decrease the degree of miscibility of the HDPE/LDPE and HDPE/LLDPE blends. Varying the branch length of LLDPE has no significant effect on the phase behaviour of HDPE/LLDPE blends. It should be noted that the validity of their techniques is still controversial, especially the basic assumption that quenching a sample from the melt state to the solid state does not change the morphology of the blends in the melt. To rule out the possibility of phase separation on crystallization, Hill's group measured diffusion rates of the components in the blends and found that it is very low for the polymers to segregate during the quenching process (Hill and Barham, 1992a). However, if such measurements were reliable, the resultant samples would have zero crystallinity. Obviously, this is not the case.

From the previous discussion, it can be noted that the common techniques used to study the miscibility of polyethylene blends indirectly include DSC, morphological, and rheological techniques. The following conclusions can be made. HDPE and LLDPE form co-crystals in the crystalline phase and are miscible in both crystalline and amorphous phases. In particular, in the melt state, the branch content of LLDPE plays an important role in determining the miscibility of these blends. More branches induce immiscibility. In contrast, the branch length of LLDPE is not an important factor. LDPE and LLDPE crystallize separately in the solid state and are immiscible in both crystalline and amorphous phases. For HDPE and LDPE blends, there is still no consensus on their miscibility; some researchers believe that these blends co-crystallize while other researchers do not follow this hypothesis.

21

2.1.2 Interaction parameters of polyethylene blends

2.1.2.1 Experimental studies

SANS is one of the few experimental techniques that can be used to determine the miscibility of polymers quantitatively because it can provide direct information on the interaction energy between the components in the blend. Another advantage of this technique is that the blends can be examined directly in the melt state. The drawback of this technique is that the required equipment is very expensive.

Wignall *et al.* (1982) first used this technique to study the miscibility of PP and PE blends in the melt state. Thereafter, Lohse (1986) applied this method to study the melt compatibility of blends of polypropylene (PP) and ethylene-propylene co-polymers (EP). Five EPs with different ethylene contents were selected to investigate the effect of ethylene content on the miscibility of such blends. It was found that PP and EP blends are not miscible in the melt, even when the ethylene content of EP is as low as 8 wt%.

Nicholson *et al.* (1990) used this technique to study blends of HDPE and hydrogenated polybutadienes (HPB) with different amounts of ethyl branches ranging from 18 to 106 per 1,000 backbone carbons. Hydrogenated polybutadienes are commonly used as model polymers of random co-polymer of ethylene and 1-butene. The reason for using model polymers is that they tend to have very narrow molecular weight distribution (i.e., $M_w/M_n < 1.1$). Due to the chemical similarity of the above-mentioned two polymers, one of the components must be deuterated or partially deuterated to provide the neutron contrast. This inevitably creates the problem that the phase behaviour of the blends may be affected by the presence of the isotope in one of the components. This effect was later studied by Graessley *et al.* (1993, 1994a). Treating the deuterated component as a

22

mixture of two different co-polymers, one was hydrogenated polybutadiene and the other was deuterated polybutadiene, they obtained the following expression for 50/50 blends of HDPE and HPB at 150 ± 15 °C: $\chi = 0.4 \times 10^{-4} + 0.014 \Delta X_{br}^2$. Here χ is the Flory-Huggins interaction parameter and ΔX_{br} is the fraction of the repeating units containing ethyl branches. The first term in the above equation was attributed to the isotopic effect while the second term to the differences in chemical composition between the components. This equation indicates that the difference in the branch content prevents miscibility. They also studied the morphology of quenched samples of the blends with SEM. They suggested that a co-polymer having more than 60 branches per 1,000 backbone carbons phase separates from HDPE with molecular weight $M_n=11,800$ at 150 °C in blends. This result was confirmed by MD simulation (Fan, 2001). In this thesis, I studied the branch content effect of LLDPE by using IGC at higher temperatures and obtained similar results (see Chapter 6).

Graessley and coworkers have also done a substantial amount of research on the miscibility of model polyolefin blends using SANS. The model polyolefins they used were hydrogenated polybutadienes (HPB). Two series of binary blends composed of four types of polybutadienes with various branch contents and molecular weight averages were investigated to study the effect of temperature, composition, and molecular weight on Flory-Huggins interaction parameters (Balsara *et al.*, 1992, Krishnamoorti *et al.*, 1994, 1995). The experimental procedure and data analysis were very similar to those of Nicholson *et al.* (1990). Based upon their experimental results, they concluded that χ values are not sensitive to the molecular weight of the components and the blend

23

composition. This is somewhat unexpected. In terms of temperature dependence, χ conforms to the form $\chi(T) = A / T + B$; here, values of A and B vary with systems. However, deuterium substitution may play an important role in the interactions between deuterated and hydrogenated polymers.

Subsequent studies by Graessley *et al.* (1993, 1994a) showed that deuteration results in a significant change in the thermodynamic interactions, but the direction of changes depends on which of the two components is deuterated. Although the magnitude of the changes vary for different blends, for a particular series of blends, the effect of deuteration changes systematically. Based on solubility parameter arguments, a simple theory was proposed and a numerical ordering of the solubility parameters of the components in blends was obtained, and could be used to infer the miscibility of the blends. The interaction parameters between linear polyethylene and poly(1-butene) with various branch contents were determined (Graessley *et al.*, 1994b). The solubility parameter differences derived from the interaction parameters were found to be consistent with those from pressure-volume-temperature (PVT) measurements.

Alamo *et al.* (1994, 1992) did extensive studies on the phase behavior of HDPE/LDPE blends in the molten and solid states by SANS and DSC. The branch content of LDPE used was about 15 branches per 1,000 backbone carbons, 2 long and 13 short. Based on their results, in the solid state blend morphology changes with the composition of the blend and cooling rates used. For slow cooling, they found that HDPE/LDPE blends are phase separated, regardless of the composition. On the other hand, co-crystallization was observed in the quenched samples. In the melt state, HDPE/LDPE blends were found to form a homogeneous liquid mixture at all

24

compositions. This contradicts to Barham's (Barham, *et al.*, 1988) finding that HDPE and LDPE are phase separated in the melt state at low HDPE concentrations. This may be attributed to the different branch contents of the LDPEs used. It was suggested that 25 branches is the critical branch content value of LDPE, above which HDPE and LDPE become immiscible, is about 25 branches (Fan *et al.*, 2001). The branch content of the LDPE used by Barham's group was 26 branches. However, the LDPE used by Alamo's group contained only 15 branches per 1,000 backbone carbons.

The effect of branch content of LLDPE on the phase behavior of HDPE/LLDPE blends was also studied using the same techniques (Alamo *et al.*, 1997). In such study, the authors used HPB to simulate butene-based LLDPE to obtain samples with high branch contents. The branch contents of HPB were in the range of 21 to 106 branches per 1,000 backbone carbons. Their results show that if the branch content is lower than 40 branches, the blends are homogenous at all concentrations. However, if the branch content is higher than 80 branches, phase separation will occur. These findings are basically consistent with Nicholson's conclusion (Nicholson *et al.*, 1990) that the branched component having more than 60 branches will induce phase separation. In addition, the critical value of branch content of LLDPE to induce immiscibility obtained from my IGC method is 50 branches per 1,000 backbone carbons (Chapter 6).

It is worth noting that the maximum spatial resolution of SANS is $103 \overset{0}{A}$. Hence, the SANS data can also be interpreted as a result of a heterogeneous melt with a large particle size at the micron level. To rule out this possibility, Agamalian *et al.* (1999) investigated the same HDPE/LDPE blend by means of ultra small angle neutron

25

scattering (USANS), which can detect particle dimensions up to 30 μm. The USANS results confirmed their former conclusion that HDPE/LDPE blends are homogenous in the melt state over the whole compositional range. They also used the technique to study the blends of HDPE and HPB with branch contents high enough to form a phase separated system (>80 branches per 1,000 backbone carbons). It was found that USANS can detect the dispersed phase directly and the domain size of the dispersed phase is about 4 μm.

Although SANS is considered as a powerful technique, controversy presents in the interpretation of experimental data. For the same set of data, Alamo $et\ al.$ (1994) used an equation derived for a miscible melt to fit the experimental data and they found that χ_{23} values are in the order of 10^{-4} at 160 °C, while Schipp and co-workers (1996) used an equation for a biphasic melt to fit their experimental data and they concluded that χ_{23} values are in the order of 10^{-3} at the same temperature. This indicates that χ obtained from the SANS technique is very sensitive to the equations used. This gives some uncertainties to SANS results.

In addition to SANS, some researchers attempted to use different techniques to determine χ of polyethylene blends. Martinez-Salazar $et\ al.$ (1992) and Plans $et\ al.$ (1992) investigated the effect of the branch content of LDPE on its phase behaviour with HDPE blends by melting point depression analysis. The branch contents of LDPEs studied were 7, 12.1, and 17.6 branches per 1,000 backbone carbons. The samples were prepared using solution mixing. The melting points of pure polymers and their blends were obtained by observing the growth and disappearance of the spherulites using an optical microscope

equipped with a hot stage under the polarized light. Based upon their experimental data, they suggested that HDPE and LDPE may form a miscible blend if the branch content of LDPE is lower than 20, and phase separation may occur if the branch content of LDPE is higher than 30. Based on these results on HDPE/LDPE blends together with the results on HDPE/LLDPE blends obtained by Nicholson *et al.* (1990), it can be said that for HDPE/LLDPE blends, the critical branch content of LLDPE to induce immiscibility is about 60 branches per 1,000 backbone carbons and that of LDPE in HDPE/LDPE blends is only about 20 branches per 1,000 backbone carbons. This suggests that long chain branches on LDPE play an important role on its miscibility with other polyethylenes.

However, it is important to note that the validity of the use of the extrapolative method to derive the equilibrium melting point of polyethylene is still questionable. Alamo *et al.* (1995) attempted to use the Hoffman-Week plot to obtain equilibrium melting temperatures of hydrogenated polybutadienes (HPBD) and failed. Later, they re-examined this issue using a linear polyethylene. They found that the T_m/T_c plot was nonlinear and the expected T_m^o could not be obtained. As a result, this affected the estimation of χ. Similar experiments have been carried out in our laboratory using DSC and we obtained results similar to those of Alamo *et al.* (as shown in Figure 2.1).

2.1.2.2 Simulation methods to predict interaction parameters of polyethylene blends

With the rapid advancement in computer hardware and software, many researchers have been able to predict the phase behavior of polyethylene blends theoretically. Economou (2000) applied the lattice-fluid theory of Sanchez and Lacombe

27

to estimate the phase behavior of binary blends of HDPE with three branched polyethylenes of variable molecular weights. The binary interaction parameters were obtained from experimental data and were used for in the simulation. The phase behavior was predicted as a function of molecular size and structure, temperature, and pressure. He claimed that his calculated results are consistent with experimental observations and with predictions from other theoretical models, qualitatively. He believed that the simple method they proposed can provide a guideline for more powerful models to estimate polyolefin blend miscibility.

Most recently, Choi and co-workers (Choi 2000, Fan *et al.*, 2001) have applied a molecular dynamics approach to study the miscibility of polyethylenes with different molecular structures. They found that both branch content and branch distribution are the primary factors controlling the phase behavior of such blends. The critical values of branch contents of LDPE and LLDPE to induce immiscibility with HDPE are 25 and 50 branches per 1,000 backbone carbons, respectively. These results are in good agreement with those obtained from other experimental techniques such as SANS (Alamo *et al.*, 1994).

Mehta and Honnel (1997) proposed a new equation-of-state model derived from the Flory-Huggins theory to investigate the effect of molecular weight and branch content on the miscibility of polyolefin blends. They employed this model to predict the phase behavior of HDPE/isotactic polypropylene (i-PP) and ethylene-propylene rubber (EPR)/i-PP blends in the melt state. They found that blend miscibility decreases with increasing the molecular weight of the components and the degree of branching. They believed that

28

their model is applicable to other polyethylene blends, such as blends of HDPE and LLDPE.

Fredrickson *et al.* (1994) calculated the combinational part of excess free energy on mixing by the Flory-Huggins theory associated with fluctuation corrections. Their results are consistent with Alamo's findings (Alamo *et al.*, 1997), which is contradict to the phase separation observation reported by Hill *et al* (1991).

2.2 Miscibility studies on polyethylene/polypropylene and polyethylene/polystyrene blends

Miscibility of polyethylene/polypropylene and polyethylene/polystyrene blends has been widely investigated in the literature and the general consensus is that these two blends are not miscible in both solid and melt states. Therefore, I will not present an extensive review in this thesis.

An extensive review of polyethylene/polypropylene blends has been presented by Teh *et al.* (1994). In general, blends of polyethylene and polypropylene have been found to be immiscible in both the solid state and the melt state although both components are composed of CH, CH_2, and CH_3 groups only. For example, by measuring the capillary viscosities, Alle and Lyngaae-Lorgensen (1980) found that the plot of shear viscosity at constant shear stress versus volume fraction of one component of the blend showed a large negative deviation from the additive rule. Therefore, they concluded that polyethylene and polypropylene blends are immiscible in the melt state.

29

Results of SANS and PVT measurements (Jeon *et al.*, 1997) showed that χ is about 0.0038, estimated based upon the reference volume of an ethylene repeating unit. Recently, Hermes *et al.* (1997) and Bucknall *et al.* (1998) investigated the HDPE/i-PP blends using a neutron reflectivity technique. They found that the interaction parameters between HDPE and i-PP blends are about 0.02 over the temperature range of 175 to 225 °C. Applying molecular simulation method for modeled polyethylene/polypropylene blend, Akten *et al.* (2001) obtained χ values of around 0.09 at 200 °C.

The polyethylene/polystyrene blend is a well known immiscible blend because of the dissimilarity in the chemical structures. SEM pictures of quenched samples of these blends show that the dispersed phase forms spherical particles in the continuous phase indicating that these blends are phase separated in the solid state. Using a neutron reflectivity in the melt state, Bucknall *et al.* (1998) found that interaction parameter between HDPE and PS has a value of 0.05 at 150 °C.

2.3 Summary

It is evident from the foregoing discussion that only a limited number of techniques can be used to determine miscibility of polyethylene blends because of the similarity of chemical structures of different polyethylenes. Most of the experimental techniques mentioned are indirect and cannot be used to investigate the samples in the melt state directly or to yield χ. The conclusions researchers made about the miscibility of polyethylene blends in melt state were mainly inferred from the investigation of solid

30

samples. The applicability of using solid state data is still controversial (Alamo *et al.*, 1994) because quenching of samples from the melt state to the solid state may change the morphology of the samples. On the other hand, some researchers studied the polyethylene blends in the liquid state using SANS and molecular simulation. Unfortunately, the SANS equipment is extremely expensive and cannot be accessed by many researchers. Molecular simulation can provide us with valuable information on this issue. However, the technique is rather limited because of the computer resources required. It is also evident that conclusions drawn from different techniques are not consistent with each other. For example, miscibility of HDPE/LDPE in the melt state and the critical branch content of LLDPE to induce phase separation in the blends with HDPE are still controversial. In addition, as mentioned in the introduction, most of the studies have focused on temperatures much lower than the processing temperatures of these materials. It is clear that developing an inexpensive but reliable experimental technique that can be used to determine miscibility around processing temperatures of polyethylenes is needed.

2.4 References

Agamalian, M., Alamo, R.G., Kim, M.H., Londono, J.D., Mandelkern, L. and Wignall, G.D. (1999) Phase Behavior of Blends of Linear and Branched Polyethylenes on Micron Length Scales via Ultra-Small-Angle Neutron Scattering, *Macromolecules*, 32, 3093-3096.

Akten, D.E., Wayne, L. and Mattice, L. (2001) Monte Carlo Simulation of Head-to-Head, Tail-to-Tail Polypropylene and its Mixing with Polyethylene in the Melt, *Macromolecules*, 34(10), 3389-3395.

Alamo, R.G., Chan, E.K.M., Mandelkern, L. and Voigt-Martin, I.G. (1992) Influence of Molecular Weight on the Melting and Phase Structure of Random Co-polymer of Ethylene, *Macromolecules*, 25, 6381-6394.

Alamo, R.G., Graessley, W.W., Krishnamoorti, R., Lohse, D.J., Londono, J.D., Mandelkern, L., Stehling, F.C. and Wignall, G.D. (1997) Small Angle Neutron Scattering Investigations of Melt Miscibility and Phase Segregation in Blends of Linear and Branched Polyethylenes as a Function of the Branch Content, Molecules, *Macromolecules*, 30, 561-566.

Alamo, R.G., Londono, J.D., Mandelkern, L., Stehling, F.C. and Wignall, G.D. (1994) Phase Behavior of Linear and Branched Polyethylenes in the Molten and Solid States by Small-Angle Neutron Scattering, *Macromolecules*, 27, 411-417.

Alamo, R.G., Viers, B.D. and Mandelkern, L. (1995) A Re-examination of the Relation between the Melting Temperature and the Crystallization Temperature: Linear Polyethylene, *Macromolecules*, 28, 3205-3213.

Alle, N. and Lyngaae-Jorgensen, J. (1980) Polypropylene and Polyethylene Blends I. Flow Behavior in Capillaries, *Rheol. Acta*, 19, 94-103.

Balsara, N.P., Fetters, L.J., Hadjichristidis, N., Lohse, D.J., Han, C.C., Graaessley, W.W. and Krishnamoorti, R. (1992) Thermodynamic Interactions in Model Polyolefin Blends Obtained by Small-Angle Neutron Scattering. *Macromolecules*, 25, 6137-6147.

32

Barham, P.J., Hill, M.H., Keller, A. and Rosney, C.C.A. (1988) Phase Separation in Polyethylene Melts, *Journal of Materials Science Letters*, 7, 1271-1275.

Bucknall, D.G., Butler, S.A., Hermers, H.E. and Higgins, J.S. (1998) Neutron Reflectivity Investigations of Semi-crystalline Polymer Interfaces, *Physica B*, 241-243, 1071-1073.

Cho, K., Ahn, T., Lee, B.H. and Choe, S. (1997) Miscibility and Processibility in Linear Low Density Polyethylene and Ethylene-Propylene-Butene-1 Terpolymer Binary Blends, *J. Appl. Polym. Sci.*, 63, 1265-1274.

Choi, P. (2000) Molecular Dynamics Studies of the Thermodynamics of HDPE/Butene-Based LLDPE Blends, *Polymer*, 41, 8741-8747.

Conde Brana, M.T. and Gedde, U.W. (1992) Morphology of Binary Blends of Linear and Branched Polyethylene: Composition and Crystallization- Temperature Dependence, *Polymer*, 33.

Crist, B. and Hill, M.J. (1997) Recent Developments in Phase Separation of Polyolefin Melt Blends, *J. Polym. Sci. B Polym. Phys.*, 35, 2329-2353.

Datta, N.K. and Birley, A.W. (1982) Thermal Analysis of Polyethylene Blends, *Plastics and Rubber Processing and Application*, 2, 237-245.

Doran M. and Choi, P (2001) Molecular Dynamics Studies of the Effects of Branching Characteristics on the Crystalline Structure of Polyethylene, *J. Chem. Phys.*, 115(6), 2827-2830.

Drummond, K.M., Hopewell, J.L. and Shanks, R.A. (2000) Crystallization of Low-Density Polyethylene- and Linear Low-Density polyethylene-Rich Blends. *J. Appl. Polym. Sci.* 78, 1009-1016.

33

Economou, E.G. (2000) Lattice-Fluid Theory Prediction of High-Density Polyethylene-Branched Polyolefin Miscibility, *Macromolecules*, 33, 4954-4960.

Fan, Z. (2001) MD and SEM Studies of Miscibility of Polyethylene Blends, Ph.D. thesis, University of Alberta.

Fan, Z., Williams, M.C. and Choi, P. (2001) Molecular Dynamics Studies of the Effects of Branching Characteristics of LDPE on its miscibility with HDPE, *Polymer*, 43(4), 1479-1502.

Fredrickson, G.H., Liu, A.J. and Bates, F.S. (1994) Entropic Corrections to the Flory-Huggins Theory of Polymer Blends: Architectural and Conformational Effects, *Macromolecules*, 27, 2503-2511.

Graessley, W.W., Krishnamoorti, R., Balsara, N.P., Fetters, L.J., Lohse, D.J., Schulz, D.N. and Sossano, J.A. (1994a) Deuteration Effects and Solubility Parameters Ordering in Blends of Saturated Hydrocarbon Polymers, *Macromolecules*, 27, 2574-2579.

Graessley, W.W., Krishnamoorti, R., Balsara, N.P., Fetters, L.J., Lohse, D.J., Schulz, D.N. and Sossano, J.A. (1993) Effect of Deuterium Substitution on Thermodynamic Interactions in Polymer Blends, *Macromolecules*, 26, 1137-1143.

Graessley, W.W., Krishnamoorti, R., Balsara, N.P., Fetters, L.J., Lohse, D.J., Schulz, D.N. and Sossano, J.A. (1994b) Thermodynamics of Mixing for Blends of Model Ethylene-Butene Co-polymers, *Macromolecules*, 27, 3896-3901.

Hermes, H.E., Higgins, J.S. and Bucknall, D.G. (1997) Investigations of the Melt Interface between Polyethylene and Polystyrene Using Neutron Reflectivity, *Polymer*, 38(4), 985-989.

Hill, M. J., Barham, P.J. and Keller, A. (1992) Phase Segregation in Blends of Linear with Branched Polyethylene: the Effect of Varying the Molecular Weight of the Linear Polymer, *Polymer*, 33(12),2530-2541.

Hill, M.J. and Barham P.J. (1994) Interpretation of Phase Behavior of Blends Containing Linear Low-Density Polyethylenes Using a Ternary Phase Diagram, *Polymer*, 35(9), 1802-1808.

Hill, M.J. and Barham, P.J. (1992a) Diffusion Effects in Blends of Linear with Branched Polyethylenes, *Polymer*, 33(23), 4891-4897.

Hill, M.J. and Barham, P.J. (1992b) Liquid-Liquid Phase Separation in Melts of Blends of Linear with Branched Polyethylenes: Morphological Exploration of the Phase Diagram, *Polymer*, 33(19), 4099-4107.

Hill, M.J. and Barham, P.J. (1995) Absence of Phase Separation Effects in Blends of Linear Polyethylene Fractions of Differing Molecular Weight, *Polymer*, 36(8), 1523-1530.

Hill, M.J. and Puig, C.C. (1997) Liquid-Liquid Phase Separation in Blends of a Linear Low-Density Polyethylene with a Low-Density Polyethylene, *J. Appl. Polym. Sci.*, 65, 1921-1931.

Hill, M.J. (1991) Liquid-Liquid Phase Separation in Binary Blends of a Branched Polyethylene with Linear Polyethylenes of Differing Molecular Weight, *Polymer*, 35(9), 1991-1993.

Hill, M.J., Barham, P.J. and van Ruiten, J. (1993) Liquid-Liquid Phase Segregation in Blends of a Linear Polyethylene with a Series of Octene Copolymers of Differing Branch Content, *Polymer*, 34(14), 2975-2679.

Hill, M.J., Barham, P.J., Keller, A. and Rosney, C.C.A. (1991) Phase Segregation in Melts of Blends of Linear and Branched Polyethylene, *Polymer*, 32(8), 1384-1393.

Hill, M.J., Morgan, R.L. and Barham, P.J. (1997) Minimum Branch Content for Detection of Liquid-Liquid Phase Separation, Using Indirect Techniques, in Blends of Polyethylene with Ehylene-Octene and Ethylene-Butene Copolymers, *Polymer*, 38(12), 3003-3009.

Hu, S.R., Kyu, T. and Stein, R.S. (1987) Characterization and Properties of Polyethylene Blends I. Linear Low-Density Polyethylene with High-Density Polyethylene, *J. Polym. Sci. B: Polym. Phys.*, 25, 71-87.

Iragorri, L.I., Rego, J.M., Katime, I., Conde Brana, M.T. and Gedde, U.W. (1992) A Crystallization Kinetics Study of Binary Blends of Linear and Branched Polyethylene, *Polymer*, 33(3), 461-466.

Jeon, H.S., Lee, J.H., Balsara, N.P., Majumdar, B., Fetters, L.J. and Faldi, A. (1997) Domain Shape Transitions in Emulsified Polyolefin Blends, *Macromolecules*, 30, 973-981.

Krishnamoorti, R., Graessley, W.W., Balsara, N.P. and Lohse, D.J. (1994) Structural Origin of Thermodynamic Interactions in Blends of Saturated Hydrocarbon Polymers, *Macromolecules*, 27, 3073-3081.

Krishnamoorti, R., Graessley, W.W., Fetters, Garner, R.T. and Lohse, D.J. (1995) Anomalous Mixing Behavior of Polyisobutylene with Other Polyolefins, *Macromolecules*, 28, 1252-1259.

Kwag, H., Rana, D., Cho, K., Rhee, J., Woo, T., Lee, B.H. and Choe, S. (2000) Binary Blends of Metallocene Polyethylene with Conventional Polyolefins: Rheological and Morphological Properties. *Polym. Engr. Sci.* 40(7), 1672-1681.

Kyu, T., Hu, S.R. and Stein, R.S. (1987) Characterization and Properties of Polyethylene Blends II. Linear Low-Density with Conventional Low-Density Polyethylene, *J. Polym. Sci. B: Polym. Phys.*, 25, 89-103.

Lee, H. and Denn, M.M. (2000) Blends of Linear and Branched Polyethylenes. *Polym. Engr. Sci.* 40(5), 1132-1142.

Lee, H., Cho, K., Ahn, T., Choe, S., Kim, I. and Park, I. (1997) Solid-State Relaxations in Linear Low-Density (1-Octene Comonomer), Low-Density, and High-Density Polyethylene Blends, *J. Polym. Sci. B: Polym. Phys.*, 35, 1633-1642.

Lohse, D.J. (1986) The Melt Compatibility of Blends of Polypropylene and Ethylene-Propylene Co-polymers, *Polym. Engr, Sci.*, 26(21), 1500-1509.

Martinez-Salazar, J., Sanchez Cuesta, M. and Plans, J. (1991) On Phase Separation in High- and Low-Density Polyethylene Blends: 1. Melting-Point Depression Analysis, *Polymer*, 32(16), 2984-2988.

Mehta, S.D. and Honnell K.G. (1997) Towards a Molecular Theory for Polyolefin Miscibility, *Proceedings of ANTEC'97*, 2648-2652.

Morgan, R.L., Hill, M.J., Barham, P.J. and Frye, C.J. (1997) Liquid-Liquid Phase Separation in Ternary Blends of Linear Polyethylene with Two Ethylene-Butene Copolymer, *Polymer*, 38(8), 1903-1909.

Muller, A.J., Balsamo, V., Da Silva, F., Rosales, C.M. and Saez, A.E. (1994) Shear and Elongational Behavior of Linear Low-Density and Low-Density Polyethylene Blends from Capillary Rheometry, *Polym. Eng. Sci.*, 34(19), 1455-1463.

Nicholson, J.C., Finerman, T.M. and Crist, B. (1990) Thermodynamics of Polyolefin Blends: Small-Angle Neutron Scattering Studies with Partially Deuterated Chains, *Polymer*, 31, 2287-2294.

Plans, J., Sanchez Cuesta, M. and Martinez-Salazar, J. (1991) On Phase Separation in High- and Low-Density Polyethylene Blends: 2. A Working Model, *Polymer*, 32(16), 2989-2991.

Ree, M., Kyu, T. and Stein, R.S. (1987) Quantitative Small-Angle Light-Scattering Studies of the Melting and Crystallization of LLDPE/LDPE Blends, *J. Polym. Sci. B: Polym. Phys.*, 25, 105-126.

Rego Lopez, J.M. and Gedde, U.W. (1989) Crystallization and Morphology of Binary Blends of Linear and Branched Polyethylene: Polarized Light Microscopy, Small-Angle Light Scattering and Thermal Analysis, *Polymer*, 30, 22-26.

Schipp, C., Hill, M.J., Barham, P.J., Cloke, V.M., Higgins, J.S. and Oiarzabal, L. (1996) Ambiguities in the Interpretation of Small-Angle Neutron Scattering from Blends of Linear and Branched Polyethylene, *Polymer*, 37(12), 2291-2297.

Tashiro, K., Izuchi, M., Kobayashi, M. and Stein, R.S. (1994) Cocrystallization and Phase Segregation of Polyethylene Blends between the D and H Species. 3. Blend

Content Dependence of the Crystallization Behavior, *Macromolecules*, 27, 1221-1227.

Tashiro, K., Stein, R.S. and Hsu, S.L. (1992) Cocrystallization and Phase Segregation of Polyethylene Blends. 1. Thermal and Vibrational Spectroscopic Study by Utilizing the Deuteration Technique, *Macromolecules*, 25, 1801-1808.

Teh, J.W., Rudin, A. and Keung, J.C. (1994) A Rewiew of Polyethylene-Polypropylene Blends and Their Compatibilization, *Advances in Polymer Technology*, 13(1), 1-23.

Thomas, D., Williamson, J., Hill, M.J. and Barham, P.J. (1993) Liquid-Liquid Phase Separation in a Ternary Blend of Polyethylenes, *Polymer*, 34(23), 4919-4923.

Wignall, G.D., Child, H.R. and Samuels, R.J. (1982) Structural Characterization of Semi-Crystalline Polymer Blends by Small Angle Neutron Scattering, *Polymer*, 23, 957-964.

Yamaguchi, M. and Abe, S. (1999a) LLDPE/LDPE Blends. I. Rheological, Thermal and Mechanical Properties. *J. Appl. Polym. Sci.* 74, 3153-3159.

Yamaguchi, M. and Abe, S. (1999b) LLDPE/LDPE Blends. II. Viscoelastic Properties in Solid State. *J. Appl. Polym. Sci.* 74, 3160-3164.

Zhao, H., Lei, Z. and Huang, B. (1998) Excimer Fluorescence Studies on the Mscibility of Polyolefins in the Amorphous Phase, *Polymer Journal*, 30(2), 149-151.

Figure 2.1 $T_m - T_c$ plot for butene-based linear low density polyethylene (Mw=105,000g/mol)
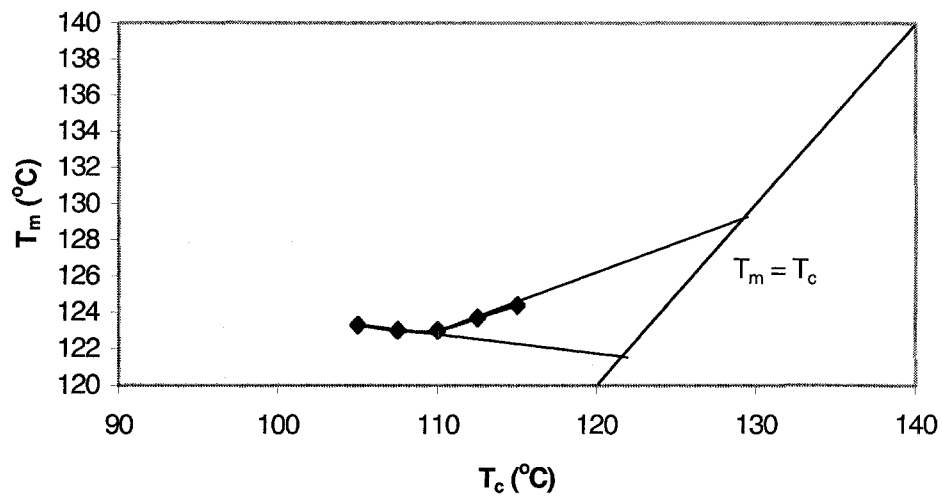
¹Chapter 3

Inverse Gas Chromatography

3.1 Introduction

The first scientist who recognized chromatography as an efficient method of separation was the Russian botanist Tswett in the late 1890s. In 1952, James and Martin constructed the first gas chromatograph (GC). Since then, GC has become one of the most powerful analytical tools available to determine the number of components and their composition in an unknown sample. The technique allows separation of extremely small quantities of materials and is applicable over a wide range of temperatures making it possible to separate materials with a wide range of volatiles (Skoog, 1998). Usually, a GC apparatus consists of the following components: a carrier gas supply, a hydrogen gas supply, an air supply, a column packed with stationary phase and secured in an oven, an inlet gas injector and a tail gas detector, as shown in Figure 3.1.

The sequence of chromatographic separation is based on the distribution of gaseous solute molecules between the mobile gaseous phase and the stationary phase. A certain amount of sample is injected into a column where the components in the sample are swept by a carrier gas and undergo a continuous sorption-desorption process. This process occurs repeatedly as the sample moves toward the end of the column as depicted

---

¹A version of Chapter 3 and Chapter 4 is published in *Polymer* (2001), 42, 1075-1081.

in Figure 3.2. Since different compounds have different distribution characteristics, each solute travels at its own rate through the column. As a result, the compounds will traverse through the column at different times. Based on this, the constituents and the relative quantities can be determined by the times and the size of the eluted peaks, respectively.

Inverse gas chromatography (IGC), as an extension of the conventional GC, was first introduced by Lavoie and Guillet (1969). The term "inverse" is used because unlike conventional GC, which is used to separate and quantify the components in the gaseous phase, the polymer being studied is coated on an inert support and packed into the chromatographic column (Al-Saigh, 1997). A series of pure solvents with known thermo-physical properties are injected into the column and interact with the polymer of interest. The thermo-physical properties of polymers are then inferred from the thermo-physical properties of solvent and the interactions between the solvent and polymer. Since the technique was introduced, it has been used widely to investigate various physical properties of polymeric systems, including the glass transition temperature, solubility parameter, diffusion coefficient and crystallinity (Tihminlioglu et al., 2000).

IGC is a very powerful tool to study the miscibility of polymer blends. The key parameter to determine the miscibility of polymer blends is the Flory-Huggins interaction parameter (χ). There are two ways to determine the interaction parameter using IGC. One is to measure the solubility parameters of the pure components in the blend and use the resultant solubility parameters to calculate interaction parameter. The other approach is to measure the interaction parameter directly. It is worth noting that using the first approach the composition dependence of χ cannot be investigated. However, it is well known that χ is a composition dependent parameter. The latter approach can be used to study the

42

effects of not only temperature but also composition on χ. In this thesis, the latter approach is adopted. In the next section of this chapter, theories used to obtain the Flory-Huggins interaction parameters directly will be introduced.

3.2 Theories

3.2.1 Thermodynamics in the IGC technique

In IGC, the parameter that manifests the elution behavior of a solvent is the specific retention volume, V_g^0, which is related to other experimental parameters as shown in the following expression (Lloyd *et al.*, 1989):

$$V_g^0 = \frac{273.15 \, t_n \, F \, J}{w \, T}$$

(3-1)

where t_n is the net retention time, which is the difference of the retention times between a selected solvent and the marker; F is the flow rate of the carrier-gas measured at the experimental temperature T; w is the mass of polymer(s) coated in the column; and J is the James-Martin correction factor that is used to correct for the pressure gradient across the column and is given by the following expression (Littlewood, 1962):

43

$$J = \frac{3}{2} \frac{\left(\dfrac{P_i}{P_o}\right)^2 - 1}{\left(\dfrac{P_i}{P_o}\right)^3 - 1}$$ (3-2)

where P_i and P_o are the inlet and outlet pressures of the column, respectively.

On the other hand, V_g^0 is also related to the partition coefficient of the solvent, which is defined as the ratio of the concentration of the solvent in the liquid phase, c_1^l, to that in the gaseous phase, c_1^g. For a column containing one polymer, the relationship reads:

$$V_g^0 = \left(\frac{c_1^l}{c_1^g}\right) v_2 \left(\frac{273.15}{T}\right)$$ (3-3)

And for a column which consists of a binary polymer blend,

$$V_g^0 = \left(\frac{c_1^l}{c_1^g}\right)(w_2 v_2 + w_3 v_3)\left(\frac{273.15}{T}\right)$$ (3-4)

In expressions (3-3) and (3-4), v_i and w_i are the specific volume and the weight fraction of polymer i in the liquid phase, respectively. It has been found that all types of polyethylenes (i.e., HDPE, LDPE or LLDPE) have the same specific volume (or density)

44

in the melt state. And the specific volume of polyethylenes can be calculated from the following empirical equations (Rudin *et al.*, 1970):

$$v = 1.282 + 9.0 \times 10^{-4}(t - 150) \qquad \text{from 150 to 260 }^{\circ}\text{C} \qquad (3\text{-}5)$$

Here, t is the temperature in degrees Celsius and v is in cm^3/g.

In a chromatographic column, a fast thermodynamic equilibrium of the solvent (which is injected in to the GC column as a probe) between the liquid and gaseous phases is established. Under this condition, the chemical potential of the solvent in the gaseous phases is equal to that in the liquid phase. This means

$$\mu_1^l = \mu_1^g \qquad (3\text{-}6)$$

Here, the chemical potential of the solvent in the gaseous phase is given by the following expression (Denbigh, 1996):

$$\mu_1^g = \mu_1^0 + RT \ln \frac{RT c_1^g}{M_1} \qquad (3\text{-}7)$$

where μ_1^0 is the chemical potential of the solvent at the standard state; R is the universal gas constant; T is the temperature; M_1 is the molecular weight of the solvent; and c_1^g is the solvent concentration in the gaseous phase.

45

The chemical potential of the solvent in the liquid phase is depicted as follows (Denbigh, 1996):

$$\mu_1^l = \mu_1^0 + RT\left(\ln \alpha_1 + \ln P_1^0 + \frac{(B_{11} - V_1)P_1^0}{RT}\right) \tag{3-8}$$

where P_1^0 is the vapor pressure of the solvent at temperature T; B_{11} is the second virial coefficient of the solvent in the gaseous phase; and α_1 is the activity of the solvent in the liquid state.

P_1^0 can be estimated from the Antoine equation (Poling $et\ al.$, 2001)

$$\ln(P_1^0) = A - \frac{B}{(T+C)} \tag{3-9}$$

where A, B and C are Antoine vapor-pressure-equation coefficients, and P_1^0 and T are in the units of mm Hg and Kelvin, respectively.

The second virial coefficients of the probe can be calculated from the modified Pitzer and Curl equations (Tsonopoulos, 1974):

$$\frac{B_{11}P_c}{RT_c} = f^0 + \omega f^1 \tag{3-10}$$

with

$$f^0 = 0.1445 - \frac{0.330}{T_r} - \frac{0.1385}{T_r^2} - \frac{0.0121}{T_r^3} - \frac{0.000607}{T_r^8} \qquad (3\text{-}11)$$

$$f^1 = 0.0637 + \frac{0.331}{T_r^2} - \frac{0.423}{T_r^3} - \frac{0.008}{T_r^8} \qquad (3\text{-}12)$$

Here, P_c and T_c are the critical pressure in atm and the critical temperature in K, respectively; T_r is the reduced temperature, which is defined as the ratio of the experimental temperature to the critical temperature of the probe; ω is the acentric factor and represents the non-sphericity of a molecule. All required constants for the above equations are taken from literature (Poling et al., 2001).

From the classical solution thermodynamics, $\ln\alpha_1$ is related to the Gibbs free energy change on mixing through the following expression:

$$RT\ln\alpha_1 = \left(\frac{\partial \Delta G_m}{\partial n_1}\right)_{n_2, n_3, P, T} \qquad (3\text{-}13)$$

To obtain α_1, an expression for Gibbs free energy on mixing is needed. For polymer solutions and blends, the most commonly used theory is the Flory-Huggins lattice theory.

47

3.2.2 The Flory-Huggins lattice theory

Paul Flory and Maurice Huggins independently modified the original lattice theory for polymer solutions (Flory, 1941 and Huggins, 1941). In this theory, both the size difference and the intermolecular interactions between solvent and polymer molecules are taken into account. The basic assumption they made is that each polymer molecule is composed of a series of segments, and each segment takes one lattice site as shown in Figure 3.3. Usually, the size of a lattice site is determined by the size of a solvent molecule; that is, each solvent molecule takes one lattice. By applying the statistical thermodynamic theories, the entropy change on mixing of a binary mixture can be expressed as (Flory, 1953):

$$\Delta S_m = -R(n_1 \ln \phi_1 + n_2 \ln \phi_2) \tag{3-14}$$

where R is the universal gas constant; n_i is the number of moles of the ith component in the mixture; and ϕ_i is the volume fraction of the ith component in the mixture.

The heat of mixing is approximated as:

$$\Delta H_m = RTn_1\phi_2\chi_{12} \tag{3-15}$$

where χ_{12} is the aforementioned Flory-Huggins interaction parameter between components 1 and 2, and is defined by:

48

$$\chi_{12} = (z - 2)\Delta g_{12} / kT \tag{3-16}$$

Here, z is the number of the first neighbors of each segment; Δg_{12} is the Gibbs free energy change for the formation of a single solvent-segment contact; and k is the Boltzmann constant.

It is worth noting that, in this theory, χ is inversely related to temperature and is independent of composition. However, it has been observed that χ varies with concentration when fitting experimental data into the Flory-Huggins theory.

Therefore, the Flory-Huggins theory for the Gibbs free energy change on mixing for a binary system can be expressed as:

$$\Delta G_{mix} = RT(n_1 \ln \phi_1 + n_2 \ln \phi_2 + n_1 \phi_2 \chi_{12}) \tag{3-17}$$

This equation describes a series of curves for the variation of the Gibbs free energy change on mixing with the volume fractions of the components at various temperatures. Generally, the curves have one of the two shapes as illustrated in Figures 3.4 and 3.5. Figure 3.4 shows a miscible blend system for the entire composition range. Figure 3.5 shows that the two components form a homogeneous mixture in the ranges $0 < \phi_2 < \phi'_{2b}$ and $\phi''_{2b} < \phi_2 < 1$; separate into two phases in the range $\phi'_{2sp} < \phi_2 < \phi''_{2sp}$; and form a metastable solution in the ranges $\phi'_{2b} < \phi_2 < \phi'_{2sp}$ and $\phi''_{2sp} < \phi_2 < \phi''_{2b}$. Here,

49

ϕ'_{2b} and ϕ''_{2b} are referred to the binodal compositions while ϕ'_{2sp} and ϕ''_{2sp} the spinodal compositions.

For two mono-dispersed polymers with degrees of polymerization x_1 and x_2, by taking the second and third derivatives of the equation 3-17 with respect to the volume fraction and setting them to zero, the following criterion for miscibility of the mixture can be derived.

$$(\chi_{12})_{cri} = \frac{1}{2}\left(\frac{1}{\sqrt{x_1}} + \frac{1}{\sqrt{x_2}}\right)^2 \qquad (3\text{-}18)$$

From the above equation, it is obvious that when $x_1 \approx x_2 \approx 1$, $(\chi_{12})_{cri} \approx 2$, which is the critical value of interaction parameter for miscible systems composed of small molecules. When $x_1 \approx 1$, and $x_2 \approx \infty$, (i.e., a polymer solution), $(\chi_{12})_{cri} \approx 0.5$. For polymer blends, $x_1 \approx x_2 \approx \infty$; therefore, $(\chi_{12})_{cri} \approx 0$.

Similarly, for a ternary system, the Gibbs free energy change on mixing can be expressed as:

$$\Delta G_{mix} = RT(n_1 \ln\phi_1 + n_2 \ln\phi_2 + n_3 \ln\phi_3 + n_1\phi_2\chi_{12} + n_1\phi_3\chi_{13} + n_2\phi_3\chi_{23}) \qquad (3\text{-}19)$$

The Flory-Huggins equation can be used to account for the equilibrium thermodynamic properties of polymer solutions, phase separation and melting point depressions. However, even though the Flory-Huggins theory is able to predict some

50

general features of the mixing process, the theory has deficiencies in many aspects. For example, in the original Flory-Huggins theory, all lattices are required to be occupied by either the solvent molecules or the segments of the polymer molecules. Therefore, there is no empty site. This implies that free volume is not allowed in the mixture. As a result, the volume change on mixing cannot be modeled. This is obviously not true for many systems, especially for polymer solutions.

Despite these shortcomings, the Flory-Huggins theory still prevails in the current polymer literature and is frequently used as the basis of many other theories. The interaction parameter is still widely used as an indicator to determine miscibility. Some modifications to the Flory-Huggins theory have been proposed by many researchers, such as the Flory-Krigbaum theory (Fried, 1995). Since the resulting expressions of such approaches are rather complex, they are seldom employed in practice.

The Flory-Huggins theory was still used in the present work because the polymers of interest have very similar thermal expansion coefficients. It is well known that the volume change on mixing comes from the different free volumes or degrees of thermal expansion of the components in a mixture. However, Rudin et $al.$ reported that the specific volumes of different types of polyethylenes are equivalent in the melt state (Rudin et $al.$, 1970). This indicates that different types of polyethylenes, regardless of their branching characteristics or content, have the same free volume and thermal expansion coefficient in the melt state. The expansion coefficient is $9.0 \times 10^{-4} cm^3 g^{-1} K^{-1}$ from 150 to 260 $^\circ$C.

51

For polypropylene, the expansion coefficient between 200 and 250 °C is $9.6\times10^{-4}\, cm^3 g^{-1} K^{-1}$. This value is comparable to that of polyethylene. I believe that the volume change on mixing of polyethylene and polypropylene is negligible. On the other hand, as pointed out by some researchers (Patterson and Robard, 1978), the volume change on mixing for polymer blends is relatively small compared to polymer-solvent systems. In many systems, the free volume contribution to the Gibbs free energy change on mixing is not significant.

3.2.3 Drawbacks in IGC measurements to determine miscibility of polymer blends

Deshpande *et al.* (1974) was the first group of researchers who used IGC to determine interaction parameters between polymers. Their results showed that IGC is capable of measuring interaction parameters between the components in a binary stationary phase. However, they also found that the calculated interaction parameters were dependent on the chemical nature of the probe. Olabisi's finding (Olabisi *et al.*, 1979) confirmed Deshpande's results that the probe dependence problem was a result of the inability of the Flory-Huggins theory to account for all the polymer-solute interactions.

Lezcano and coworkers (1992) attributed the weakness of Flory-Huggins theory to one of the major assumptions made in the theory, which is the enthalpic part of the Gibbs function for the solvent-polymer-polymer ternary system was simply an addition of the binary contributions. They proposed a method to determine the so-called true

52

interaction parameter by combining Flory's equation-of-state theory with the original Flory-Huggins theory. They showed that the probe dependence problem is minimized.

Al-Saigh and Munk (1984) suggested that uncontrolled experimental artifacts and errors could have caused the observed variability of χ_{23} with solvents. Later, they pointed out that the solvent dependence observation is real.

Shi and Schreiber (1991) tackled the problem by correcting the concentrations used in the original Flory-Huggins expression based upon the argument that the mixed stationary phase was not homogeneous (i.e., the surface and bulk concentrations were not the same), but they could not totally eliminate the problem.

Chee (1990) developed a novel method for determining the probe independent polymer-polymer interaction density parameter, but not the χ_{23}, by combining the original Flory-Huggins lattice and Hildebrand-Scatchard solubility theories.

Sanchez and Lacombe(1978) applied an equation-of-state approach and found that the contribution of the excess volume effect (one of the major deficiencies of the Flory-Huggins lattice theory) to the solvent dependence problem is not significant.

Su and Patterson (1977) suggested that the probe dependence problem is attributed to the nonrandom partitioning of the probe with the two components of the stationary phase. This effect appears in the difference between χ_{12} and χ_{13} and is described as the $\Delta\chi$ effect. To eliminate the probe dependence problem, they suggested that probes meeting $\chi_{12}=\chi_{13}$ must be selected. However, this is impossible practically.

In the study of the blend of polystyrene and polybutadiene, Farooque and Deshpande (1992) used four different approaches such as Flory's equation of state,

53

Sanchez's equation-of-state, Chee's method and their own method to calculate the interaction parameters. It was concluded that the results from different methods are not in good agreement with each other.

3.2.4 Modification of the Flory-Huggins lattice theory for IGC measurements

As I mentioned previously, traditionally, when the Flory-Huggins lattice theory is applied to a solvent-polymer system (Flory, 1953), the molar volume of the solvent (V_1) is usually taken as the reference volume (V_0) to define the size of the lattice. Difficulties arise when one wants to compare interaction strengths between different solvents with the same polymer since these interaction parameters are calculated based upon different lattice sizes. As a result, the apparent differences in the interaction parameters among different solvents with the same polymer do not necessarily emanate completely from the differences in the intermolecular interactions but also the lattice sizes used. This is problematic especially when the ternary version of the Flory-Huggins theory is used to correlate experimental data involving more than one solvent. This is essentially the situation encountered in all IGC measurements and in my opinion, the major cause for the observed solvent dependence problem.

The question is which V_0 should be used in the data analysis when a number of solvents are used. Based on the spirit of the original Flory-Huggins lattice theory, the smallest one among the molar volumes of the solvents and polymers comprising the mixture should be chosen. Here, for the polymers, the molar volumes of their repeating units rather than those of the whole molecules should be considered. Therefore, for this

54

particular work, the molar volume of an ethylene repeating unit should be chosen as the reference volume since all solvents used have molar volumes larger than that of the ethylene repeating unit. And the molar volume of the ethylene repeating unit was calculated based upon the experimental melt density and number average molecular weight of HDPE at the chosen experimental temperatures.

With the adoption of such a reference volume, the Gibbs free energy change on mixing for a solvent-polymer system is given as follows:

$$\Delta G_m = RT \left(n_1 \ln \phi_1 + n_2 \ln \phi_2 + n_1 \phi_2 \chi_{12} \frac{V_1}{V_0} \right). \tag{3-20}$$

Note that if V_1 is used as the reference volume, it follows that the V_1/V_0 term in the above expression will become 1 (i.e., the original Flory-Huggins expression for ΔG_m).

For a ternary system that consists of one solvent and two polymers, the expression takes the following form:

$$\Delta G_{mix} = RT \left(n_1 \ln \phi_1 + n_2 \ln \phi_2 + n_3 \ln \phi_3 \right. $$
$$\left. + n_1 \phi_2 \chi_{12} \frac{V_1}{V_0} + n_1 \phi_3 \chi_{13} \frac{V_1}{V_0} + n_2 \phi_3 \chi_{23} \frac{V_2}{V_0} \right) \tag{3-21}$$

In the above expressions, V_0 is the molar volume of the reference, and V_1 and V_2 correspond to the molar volume of the solvent and the polymer, respectively. χ_{12}, χ_{13}, and χ_{23} are the Flory-Huggins binary interaction parameters.

55

Similarly, by taking the second and third derivatives of the equation 3-20 with respect to the volume fraction and setting them to zero, the following criterion for determining miscibility of the mixture can be expressed as:

$$(\chi_{12})_{cri} = \frac{1}{2}\left(\sqrt{\frac{V_0}{V_1}} + \sqrt{\frac{V_0}{V_2}}\right)^2 \qquad (3\text{-}22)$$

For a solution composed of small molecules, the critical value can be calculated from the above expression directly. For a polymer solution, $V_2 \approx \infty$, $(\chi_{12})_{cri} = \frac{1}{2}\frac{V_0}{V_1}$. It should be noticed that this value is different from the one obtained from the original Flory-Huggins theory owing to the effect of using a common reference volume. For a polymer blend, $(\chi_{12})_{cri} \approx 0$.

By taking the first derivative on the modified Flory-Huggins theory (equations 3-20 and 3-21), for a pure liquid phase, $(\partial \Delta G_m / \partial n_1)$ reads:

$$\left(\frac{\partial \Delta G_m}{\partial n_1}\right)_{n_2,n_3=0,P,T} = RT\left(\ln \phi_1 + 1 - \frac{V_1}{V_2} + \chi_{12}\frac{V_1}{V_0}\right) \qquad (3\text{-}23)$$

And if the liquid phase contains a binary polymer blend,

56

$$\left(\frac{\partial \Delta G_m}{\partial n_1}\right)_{n_2,n_3,P,T} = RT\left(\ln\phi_1 + 1 - \frac{V_1}{V_2}\phi_2 - \frac{V_1}{V_3}\phi_3 \right.$$
$$\left. + \phi_2\chi_{12}\frac{V_1}{V_0} + \phi_3\chi_{13}\frac{V_1}{V_0} - \phi_2\phi_3\chi_{23}\frac{V_1}{V_0}\right) \qquad (3\text{-}24)$$

As mentioned previously, V_1 is the molar volume of the probes at the temperature of interest, and can be calculated based on the molecular weight and the density of the probe. Here, a modified form of the Rackett equation is chosen to obtain the density of the probes at different temperatures, as shown in the following expressions (Rackett, 1970):

$$\rho = A \times B^{-(1-T_r)^{2/7}} \qquad (3\text{-}25)$$

where ρ is the saturated liquid density (g/cm^3); A and B are the correlation constants, which are obtained from literature (Yaws, 1992).

By combining expressions (3-23) and (3-8) and equating the resultant expression to expression (3-7), after some manipulation, the final expression is:

$$\chi_{12} = \frac{V_0}{V_1}\left(\ln\frac{273.15\,R\,v_2}{V_g^0 V_1 P_1^0} - 1 + \frac{V_1}{M_2 v_2} - \frac{(B_{11} - V_1)}{RT}P_1^0\right) \qquad (3\text{-}26)$$

57

By performing the similar manipulation of the corresponding expressions for ternary systems, one obtains the following expression:

$$\phi_2 \chi_{12} + \phi_3 \chi_{13} - \phi_2 \phi_3 \chi_{23} = \frac{V_0}{V_1} \left[\ln \frac{273.15 R (w_2 v_2 + w_3 v_3)}{V_g^0 V_1 P_1^0} - 1 \right.$$
$$\left. + \frac{V_1}{M_2 v_2} + \frac{V_1}{M_3 v_3} - \frac{(B_{11} - V_1)}{RT} P_1^0 \right]$$

(3-27)

For convenience, I define a new variable here, $\chi_{1(23)}$, as shown in the following expression to replace the left hand side of the above expression. $\chi_{1(23)}$ can be thought of as the interaction between the solvent and the polymer blend.

$$\chi_{1(23)} = \phi_2 \chi_{12} + \phi_3 \chi_{13} - \phi_2 \phi_3 \chi_{23}$$

(3-28)

Equation (3-28) predicts that a plot of $\chi_{1(23)}$ versus $(\phi_2 \chi_{12} + \phi_3 \chi_{13})$ yields a straight line with a slope of 1 and an intercept of $-\phi_2 \phi_3 \chi_{23}$. Therefore, attainment of solvent independent χ_{23} for a blend with polymer concentrations ϕ_2 and ϕ_3 and (note that $\phi_1 \cong 0$) essentially boils down to the determination of χ_{12}, χ_{13}, and $\chi_{1(23)}$. By substituting the experimental data of specific retention volume and the physiochemical data of the solvents into equations (3-26) and (2-27), χ_{12}, χ_{13}, and $\chi_{1(23)}$ can be calculated. Consequently, the interaction parameter between two polymers (χ_{23}) can be obtained from the intercept of the plot of $\chi_{1(23)}$ versus $(\phi_2 \chi_{12} + \phi_3 \chi_{13})$.

58

3.2.5 Reliability of the IGC approach

From the experimental point of view, uncertainties of IGC measurements are caused by the measurement errors of the flow rate of the carrier gas, the net retention time and the mass of polymer(s) in the column. These errors lead to the uncertainties in χ_{12}, χ_{13}, and $\chi_{1(23)}$. They are rather small and usually within a range of 5%. However, due to error propagation, large errors are inevitably obtained for χ_{23} (for the detailed procedures, refer to Appendix B).

In addition, the inherent weakness of the Flory-Huggins theory also gives additional uncertainties to the final results of χ_{23}. First of all, IGC is a method in which a third solvent is used for measuring the binary interaction parameters. Even though the concentration of the third solvent in the polymer blend is close to infinitely dilute, the solvent still affects the interactions between the polymers, and consequently, one should not expect that χ values obtained from IGC are comparable to those from the technique without using a third solvent. On the other hand, χ_{23} obtained from IGC is dependent on the functional form of the entropy part of the Flory-Huggins theory. It is well known that this theory overestimates the entropy gain. This in turn may affect the estimation of χ_{12}, χ_{13}, and $\chi_{1(23)}$. This may explain why IGC tends to give χ_{23} values about one to two orders of magnitude larger than those obtained from SANS technique.

59

3.3 Experimental set-up and procedures

3.3.1 Solutes

Twelve different organic substances composed of aliphatic and aromatic hydrocarbons were used as probes, which are listed in Table 3.1. These solvents were chosen because their thermo-physical data were readily available and the corresponding results of the IGC measurements could be used to calculate the Henry's law constants of the solvents, which are useful for the design of the solution polymerization process adopted by NOVA Chemicals Corporation (NOVA), one of the sponsors for the present work. For example, 1-hexene and 1-octene are very common co-monomers to produce LLDPE. Therefore, knowledge of the solubility of the co-monomers in the LLDPE is critical for designing the corresponding reactor properly. In fact, my data have been utilized by NOVA for this purpose. All solutes were purchased from Fisher Scientific Company (Canada). They were reagent grade and used without further purification. The critical properties, correlation constants and Antoine vapour-pressure-equation coefficients of the solutes are not given here. One can obtain them from references (Laws, 1992 and Poling *et al.*, 2001).

3.3.2 Polyethylene samples used

In this work, all polyethylene samples used were supplied by NOVA. For HDPE/LDPE blends, we chose one HDPE and one LDPE. For HDPE/LLDPE blends, one HDPE and five LLDPEs with different branch contents were used. The blends between one LDPE and twelve LLDPEs with different characteristics were studied. The

60

details of the molecular characteristics of those samples will be presented in the following chapters.

3.3.3 Sample Preparation

Columns consisted of pure polymers or their blends were prepared using the same procedures. The following summarizes such details. Polymer pellets (usually around 1.4 g) were added to a flask (1 L) containing about 200 mL xylenes. Here, if a blend was of interest, the amount of the pure components that corresponded to the weight fractions of the blends was added. The flask was then assembled to a rotary vaporator equipped with an oil bath and a hot stage heater. The flask was immersed half way into the oil bath and heated to between 100 to 120 °C under constant rotation (condenser and vacuum off). When the polymer was totally dissolved, about 11 g inert solid support Chromosorb with acid washed (WAW) (60/80 mesh; Sigma-Aldrich Canada Ltd.) was added into the solution. The flask containing the resultant slurry was then put back into the oil bath and kept at the same temperature and rate of rotation for three hours. To deposit the polymer(s) onto the surfaces of the solid support, the solvent was evaporated by vacuum. The evaporated solvent vapor was condensed and collected in second flask (1 L). The vacuum, oil bath heater, and rotating motor were turned off when the sample was dried. The coated Chromosorb was removed from the flask and put into a sample dish and dried in a vacuum oven at 50 °C for 4 hours.

3.3.4 Determination of loading of polymers on the support

As described in the previous section, the amount of polymer used was required for the determination of the specific retention volume (equation 3-1). In this regard, the amount of polymer deposited on the Chromosorb was determined by an ashing method with the blank correction. The procedure is described as follows.

1. Weighed three empty crucibles using an electronic balance and recorded the weight.

2. Added a certain amount of sample into the crucibles and weighed again.

3. Put the crucibles into a furnace at 850 to 870 °C for 12 hours to burn up polymers.

4. Weighed the residue sample and crucibles, and calculated the loading of polymers on the support.

To calculate the mass loss of the solid support, the same procedure was also applied to the pure Chromosorb to determine the mass loss of the solid support. This was used as a correction in the calculation of polymer loading The final loadings were calculated based on the blank corrections.

It has been found that the optimal loading of polymer in a column is from 6 to 10%. Here, loading is defined as the ratio of the mass of polymer to that of the Chromosorb used in an IGC column. If the loading is too low (<5%), the solid support will not be totally covered by the polymer and this will significantly affect the retention time of the probe. However, if the loading is too high, the layer of polymer covering the support will be too thick and consequently, the probe cannot penetrate into the layer of the polymer and reach thermodynamic equilibrium state promptly. In this case, the equations I described in the previous sections will not be applicable. There are a few ways to determine whether the probe reaches the thermodynamic equilibrium state with

62

the polymer. One is based on the shape of the gas chromatogram of the solvent. A symmetric and sharp peak indicates that the equilibrium state is established (Young, 1968). Another way is plotting the natural logarithm of specific retention volumes (ln V_g^o) against the inverse of the temperature (1/T). A linear relationship between ln V_g^o and 1/T also suggests the attainment of the equilibrium state. The slopes of these lines can be used to obtain the heat of sorption, which is given by:

$$\Delta H_s = \frac{-Rd\ln V_g^o}{d\left(\dfrac{1}{T}\right)} \tag{3-29}$$

where ΔH_s is the heat of sorption and R is the universal gas constant (Lipson et al., 1981).

3.3.5 Morphology of the coated samples

Figures 3.6 to 3.9 illustrate the surface morphology of the coated and non-coated Chromosorb particles. Figures 3.6 and 3.7 are scanning electron micrographs of the Chromosorb particles with different magnifications. The Chromosorb used was a silicon based, micron level white powder. It can be seen from the pictures that the Chromosorb was a porous material. As a result, the polymer was actually deposited onto the inner surfaces of the particles. Because of the porosity of the Chromosorb, the surface area is very large. The nominal value of the surface area of the Chromosorb supplied by the manufacturer, was about 150 m^2/g. Based on this value, the average thickness of the

63

polymer coated on the Chromosorb was only 50 nm if a 7 wt% loading was used. It is worth noting that the thickness of the polymer layer coated on the Chromosorb is not uniform. And the variation in thickness may affect the retention times of the solvents. However, I did not incorporate such a factor in the calculations of χ because all the equations described in this chapter are only valid under the condition that the thickness of the polymer layer is consistent.

Figures 3.8 and 3.9 are the micrographs of the Chromosorb coated with LDPE. The detailed characteristics of this polymer can be found in Chapter 4. The loading was 10 wt%. The morphological characteristics of the coated sample were similar to that of the non-coated sample because the polymer layer on the support was indeed very thin.

When a sample composed of polyethylene blends was prepared, the constituent polymers might precipitate from the solvent successively because of the difference of their solubility in the solvent. The one with higher molecular weight (i.e., melting temperature) will separate out and deposit onto the surface of the Chromosorb first. The polymer with lower melting temperature will deposit on the surface of the polymer already deposited. Consequently, these two polymers will form two separated layers of materials on the Chromosorb, and the molecules of these two polymers only interact with each other at the interface. If this is the case, the equations described in the previous section will not be applicable. Therefore, this kind of sample cannot be used to determine the interaction parameters. To rule out this possibility, a temperature rising elution fractionation (TREF) experiment was carried out to determine if mixtures with uniform composition were obtained. The polymer used was LLDPE because LLDPE was composed of both linear and branch molecules. Two kinds of samples were used for

comparison. One was the sample prepared for the IGC experiment (IGC sample). And the other was prepared using the conventional method for TREF (TREF sample) (Zhang *et al.*, 2000).

In a TREF sample, the linear molecules usually deposit first and form the inner layer and the branched molecules deposited on the top of the linear molecules. Therefore, two elution peaks are obtained from the TREF sample as shown in Figure 3.10. The peak at higher temperature corresponds to the linear component in the LLDPE sample while the broad peak at the lower temperature corresponds to the branched molecules.

Figure 3.11 shows the TREF profile for the IGC sample. It can be seen from this figure that only one peak was obtained and the elution temperature was between the temperatures of the two peaks obtained for the TREF sample. This indicates that the polymer molecules of the IGC sample only formed one layer of material consisting of both linear and branched molecules on the solid support. This result is not surprising. To separate the linear and branched molecules, preparation for a TREF sample usually needs more than 24 hours. For an IGC sample, the coating process usually takes one hour to complete. As a result, polymer molecules with different molecular structures precipitated from the solvent almost at the same time. On the other hand, the IGC sample was prepared under rotation so that the molecules were mixed and deposited on the solid support randomly.

In addition to the difference of melting temperatures between the components in the blend, their surface energy difference may also lead to the non-random distribution of the constituents in the blend deposited on the Chromosorb. In particular, for HDPE and PS blend, the polarity of PS is stronger than that of HDPE owing to its aromatic rings.

65

Since the Chromosorb used contained OH groups, the interaction between PS and the Chromosorb would be stronger than that between HDPE and the Chromosorb. As a result, PS might deposit on the Chromosorb first and form an inner layer. However, I believe this is not the case. This is because in the absence of oxygen, the polarity of PS is only slightly stronger than that of HDPE and still very weak compared to the polarity of the Chromosorb. Moreover, the rotation during the sample preparation also prevented the non-random distribution. Therefore, I feel justified to assume that PS and HDPE molecules deposited on the Chromosorb randomly.

3.3.6 Adsorption and absorption of the probe molecule on the polymer melt

When the probe molecules pass through the column, there exist two sorption mechanisms. One is the adsorption of the probe on the surface of polymer melt and the other is the absorption in the bulk of the melt. It has been shown that for a semi-crystalline polymer (e.g., polyethylene), the adsorption process dominates if the experimental temperature is below the polymer's glass transition temperature. In contrast, the adsorption can be neglected at temperatures higher than the melting temperature of the polymer (Guillet et al., 1989). Since the temperature range in which I was interested was much higher than the melting temperatures of the polymers I studied in this work, I only considered the absorption process. Furthermore, it has long been recognized that the contribution of the adsorption of a non-polar solute to the corresponding measured retention volume is negligible compared with that of the absorption process (Young

66

1968). The probes used in this work (Table 3.1) had no strong polarity. Therefore, the adsorption of the probe on the polymer should be insignificant, if there is any.

3.3.7 Column preparation

Stainless steel tubes were used as the IGC columns. Their interior was first washed with acetone and dried. The inner diameter of the tubes used was 0.18 cm and the nominal length 100 cm. To put coated Chromosorb powder into the tube, one end of it was plugged with a small amount of glass wool. The coated Chromosorb was then introduced into the tube through its other end, with gentle tapping. After packing, this end was also plugged with glass wool. The weight of the packing was measured before and after packing and the weight of the sample inside the column was then calculated. The column was coiled and placed into the oven of a GC. Soap water was used to detect the leakage of the connections between GC and column. Each column was conditioned in the GC at 60 °C for 2 days under a helium flow (20 mL/min) to eliminate residual solvent before data collection. The variation from column to column was checked by packing two parallel columns with the same sample and it was found that the data were highly reproducible.

3.3.8 Instrumentation

Measurements were carried out using a Hewlett-Packard 4890 gas chromatograph, equipped with a flame ionization detector (FID). Pre-purified helium

67

was used as the carrier gas at flow rates over the range from 18 to 25 mL/min, which were measured at the corresponding experimental temperatures with the use of a soap bubble flowmeter. The inlet and outlet pressures of the column were monitored with the manometers. To measure the retention time of each solvent, three injections of $1\mu L$ of its vapor were made manually using a Hamilton syringe (5 μL capacity; Sigma-Aldrich Canada Ltd.). The reproducibility was within 3%. To measure the dead time, methane was used as the marker. The net retention time was determined by subtracting the retention time of methane from that of the solvent.

3.4 Summary

Thermodynamic theories of polymer solutions have been reviewed, especially the Flory-Huggins lattice theory. Even though deficiencies exist in the theory, which result from the limitations of both the model and the assumptions employed in its derivation, the Flory-Huggins lattice theory is still widely used in practice due to its simplicity. For the IGC technique, it has been shown to be a very successful method to obtain Flory-Huggins interaction parameters. However, a severe drawback prevents the technique from gaining more popularity; that is, the obtained interaction parameters vary with the nature of the solvent used in the experiment. By reexamining the equations used in this technique, it was found that the probe dependence problem stems from the improper choice of the reference volume used to define the size of the lattice in the Flory-Huggins theory. A new analytical method to obtain the probe independent interaction parameter

68

was proposed by modifying the original Flory-Huggins theory with a common reference volume. The validity of the proposed method was tested by applying it to various polyolefin blends and the results will be presented in the next few chapters.

3.5 References

Al-Saigh, Z.Y. and Munk P. (1984) Study of Polymer-Polymer Interaction Coefficients in Polymer Blends Using Inverse Gas Chromatography, *Macromolecules*, 17, 803-809.

Al-Saigh, Z.Y. (1997) Review: Inverse Gas Chromatography for the Characterization of Polymer Blends, *Int. J. Polym. Anal. Charact.*, 3, 249-291.

Chee, K.K. (1990) Estimation of Polymer-Polymer Interaction Density Parameter by Inverse Gas Chromatography, *Polymer*, 31, 1711-1714.

Denbigh, K.G. (1996) Principles of Chemical Equilibrium, Cambridge University Press, 4th edition.

Deshpande, D.D., Patterson, D., Schreiber H.P. and Su C. S. (1974) Thermodynamic Interactions in Polymer Systems by Gas-Liquid Chromatography. IV. Interactions between Components in a Mixed Stationary Phase, *Macromolecules*, 7, 530-535.

Farooque, A.M. and Deshpande D.D. (1992) Studies of Polystyrene-Polybutadiene Blend System by Inverse Gas Chromatography, *Polymer*, 33(23), 5005-5018.

Flory, P.J. (1941) Thermodynamics of High Polymer Solutions, *J. Chem. Phys.*, 9, 660.

Flory, P.J. (1953) Principles of Polymer Chemistry, Cornell University Press, New York.

Fried, J.R. (1995) Polymer Science and Technology, Prentice-Hall , Inc., New Jersey.

Gulliet, J.E., Romansky, M., Price, G.J. and van der Mark, R. (1989) Inverse Gas Chromatography, American Chemical Society.

Huggins, M.L. (1941) Solutions of Long Chain Compounds, *J. Chem. Phys.*, 9, 440.

Lavoie, A. and Guillet, E.J. (1969) Estimation of Glass Transition Temperatures from Gas Chromatographic Studies on Polymers, *Macromolecules*, 2, 443-446.

Lezcano, E.G., Salom Coll, C. and Prolongo, M.G. (1992) Thermodynamic Study of Poly(4-hydroxystyrene)/Poly(vinylacetate) Blends by Inverse Gas Chromatography, *Macromolecules*, 25, 6849-6854.

Lipson J.E.G. and Guillet, J.E. (1981) Studies of Polar and Nonpolar Probes in the Determination of Infinite-Dilution Solubility Parameters, *J. Polym. Sci., Polym. Phys. Edn.*, 19, 1199-1209.

Littlewood, A.B. (1962) Gas Chromatography, Academic Press, New York.

Lloyd, D.R., Ward, T.C. and Schreiber, H.P., editors. (1989) ACS Symposium Series 391, American Chemical Society, Washington, D. C.

Olabisi, O., Robeson, L.M. and Shaw, M.T. (1979) Polymer-Polymer Miscibility, Academic Press, New York.

Patterson, D. and Robard, A. (1978) Thermodynamics of Polymer Compatibility, *Macromolecules*, 11(4), 690-695.

Poling, B.E., Prausnitz, J.M. and O'Connell, J.P. (2001) The Properties of Gases and Liquids, 5th ed.; McGraw-Hill Book Co., New York.

Rackett, H.G. (1970) Equation of State for Saturated Liquids *J. Chem. Eng. Data*, 15, 514-517.

Rudin, A., Chee, K.K. and Shaw, J.H. (1970) Specific Volume and Viscosity of Polyolefin Melts, *J. Polym. Sci., Part C*, 30, 415-427.

Sanchez, I.C. and Lacombe, R.H. (1978) Statistical Thermodynamics of Polymer Solutions, *Macromolecules*, 11(6), 1145-1156.

Shi, Z.H. and Schreiber, H.P. (1991) On the Application of Inverse Gas Chromatography to Interactions in Mixed Stationary Phases, *Macromolecules*, 24, 3522-3527.

Skoog, D.A. (1998) Principles of Instrumental Analysis, 5rd ed.; Saunders College Publishing, New York.

Su, C.S. and Patterson D. (1977) Determination by Gas-Liquid Chromatography of the Polystyrene-Poly(vinyl methyl ether) Interaction, *Macromolecules*, 10, 708-711.

Tihminlioglu, F., Danner, R. P., Lutzow, N. and Duda, L. (2000) Solvent Diffusion in Amorphous Polymers: Polyvinyl Acetate-Toluene System, *J. Polym. Sci. Part B Polym. Phys*, 38, 2429-2435.

Tsonopoulos, C. (1974) An Empirical Correlation of Second Virial Coefficients, *AIChE J.*, 20, 263-272.

Yaws, C.L. (1992) Thermodynamic and Physical Properties Data, Gulf Publishing Co., Houston, Texas.

Young, C.L. (1968) The Use of Gas-Liquid Chromatography for the Determinations of Thermodynamic Properties, *Chromatog. Rev.*, 10, 99-128.

Zhang, M., Lynch, D.T. and Wanke, S.E. (2000) Characterization of Commercial Linear Low-Density Polyethylene by TREF-DSC and TREF-SEC Cross-Fractionation, *J. Appl. Polym. Sci.*, 75(7), 960-967.

Table 3.1 Solutes selected as probes in this work.

n-Pentane	n-Hexane	n-Heptane
n-Octane	n-Nonane	n-Dodecane
1-Hexene	1-Octene	Cyclohexane
Benzene	Toluene	Xylenes

73

Figure 3.1 Schematic diagram of a gas chromatographic apparatus. (1) Carrier gas cylinder; (2) Sample injector; (3) Manometer; (4) Column; (5) Detector; (6) Bubble flowmeter; (7) Recorder; (8) Hydrogen gas cylinder; (9) Air cylinder.

74
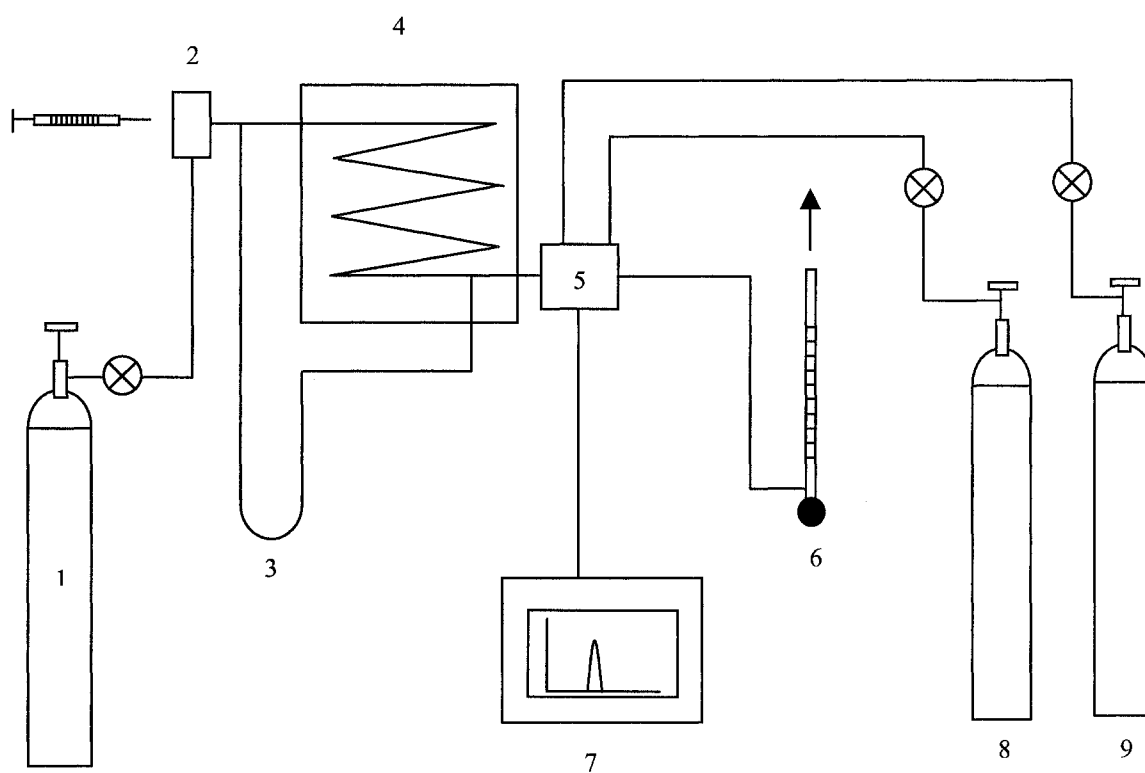
Figure 3.2 Schematic illustration of a GC column

●
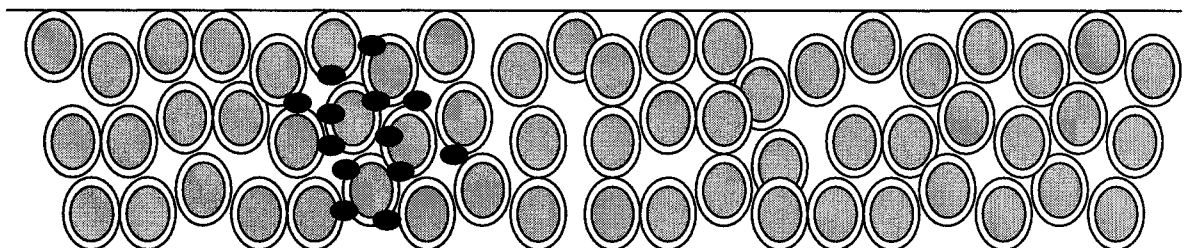
Probe molecule

Coated samples

75

Figure 3.3 Schematic representation of a lattice model of a polymer solution
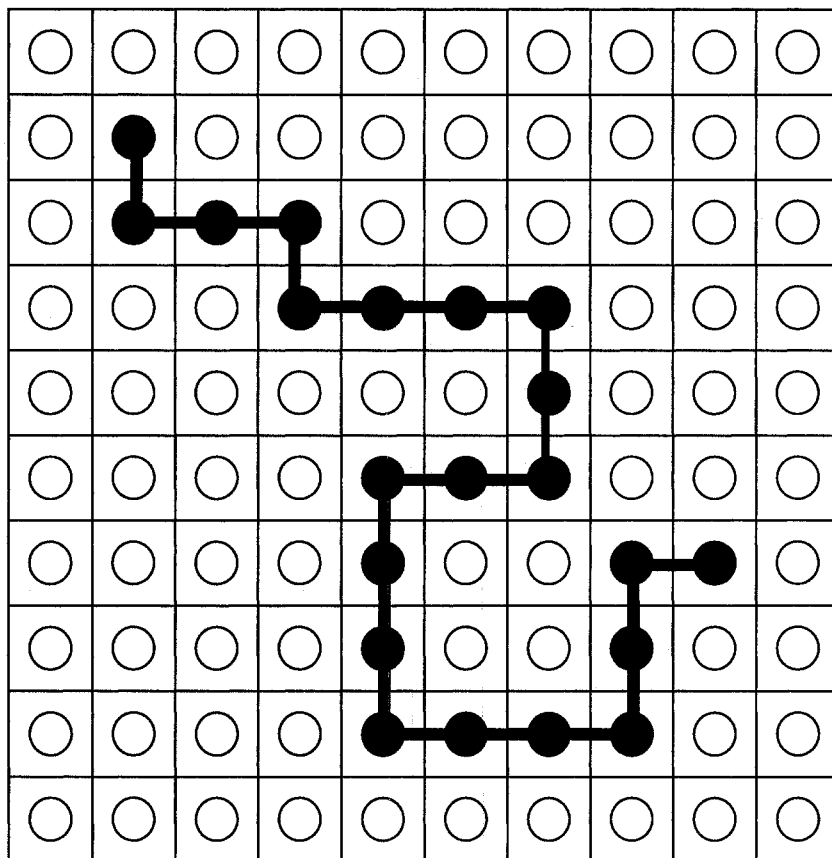
Figure 3.4 Gibbs free energy on mixing vs. concentration diagram for miscible systems.
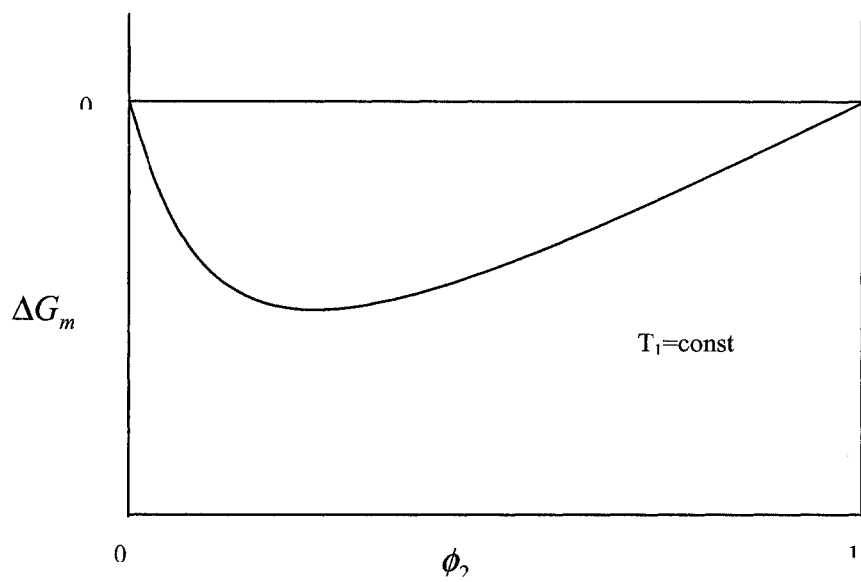
Figure 3.5 Gibbs free energy on mixing vs. concentration diagram for partially miscible systems.

77
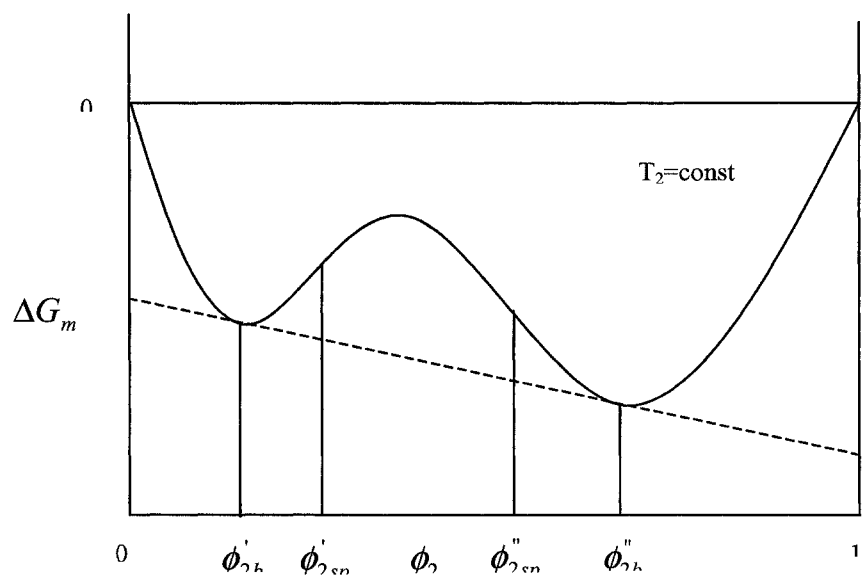
Figure 3.6 Scanning electron micrograph (SEM) of a Chromosorb particle
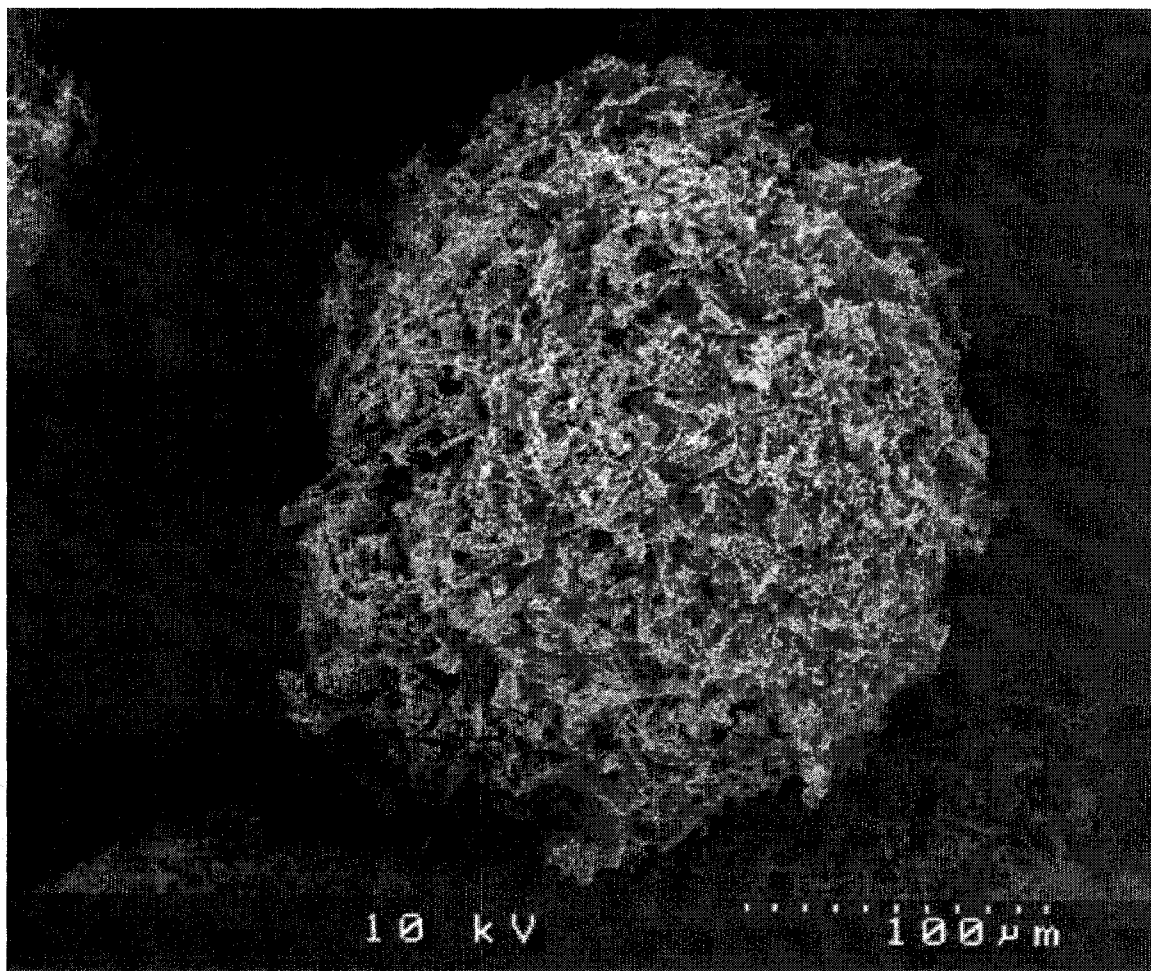
Figure 3.7 SEM image of the surface of the same non-coated Chromosorb particle as

shown in Figure 3.6 at higher magnification

79
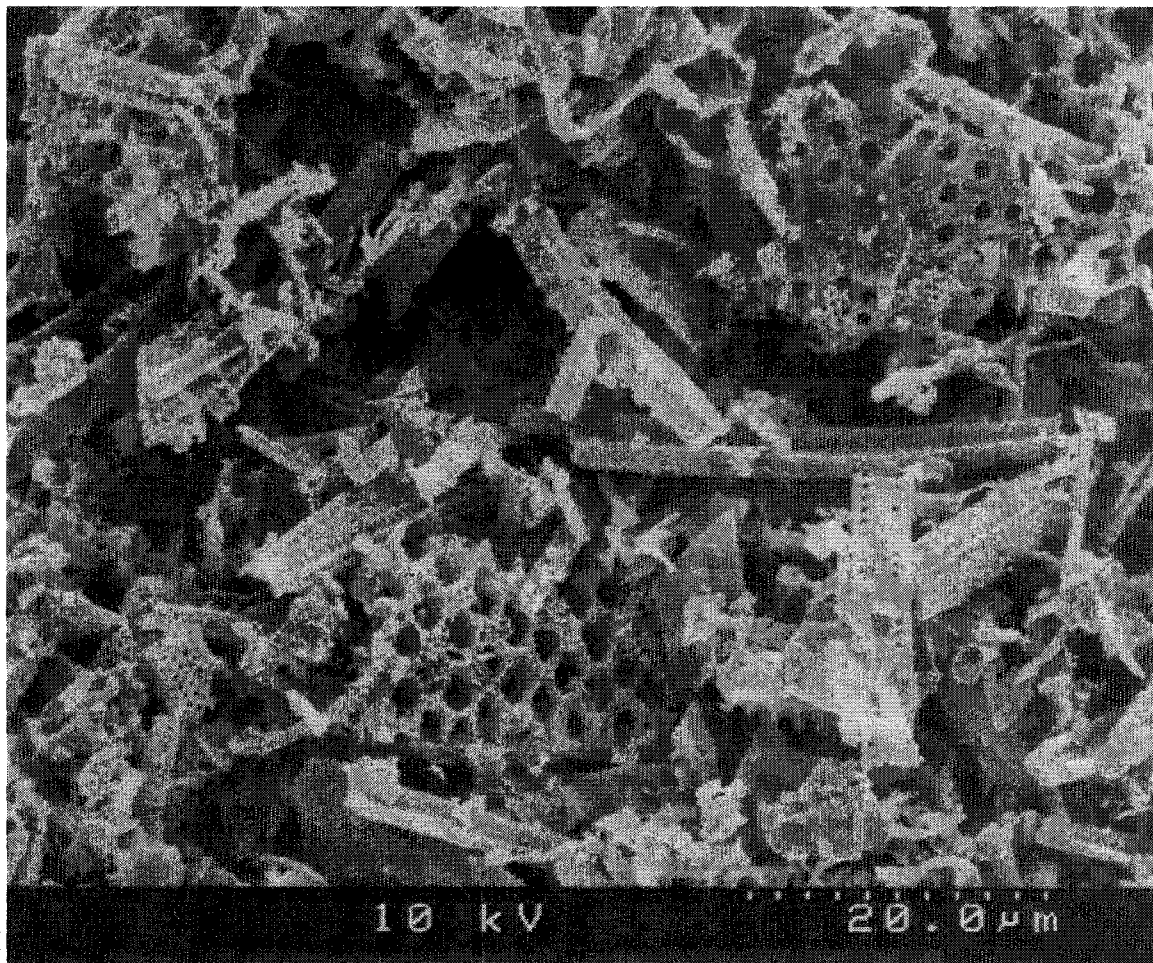
Figure 3.8 SEM image of a Chromosorb particle coated with 10% LDPE

80
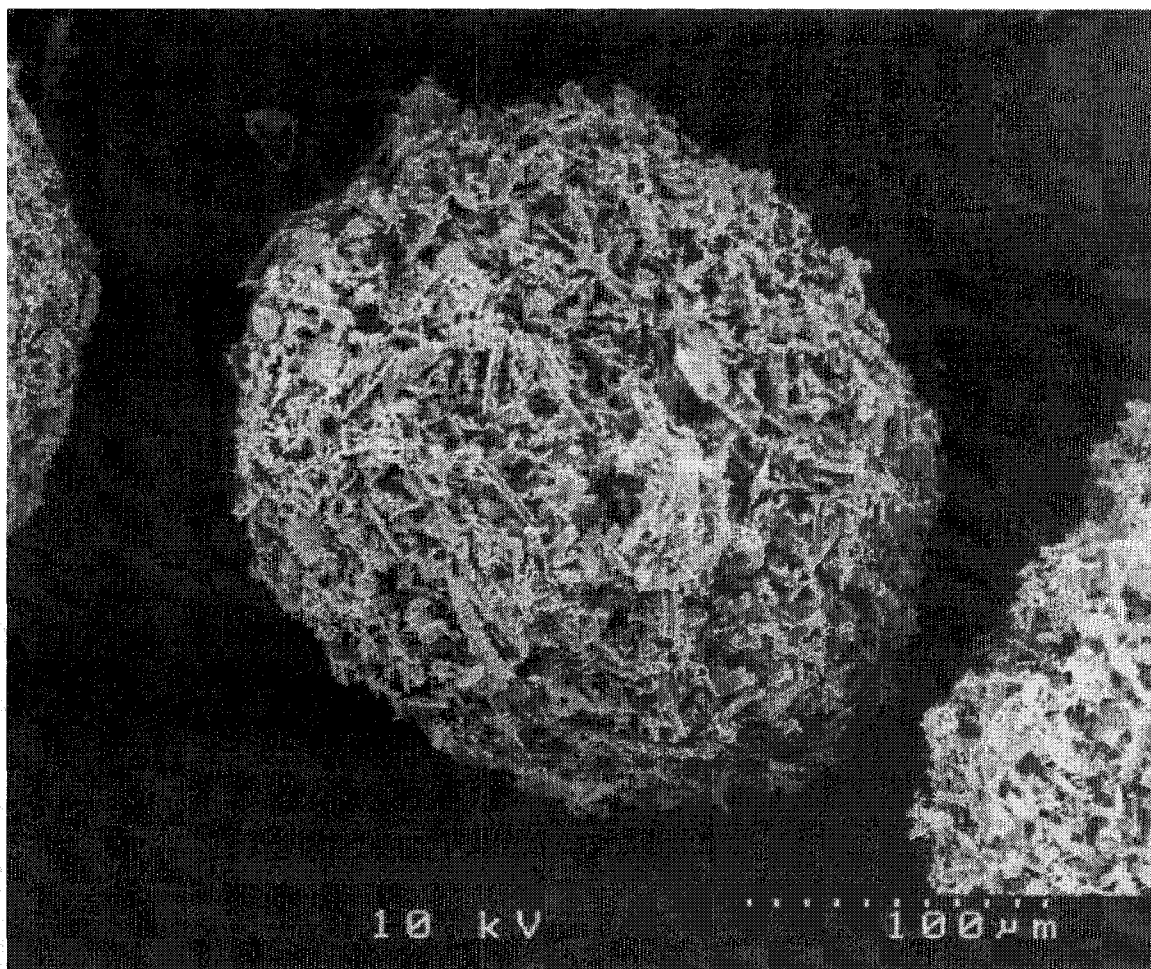
Figure 3.9 SEM image of the surface of the same Chromosorb particle coated with 10%

LDPE as shown in Figure 3.8 at higher magnification

81
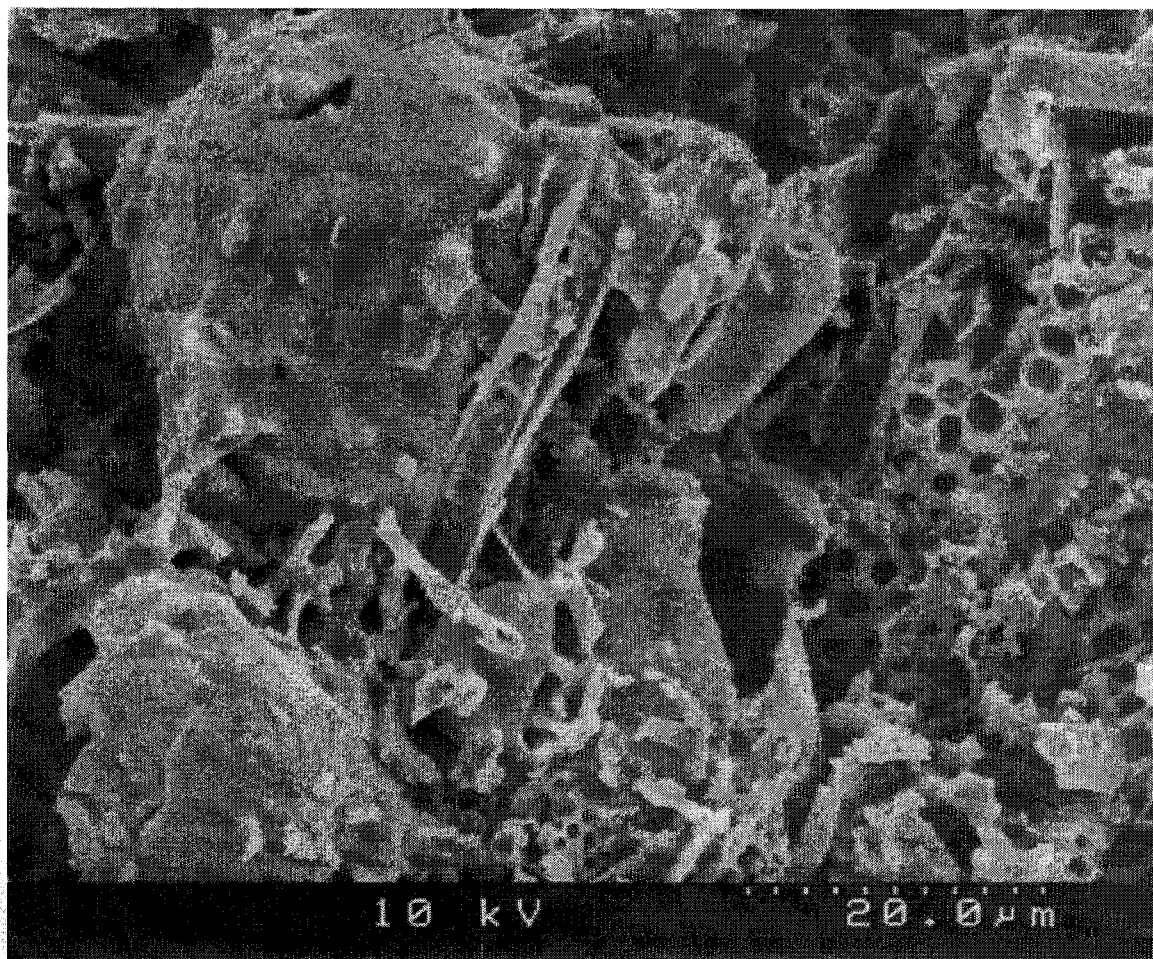
Figure 3.10 TREF profile for LLDPE sample prepared by the conventional TREF method
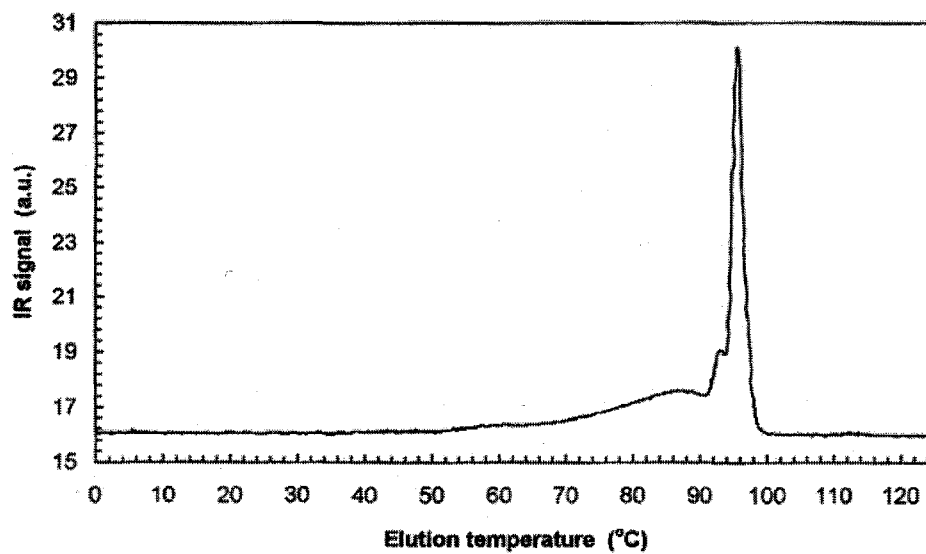
Figure 3.11 TREF profile for LLDPE sample prepared for IGC

82
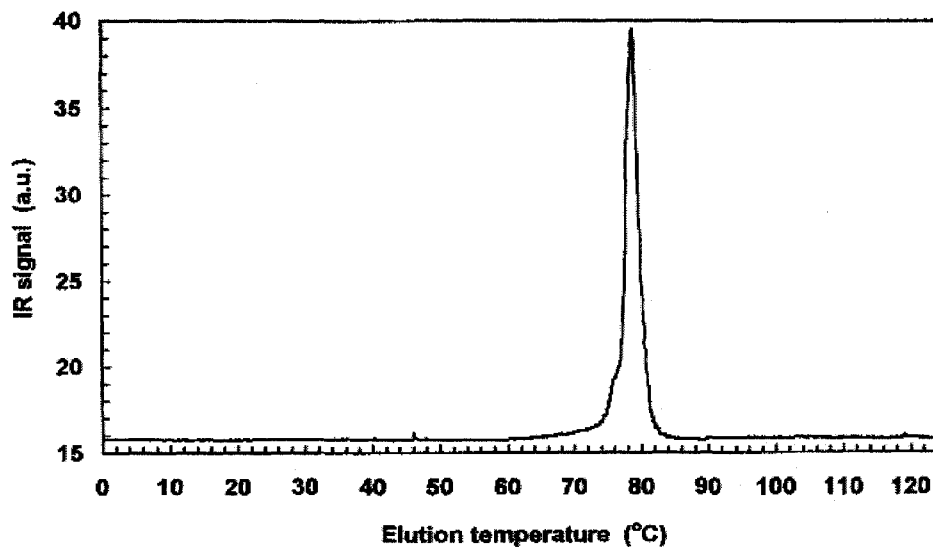
Chapter 4

Miscibility studies of HDPE and LDPE blends

4.1 Introduction

Chapter 3 reexamined the theories and equations used in the IGC measurements. It was discovered that the solvent dependence problem might essentially originate from the improper choices of the reference volumes used in the calculations of the binary interaction parameters between various solvents and the pure polymers as well as their blends. By modifying the original Flory-Huggins theory with the common reference volume concept, a new data analysis method to obtain probe independent interaction parameters was proposed.

In this chapter, the new approach is illustrated using the HDPE/LDPE blend since the materials are readily available and have been studied extensively by other researchers using techniques such as DSC, SANS, and TEM (Hill *et al.*, 1991, Hill and Barham, 1995, Alamo *et al.*, 1994, 1997, Agamalian *et al.*, 1999).

4.2 Experimental

4.2.1 Materials

Both HDPE and LDPE samples used in this work were supplied by NOVA Chemical Corporation (Calgary, AB). The LDPE used was a homo-polymer made by a high-pressure process. The molecular weight averages and branch contents of the polymers, which were determined by gel permeation chromatography (GPC) and Fourier transform infrared spectroscopy (FTIR), are listed in Table 4.1. This information was supplied by NOVA. Five columns including two pure polymers and three blends with various compositions were prepared using the procedure described in Chapter 3. The loadings and weights of polymer coated in the columns, which were obtained by the ashing process, are listed in Table 4.2.

4.2.2 Operating conditions

The operating conditions of the GC columns are specified as follows:

1. Oven temperatures: 170, 190, 210 and 230 $^{\circ}$C;

2. Injection temperature: 150 $^{\circ}$C;

3. Inlet pressure: 200 to 250 kPa;

4. Outlet pressure: Atmospheric pressure;

5. Carrier gas: Purified helium;

6. Flowrate of carrier gas: 18 to 25 ml/min;

7. Detector: Flame ionization detector;

8. Temperature of the detector: 150 $^{\circ}$C;

9. Volume of the vapor of the solvent injected into the column: 1 μL ;

10. Software for data collection: HPChem station.

4.3 Results and discussion

Figure 4.1 shows the gas chromatograms for n-hexane interacting with a stationary phase coated with LDPE at 170, 190, 210, and 230 °C. It can be seen from these graphs that the peaks are sharp and symmetrical at different temperatures. This proves that the probe molecules reached a thermodynamic equilibrium state in the stationary and gaseous phases within the temperature range of interest, as discussed in Chapter 3 (Young, 1968). The retention time was obtained from the maximum of the peak. Similar gas chromatograms for other probes in LDPE and for all probes in HDPE and three LDPE/HDPE blends (each blend had different composition) at different temperatures are omitted for clarity.

The measured retention times and the calculated specific retention volumes of the probe molecules for pure LDPE, HDPE and their 50/50 blend at different temperatures are summarized in Tables 4.3, 4.4, 4.5, 4.6, 4.7 and 4.8. The retention times for 30/70 and 70/30 blends are listed in Appendix C and the corresponding specific retention volumes can be calculated from equation 3-1. Each reported retention time corresponded to the average of the results of three injections. All data were usually within 1% of the mean value. In addition, the measured retention times have been verified to be repeatable from

84

day to day and from column to column through a preliminary experiment carried out by a former summer student.

In all cases, the retention time decreased with increasing temperature as shown in Tables 4.3 to 4.5. The magnitude of decrease increased with increasing chain length of the aliphatic molecules. For example, for n-hexane, retention time decreases 10% from 170 to 230 °C while 16% for n-heptane and 30% for n-nonane in the same temperature range. This was due to the increase in the speed of absorption and desorption of the probe in the vapor and liquid phases as well as the decrease in the viscosity of the carrier gas. However, in the case of methane, the decrease in the retention time was only 5% so that it was only attributed to the second factor, i.e., the decrease in the viscosity of the carrier gas. Therefore, it seems reasonable to assume that methane does not interact with the liquid phase.

The specific retention volume also decreased with increasing temperature as shown in Tables 4.6 to 4.8. For example, the specific retention volume of n-heptane for pure LDPE decreased from 6.44 g/cm^3 at 170 °C to 2.69 g/cm^3 at 230 °C. This was due to the fact that the retention time decreased with increasing temperature. Within a series of similar type of probe molecules, the specific retention volume increased with increasing the length of the molecules.

The natural logarithm of specific retention volumes (ln V_g^o) of some selected probes for 50/50 HDPE and LDPE blend were plotted against the inverse of the temperature (1/T) (Figure 4.2). It can be seen that the data points of ln V_g^o at different temperatures were well described by equation 3-29 and linear relationships were obtained. Therefore, I feel justified assuming that the probe was at thermodynamic

85

equilibrium state where the probe partitioned in both the liquid and gaseous phases according to the thermodynamic equations described in the previous chapter.

The specific retention volumes of same probe for pure HDPE and LDPE were very comparable to each other as shown in Tables 4.6 and 4.7. In most of the cases, the difference was within 5%. This indicates that the interaction between the probe and HDPE was similar to that between the same probe and LDPE. This is reasonable owing to the chemical similarity of the two polymers comprising the blend.

Table 4.8 lists the specific retention volumes of the probes for the column packed with 50/50 HDPE/LDPE blend. From this table, it can be seen that the specific retention volume of the same probe for HDPE/LDPE blend showed a slightly positive deviation from the linear combination of the specific retention volumes of two pure components. This indicates that the probes did not interact strongly with the polymers in the blend. However, it is worth noting that the use of composition dependence of specific retention volume is not a reliable way to determine the miscibility of the blends, as suggested by other authors (Al-Saigh and Chen, 1991). This is because even for the same pair of polymers, the composition dependence of specific retention volume varies considerably depending on the type of probes. The probes with a strong interaction with the blends can lead to a negative deviation while those do not interact strongly with the blends usually follow a linear relationship or a small positive deviation.

By substituting the calculated specific retention volume, V_g^0, in expressions (3-26) and (3-27), Flory-Huggins interaction parameters between the selected solvents and the pure polymers (i.e., χ_{12} and χ_{13}), and their 50/50 blends (i.e., $\chi_{1(23)}$) were calculated at 170, 190, 210, and 230 °C and are summarized in Tables 4.9 and 4.10. The corresponding

86

$\chi_{1(23)}$ for 30/70 and 70/30 blends are listed in Appendix D. Note that the obtained interaction parameters were calculated based on the common reference volume (i.e., the molar volume of the ethylene repeating unit at the corresponding experimental temperature). It can be seen from the tables that for an aliphatic type of probe molecules, the interaction parameter decreased slightly with increasing chain length of the molecule. This indicates that the interactions between longer probe molecules and polymers were stronger than the interactions between shorter probe molecules and polymers. However, this does not necessarily mean that miscibility between probe molecules and polymer increases with increasing chain length of the probe molecules because the critical interaction parameter value for a polymer solution is also affected by the molar volume (or molecular size) of the probe molecules as mentioned in Chapter 3.

In terms of the temperature dependence of χ_{12}, χ_{13}, and $\chi_{1(23)}$, the interaction parameters decreased with increasing temperature, as expected. It is because from the definition of the original Flory-Huggins interaction parameter as shown in Chapter 3:

$$\chi_{12} = (z - 2)\Delta g_{12} / kT \qquad (3\text{-}16)$$

In this equation, if z, k and Δg_{12} are independent of temperature, χ_{12} has an inverse dependence on temperature.

As discussed in Chapter 3, it was suggested that to eliminate the probe dependence problem, one should choose the probes that give $\chi_{12}=\chi_{13}$ (zero $\Delta\chi$) to minimize the effect of the nonrandom partitioning of the probe within the two

87

components of the stationary phase (Su and Patterson, 1977). This is impossible in most of the systems. However, in the system containing HDPE and LDPE, it is evident in Tables 4.9 and 4.10 that both χ_{12} and χ_{13} are rather close to each other indicating that most of the solvents used satisfied the zero $\Delta\chi$ criterion. It is worth noting that the criterion is also met even though the individual molar volumes of the solvents are used as reference volumes in the calculations of χ_{12} and χ_{13}. But when such interaction parameters were used for the plots of $\chi_{1(23)}$ versus ($\phi_2\chi_{12} + \phi_3\chi_{13}$), the data scattered considerably and the linearity, characterized by R^2, was poor (see Figure 4.3). This suggests that even if the zero $\Delta\chi$ criterion was met, the solvent independent interaction parameter still could not be obtained.

In contrast, when the molar volume of the ethylene-repeating unit was used, the resultant data conformed remarkably well to equation (3-28). This observation is significant because this means that unique interaction parameters can be obtained from the intercepts of the regression lines. Figure 4.4 illustrates plots of $\chi_{1(23)}$ versus ($\phi_2\chi_{12}+\phi_3\chi_{13}$) for the same 50/50 blend. As can be seen from Figure 4.4, the linearity is excellent (high R^2 values) in all cases and the slopes are quite close to the expected value of 1. This result indicates that choosing a common reference volume is necessary for obtaining a solvent independent interaction parameter from IGC measurements. However, it is not clear whether using zero $\Delta\chi$ solvents is a necessary condition for the above described findings.

The solvent independent χ_{23} values were determined from the intercepts of these regression lines. The corresponding uncertainties were calculated based upon the

88

measurement errors of the flow rate of the carrier gas, net retention time and mass of polymer(s) in the column. The procedures used to calculate errors are shown in Appendix B. Both average χ_{23} values and their associated error bars are summarized in Table 4.11.

Figure 4.5 depicts the temperature dependence of χ_{23}. It can be seen from this figure that the experimental errors are very large and in some cases, it is very difficult to determine the miscibility from these data because accounting for the error, χ included zero, which is the critical value for miscibility. This implies that to measure extremely small χ accurately, reducing experimental errors is necessary.

For 30/70 and 50/50 HDPE/LDPE blends, χ_{23} did not show strong dependence on temperature as shown in Figure 4.5. For blend containing 70% HDPE, considering the errors, χ_{23} did not change much from 170 to 210 $^{\circ}$C. However, χ_{23} at 230 $^{\circ}$C is much smaller than that at 210 $^{\circ}$C exhibiting a decrease of χ_{23} with increasing temperature. This is consistent with the theoretical prediction by equation 3-16 that increasing temperature decreases the value of χ_{23}. A similar trend was also obtained from recent molecular dynamics (MD) calculations for a modeled HDPE/LDPE system over the same temperature range (Fan *et al.*, 2001). It should be noted that the MD results were obtained without the use of a third solvent and based upon the molar volume of the ethylene-repeating unit. In addition, it is worth pointing out that the MD simulation approach suffers from the same problem as the IGC method; that is, the errors for χ_{23} are very large. Other researchers used SANS to study this blend. Based upon their results obtained at a lower temperature range (from 140 to 160 $^{\circ}$C), χ_{23} exhibits a decreasing trend with

89

increasing temperature (Alamo, *et al.*, 1994). This is consistent with the present findings at higher temperatures.

Figure 4.6 shows the plot of χ_{23} versus weight fraction of HDPE at four temperatures. It can be seen from this figure that, considering the large uncertainties, χ_{23} did not change much with changing the weight fraction of HDPE from 30% to 70% at 170, 190 and 230 °C. This result is in agreement with SANS result at 160 °C (Alamo, *et al.*, 1994). However, at 210 °C, χ_{23} showed an increasing trend with increasing the concentration of HDPE. The magnitude of the increase in χ_{23} was not attributed to the error bars. This indicates that at 210 °C increasing concentration of HDPE decreased the miscibility of HDPE/LDPE blend. The results of composition dependence of χ_{23} from MD simulation are not available because the MD simulation is based on the solubility parameter approach and the composition dependence of χ_{23} cannot be studied.

From the above discussion, it is evident that HDPE/LDPE blend showed an unexpected miscibility behavior at 210 °C; that is, χ_{23} increased with increasing the composition of HDPE. This may be explained by the local orders of polyethylene melts. It is believed that even in polyethylene melts, there exist some local orders. Hussein *et al.* (2000) found a "thermal" transition at 210 °C in many commercial polyethylenes using DSC. They contended that these local orders create mismatch of the molecular conformations of different polyethylene structures and lead to immiscibility of the blends.

Quantitatively speaking, χ_{23} values from the current IGC measurements are in the order of 10^{-3} to 10^{-2} depending on the experimental conditions. The associated errors are in the order of 10^{-2}. However, χ_{23} values obtained from MD simulations are in the order

90

of 10^{-4} to 10^{-3} over the same temperature range. The discrepancy between IGC and MD results is expected. In order to save the computational time, in MD simulation, the number average molecular weights of HDPE and LDPE models were only 14,000 g/mol, which was much lower than that of the samples I used (M_n=28,000 g/mol). On the other hand, the models considered in MD simulation were monodisperse, but the polydispersities of HDPE and LDPE used in the present work were 4.9 and 5.5, respectively. These differences in the molecular weight and molecular structures may cause the difference in χ_{23} values.

In terms of χ_{23} values obtained from SANS analysis for HDPE/LDPE blend, the results are not consistent in the literature, depending on the equations used to fit the experimental data. Alamo and co-workers (1994) used an equation derived for a miscible melt to fit the experimental data and they found that χ_{23} values are in the order of 10^{-4} at 160 °C, while Schipp and co-workers (1996) used an equation for a biphasic melt to fit a similar set of experimental data and they concluded that χ_{23} values are in the order of 10^{-3} at the same temperature. It was suggested that this one order of magnitude difference in χ_{23} values are caused by using different equations to fit the experimental data. This indicates that χ_{23} obtained from SANS technique is very sensitive to the equations used to fit data. However, compared the results in the present work with SANS results, it can be seen that my χ_{23} values at 170 °C are in the same order of magnitude with Schipp's results. Unfortunately, the errors of χ_{23} obtained in the present work are rather large, which makes the comparison between the present data with those of others very difficult.

This suggests once again that reducing errors is necessary, especially, for blends exhibiting small χ_{23}.

4.4 Summary

In summary, the miscibility of blends containing HDPE and LDPE has been investigated by inverse gas chromatography. The solvent independent Flory-Huggins interaction parameters of the blends were obtained by selecting a proper common reference volume for analyzing the IGC data. It was found that the interaction parameters between the pure polymers and the selected solvents satisfied the zero $\Delta\chi$ criterion suggested by Su and Patterson (1977). However, it is uncertain that whether such an approach can be used in the case of using solvents that do not meet the zero $\Delta\chi$ criterion. But it is anticipated that the method should be applicable to other polyolefin blends. In Chapter 5, I will discuss the results of the application of the present approach to the HDPE/PS and HDPE/i-PP blends in which they do not meet the zero $\Delta\chi$ criterion owing to the different chemical structures between the two components in the blends. The measured χ_{23} from the newly developed procedure for the HDPE/LDPE blend was found to be temperature and concentration dependent, as expected. It was found that for blend containing 70% HDPE, χ_{23} at 210 °C was much larger than that at 230 °C. For the concentration dependence, it seems that χ_{23} at 210 °C increased with increasing the concentration of HDPE in the blend. These results were in qualitative agreement with those obtained by molecular dynamics simulations.

92

4.5 References

Agamalian, M., Alamo, R.G., Kim, M.H., Londono, J.D., Mandelkern, L. and Wignall, G.D. (1999) Phase Behavior of Blends of Linear and Branched Polyethylenes on Micron Length Scales via Ultra-Small-Angle Neutron Scattering, *Macromolecules*, 32, 3093-3096.

Alamo, R.G., Graessley, W.W., Krishnamoorti, R., Lohse, D.J., Londono, J.D., Mandelkern, L, Stehling, F.C. and Wignall, G.D. (1997) Small Angle Neutron Scattering Investigations of Melt Miscibility and Phase Segregation in Blends of Linear and Branched Polyethylenes as a Function of the Branch Content, *Macromolecules*, 30, 561-566.

Alamo, R.G., Londono, J.D., Mandelkern, L., Stehling, F.C. and Wignall, G.D. (1994) Phase Behavior of Linear and Branched Polyethylenes in the Molten and Solid States by Small-Angle Neutron Scattering, *Macromolecules*, 27, 411-417.

Al-Salgh, Z. and Chen, P. (1991) Characterization of Semicrystalline Polymers by Inverse Gas Chromatography. 2. A Blend of Poly(vinylidene fluoride) and Poly(ethyl methacrylate), *Macromolecules*, 24, 3788-3795.

Fan, Z., Williams, M.C. and Choi, P. (2001) Molecular Dynamics Studies of the Effects of Branching Characteristics of LDPE on its miscibility with HDPE, *Polymer*, 43(4), 1479-1502.

Graessley, W.W., Krishnamoorti, R., Balsara, N.P., Butera, R.J., Fetters, L.J., Lohse, D.J., Schulz, D.N. and Sissano, L.A. (1994) Thermodynamics of Mixing for Blends of Model Ethylene-Butene Copolymers, *Macromolecules*, 27, 3896-3901.

Hill, M.J. and Barham, P.J. (1995) Absence of Phase Separation Effects in Blends of Linear Polyethylene Fractions of Differing Molecular Weight, *Polymer*, 36(8), 1523-1530.

Hill, M.J., Barham, P.J., Keller, A. and Rosney, C.C.A. (1991) Phase Segregation in Melts of Blends of Linear and Branched Polyethylene, *Polymer*, 32(8), 1384-1393.

Hussein, I.A. and Williams, M.C. (2000) DSC Evidence for Microstructure and Phase Transitions in Polyethylene Melts at High Temperatures, *Macromolecules*, 33, 520-522.

Schipp, C., Hill, M.J., Barham, P.J., Cloke, V.M., Higgins, J.S. and Oiarzabal, L. (1996) Ambiguities in the Interpretation of Small-Angle Neutron Scattering From Blends of Linear and Branched Polyethylene, *Polymer*, 37(12), 2291-2297.

Su, C.S., Patterson D. (1977) Determination by Gas-Liquid Chromatography of the Polystyrene-Poly(vinyl methyl ether) Interaction, *Macromolecules*, 10, 708-711.

Young, C.L. (1968) The Use of Gas-Liquid Chromatography for the Determination of Thermodynamic Properties, *Chromatog. Rev.*, 10, 130-155.

Table 4.1 Characteristics of HDPE and LDPE used

Resin	Density @ 25 °C (g/cm^3)	M_n	M_w	Branch content, branches/1,000 carbon atoms
HDPE	0.957	28,000	137,000	~0
LDPE	0.919	17,000	94,000	22

Table 4.2 Loadings and mass of HDPE, LDPE and their blends used in the GC columns

Column number	Composition (weight% of HDPE)	Loading (% w/w)	Mass of polymer (g)
1	100%HDPE	8.80	0.05396
2	100%LDPE	7.14	0.04920
3	30% HDPE+70%LDPE	8.55	0.05431
4	50% HDPE+50%LDPE	8.05	0.05411
5	70% HDPE+30%LDPE	6.76	0.04173

95

Table 4.3 Measured retention times of the selected probes for the column packed with pure LDPE at 170, 190, 210 and 230 °C.

PROBE	RETENTION TIME (min)			
	170 °C	190 °C	210 °C	230 °C
Methane	0.136	0.136	0.132	0.130
1 – Hexene	0.159	0.153	0.148	0.143
1-Octene	0.206	0.182	0.171	0.16
Benzene	0.18	0.169	0.162	0.152
Cyclohexane	0.183	0.169	0.162	0.153
n-Hexane	0.161	0.154	0.15	0.143
n-Dodecane	0.675	0.45	0.34	0.267
n-Heptane	0.178	0.166	0.158	0.151
n-Nonane	0.255	0.219	0.194	0.177
n-Octane	0.206	0.186	0.171	0.163
Toluene	0.213	0.193	0.18	0.168
Xylenes	0.27	0.231	0.205	0.186

Table 4.4 Measured retention times of the selected probes for the column packed with pure HDPE at 170, 190, 210 and 230 °C.

PROBE	RETENTION TIME (min)			
	170 °C	190 °C	210 °C	230 °C
Methane	0.143	0.141	0.140	0.136
1 – Hexene	0.169	0.162	0.157	0.151
1-Octene	0.217	0.198	0.181	0.17
Benzene	0.193	0.182	0.171	0.163
Cyclohexane	0.195	0.183	0.173	0.163
n-Hexane	0.171	0.164	0.158	0.152
n-Dodecane	0.754	0.513	0.383	0.298
n-Heptane	0.191	0.177	0.171	0.16
n-Nonane	0.272	0.23	0.211	0.19
n-Octane	0.222	0.201	0.185	0.171
Toluene	0.23	0.205	0.193	0.176
Xylenes	0.293	0.249	0.224	0.197

Table 4.5 Measured retention times of the selected probes for the column packed with 50% HDPE and 50% LDPE at 170, 190, 210 and 230 °C.

PROBE	RETENTION TIME (min)			
	170 °C	190 °C	210 °C	230 °C
Methane	0.136	0.134	0.133	0.130
1 – Hexene	0.163	0.155	0.149	0.144
1-Octene	0.213	0.19	0.175	0.163
Benzene	0.187	0.173	0.164	0.156
Cyclohexane	0.189	0.174	0.165	0.156
n-Hexane	0.164	0.156	0.151	0.146
n-Dodecane	0.756	0.51	0.374	0.296
n-Heptane	0.185	0.171	0.162	0.154
n-Nonane	0.272	0.23	0.203	0.183
n-Octane	0.218	0.194	0.178	0.165
Toluene	0.226	0.201	0.184	0.172
Xylenes	0.287	0.244	0.214	0.192

Table 4.6 Calculated specific retention volumes of the selected probes for the column

packed pure LDPE at 170, 190, 210 and 230 °C.

PROBE	SPECIFIC RETENTION VOLUME (cm^3/g)			
	170 °C	190 °C	210 °C	230 °C
1 – Hexene	3.53	2.46	2.14	1.67
1-Octene	10.74	6.66	5.21	3.85
Benzene	6.75	4.78	4.01	2.82
Cyclohexane	7.21	4.78	4.01	2.95
n-Hexane	3.84	2.61	2.41	1.67
n-Dodecane	82.70	45.49	27.80	17.56
n-Heptane	6.44	4.35	3.47	2.69
n-Nonane	18.26	12.02	8.29	6.02
n-Octane	10.74	7.24	5.21	4.23
Toluene	11.81	8.26	6.42	4.87
Xylenes	20.56	13.76	9.76	7.18

Table 4.7 Calculated specific retention volumes of the selected probes for the column

packed with pure HDPE at 170, 190, 210 and 230 °C.

PROBE	SPECIFIC RETENTION VOLUME (cm^3/g)			
	170 °C	190 °C	210 °C	230 °C
1 – Hexene	3.38	2.57	1.96	1.62
1-Octene	9.61	6.98	4.72	3.67
Benzene	6.50	5.02	3.57	2.92
Cyclohexane	6.76	5.14	3.80	2.92
n-Hexane	3.64	2.82	2.07	1.73
n-Dodecane	79.38	45.55	28.00	17.50
n-Heptane	6.24	4.41	3.57	2.59
n-Nonane	16.76	10.90	8.18	5.83
n-Octane	10.26	7.35	5.19	3.78
Toluene	11.30	7.84	6.11	4.32
Xylenes	19.49	13.22	9.68	6.59

100

Table 4.8 Calculated specific retention volumes of the selected probes for the column

packed with 50% HDPE and 50% LDPE at 170, 190, 210 and 230 °C.

PROBE	SPECIFIC RETENTION VOLUME (cm^3/g)			
	170 °C	190 °C	210 °C	230 °C
1 – Hexene	3.77	2.73	1.98	1.61
1-Octene	10.75	7.28	5.19	3.80
Benzene	7.12	5.07	3.83	3.00
Cyclohexane	7.40	5.20	3.96	3.00
n-Hexane	3.91	2.86	2.23	1.84
n-Dodecane	86.55	48.85	29.79	19.13
n-Heptane	6.84	4.81	3.58	2.77
n-Nonane	18.99	12.47	8.65	6.11
n-Octane	11.45	7.79	5.56	4.03
Toluene	12.56	8.70	6.30	4.84
Xylenes	21.08	14.29	10.01	7.15

101

Table 4.9 Measured Flory-Huggins interaction parameters between the selected solvents and pure HDPE, LDPE and their 50/50 blend 170 and 190 °C.

PROBE	170 °C			190 °C		
	χ_{12}	χ_{13}	$\chi_{1(23)}$	χ_{12}	χ_{13}	$\chi_{1(23)}$
1 – Hexene	0.15	0.14	0.13	0.13	0.14	0.12
1-Octene	0.13	0.11	0.11	0.11	0.12	0.10
Benzene	0.24	0.22	0.21	0.21	0.22	0.20
Cyclohexane	0.15	0.13	0.12	0.13	0.15	0.13
n-Hexane	0.14	0.13	0.13	0.12	0.13	0.12
n-Dodecane	0.078	0.072	0.066	0.074	0.075	0.065
n-Heptane	0.13	0.12	0.11	0.12	0.12	0.10
n-Nonane	0.11	0.098	0.092	0.11	0.093	0.087
n-Octane	0.12	0.11	0.10	0.11	0.11	0.095
Toluene	0.19	0.17	0.16	0.18	0.17	0.15
Xylenes	0.15	0.14	0.13	0.14	0.13	0.13

102

Table 4.10 Measured Flory-Huggins interaction parameters between the selected solvents and pure HDPE, LDPE and their 50/50 blend 210 and 230 °C.

PROBE	210 °C			230 °C		
	χ_{12}	χ_{13}	$\chi_{1(23)}$	χ_{12}	χ_{13}	$\chi_{1(23)}$
1 – Hexene	0.11	0.093	0.11	0.043	0.040	0.044
1-Octene	0.12	0.099	0.099	0.097	0.089	0.091
Benzene	0.21	0.17	0.19	0.17	0.18	0.16
Cyclohexane	0.12	0.11	0.11	0.11	0.11	0.10
n-Hexane	0.11	0.089	0.093	0.056	0.061	0.046
n-Dodecane	0.071	0.072	0.062	0.069	0.069	0.058
n-Heptane	0.094	0.099	0.093	0.087	0.081	0.076
n-Nonane	0.089	0.087	0.080	0.080	0.075	0.073
n-Octane	0.100	0.099	0.088	0.091	0.073	0.081
Toluene	0.15	0.14	0.14	0.15	0.12	0.12
Xylenes	0.13	0.12	0.12	0.13	0.11	0.11

103

Table 4.11 Measured solvent independent polymer-polymer χ_{23}

HDPE (WT%)	170 °C	190 °C	210 °C	230 °C
30	0.0098±0.028	0.073±0.029	0.025±0.031	0.0065±0.019
50	0.0040±0.024	0.039±0.024	0.034±0.028	-0.00080±0.016
70	0.033±0.032	0.060±0.032	0.098±0.038	-0.0024±0.021

104

Figure 4.1 Gas chromatograms for n-hexane interacting with a stationary phase coated

with LDPE at four temperatures (a) T=170 °C; (b) T=190 °C; (c) T=210 °C; (d) T=230 °C

(a)

(b)

(c)

(d)

105
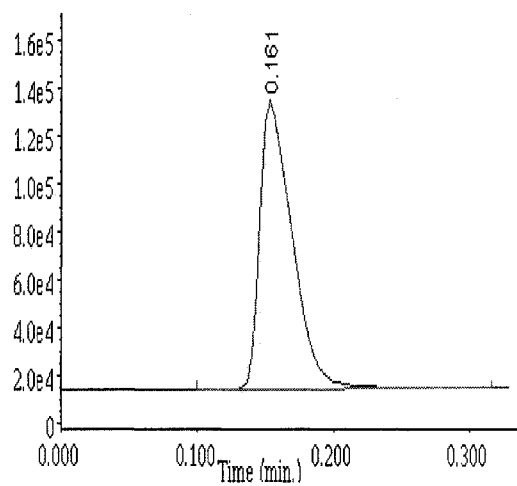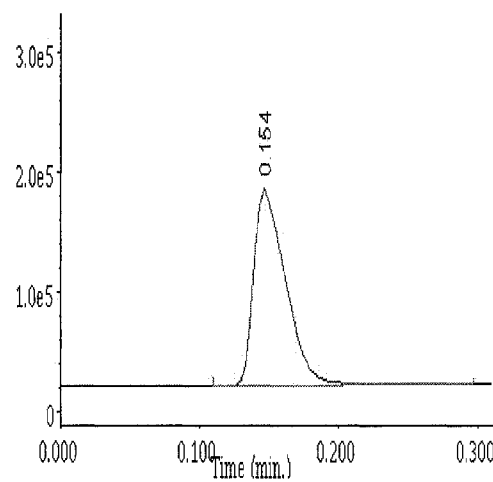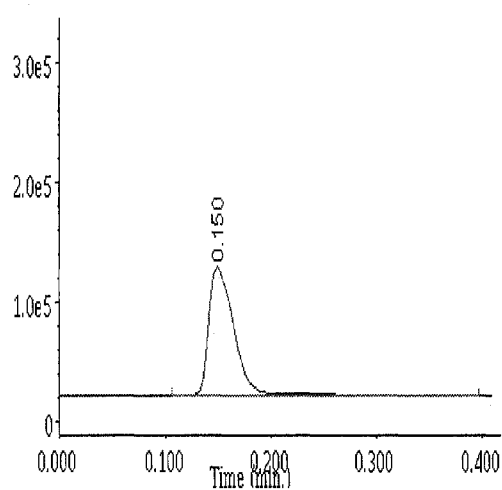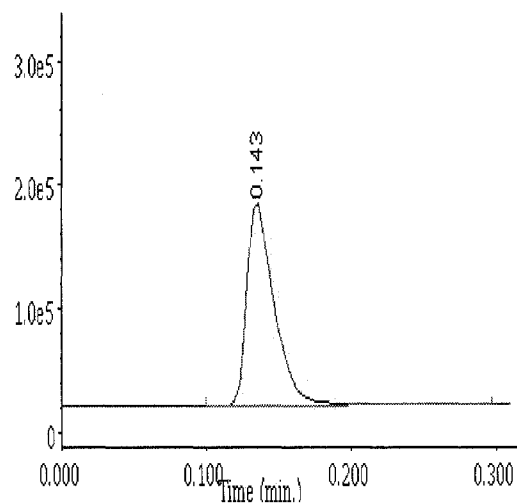
Figure 4.2 Dependence of $\ln V_g^0$ on the inverse of temperature for a 50/50 HDPE and

LDPE blend.

106
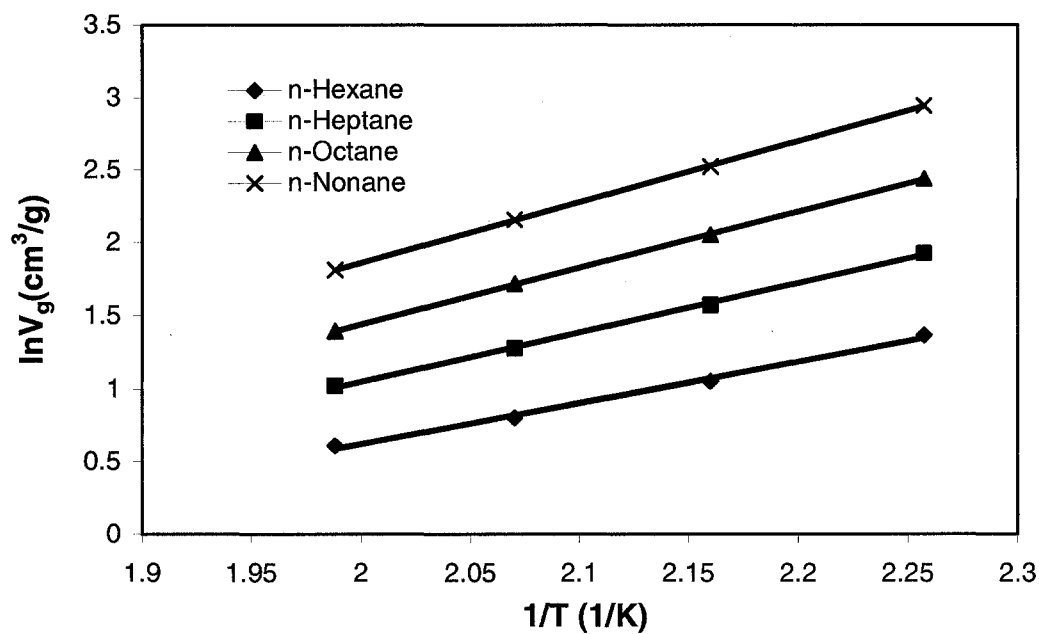
Figure 4.3 Plots of $\chi_{1(23)}$ vs $(\phi_2\chi_{12}+\phi_3\chi_{13})$ for the 50:50 HDPE/LDPE blends at four elevated temperatures. (a) T=170 $^\circ$C; (b) T=190 $^\circ$C; (c) T=210 $^\circ$C; (d) T=230 $^\circ$C (solvent as V$_0$)

(a)

(b)

(c)

(d)

107
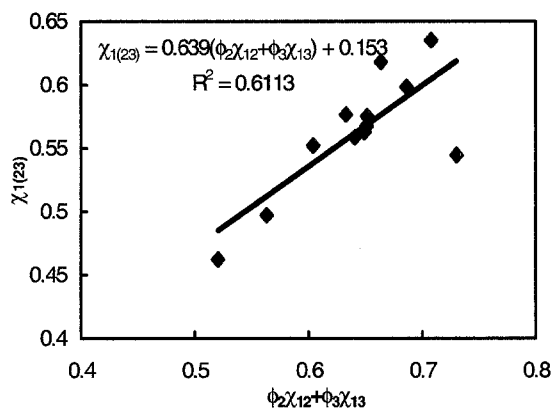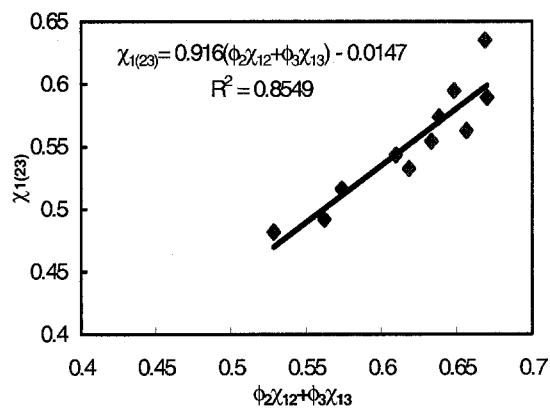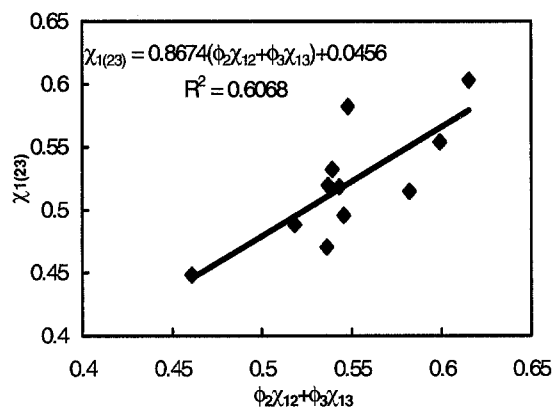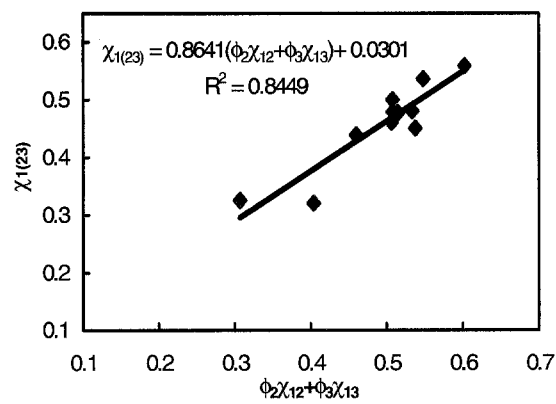
Figure 4.4 Plots of $\chi_{1(23)}$ vs $(\phi_2\chi_{12}+\phi_3\chi_{13})$ for the 50:50 HDPE/LDPE blends at four

elevated temperatures. (a) T=170 °C; (b) T=190 °C; (c) T=210 °C; (d) T=230 °C

$\chi_{1(23)} = 0.898(\phi_2\chi_{12}+\phi_3\chi_{13}) - 0.001$
$R^2 = 0.9939$

(a)

$\chi_{1(23)} = 0.9709(\phi_2\chi_{12}+\phi_3\chi_{13}) - 0.0098$
$R^2 = 0.9908$

(b)

$\chi_{1(23)} = 1.0307(\phi_2\chi_{12}+\phi_3\chi_{13}) - 0.0084$
$R^2 = 0.9817$

(c)

$\chi_{1(23)} = 0.9238(\phi_2\chi_{12}+\phi_3\chi_{13}) + 0.0002$
$R^2 = 0.9848$

(d)

108
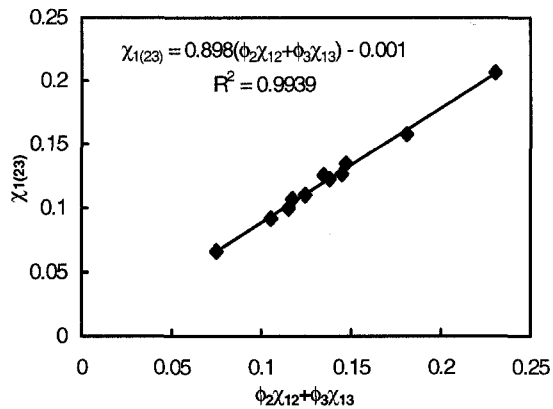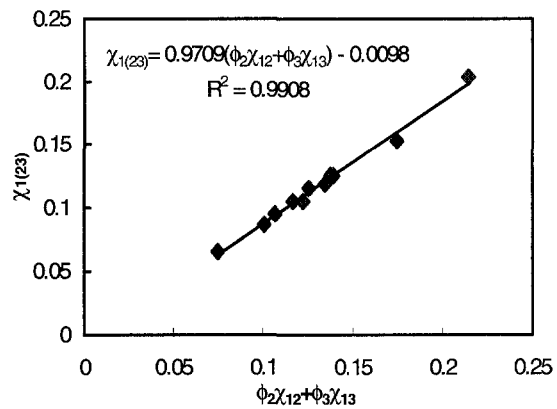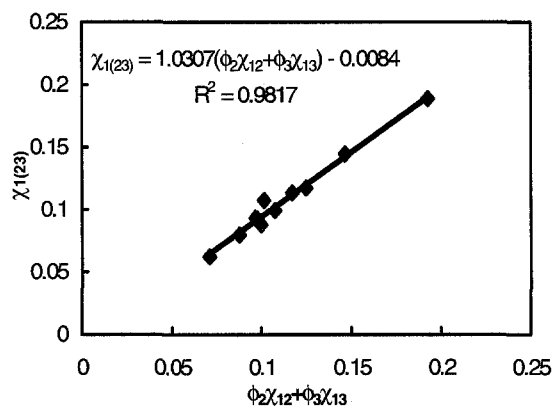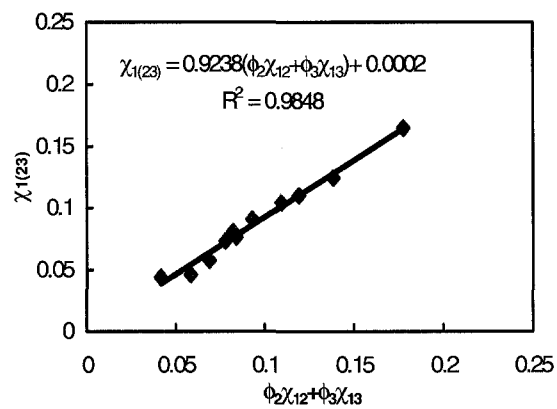
Figure 4.5 Temperature dependence of χ_{23} for the HDPE/LDPE blends at various
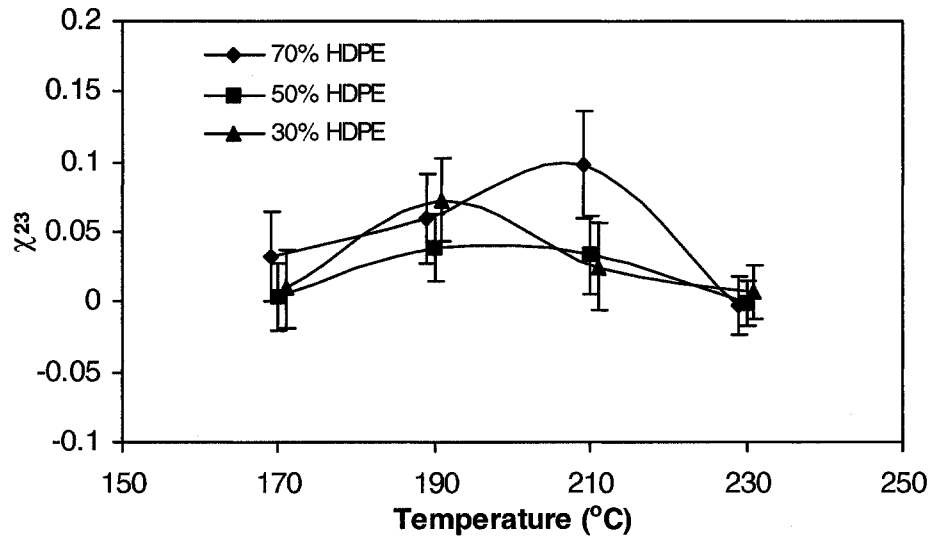
compositions

Figure 4.6 Dependence of χ_{23} on composition of the HDPE/LDPE blends at various

temperatures

109
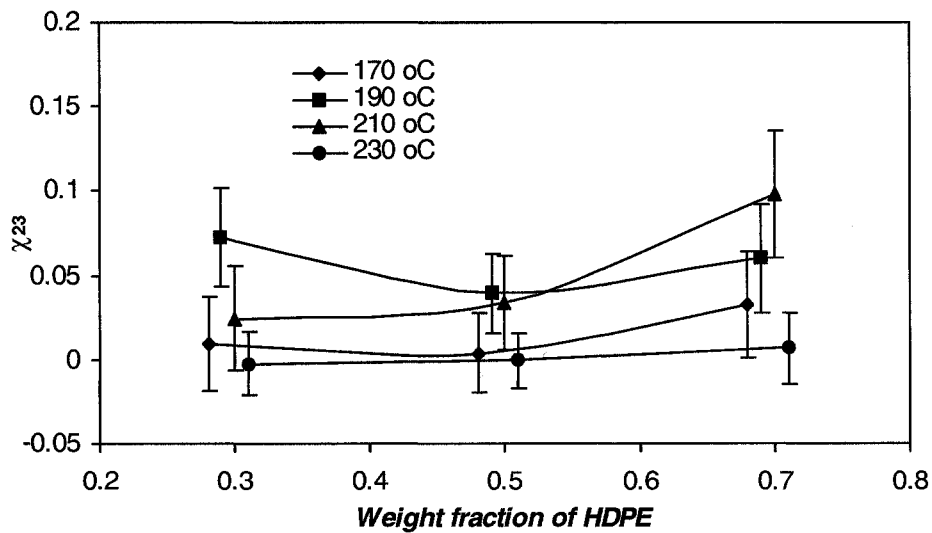
Chapter 5

Miscibility studies on HDPE/i-PP and HDPE/PS

blends

5.1 Introduction

In the previous chapter, I have demonstrated that the IGC technique combined with the data analysis approach proposed in this work provides a reasonable way to estimate interaction parameters for HDPE/LDPE blends. However, examination of the data shows that my χ values are about one to two orders of magnitude larger than those obtained from MD simulations on the comparable systems over the same temperature range. At 170 $^{\circ}$C, my χ values are one order of magnitude larger than SANS results obtained by Alamo et al. (1994). Therefore, I applied the method to two well-known immiscible systems, HDPE/i-PP and HDPE/PS blends, to check if the proposed data analysis approach could yield reasonable interaction parameters. Moreover, as discussed in Chapter 4, since the HDPE/LDPE blends and solvents meet the zero $\Delta\chi$ criterion due to the similarity of chemical structure of the polyethylenes used, it is interesting to apply this approach to the aforementioned blends and to check if it also applies to cases where solvents used do not meet the zero $\Delta\chi$ criterion. Because of the difference in chemical

110

structures between HDPE, i-PP, and PS, it is expected that these blends with most of the solvents used would not meet the zero $\Delta\chi$ criterion.

The miscibility of HDPE/i-PP and HDPE/PS blends has been widely investigated in the polymer literature and consistent conclusions have been made that these blends are not miscible in the melt state. In particular, Hermes *et al.* (1997) and Bucknall *et al.* (1998) investigated these blends using a neutron reflectivity technique. They found that the interaction parameters between HDPE and i-PP blends are about 0.02 in the temperature range of 175 to 225 °C. In terms of HDPE/PS blends, their results showed that χ exhibits a value of 0.05 at 150 °C. The composition dependence of χ cannot be investigated with the use of this technique.

5.2 Experimental

5.2.1 Materials and operating conditions

Binary blends of HDPE with i-PP and with PS were investigated at three different compositions and four temperatures in the range from 170 °C to 230 °C. Here, the HDPE sample was supplied by NOVA (Calgary, AB). The i-PP sample was from Dow Chemicals (US) and the PS sample from Exxon Chemicals (US). The molecular weight averages and density of HDPE, PS, and i-PP provided by the manufacturers are listed in Table 5.1. For each pair of the blends, five columns were prepared including two pure polymers and three binary blends at different compositions (30, 50, and 70 wt%). The procedures used to prepare the columns were exactly the same as those described in

111

Chapter 3. The loadings and mass of polymer coated in each column are listed in Table 5.2. It can be seen from the table that the loadings of polymer for all columns were in the reasonable range, which were from 6 to 10 wt%. The flowrate of carrier gas was about 20 mL/min. The inlet pressure of the column was from 200 to 250 kPa and the outlet pressure was the atmospheric pressure. The operating conditions of GC were the same as described in Chapter 4.

5.3 Results and discussion

5.3.1 Reexamination of the zero $\Delta\chi$ criterion proposed by Su and Patterson

The measured retention times of the marker and different probes for pure i-PP, PS, HDPE and 30/70, 50/50, 70/30 i-PP/HDPE and PS/HDPE blends at different temperatures are summarized in Appendix C. The corresponding specific retention volumes can be calculated from equation 3-1. Each reported retention time corresponded to the average of three injections. For each specific column, the retention time decreased with increasing temperature and within a series of similar type of probe molecules, the retention time increased with increasing size of the molecules. The specific retention volume also decreased with increasing temperature and decreased with increasing length of the solvent molecules. This observation is similar to that of HDPE/LDPE blends and the reason was given in Chapter 4.

Substituting those specific retention volumes, along with the corresponding physiochemical properties of polymers and solvents, into equations 3-26 and 3-27,

112

interaction parameters for the pure polymers, χ_{12} and χ_{13}, and their blends $\chi_{1(23)}$ were obtained. Here, the specific volumes of PS at high temperatures were calculated from the following equation (Mark and Kroschwitz, 1985):

$$v = (1.0865 - 6.19 \times 10^{-4} T + 1.36 \times 10^{-7} T^2)^{-1} \qquad (5\text{-}1)$$

And the specific volumes of i-PP at the experimental temperatures were obtained from the literature (Rudin *et al.*, 1970).

All χ_{12}, χ_{13}, and $\chi_{1(23)}$ for different solvents for the 50/50 HDPE/PS blend at the chosen experimental temperatures are listed in Tables 5.3 and 5.4. The corresponding $\chi_{1(23)}$ for the 30/70 and 70/30 blends are summarized in Appendix D. It can be seen from the data that the χ_{12} for all solvents are different from χ_{13}. The difference is from 20 to 60% depending on the solvent and this is beyond the errors of χ, which is about 5%. Note that all binary interaction parameters here were calculated based upon the molar volume of the ethylene-repeating unit. By comparing χ_{12} and χ_{13} values, it was found that for alkane and alkene types of solvents, χ_{12} was smaller than χ_{13}, but for aromatic type of solvents, χ_{12} was larger than χ_{13}. This is because chemical structures of alkane and alkene types of solvents are closer to the chemical structure of HPDE than to that of PS and based on the theory that like dissolves like, HDPE should be easier to dissolve in alkane and alkene types of solvents than PS. Therefore, for these types of solvents, χ_{12} tends to be smaller than χ_{13}. Similarly, the chemical structure of aromatic type of solvents is more

similar to that of PS than HDPE because of the presence of the aromatic rings in both PS and the solvents. This leads to the situation that χ_{13} is smaller than χ_{12}.

According to Su and Patterson's argument (Su and Patterson, 1977), the difference between χ_{12} and χ_{13} reflects the degree of nonrandom partitioning of solvent molecules in the two constituent polymers in their blend. They believed that it was the nonrandom partitioning of solvent molecules that caused the solvent dependence problem. The reason is explained as follows. In IGC measurements, to obtain the interaction parameter of two polymers, χ_{23}, a ternary system composed of two polymers and one solvent are used and are calculated from χ_{12}, χ_{13}, and $\chi_{1(23)}$, as shown in equation 3-28:

$$\chi_{1(23)} = \phi_2 \chi_{12} + \phi_3 \chi_{13} - \phi_2 \phi_3 \chi_{23} \qquad (3\text{-}28)$$

Here, χ_{12} and χ_{13} are obtained from the binary system composed of a pure polymer and a solvent. However, it is obvious that χ_{12} obtained from the binary system must be different from that in the ternary system because of the presence of the third component (polymer 3). So is χ_{13}. Consequently, using different solvents will produce different χ_{23}. Therefore, they suggested that in order to obtain the solvent independent interaction parameter, one should use the solvent that meets $\chi_{12} = \chi_{13}$ or $\Delta\chi=0$. As a result, the presence of polymer 3 will not alter the interaction between polymer 2 and the solvent so that χ_{12} in the ternary system is the same as that obtained from the binary system. However, in my opinion, this non-random partitioning is the not real cause to the probe dependence

114

problem. By extending Su and Patterson's argument, if the third component has significant effect on the interaction between the other two components, the presence of the solvent will also interfere with the interaction between the two polymers. Obviously, each solvent will have different influence on the measured χ_{23} even when the solvents used meet the criterion of $\chi_{12} = \chi_{13}$. As a result, χ_{23} obtained using different solvents will still be different. Therefore, in order to obtain the probe independent χ_{23}, the solvent and the polymers should meet $\chi_{12} = \chi_{13} = \chi_{23}$ instead of $\chi_{12} = \chi_{13}$. In reality, this is totally impossible. From the above discussion, it can be concluded that the probe dependence problem arises from two contributions. One is the misuse of reference volume as explained in Chapter 3 and the other is the non-zero $\Delta\chi$ effect. In Chapter 4, I have demonstrated that the former contribution can be eliminated. However, the latter is inherent in all the IGC measurements and cannot be removed.

Based on the results on the HDPE/PS blend, χ_{12} for all solvents are different from χ_{13} indicating that the solvents used did not meet the zero $\Delta\chi$ criterion. However, when $\chi_{1(23)}$ was plotted against $(\phi_2\chi_{12} + \phi_3\chi_{13})$ for the same set of data, it was found that all data points followed a straight line with reasonably good linearity as shown in Figure 5.1. This suggests that the data can be described quite well by equation 3-28 even if χ_{12} and χ_{13} differed considerably. Therefore, a solvent independent χ can still be obtained between the two polymers by using the data analysis method proposed in the present work although the solvent molecules exhibited nonrandom partitioning. This result indicates that the effect of the solvent on the interaction of the two polymers is negligible.

115

The probe dependence problem observed is mainly attributed to the improper use of the reference volume.

5.3.2 Polymer-polymer interaction parameters for the HDPE/i-PP and HDPE/PS systems

All χ_{12}, χ_{13}, and $\chi_{1(23)}$ for different solvents for the 30/70, 50/50, and 70/30 HDPE/i-PP blends at the chosen experimental temperatures are listed in Appendix D. By plotting $\chi_{1(23)}$ against $(\phi_2\chi_{12} + \phi_3\chi_{13})$, χ_{23} values for HDPE and i-PP blends at different compositions and temperatures were obtained from the intercepts of the lines and are listed in Table 5.5 along with the associated errors. The corresponding values of χ_{23} for HDPE and PS blends are listed in Table 5.6.

From Table 5.5, it can be seen that χ values of HDPE/i-PP blends vary from 0.04 to 0.13 and most of which are higher than 0.05 with errors about 0.03. It should be noted that χ values were calculated based on the reference volume of the molar volume of the ethylene-repeating unit. These results are very comparable to the value of 0.02 over the same temperature range obtained from neutron reflectivity technique (NR) by Bucknall *et al.* (1998). It is worth noting that in neutron reflectivity measurements, the interaction parameter was obtained by measuring the thickness of the interface formed by the blend component polymers. Therefore, this technique cannot be used to study the effect of composition of the blend on the interaction parameter. Akten *et al.* (2001) applied molecular simulation method to the HDPE/i-PP system and obtained a χ value of 0.09 at

116

200 °C, which is in good agreement with the present results. Similar results were also obtained by Rajasekaran *et al.* (1995) by using a modeling method based on the polymer reference interaction site model (PRISM). Their interaction parameters between HDPE and i-PP are from 0.025 to 0.035, depending on the composition of the blend. However, when I compared my results with those from SANS (Jeon *et al.*, 1997), it was found that my χ values were at least one order of magnitude larger than theirs, which is 3.8×10^{-3}. Here, the discrepancy of the χ_{23} values obtained from NR and SANS is still not well understood. Nonetheless, the obtained χ values for HDPE and i-PP blends indicate that these blends are not miscible.

From the above discussion, I ruled out the possibility that the third solvent used in the IGC experiment caused the problem that my χ values are one order of magnitude larger than those obtained from SANS because the third solvent was not utilized in both SANS and neutron reflectivity measurements. However, my χ values are in the same order of magnitude with those obtained from neutron reflectivity, while one order of magnitude larger than those obtained from SANS.

Table 5.6 shows χ values for the HDPE/PS blends and they are in the range of 0.04 to 0.19 based on the same reference volume as I used for the HDPE/i-PP blends. The errors for χ were determined to be 0.03. Hermes *et al.*, (1997) used the neutron reflectivity to study similar systems and found that χ values are in the range of 0.038 to 0.08 at 150 °C. By comparison, χ values obtained in this work are consistent with Hermes's results. These results confirm that HDPE and PS form an immiscible blend. No data obtained by SANS technique were found for this system in the literature.

117

5.3.3 Temperature and composition dependency of χ for the HDPE/i-PP system

Figure 5.2 shows the temperature dependence of χ of HDPE and i-PP blends at three different compositions. It can be seen from this figure that no strong temperature dependence was observed for blends with 50% and 70% i-PP. In contrast, χ increased with increasing temperature for blend with 30% i-PP, suggesting that this blend shows a lower critical solution temperature (LCST) type of phase diagram. This type of phase diagram is also observed in the polypropylene and saturated polyisoprene (SPI) blend (Reichart *et al.*, 1997) and the deuterated polybutadiene (DPB) and protonated polybutadiene (HPB) blends with high vinyl content of HPB (Jinnai *et al.*, 1992). In Figure 5.2, the dotted line represents Bucknall's results obtained by neutron reflectivity. The three data points were at 175, 200 and 225 °C, respectively. It can be seen that their χ is insensitive to temperature. The value of χ at 200 °C is slightly smaller than those at 175 and 225 °C. This is consistent with my results for 50/50 and 30/70 HDPE/i-PP blends. My χ also shows a slightly negative deviation at intermediate temperatures. However, it is important to point out that because of the large errors associated with the measured χ values, this negative deviation is questionable.

In Figure 5.3, χ parameters for HDPE and i-PP blends at different temperatures were plotted against the composition of i-PP in the blends. At 190 and 170 °C, χ has weaker dependence on the composition. For blends at 210 and 230 °C, χ decreased with increasing the composition of i-PP from 30% to 50% and did not change much from 50% to 70%. This asymmetric composition dependence of χ has been predicted by Rajasekaran *et al.* (1995) using the PRISM theory. It was believed that the local,

118

nonrandom packing of PE and i-PP in the blend leads to this phenomenon. It was found that in the HDPE/i-PP blend, HDPE is easier to cluster than i-PP owing to the unfavorable cross correlations between HDPE and i-PP chains in the blend. These clusters make HDPE and i-PP distribute non-randomly in the blend system. Increasing the concentration of HDPE will increase this non-randomness, and will also increase the immiscibility of the blend.

5.3.4 Temperature and composition dependence of χ for the HDPE/PS system

Figure 5.4 depicts the temperature dependence of χ at various compositions for the HDPE/PS blends. Based on the results shown in this figure, χ does not vary significantly with temperature for blends containing 50 and 70% PS. For the blend having 30% PS, χ increased with increasing temperature, especially from 210 to 230 °C indicating a LCST. This finding is similar to that for blend composed of 70% HDPE and 30% i-PP. This behavior has been commonly observed for the blends when there are specific intermolecular associations between the components such as hydrogen bonding. However, for HDPE/i-PP and HDPE/PS blends, there exists no specific interaction. Freed *et al.* (1998) explained the LCST phase diagram for systems without specific interactions based on the lattice cluster theory (LCT). They believed that the LCST phase behavior is attributed to the competition between the exchange energy and the entropic destabilization from the structural disparity.

119

Figure 5.5 shows the composition dependence of χ for the HDPE/PS blend at four different temperatures. For blends at 170, 190 and 210 °C, there exists a fairly weak composition dependence of χ. In contrast, for blends at 230 °C, χ decreased with increasing in the composition range of PS from 30% to 50% and had no significant change from 50% to 70%. A similar trend has been obtained for HDPE/i-PP blend at 210 and 230 °C and an explanation has also been provided in the previous section.

5.4 Summary

In this chapter, the miscibility of HDPE/i-PP and HDPE/PS blends was studied at three compositions and four temperatures using IGC technique along with the proposed data analysis method. From the results, the following conclusions were drawn. First, I found that the data analysis approach I proposed in Chapter 3 was applicable to the systems in which the zero $\Delta\chi$ criterion was not fulfilled, (i.e., the solvent molecules exhibit nonrandom partitioning in the two components of the blend). Secondly, the interaction parameters of HDPE/i-PP and HDPE/PS blends obtained in this work were consistent with those from neutron reflectivity measurements. However, my χ values of HDPE/i-PP blends were at least one order of magnitude larger than those obtained by the SANS technique. No data were found for HDPE/PS blends by SANS. It is not clear to us that whether neutron reflectivity or SANS yields more reliable χ. Nevertheless, my results were in good agreement with those obtained from neutron reflectivity. This lends some support to the approach I proposed.

120

For 70/30 HDPE/i-PP and 70/30 HDPE/PS blends, χ increased with increasing temperature indicating that the blends exhibited a LCST. For blends HDPE/i-PP at 210 and 230 °C and HDPE/PS at 230 °C, χ decreased with increasing the composition of i-PP from 30% to 50% and does not change much from 50% to 70% due to the non-random packing of two components. In terms of composition and temperature dependence of χ for those two blends at other temperatures and compositions, no obvious trend was identified considering the large errors associated with the measured χ values.

5.5 References

Akten, D.E., Wayne, L. and Mattice, L. (2001) Monte Carlo Simulation of Head-to-Head, Tail-to-Tail Polypropylene and Its Mixing with Polyethylene in the Melt, *Macromolecules*, 34(10), 3389-3395.

Bucknall, D.G., Butler, S.A., Hermes, H.E. and Higgins, J.S. (1998) Neutron Reflectivity Investigations of Semi-crystalline Polymer Interfaces, *Physica B*, 241-243, 1071-1073.

Freed, K.F. and Dudowicz, J. (1998) Lattice Cluster Theory for Pedestrians: The Incompressible Limit and the Miscibility of Polyolefin Blends, *Macromolecules*, 31, 6681-6690.

Hermes, H.E., Higgins, J.S. and Bucknall, D.G. (1997) Investigations of the Melt Interface between Polyethylene and Polystyrene Using Neutron Reflectivity, *Polymer*, 38(4), 985-989.

Jeon, H.S., Lee, J.H., Balsara, N.P., Majumdar, B., Fetters, L.J. and Faldi, A. (1997) Domain Shape Transitions in Emulsified Polyolefin Blends, *Macromolecules*, 30, 973-981.

Jinnai, H., Hasegawa, H. and Hashimoto, T. (1992) Inversion of the Phase Diagram from UCST to LCST in Deuterated Polybutadiene and Protonated Polybutadiene Blends, *Macromolecules*, 25, 6078-6080.

Mark, H.F. and Kroschwitz, J.I. (1985) Encyclopedia of Polymer Science and Engineering, 2nd ed., New York.

Rajasekaran, J.J., Curro, J.G. and Honeycutt, J.D. (1995) Theory for the Phase Behavior of Polyolefin Blends: Application to the Polyethylene/Isotactic Polypropylene Blend, *Macromolecules*, 28, 6843-6853.

Reichart, G.C., Graessley, W.W., Register, R.A., Krishnamoorti, R. and Lohse, D.J. (1997) Anomalous Attractive Interactions in Polypropylene Blends, *Macromolecules*, 30, 3036-3041.

Rudin, A., Chee, K.K. and Shaw, J.H. (1970) Specific Volume and Viscosity of Polyolefin Melts, *J. Polym. Sci., Part C*, 30, 415-427.

Su, C.S. and Patterson D. (1977) Determination by Gas-Liquid Chromatography of the Polystyrene-Poly(vinyl methyl ether) Interaction, *Macromolecules*, 10, 708-711.

Table 5.1 Characteristics of HDPE, i-PP and PS used

RESIN	DENSITY @ 25 ^{O}C (g/cm^3)	M_n	M_w
HDPE	0.962	13,700	49,400
i-PP	0.90	N/A	270,000
PS	1.04	200,000	N/A

123

Table 5.2 Loadings and mass of HDPE, i-PP, PS and their blends used in the GC columns

COLUMN NUMBER	COMPOSITION (wt% of HDPE)	LOADING (% w/w)	MASS OF POLYMER (g)
1	100% HDPE	8.80	0.05396
2	100% i-PP	7.09	0.04582
3	30% HDPE+70% i-PP	6.95	0.04303
4	50% HDPE+50% i-PP	8.32	0.05273
5	70% HDPE+30% i-PP	7.15	0.04726
6	100% PS	8.85	0.05658
7	30% HDPE+70% PS	8.66	0.05986
8	50% HDPE+50% PS	8.45	0.05207
9	70% HDPE+30% PS	8.35	0.05791

Table 5.3 Measured Flory-Huggins interaction parameters between the selected solvents and pure HDPE, PS and their 50/50 blend 170 and 190 °C.

PROBE	170 °C			190 °C		
	χ_{12}	χ_{13}	$\chi_{1(23)}$	χ_{12}	χ_{13}	$\chi_{1(23)}$
1 – Hexene	0.15	0.19	0.16	0.13	0.18	0.14
1-Octene	0.13	0.16	0.14	0.11	0.15	0.13
Benzene	0.24	0.17	0.19	0.21	0.16	0.19
Cyclohexane	0.15	0.18	0.16	0.13	0.18	0.16
n-Hexanes	0.14	0.18	0.16	0.12	0.19	0.14
n-Dodecane	0.08	0.13	0.10	0.07	0.11	0.09
n-Heptane	0.13	0.18	0.13	0.12	0.18	0.14
n-Nonane	0.11	0.16	0.12	0.11	0.16	0.12
n-Octane	0.12	0.16	0.13	0.11	0.16	0.13
Toluene	0.19	0.13	0.15	0.18	0.16	0.15
Xylenes	0.15	0.12	0.13	0.14	0.13	0.13

125

Table 5.4 Measured Flory-Huggins interaction parameters between the selected solvents and pure HDPE, PS and their 50/50 blend 210 and 230 °C.

PROBE	210 °C			230 °C		
	χ_{12}	χ_{13}	$\chi_{1(23)}$	χ_{12}	χ_{13}	$\chi_{1(23)}$
1 – Hexene	0.11	0.13	0.11	0.04	0.07	0.05
1-Octene	0.12	0.14	0.12	0.10	0.11	0.09
Benzene	0.21	0.15	0.18	0.17	0.13	0.14
Cyclohexane	0.12	0.15	0.13	0.11	0.13	0.12
n-Hexanes	0.11	0.13	0.11	0.06	0.09	0.06
n-Dodecane	0.07	0.09	0.06	0.07	0.08	0.05
n-Heptane	0.09	0.13	0.12	0.09	0.13	0.09
n-Nonane	0.09	0.12	0.10	0.08	0.14	0.08
n-Octane	0.10	0.12	0.11	0.09	0.14	0.10
Toluene	0.15	0.11	0.13	0.15	0.13	0.12
Xylenes	0.13	0.10	0.11	0.13	0.12	0.10

126

Table 5.5 Measured polymer-polymer interaction parameters between HDPE and i-PP.

HDPE (wt%)	170 °C	190 °C	210 °C	230 °C
30%	0.074±0.026	0.051±0.024	0.062±0.022	0.070±0.015
50%	0.053±0.021	0.043±0.020	0.031±0.019	0.064±0.013
70%	0.048±0.028	0.062±0.027	0.10±0.025	0.13±0.018

Table 5.6 Measured polymer-polymer interaction parameters between HDPE and PS.

HDPE (wt%)	170 °C	190 °C	210 °C	230 °C
30%	0.13±0.048	0.051±0.040	0.116±0.038	0.092±0.024
50%	0.042±0.030	0.046±0.030	0.032±0.019	0.049±0.018
70%	0.061±0.035	0.070±0.040	0.066±0.031	0.19±0.024

Figure 5.1 Plots of $\chi_{1(23)}$ vs $(\phi_2\chi_{12}+\phi_3\chi_{13})$ for the 50:50 HDPE/PS blends at four elevated temperatures. (a) T=170 °C; (b) T=190 °C; (c) T=210 °C; (d) T=230 °C

$$\chi_{1(23)} = 1.0048(\phi_1\chi_{12}+\phi_1\chi_{13}) - 0.0104$$
$$R^2 = 0.9577$$

(a)

$$\chi_{1(23)} = 1.031(\phi_1\chi_{12}+\phi_1\chi_{13}) - 0.0114$$
$$R^2 = 0.8567$$

(b)

$$\chi_{1(23)} = 1.0147(\phi_1\chi_{12}+\phi_1\chi_{13}) - 0.008$$
$$R^2 = 0.9497$$

(c)

$$\chi_{1(23)} = 0.9737(\phi_1\chi_{12}+\phi_1\chi_{13}) - 0.0123$$
$$R^2 = 0.9093$$

(d)

128
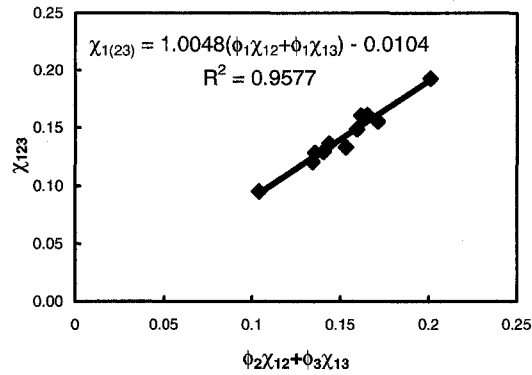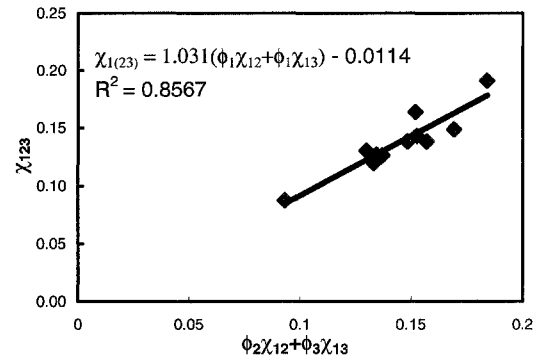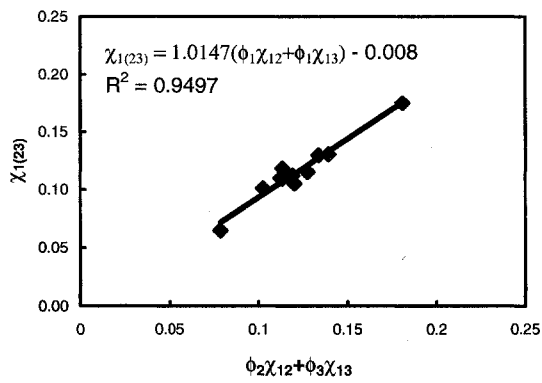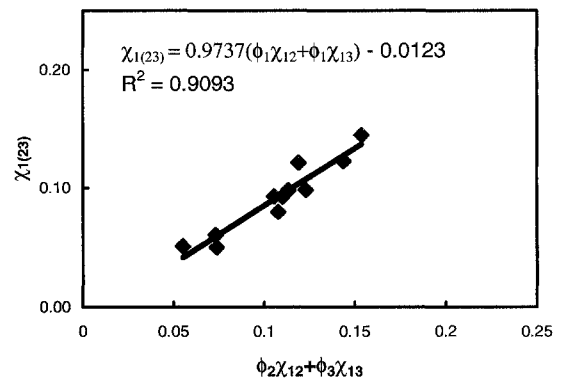
Figure 5.2 Temperature dependence of χ_{23} for HDPE/i-PP blends at various compositions
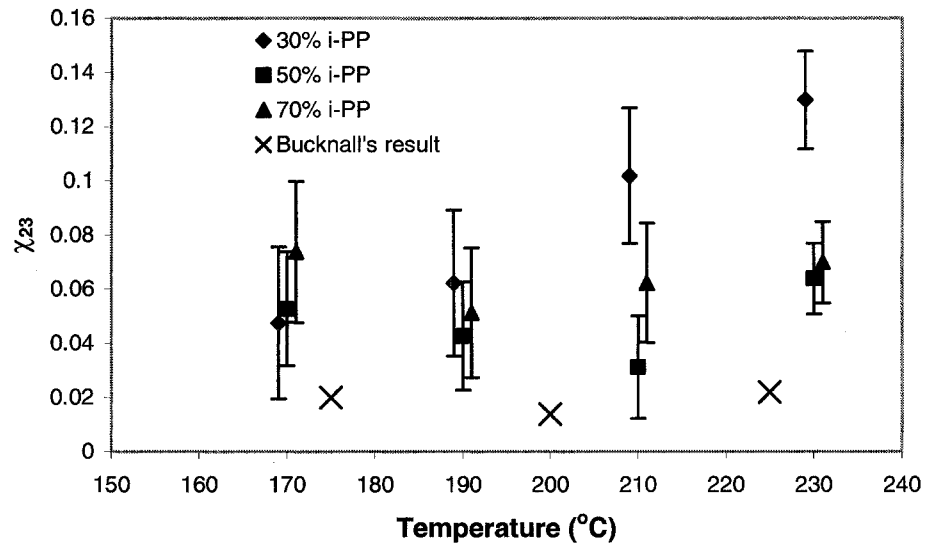
Figure 5.3 Composition dependence of χ_{23} of HDPE/i-PP blends at various temperatures

129
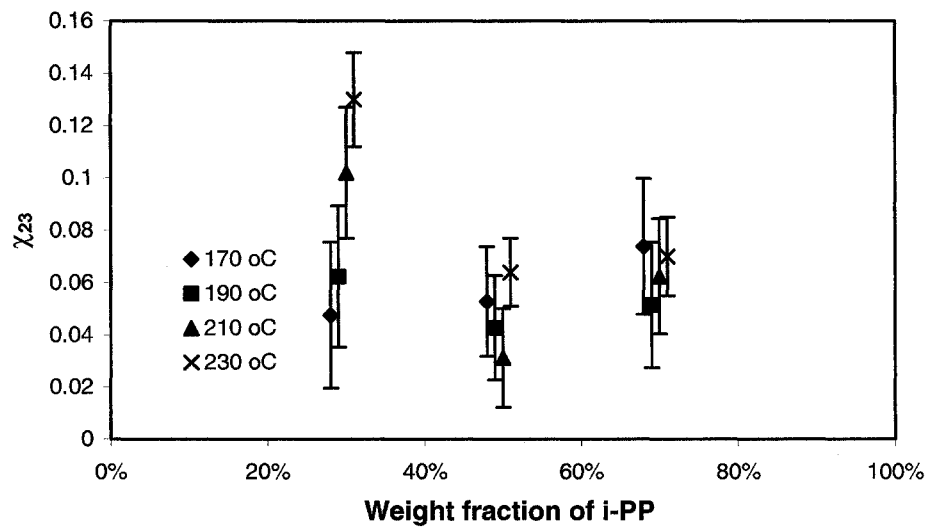
Figure 5.4 Temperature dependence of χ_{23} for HDPE/PS blends at various compositions
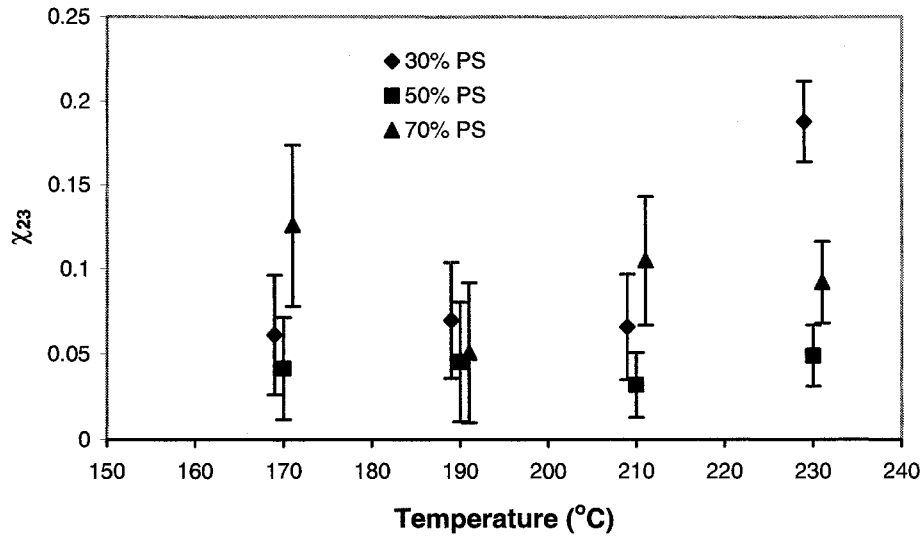
Figure 5.5 Composition dependence of χ_{23} of HDPE/PS blends at various temperatures

130
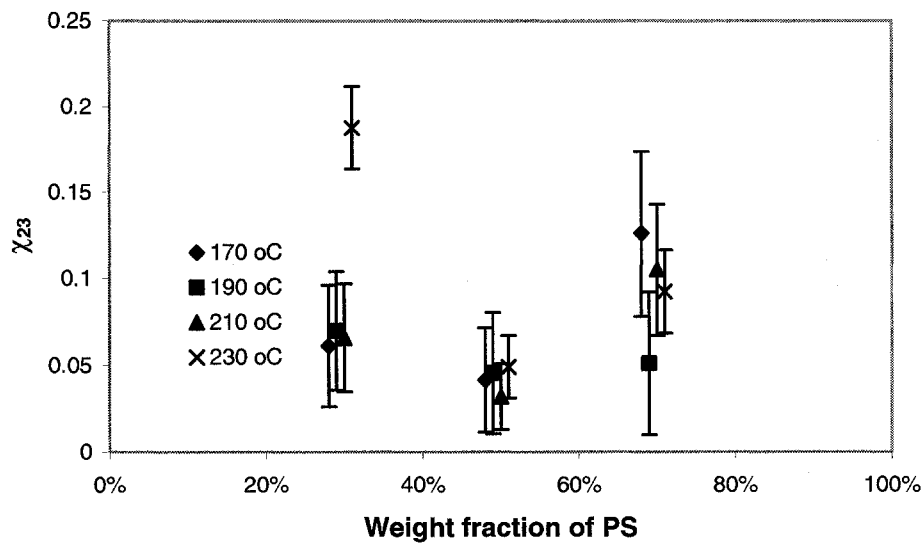
Chapter 6

Effect of branch content of LLDPE on its miscibility with HDPE

6.1 Introduction

In Chapters 4 and 5, I demonstrated that my data analysis method could be used to obtain the solvent independent Flory-Huggins interaction parameters (χ) for polyolefin blends. However, the values obtained for the HDPE/LDPE blends were one to two orders of magnitude larger than those values obtained by SANS and MD simulations on comparable systems. And for the HDPE/i-PP and HDPE/PS blends, the measured χ values agreed very well with those obtained from neutron reflectivity measurements and Monte Carlo simulations, but they were one order of magnitude larger than those from SANS. Therefore, it is uncertain which of the above techniques would yield the most reliable χ values. However, I speculate that the trends of χ values obtained from various techniques including IGC (e.g., temperature dependence, branch content dependence, etc.) may be similar to each other.

To prove this, I decided to apply the technique to study the effect of branch content of octene-based LLDPE on its miscibility with HDPE at elevated temperatures because such systems have been extensively studied and the branch content dependence

131

of χ is available. In particular, Hill *et al.* (1993), by means of DSC and TEM, found that such blends containing LLDPE with branch contents above 60 show extensive phase separation behavior. Alamo *et al.* (1997) used the SANS technique and studied the miscibility between HDPE and a model polymer, HPB (to simulate butene-based LLDPE) and suggested that these blends are miscible if the branch content of LLDPE is lower than 40 branches per 1,000 backbone carbons; immiscible if the branch content of LLDPE is higher than 80 branches per 1,000 backbone carbons. Rhee and Crist (1991) also studied the branch content effect of HPB on its miscibility with HDPE using SANS. Their results suggested that 60 branches per 1,000 backbone carbons is the critical value to induce the phase separation for the HDPE/LLDPE blends. Recent molecular modeling results based upon molecular dynamics simulation at temperatures as high as 250 °C have also indicated that 40 branches, regardless of the branch length, is the threshold value above which phase separation occurs in those blends (Choi, 2000).

6.2 Experimental

6.2.1 Materials and operating conditions

Binary blends composed HDPE and LLDPEs with different branch contents ranging from 3 to 87 branches per 1,000 backbone carbons were studied. The polyethylene samples used were commercial products. In particular, the HDPE and three LLDPEs samples (LLDPE-1, LLDPE-2 and LLDPE-3) were supplied by NOVA, while the remaining LLDPE samples were supplied by EXXON Chemicals. All LLDPEs were

132

octene-based copolymers. The molecular weight averages and branch contents of the polymers provided by the manufacturers are listed in Table 6.1. The IGC columns were prepared using the same procedures as described in Chapter 3. The loadings and mass of polymer coated in the columns are listed in Table 6.2. It can be found that the loadings of polymer for all columns were in the reasonable range, which was from 6 to 10 wt%. For each pair of the blends, three different compositions (30, 50 and 70 wt%) and four elevated temperatures (170, 190, 210, and 230 °C) were studied. The inlet pressure of the column was from 200 to 250 kPa and the outlet pressure was the atmospheric pressure. The operating conditions of GC were the same as those used for the blends described in the previous chapters.

6.3 Results and discussion

6.3.1 Polymer-polymer interaction parameters between HDPE and various LLDPEs

The measured retention times of the marker and different probes for the pure HDPE, each LLDPE, and their 30/70, 50/50, and 70/30 blends at different temperatures are summarized in Appendix C. The corresponding specific retention volumes can be calculated using equation 3-1. For each specific column, net retention time decreased with increasing temperature and within a series of similar type of probe molecules, net retention time increased with increasing size of the molecules. The specific retention volume also decreased with increasing temperature and decreased with increasing size of the solvent molecules, basically, following the same trends as those of the HDPE/LDPE blends.

133

By substituting the specific retention volumes into equations 3-26 and 3-27, interaction parameters between the selected solvents and the pure polymers as well as their corresponding blends were calculated and all the results are summarized in Appendix D. Tables 6.3 and 6.4 show such data for the blends consisted of HDPE and LLDPE-1 as well as HDPE and LLDPE-5. Note that values in the parenthesis are the interaction parameters between the probes and the pure LLDPE-5, which had a higher branch content than that of LLDPE-1. It can be seen from these tables (also those in Appendix D) that for all probes, χ_{12} is very similar to χ_{13}, although there is a trend that χ_{12} is slightly smaller than χ_{13}. These small differences between χ_{12} and χ_{13} reflect the differences of the same probe molecule interacting with polymers having different molecular structures. Most of the probes are linear molecules. Therefore, based on the theory that like dissolves like, these probes are easier to dissolve in the HDPE, which is also a linear molecule, than in the LLDPE, which contains branches. This difference between χ_{12} and χ_{13} becomes significant for the HDPE/LLDPE-5 blend because LLDPE-5 blend contains more branches (87 branches per 1,000 backbone carbons) than LLDPE-1 (3 branches per 1,000 backbone carbons).

These χ_{12}, χ_{13}, and $\chi_{1(23)}$ data were then used to determine χ_{23} by plotting $\chi_{1(23)}$ against ($\phi_2\chi_{12} + \phi_3\chi_{13}$) according to equation 3-28. The corresponding plots of HDPE/LLDPE-1 blends at four elevated temperatures are shown in Figure 6.1. It is evident from this figure that the resultant plots, similar to those shown in the two previous chapters, exhibited linear relationships with slopes close to 1. Similar results were obtained for blends containing HDPE and other LLDPEs at various compositions

134

and temperatures. It can be concluded that the approach I proposed to obtain probe independent interaction parameter is also applicable to the blends of HDPE and LLDPE. This result confirmed the claim in Chapter 5 that the solvent independent interaction parameter between two polymers could be obtained even if the zero $\Delta\chi$ criterion was not satisfied. The non-random partitioning contribution to the solvent dependence problem is negligible and the real reason to cause the problem is the improper choice of the reference volume as discussed in Chapter 3.

From the intercepts of these lines, the resultant χ_{23} and the associated errors were calculated for all blends at three compositions and four temperatures and are summarized in Table 6.5. From this table, it can be found that in most of the cases, the absolute value of χ_{23} is in the order of 10^{-3} to 10^{-2} and the associated errors are in the order of 10^{-2}. Here, χ_{23} of the blends containing LLDPE with low branch contents (LLDPE-1, LLDPE-2 and LLDPE-3) were negative. In contrast, χ_{23} of blends containing LLDPE with high branch contents (LLDPE-4 and LLDPE-5) showed positive values. The negative values of χ_{23} are unexpected since HDPE and LLDPE interact with each other via van der Waals forces. Therefore, their interaction energy is expected to conform to the geometric mean assumption, and the measured interaction parameters should be positive. Here, it is worth noting that in the work of Jinnai *et al.*, (1992) they observed negative interaction parameters for blends containing high, instead of low, vinyl content polybutadienes. Graessley *et al.* (1994) also reported negative values of χ_{23} for blends of hydrogenated polybutadiene and hydrogenated polyisoprene. However, the results of Choi (2000) show

135

no negative values of χ_{23}. This is because the solubility parameter formulation was used in his MD simulations:

$$\chi_{23} = \frac{V_0}{RT}(\delta_2 - \delta_3)^2 \qquad (6\text{-}1)$$

where δ_2 and δ_3 are the solubility parameters of polymers 2 and 3, respectively and are calculated from simulation; V_0 is the reference volume in the lattice theory. It can be seen that negative χ_{23} is impossible. The real reason for the negative χ_{23} observed in my data is still not understood.

6.3.2 Composition dependence of χ_{23} of the HDPE/LLDPE blends

For each pair of the HDPE/LLDPE blends, the composition dependence of χ_{23} at various temperatures is shown in Figures 6.2-6.6. It can be seen that if the branch content of LLDPE was 3 branches per 1,000 backbone carbons (LLDPE-1), χ_{23} exhibited a minimum value at the middle concentration range, regardless of temperature, indicating that HDPE and LLDPE blends are more miscible at this composition, as shown in Figure 6.2. For blends with LLDPE having higher branch contents, χ_{23} showed a similar trend with respect to compositions at all temperatures as that for the blend containing LLDPE-1. However, there are some exceptions. In particular, for blends containing LLDPE-3 at 190 °C and LLDPE-5 at 230 °C, χ_{23} showed an opposite trend. In general, HDPE/LLDPE

136

blends seem more miscible at the intermediate concentrations although the errors are rather large that the variation of χ_{23} with composition is overshadowed by the uncertainties of χ_{23}.

It has been reported that the composition dependence of χ_{23} for weakly interacting blends such as the ones considered here is approximately parabolic (Taylor, *et al.*, 1996):

$$\chi(\phi, T) = A(T) + \frac{B(T)}{\phi_2\phi_3} \qquad (6\text{-}2)$$

In the above equation, χ_{23} is a function of composition and temperature. *A(T)* and *B(T)* are the temperature coefficients, and ϕ_2 and ϕ_3 are the weight fractions of polymers 2 and 3 in the blend. It was found the coefficient *B(T)* is usually positive, resulting in an increasing trend at the composition extremes. Also, according to this equation, χ_{23} changes dramatically at either $\phi_2<0.2$ or $\phi_3<0.2$, and changes slightly at the intermediate compositions. In the IGC experiments, the composition range I studied was from 0.3 to 0.7. Therefore, it is not sure whether the composition dependence of χ_{23} at low concentration of either one of the polymers exhibiting the behaviour as suggested by equation 6-2 or not. However, the data seem to support the equation.

137

6.3.3 Temperature dependence of χ_{23} of the HDPE/LLDPE blends

Figures 6.7 to 6.9 depict the plots of χ_{23} versus temperature for all blends at three compositons, 30/70, 50/50, and 70/30. It can be seen from these figures that χ_{23} are not very sensitive to temperature. For the 30/70 blends, the general trend is that χ_{23} slightly decreased with increasing temperature. These results are consistent with the results on the blends of hydrogenated polybutadienes and linear polyethylene blends obtained from SANS and PVT measurements (Graessley *et al.*, 1994 and Han *et al.*, 1999). The temperature range that these research groups investigated was from 25 to 167 °C.

Figure 6.8 shows the temperature dependence of χ_{23} for all 50/50 blends. It can be seen that the temperature dependence of χ_{23} showed an inverse relationship for the blend containing LLDPE with a branch content of three. On the other hand, χ_{23} increased with increasing temperature for the blend containing LLDPE with 87 branches. Such observations parallel what Jinnai *et al.* observed some years ago on blends consisted of deuterated and protonated polybudatiene (Jinnai *et al.*, 1992). All 70/30 blends, taking the errors into account, no obvious trend could be identified, as shown in Figure 6.9.

Based on the results, it can be concluded that χ_{23} is not necessary to follow an inverse relationship with temperature. According to the Flory-Huggins theory, it is expected that χ_{23} decreases with increasing temperature as shown in the following expression:

$$\chi_{23} = (z - 2)\Delta g_{23} / kT \qquad (3\text{-}16)$$

138

In the original Flory-Huggins theory, Δg_{23} is considered to be a temperature-independent term. However, if I substitute the above equation into the following equation for the enthalpy change on mixing:

$$\Delta H_m = kTn_2\phi_3\chi_{23} \tag{3-15}$$

It yields:

$$\Delta H_m = (z-2)n_2\phi_3\Delta g_{23} \tag{6-3}$$

From the above equation, if Δg_{23} is independent of temperature, ΔH_m will be also temperature independent. Obviously, this is not correct. Therefore, Δg_{23} must be a function of temperature. This, in turn, makes χ_{23} a parameter that depends on temperature in a complex way. Depending on the functional relationship of Δg_{23} on temperature, χ_{23} may increase, decrease or weakly depend on temperature. Until now, the relationship between Δg_{23} and temperature has not been fully developed. Different temperuature dependence of χ_{23} has been reported in the literature (Jinnai et al. 1992). For example, in the study of blends composed of deuterated polybutadiene (DPB) and protonated polybutadiene (HPB) with different vinyl contents by SANS, Jinnai et al., (1992) found if the vinyl contents of HPB is lower than 40%, χ_{23} decreases with increasing temperature; if higher than 65%, χ_{23} increases with increasing temperature, and no temperature dependence was observed for the blend with the intermediate vinyl contents.

139

Unfortunately, the IGC approach cannot capture the small difference of χ_{23} due to the large errors associated with the measured χ_{23}. The temperature dependence of χ_{23} described previous may be questionable and reducing the errors is extremely important for identifying the composition and temperature dependence of χ_{23}.

6.3.4 Effect of the branch content of LLDPE on χ_{23} of the HDPE/LLDPE blends

When χ_{23} values were plotted against the branch content of LLDPE as shown in Figures 6.10-6.12, it can be seen that χ_{23} values were all negative if the branch content of LLDPE is lower than 50 for all temperatures and compositions of the blends. When the branch content of LLDPE was higher than 50, χ_{23} values became positive and deviated significantly from zero when the branch content was 87. This increasing trend of χ_{23} indicates that phase separation may occur in the blends containing LLDPE with high branch contents.

A similar miscibility trend for comparable systems was observed from SANS (Alamo *et al.*, 1997) at a lower temperature range and from the MD simulation (Choi, 2000) at comparable temperatures. Alamo *et al.* found that at 160 °C if the branch content of LLDPE is lower than 40, HDPE/LLDPE blends are miscible, while if the branch content of LLDPE is higher than 80, the blends are immiscible. Choi's results showed that 50 is the cutoff value to induce immiscibility. The present IGC results are in good agreement with these findings.

140

From a molecular structure perspective, such branch content dependence of χ_{23} is not unreasonable. This is because by adding more branches to the backbone of a polyethylene molecule, the distribution of the torsional angles of the backbone is disturbed. As a result, linear and branched molecules will have different local structures and such differences will lead to phase separation even though the molecules interact via similar van der Waals interactions. Moreover, the interaction energy of the CH_2, CH_3 and CH groups is not exactly the same and would also contribute to the immiscibility. The major interacting groups existing in the HDPE molecules are the CH_2 groups. Due to the presence of the branches in LLDPE molecules, the above mentioned three types of interacting groups exist in the LLDPE molecules. Increasing the number of branches on the LLDPE molecules would increase the number of non-CH_2 group interactions. Consequently, the HDPE molecules composed of only CH_2 groups (neglecting the end groups) will separate from highly branched LLDPE molecules, which contain numerous CH_3 and CH groups. The present results are also consistent with an experimental observation that if the branch content distribution of LLDPE chain molecules is broad enough, the highly branched molecules (> 100 branches per 1,000 backbone carbons) phase separate from the lightly branched matrix (Mirabella $et\ al.$, 1988).

6.4 Summary

The miscibility between HDPE and LLDPE with variable branch contents over their processing temperature range was studied at three compositions by IGC along with

141

the data analysis method proposed in Chapter 3. Based on the obtained results, this data analysis method was found applicable to the HDPE/LLDPE systems. The results showed that for the same pair of HDPE and LLDPE blend at different compositions, 50/50 blend was more miscible than those at other compositions. The effect of temperature on miscibility depends on the composition of the blends and the branch content of LLDPE studied. In particular, I found that the branch content of LLDPE strongly influenced the miscibility of the blends. And it seems that large differences in branch contents of the constituent polyethylenes induced immiscibility. My data suggested that when the branch content was higher than 50 branches per 1,000 backbone carbons, the blend might phase separate. In general, my findings are in good agreement with those determined by SANS measurements and MD simulations.

6.5 References

Alamo, R.G., Graessley, W.W., Krishnamoorti, R., Lohse, D.J., Londono, J.D., Mandelkern, L., Stehling, F.C. and Wignall, G.D. (1997) Small Angle Neutron Scattering Investigations of Melt Miscibility and Phase Segregation in Blends of Linear and Branched Polyethylenes as a Function of the Branch Content, Molecules, *Macromolecules*, 30, 561-566.

Choi, P. (2000) Molecular Dynamics Studies of the Thermodynamics of HDPE/Butene-Based LLDPE Blends, *Polymer*, 41, 8741-8747.

Graessley, W.W., Krishnamoorti, R., Balsara, N.P., Fetters, L.J., Lohse, D.J., Schulz, D.N. and Sossano, J.A. (1994) Thermodynamics of Mixing for Blends of Model Ethylene-Butene Co-polymers, *Macromolecules*, 27, 3896-3901.

Han, S.J., Lohse, D.J., Condo, P.D. and Sperling, L.H. (1999) Pressure-Volume-Temperature Properties of Polyolefin Liquids and Their Melt Miscibility, *Journal of Polymer Science: Part B: Polymer Physics*, 37, 2835-2844.

Hill, M.J., Barham, P.J. and van Ruiten, J. (1993) Liquid-Liquid Phase Segregation in Blends of a Linear Polyethylene with a Series of Octene Copolymers of Differing Branch Content, *Polymer*, 34(14), 2975-2679.

Jinnai, H., Hasehawa, H. and Hashimoto, T. (1992) Inversion of the Phase Diagram from UCST to LCST in Deuterated Polybutadiene and Protonated Polybutadiene blends, *Macromolecules*, 25, 6078-6080.

Mirabella, F.M., Westphal, S.P., Fernando, P.L., Ford, E.A, and Williams, J.G. (1988) Morphological Explanation of the Extraordinary Fracture-Toughness of Linear Low-Density Polyethylenes, *J. Polym. Sci. (B) Polym. Phys.*, 26, 1995-2005.

Rhee, J. and Crist, B. (1991) Thermodynamics and Phase Separation in Melt Blends of Polyethylene and Model Copolymers, *Macromolecules*, 24, 5663-5669.

Taylor, J.K., Debenedetti, P.G., Graessley, W.W. and Kumar, S.K. (1996) Compressibility Effects in the Analysis and Interpretation of Neutron Scattering Data from Polymer Blends, *Macromolecules*, 29, 764-773.

Table 6.1 Characteristics of HDPE and LLDPEs

RESIN	DENSITY @ 25 $^{\circ}$C (g/cm^3)	M_n	M_w	BRANCH CONTENT BRANCHES/1,000 CARBON ATOMS
HDPE	0.962	13,700	49,400	~0
LLDPE-1	0.938	34,600	69,200	3.1
LLDPE-2	0.922	38,700	77,400	11.4
LLDPE-3	0.914	20,300	69,000	18.1
LLDPE-4	0.874	53,800	96,900	49.7
LLDPE-5	0.881	52,000	104,000	87.2

144

Table 6.2 Loadings and mass of HDPE, LLDPEs and their blends used in the GC columns

COLUMN NUMBER	COMPOSITION (weight% of HDPE)	LOADING (% w/w)	MASS OF POLYMER (g)
1	100%HDPE	8.80	0.05396
2	100%LLDPE-1	7.14	0.04920
3	30% HDPE+70%LLDPE-1	8.55	0.05431
4	50% HDPE+50%LLDPE-1	8.05	0.05411
5	70% HDPE+30%LLDPE-1	6.76	0.04173
6	100%LLDPE-2	7.14	0.04920
7	30% HDPE+70%LLDPE-2	8.55	0.05431
8	50% HDPE+50%LLDPE-2	8.05	0.05411
9	70% HDPE+30%LLDPE-2	6.76	0.04173
10	100%LLDPE-3	7.14	0.04920
11	30% HDPE+70%LLDPE-3	8.55	0.05431
12	50% HDPE+50%LLDPE-3	8.05	0.05411
13	70% HDPE+30%LLDPE-3	6.76	0.04173
14	100%LLDPE-4	7.14	0.04920
15	30% HDPE+70%LLDPE-4	8.55	0.05431
16	50% HDPE+50%LLDPE-4	8.05	0.05411
17	70% HDPE+30%LLDPE-4	6.76	0.04173
18	100%LLDPE-5	7.14	0.04920
19	30% HDPE+70%LLDPE-5	8.55	0.05431
20	50% HDPE+50%LLDPE-5	8.05	0.05411
21	70% HDPE+30%LLDPE-5	6.76	0.04173

Table 6.3 Measured Flory-Huggins interaction parameters between the selected solvents and pure HDPE, LLDPE-1 (LLDPE-5) and their 50/50 blend 170 and 190 °C.

PROBE	170 °C			190 °C		
	χ_{12}	χ_{13}	$\chi_{1(23)}$	χ_{12}	χ_{13}	$\chi_{1(23)}$
1 – Hexene	0.11	0.12 (0.13)	0.16	0.10	0.10 (0.12)	0.14
1-Octene	0.09	0.10 (0.11)	0.14	0.08	0.10 (0.11)	0.13
Benzene	0.19	0.20 (0.23)	0.27	0.18	0.20 (0.21)	0.25
Cyclohexane	0.11	0.11 (0.13)	0.18	0.11	0.11 (0.13)	0.17
n-Hexanes	0.10	0.11 (0.13)	0.15	0.09	0.10 (0.12)	0.13
n-Dodecane	0.05	0.06 (0.07)	0.09	0.04	0.05 (0.06)	0.08
n-Heptane	0.10	0.10 (0.11)	0.14	0.09	0.10 (0.11)	0.13
n-Nonane	0.08	0.08 (0.11)	0.12	0.07	0.08 (0.09)	0.11
n-Octane	0.08	0.09 (0.10)	0.13	0.08	0.09 (0.10)	0.12
Toluene	0.14	0.15 (0.17)	0.21	0.13	0.14 (0.17)	0.20
Xylenes	0.11	0.12 (0.14)	0.17	0.10	0.11 (0.13)	0.17

146

Table 6.4 Measured Flory-Huggins interaction parameters between the selected solvents and pure HDPE, LLDPE-1 (LLDPE-5) and their 50/50 blend 210 and 230 °C.

PROBE	210 °C			230 °C		
	χ_{12}	χ_{13}	$\chi_{1(23)}$	χ_{12}	χ_{13}	$\chi_{1(23)}$
1 – Hexene	0.08	0.09 (0.08)	0.12	0.03	0.04 (0.04)	0.06
1-Octene	0.07	0.09 (0.10)	0.13	0.08	0.09 (0.10)	0.11
Benzene	0.17	0.19 (0.20)	0.25	0.15	0.19 (0.18)	0.22
Cyclohexane	0.10	0.11 (0.12)	0.16	0.09	0.13 (0.10)	0.14
n-Hexanes	0.07	0.08 (0.09)	0.11	0.04	0.06 (0.05)	0.08
n-Dodecane	0.02	0.05 (0.05)	0.07	0.04	0.05 (0.05)	0.07
n-Heptane	0.09	0.10 (0.10)	0.12	0.08	0.09 (0.08)	0.11
n-Nonane	0.06	0.07 (0.08)	0.10	0.07	0.07 (0.07)	0.10
n-Octane	0.07	0.08 (0.08)	0.12	0.07	0.08 (0.08)	0.11
Toluene	0.12	0.14 (0.14)	0.19	0.13	0.13 (0.14)	0.18
Xylenes	0.09	0.11 (0.11)	0.15	0.10	0.12 (0.11)	0.15

147

Table 6.5 Measured polymer-polymer interaction parameters between HDPE and LLDPEs.

LLDPE	HDPE (WT%)	170 ^{O}C	190 ^{O}C	210 ^{O}C	230 ^{O}C
1	30%	-0.007±0.022	-0.027±0.02	-0.043±0.016	-0.020±0.015
	50%	-0.048±0.018	-0.072±0.016	-0.078±0.014	-0.075±0.012
	70%	-0.026±0.022	-0.043±0.02	-0.030±0.018	-0.063±0.014
2	30%	-0.030±0.024	-0.011±0.022	-0.030±0.021	-0.047±0.015
	50%	-0.034±0.019	-0.014±0.017	-0.018±0.017	-0.064±0.012
	70%	-0.021±0.022	-0.039±0.02	-0.005±0.02	-0.041±0.015
3	30%	-0.012±0.021	-0.004±0.019	-0.024±0.018	-0.020±0.014
	50%	-0.026±0.019	-0.005±0.17	-0.022±0.016	-0.034±0.012
	70%	-0.009±0.021	-0.023±0.019	-0.006±0.018	-0.014±0.014
4	30%	0.013±0.021	0.015±v0.021	0.002±0.019	0.042±0.015
	50%	0.008±0.019	0.014±0.018	0.006±0.017	0.014±0.013
	70%	0.016±0.021	0.015±0.02	0.022±0.019	0.011±0.015
5	30%	0.017±0.02	0.025±0.019	0.041±0.017	0.023±0.013
	50%	0.005±0.02	0.014±0.02	0.022±0.018	0.037±0.013
	70%	0.022±0.022	0.026±0.02	0.019±0.019	0.009±0.014

Figure 6.1 Plots of $\chi_{1(23)}$ versus $(\phi_2\chi_{12}+\phi_3\chi_{13})$ for the 50:50 HDPE/LLDPE-1 blends at

four elevated temperatures. (a) T=170 °C; (b) T=190 °C; (c) T=210 °C; (d) T=230 °C

(a)

(b)

(c)

(d)

149
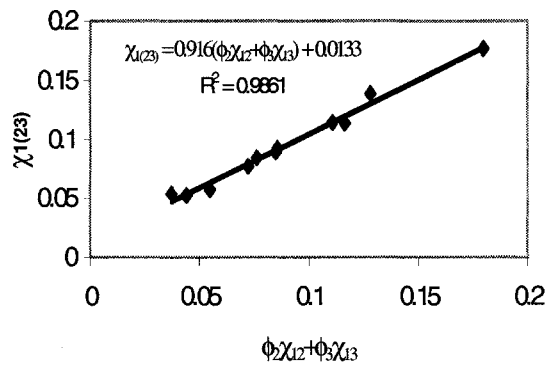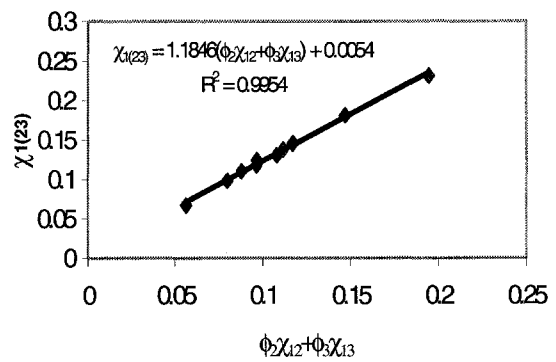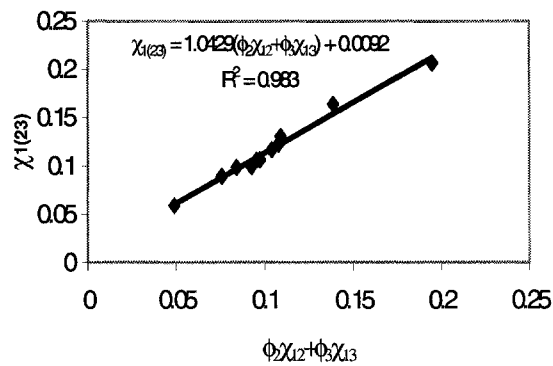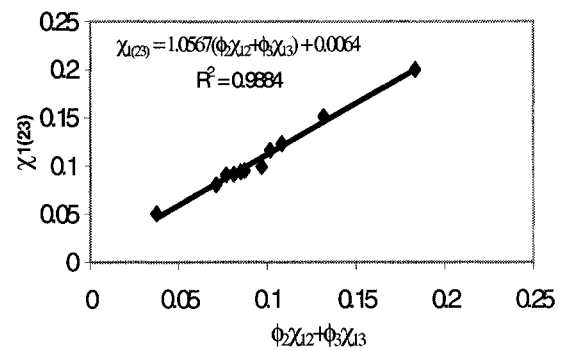
Figure 6.2 Composition dependence of χ_{23} of the HDPE/LLDPE-1 blends at various temperatures
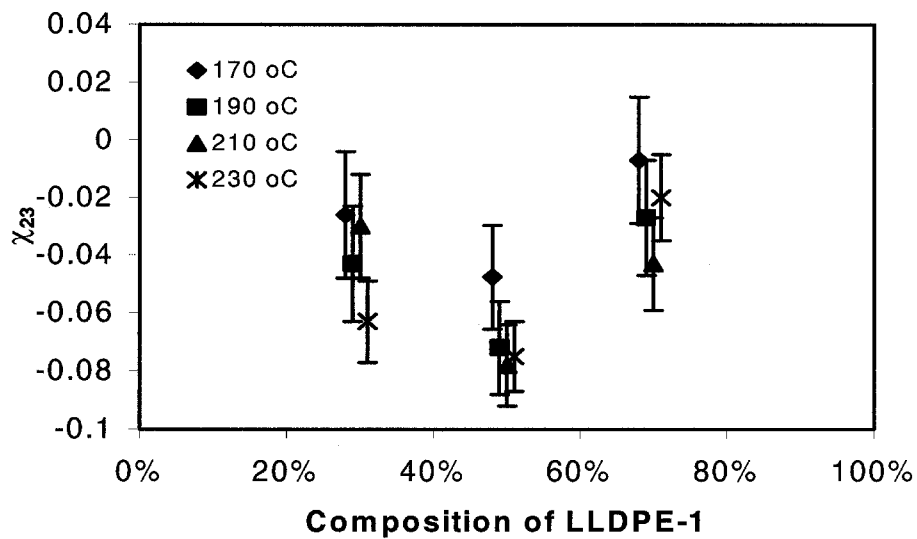
Figure 6.3 Composition dependence of χ_{23} of the HDPE/LLDPE-2 blends at various temperatures

150
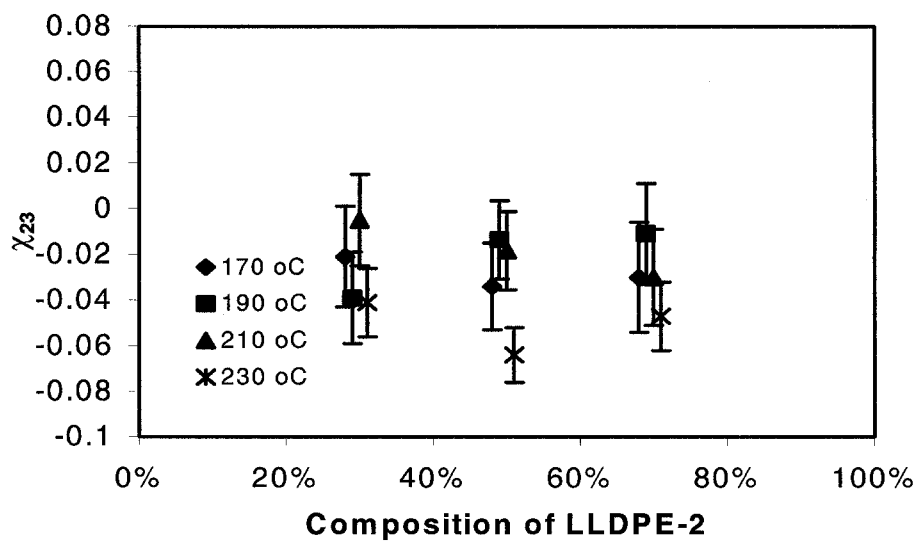
Figure 6.4 Composition dependence of χ_{23} of the HDPE/LLDPE-3 blends at various temperatures

Composition of LLDPE-3
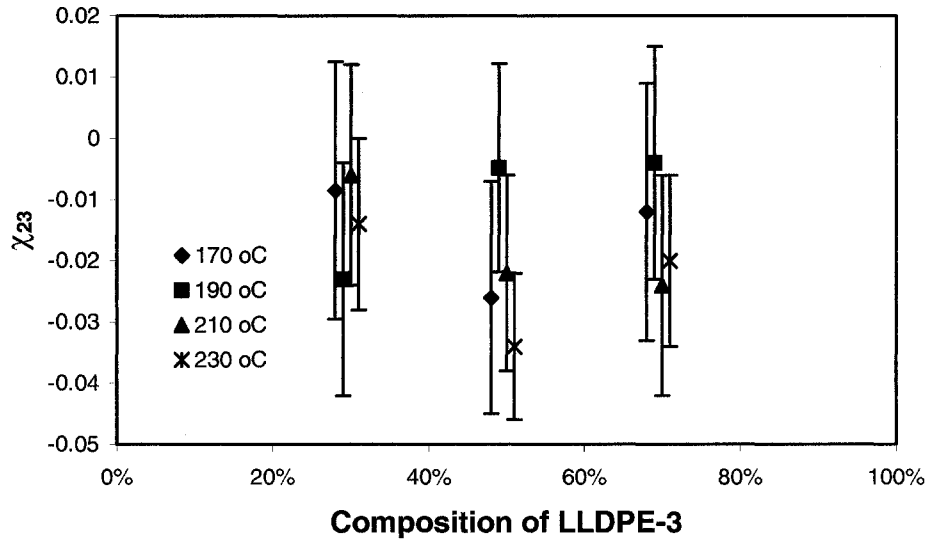
Figure 6.5 Composition dependence of χ_{23} of the HDPE/LLDPE-4 blends at various temperatures

Composition of LLDPE-4

151
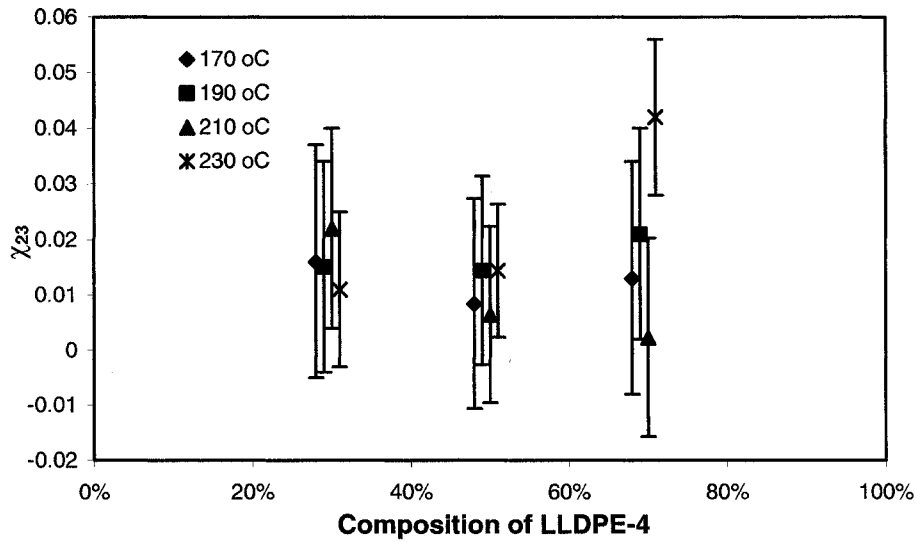
Figure 6.6 Composition dependence of χ_{23} of the HDPE/LLDPE-5 blends at various temperatures
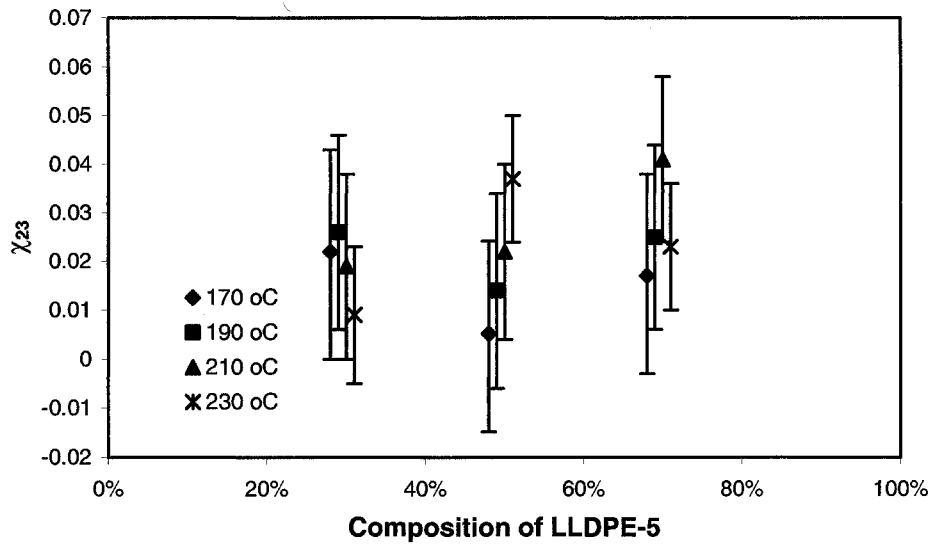
Figure 6.7 Temperature dependence of χ_{23} of the 30/70 HDPE/LLDPEs blends

152
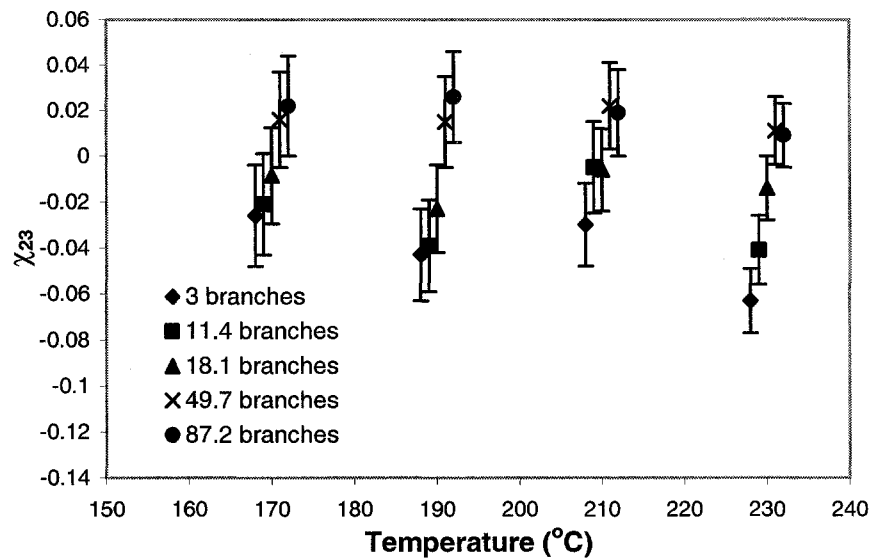
Figure 6.8 Temperature dependence of χ_{23} of the 50/50 HDPE/LLDPEs blends
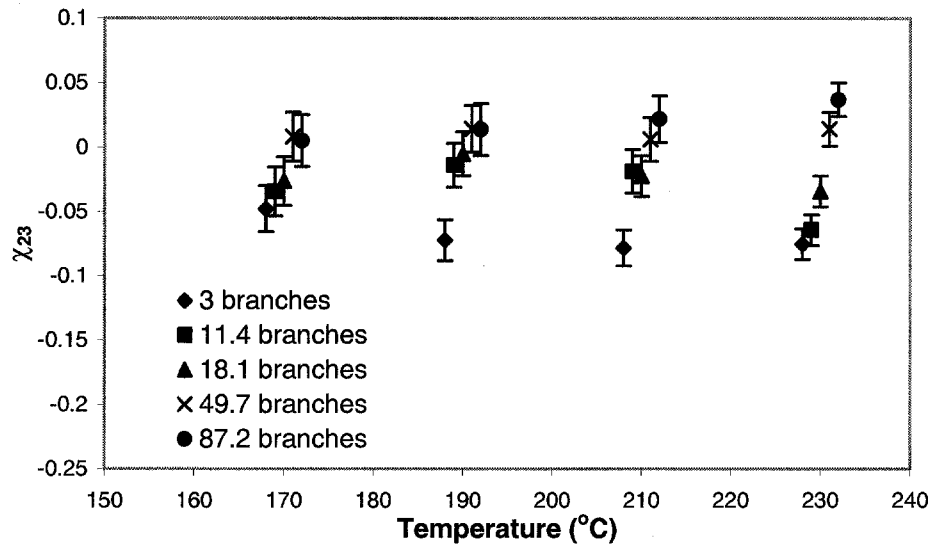
Figure 6.9 Temperature dependence of χ_{23} of the 70/30 HDPE/LLDPEs blends

153
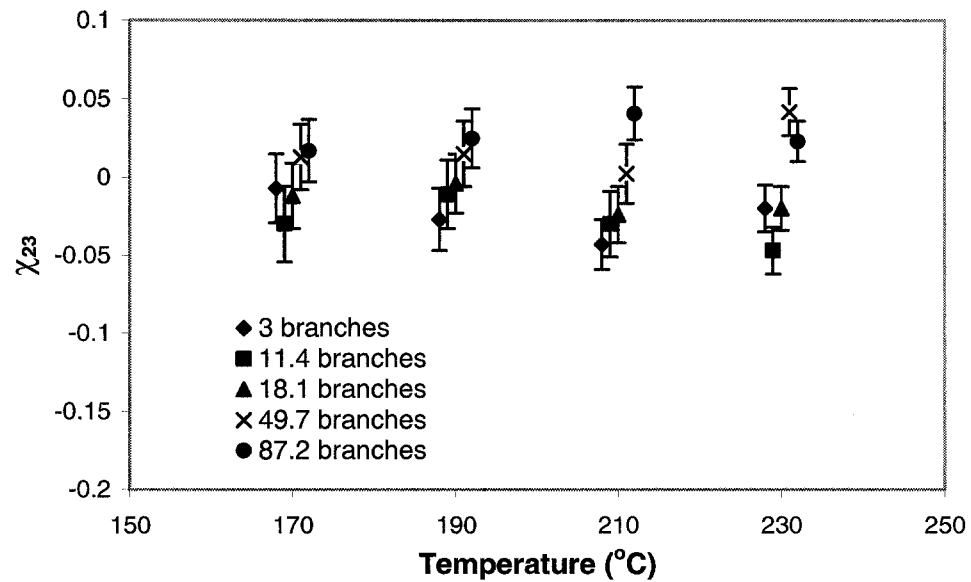
Figure 6.10 Effect of branch content of LLDPEs on the interaction parameters of the 50/50 HDPE/LLDPEs blends at various temperatures
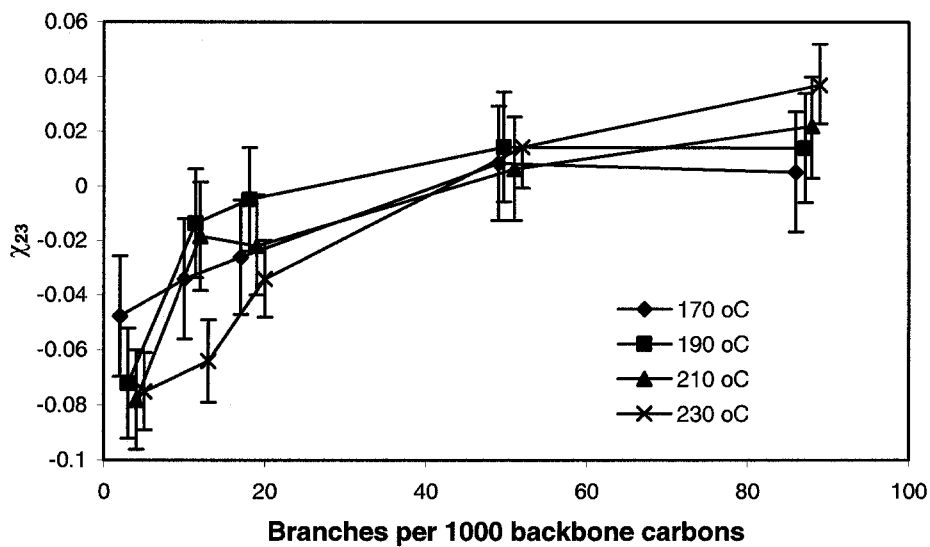
Figure 6.11 Effect of branch content of LLDPEs on the interaction parameters of the 30/70 HDPE/LLDPEs blends at various temperatures

154
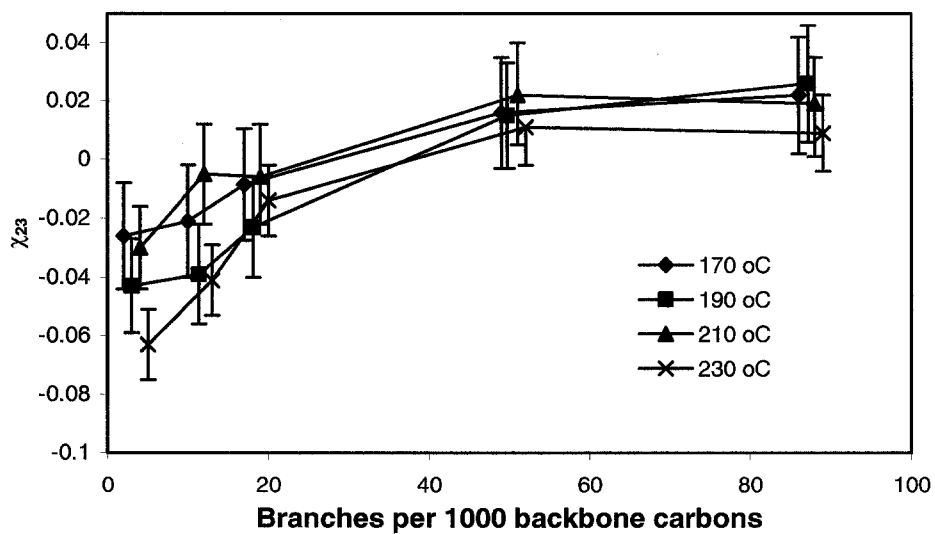
Figure 6.12 Effect of branch content of LLDPEs on the interaction parameters of the 70/30 HDPE/LLDPEs blends at various temperatures
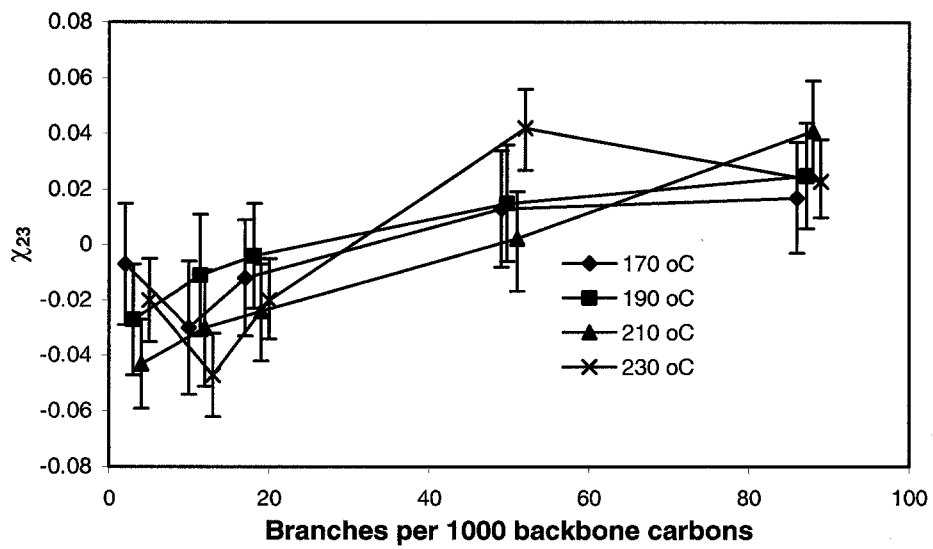
Chapter 7

Miscibility studies of LLDPE/LDPE blends

7.1 Introduction

In Chapter 3, I proposed a new data analysis method to obtain probe independent Flory-Huggins interaction parameters by IGC measurements. To verify the validity of this approach, I applied it to the HDPE/LDPE, HDPE/i-PP, HDPE/PS, and HDPE/LLDPE systems because of the existence of the extensive data on these blends in the literature. My results on the HDPE/i-PP and HDPE/PS blends suggested that the interaction parameters obtained from my method are consistent with those from neutron reflectivity (NR) and Monte Carlo simulations while they are about one order of magnitude larger than those obtained from SANS. There are no data available from NR measurements for the HDPE/LDPE and HDPE/LLDPE blends. However, when I compared my results with those from SANS, similar trends of the interaction parameters have been captured although the absolute values of interaction parameters from my work and SANS do not agree with each other. Based upon these results, it seems that IGC combined with my data analysis method provides a reasonably reliable low-cost alternative to estimate these parameters. Therefore, I have applied the technique to measure the interaction parameters of different LLDPE/LDPE blends.

LLDPE plays a very important role in the film industry because of its good mechanical properties. To obtain better processing properties, LLDPE is usually blended with other materials. It has been estimated that 60 to 70% of LLDPE enters the market as blends. In particular, LLDPE is blended with LDPE to improve processability and transparency. Determining miscibility of LLDPE and LDPE is quite important for successfully utilizing such systems in industry. However, studies on this topic in the literature are still lacking, especially, in the melt state. Hill and coworkers investigated the phase behavior of LLDPE/LDPE blends at 160 °C by means of DSC and TEM. The LLDPE they used has 15 branches and LDPE has overall 25 (10 long and 15 short) branches per 1,000 backbone carbons. Their results suggested that LDPE and LLDPE blends exhibit a closed loop shape phase diagram, which means that the blends are immiscible at intermediate temperature range (Hill and Puig, 1997). However, as mentioned previously, the techniques they used are still controversial to study the miscibility of polymer blends in the melt state.

To date, most studies on miscibility of LLDPE/LDPE blends have only focused on temperatures slightly above the melting temperatures of polyethylene (below 160 °C). To utilize miscibility information for improving the processing of these materials, it is more important to study the miscibility of those blends around their processing temperatures, which are around 200 °C. This work focuses on examining the effect of the molecular architecture and other characteristics of LLDPE on its miscibility with one LDPE at four elevated temperatures using IGC combined with the proposed data analysis method. Twelve LLDPEs with different branch contents, melt index, and branch

157

distribution were studied. The experimental results of these blends are discussed in this chapter.

7.2 Experimental

7.2.1 Materials and operating conditions

One LDPE and twelve LLDPEs were studied. Six LLDPE samples were polymerized using a Ziegler-Natta catalyst and the remaining six LLDPE samples were produced using a metallocene catalyst. All LLDPE samples were laboratory polymerized octene-based copolymers. Both LDPE and LLDPE samples were supplied by NOVA. The average molecular weights and branch contents, and melt index of the polymers are listed in Table 7.1. Here, "a" series stands for the Ziegler-Natta type LLDPE and "m" series stands for the metallocene type LLDPE. For each pair of LDPE and LLDPE, five columns were prepared including two pure polymers and three binary blends at different compositions (30, 50 and 70 wt%). The procedures used to prepare the columns were described in Chapter 3. The loadings and mass of polymer coated of the columns are listed in Table 7.2. For each column, four elevated temperatures (170, 190, 210, and 230 °C) were studied. The inlet pressure of the column was from 200 to 250 kPa and the outlet pressure was the atmosphere pressure. The operating conditions of GC were the same as described in Chapter 4.

158

7.3 Results and discussion

7.3.1 Polymer-polymer interaction parameters between LDPE and various LLDPEs

The measured retention times of the marker and different probes for the pure LDPE, each of the pure LLDPEs, and their 30/70, 50/50, and 70/30 blends at different temperatures are summarized in Appendix C. The corresponding specific retention volumes can be calculated from equation 3-1. For each specific column, variation of net retention time and net retention volume with temperature and the size of solvent molecules showed the same trends as those for the HDPE/LDPE and HDPE/LLDPE blends.

By substituting the specific retention volumes into equations 3-26 and 3-27, interaction parameters between the selected solvents and the pure polymers as well as their corresponding blends were calculated and summarized in Appendix D. Tables 7.3 and 7.4 shows the data for the 50/50 LLDPE-a1/LDPE blend at the experimental temperatures. From these tables it can be seen that the values of χ_{12} and χ_{13} are very comparable because LLDPE and LDPE have similar molecular structures, i.e., both LLDPE and LDPE have branches. However, in most of the cases, χ_{12} is slightly smaller than χ_{13} for the same solvent, which reflects the subtle difference in the molecular structures of LLDPE-a1 and LDPE. From Table 7.1, it can be found that the major difference between LLDPE-a1 and LDPE is the branch content. In particular, the branch contents of LLDPE-a1 and LDPE were 12 and 22 branches per 1,000 backbone carbons, respectively. As discussed in Chapter 6, most probes used were linear molecules and

159

easier to dissolve in the polymer with fewer branches. As a result, χ_{12} is slightly smaller than χ_{13}.

These data were then used to determine χ_{23} by plotting $\chi_{1(23)}$ against $(\phi_2\chi_{12} + \phi_3\chi_{13})$ using equation 3-28. The corresponding plots of 50/50 LLDPE-a1/LDPE blends at four elevated temperatures are shown in Figure 7.1. Figure 7.2 is the corresponding plot for the 50/50 LLDPE-m1/LDPE blend. It can be seen from these figures that equation 3-28 describes the experimental data remarkably well that the linearity of the regression line is quite good (R^2 close to 1) and the slopes are also very close to the expected value of 1. It can be concluded that the approach I proposed to obtain probe independent interaction parameters is also applicable to the LDPE and LLDPE (both metallocene catalyst LLDPE and Ziegler-Natta catalyst LLDPE) systems. Based on the intercepts of these lines, the resultant χ_{23} associated with errors were calculated for all blends at three compositions and four temperatures and are summarized in Table 7.5. The procedures for calculating errors are described in Appendix B. It can be seen from this table that for all blends, χ_{23} is in the order of 10^{-3} to 10^{-2} and the errors are in the order of 10^{-2}. In some cases, χ_{23} is negative and almost all these negative values of χ_{23} occurred at 230 °C.

7.3.2 Composition dependence of χ_{23} of binary blends with LDPE and different LLDPEs

Figures 7.3-7.14 depict the composition dependence of χ_{23} for the LLDPE/LDPE blends at four elevated temperatures. From these figures, it can be seen that in most of the

160

cases (except for blends containing LLDPE-a1 and LLDPE-a2), χ_{23} decreased with increasing concentration of LLDPE at 210 °C. For most of the blends, χ_{23} did not vary significantly with composition at 170 and 190 °C. At 230 °C, no general trend between χ_{23} and concentration of the blends could be obtained owing to the large errors associated with χ_{23}.

In general, χ_{23} decreased with increasing concentration of LLDPE (i.e., decreasing concentration of LDPE) at 210 °C for most of the blends. Therefore, my results suggested that adding more LDPE to the blend is more likely to cause phase separation at 210 °C. These results are consistent with findings of Hussein *et al.* (2001). In their work, only one pair of LLDPE and LDPE blend was studied. The LLDPE was a butene-based Ziegler-Natta product with M_w=105,000 g/mol. The LDPE had M_w=100,000 g/mol. The branch contents of LLDPE and LDPE were both 22 branches per 1,000 backbone carbons. Based on their rheological study, they found that at 220 °C the LLDPE/LDPE blend is immiscible around the 50/50 composition range. Miscibility is likely to occur in the LLDPE-rich blends. It is worth noting that the rheological study can only determine the miscibility qualitatively, and no χ_{23} can be obtained. The authors proposed that the immiscibility was attributed to the heterogeneity of the LLDPE sample and it was the highly branched molecules in the Ziegler-Natta LLDPE that caused the immiscibility. However, this argument cannot be used to explain the composition dependence of χ_{23} at 210 °C observed in my work for the blends containing the metallocene type of LLDPE as such heterogeneity does not exist. In my view, it is the LDPE that should be responsible for large χ_{23} values obtained at high LDPE

concentrations. This is because LDPE molecules contain both short and long branches. Here, it should be noted that Fan (2001) found that the critical branch content of LLDPE to induce immiscibility with HDPE is 50 branches per 1,000 backbone carbons, while that of LDPE is only 25. Therefore, the immiscibility of LLDPE/LDPE blends at high LDPE (low LLDPE) concentrations is attributed to the mismatch in the molecular conformations between components of the blends owing to the presence of long chain branching in the LDPE sample.

From a molecular point of view, the long branches on the LDPE molecules are bulky and form a network-like structure as illustrated in Figure 1.1. To a certain extent, a LDPE molecule can be considered as a structure that consists of crosslinked LLDPE molecules. These network-like LDPE molecules will exclude the LLDPE molecules in their surroundings. Therefore, miscibility of these two polymers is reduced. Moreover, increase in the concentration of LDPE will increase the number of long branches in the blend. And these long branches will further decrease the miscibility of the blend.

7.3.3 Temperature dependence of χ_{23} of the LLDPE/LDPE blends

Figures 7.15 to 7.26 are plots of χ_{23} versus temperature for the same sets of LLDPE/LDPE blends described in the previous section. It can be seen from these figures that in most of the cases (except for the blends containing LLDPE-a3 and LLDPE-m6), 30/70 LLDPE/LDPE blends including those containing Ziegler-Natta type of LLDPEs and metallocene type of LLDPEs, χ_{23} exhibited maxima at 210 °C. These results

162

suggested that the blends have both a lower critical solution temperature (LCST) and an upper critical solution temperature (UCST), indicating a closed-loop phase diagram.
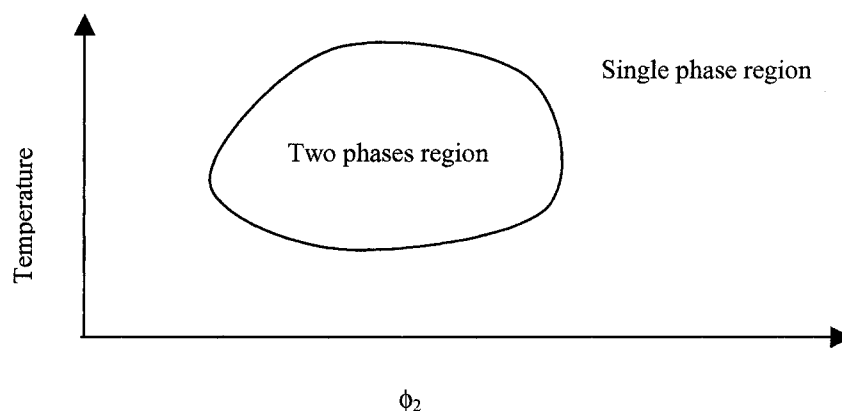
This closed-loop shape phase diagram is consistent with the findings of Hill and Puig (1997) on comparable systems. This kind of phase diagram cannot be explained by the original Flory-Huggins lattice theory because based on this theory, χ_{23} decreases with increasing temperature. The unexpected large χ_{23} value at 210 °C may be caused by the existence of the local orders in the polyethylene melts as described in Chapter 4. A thermal transition corresponding to these local orders has been found in the polyethylene melts at 210 °C.

For the 70/30 LLDPE/LDPE blends, χ_{23} showed a decreasing trend with temperature, especially from 210 to 230 °C. These results suggested that for blends containing more LLDPE, the temperature dependence of χ_{23} follows the prediction of the

163

original Flory-Huggins theory. For 50/50 LLDPE/LDPE blends, no general trend could be identified because of the large uncertainties associated with χ_{23}.

7.3.4 Effect of characteristics of LLDPE on its miscibility with LDPE

As mentioned previously, twelve LLDPEs were studied in this work to elucidate the effect of different characteristics of LLDPEs on their miscibility with LDPE. The characteristics of those LLDPEs are listed in Table 7.1. For example, between a1 and a2, I attempted to study the effect of branch content while between a3 and a4, the effect of polydispersity on miscibility. However, it can be seen from Table 7.5 and Figures 7.3 to 7.26 that χ_{23} values for the blends containing the LLDPEs are fairly close to each other at a given temperature and composition. The temperature dependence and the composition dependence of χ_{23} for different blends are also very similar. These observations imply that the present approach is not sensitive enough to detect the differences between the LLDPE/LDPE blends studied in the present work. I speculated that this might due to the small variation of each characteristic I intended to investigate. Use of broader ranges of the characteristics of LLDPE samples is suggested. It should also be emphasized that the samples used were lab products and it is very difficult to alter just one characteristic without changing the others. It can be seen from the data in Table 7.1 that not only the branch contents of a1 and a2 were different but also their polydispersities. These two factors may offset each other. As a result, the measured χ_{23} may not fully reflect the effect of the characteristic that one originally intends to study.

164

7.4 Summary

In this chapter, the miscibility between LDPE and different LLDPEs has been investigated by means of inverse gas chromatography along with the data analysis method proposed in Chapter 3. Twelve LLDPE samples, each of which having different characteristics, have been studied at three compositions and four temperatures. It was found that the experimental data could be well-described by equation 3-28 and the solvent independent interaction parameters were obtained for each pair of the blends. My results suggested that LLDPE/LDPE blends seemed to be miscible at 170 °C and 230 °C, but not at 210 °C because χ_{23} versus temperature plots exhibited maxima at around 210 °C. In terms of the composition effect, at 210 °C, χ_{23} decreased with increasing proportion of LLDPE in the blend. These results are in agreement with other researcher's findings (Hussein *et al.*, 2001). However, no obvious trend could be identified at other temperatures owing to the large errors associated with the measured χ_{23}. In terms of the effect of the characteristics of LLDPE used on miscibility, no meaningful conclusions could be drawn. This may be due to the fact that the range of variation of each characteristic that I am interested in is too narrow.

7.5 References

Fan, Z. (2001) MD and SEM Studies of Miscibility of Polyethylene Blends, Ph.D. thesis, University of Alberta.

Hill, M.J. and Puig, C.C. (1997) Liquid-Liquid Phase Separation in Blends of a Linear Low-Density Polyethylene with a Low-Density Polyethylene, *J. Appl. Polym. Sci.*, 65, 1921-1931.

Hussein, I.A. and Willians, M.C. (2001) Rheological Study of the Miscibility of LLDPE/LDPE Blends and the Influence of T_{mix}, *Polymer Engineering and Science*, 41(4), 696-701.

Table 7.1 Characteristics of LDPE and LLDPEs

RESIN	DENSITY @ 25 °C (g/cm³)	M_n	M_W	MELT INDEX	BRANCH CONTENT BRANCHES/1,000 CARBON ATOMS
LDPE	0.919	17,000	94,000	0.75	~22
LLDPE-a1	0.923	20,500	102,500	1.02	12.9
LLDPE-a2	0.902	17,300	105,530	1.02	35.0
LLDPE-a3	0.924	18,800	122,200	0.4	11.9
LLDPE-a4	0.923	26,400	116,160	0.65	12.7
LLDPE-a5	0.921	20,800	116,480	0.60	15.6
LLDPE-a6	0.919	25,500	112,200	0.70	15.3
LLDPE-m1	0.922	38,700	77,400	2.6	11.4
LLDPE-m2	0.902	25,700	69,390	3.2	30.4
LLDPE-m3	0.919	15,300	47,430	14.7	15.3
LLDPE-m4	0.917	10,500	99,750	0.72	19.6
LLDPE-m5	0.920	34,800	104,400	0.68	9.8
LLDPE-m6	0.917	33,200	92,960	0.92	10.6

Table 7.2 Loadings and mass of LLDPEs, LDPE and their blends used in the GC columns

COLUMN NUMBER	COMPOSITION (weight% of HDPE)	LOADING (% w/w)	MASS OF POLYMER (g)
1	100%LDPE	8.80	0.05396
2	100%LLDPE-1a	9.51	0.05987
3	30% LDPE+70%LLDPE-a1	7.68	0.04472
4	50% LDPE+50%LLDPE-a1	9.63	0.06058
5	70% LDPE+30%LLDPE-a1	8.49	0.05147
6	100%LLDPE-a2	6.53	0.03797
7	30% LDPE+70%LLDPE-a2	8.32	0.05163
8	50% LDPE+50%LLDPE-a2	8.87	0.05585
9	70% LDPE+30%LLDPE-a2	7.79	0.04644
10	100%LLDPE-a3	8.11	0.05296
11	30% LDPE+70%LLDPE-a3	7.20	0.04355
12	50% LDPE+50%LLDPE-a3	8.38	0.05031
13	70% LDPE+30%LLDPE-a3	9.66	0.06371
14	100%LLDPE-a4	8.52	0.05065
15	30% LDPE+70%LLDPE-a4	8.05	0.04890
16	50% LDPE+50%LLDPE-a4	9.01	0.05466
17	70% LDPE+30%LLDPE-a4	10.33	0.06269
18	100%LLDPE-a5	8.37	0.05211
19	30% LDPE+70%LLDPE-a5	9.39	0.05986
20	50% LDPE+50%LLDPE-a5	8.74	0.05088
21	70% LDPE+30%LLDPE-a5	9.90	0.06221
22	100%LLDPE-a6	7.07	0.03792
23	30% LDPE+70%LLDPE-a6	6.57	0.04009
24	50% LDPE+50%LLDPE-a6	8.60	0.05500
25	70% LDPE+30%LLDPE-a6	8.93	0.05429
26	100%LLDPE-m1	7.50	0.04715
27	30% LDPE+70%LLDPE-m1	9.41	0.05998
28	50% LDPE+50%LLDPE-m1	8.81	0.05626
29	70% LDPE+30%LLDPE-m1	8.28	0.05373
30	100%LLDPE-m2	9.97	0.06787
31	30% LDPE+70%LLDPE-m2	8.69	0.05562
32	50% LDPE+50%LLDPE-m2	9.13	0.05803

168

COLUMN NUMBER	COMPOSITION (WEIGHT% OF HDPE)	LOADING (% W/W)	MASS OF POLYMER (G)
33	70% LDPE+30%LLDPE-m2	9.94	0.06173
34	100%LLDPE-m3	8.77	0.05583
35	30% LDPE+70%LLDPE-m3	9.31	0.06001
36	50% LDPE+50%LLDPE-m3	9.24	0.05987
37	70% LDPE+30%LLDPE-m3	9.32	0.06112
38	100%LLDPE-m4	8.56	0.05337
39	30% LDPE+70%LLDPE-m4	7.62	0.04670
40	50% LDPE+50%LLDPE-m4	7.33	0.04819
41	70% LDPE+30%LLDPE-m4	8.57	0.06014
42	100%LLDPE-m5	6.85	0.04336
43	30% LDPE+70%LLDPE-m5	8.95	0.05824
44	50% LDPE+50%LLDPE-m5	8.31	0.05393
45	70% LDPE+30%LLDPE-m5	9.29	0.05880
46	100%LLDPE-m6	8.57	0.05737
47	30% LDPE+70%LLDPE-m6	7.67	0.05112
48	50% LDPE+50%LLDPE-m6	7.84	0.05463
49	70% LDPE+30%LLDPE-m6	9.49	0.06812

Table 7.3 Measured Flory-Huggins interaction parameters between the selected solvents and pure LLDPE-a1, LDPE and their 50/50 blend 170 and 190 °C.

PROBE	170 °C			190 °C		
	χ_{12}	χ_{13}	$\chi_{1(23)}$	χ_{12}	χ_{13}	$\chi_{1(23)}$
1 – Hexene	0.13	0.14	0.13	0.10	0.14	0.13
1-Octene	0.11	0.11	0.10	0.10	0.12	0.10
Benzene	0.21	0.22	0.21	0.20	0.22	0.20
Cyclohexane	0.13	0.13	0.12	0.11	0.15	0.12
n-Hexane	0.12	0.13	0.12	0.09	0.13	0.10
n-Dodecane	0.06	0.07	0.06	0.05	0.07	0.06
n-Heptane	0.11	0.12	0.11	0.09	0.12	0.10
n-Nonane	0.09	0.10	0.09	0.09	0.09	0.08
n-Octane	0.10	0.11	0.10	0.09	0.11	0.09
Toluene	0.16	0.17	0.16	0.15	0.17	0.15
Xylenes	0.15	0.14	0.13	0.12	0.13	0.13

170

Table 7.4 Measured Flory-Huggins interaction parameters between the selected solvents and pure LLDPE-a1, LDPE and their 50/50 blend 210 and 230 °C.

PROBES	210°C			230°C		
	χ_{12}	χ_{13}	$\chi_{1(23)}$	χ_{12}	χ_{13}	$\chi_{1(23)}$
1 – Hexene	0.09	0.09	0.07	0.04	0.04	0.04
1-Octene	0.09	0.10	0.08	0.08	0.09	0.09
Benzene	0.18	0.17	0.17	0.16	0.18	0.17
Cyclohexane	0.11	0.11	0.10	0.10	0.11	0.10
n-Hexanes	0.09	0.09	0.06	0.06	0.06	0.06
n-Dodecane	0.05	0.07	0.05	0.04	0.07	0.05
n-Heptane	0.10	0.10	0.08	0.08	0.08	0.08
n-Nonane	0.07	0.09	0.07	0.07	0.08	0.08
n-Octane	0.08	0.10	0.08	0.09	0.07	0.07
Toluene	0.14	0.14	0.14	0.15	0.12	0.13
Xylenes	0.11	0.12	0.11	0.11	0.11	0.11

171

Table 7.5 Measured polymer-polymer interaction parameters between LDPE and LLDPEs.

LLD PE	LDPE (WT%)	170 ^{O}C	190 ^{O}C	210 ^{O}C	230 ^{O}C
a1	30%	0.045±0.026	0.016±0.026	0.10±0.025	0.041±0.017
	50%	0.0084±0.022	0.031±0.022	0.078±0.022	-0.006±0.014
	70%	0.00048±0.03	0.035±0.03	0.12±0.033	0.019±0.021
a2	30%	0.023±0.031	0.029±0.031	0.11±0.031	0.042±0.02
	50%	0.012±0.025	0.021±0.023	0.027±0.024	-0.026±0.015
	70%	0.038±0.031	0.027±0.028	0.0784±0.032	0.0052±0.019
a3	30%	0.0029±0.026	-0.0073±0.025	0.014±0.023	0.024±0.018
	50%	0.026±0.025	0.046±0.024	0.022±0.024	-0.0056±0.017
	70%	0.0085±0.031	0.078±0.031	0.074±0.035	-00028±0.021
a4	30%	0.021±0.025	0.029±0.025	0.033±0.023	-0.035±0.015
	50%	0.014±0.023	0.055±0.024	0.057±0.023	-0.016±0.014
	70%	0.027±0.029	0.078±0.029	0.12±0.031	0.063±0.018
a5	30%	-0.013±0.025	-0.012±0.026	0.0038±0.027	-0.082±0.016
	50%	0.0068±0.024	0.015±0.023	0.081±0.026	0.014±0.016
	70%	0.0042±0.027	0.033±0.026	0.011±0.03	0.017±0.018
a6	30%	0.038±0.037	0.013±0.03	0.011±0.028	-0.042±0.017
	50%	0.048±0.033	0.054±0.024	0.061±0.025	0.041±0.017
	70%	0.022±0.034	0.014±0.033	0.14±0.037	0.054±0.02
m1	30%	0.023±0.028	0.052±0.026	0.068±0.026	0.00043±0.018
	50%	0.015±0.024	0.084±0.023	0.12±0.024	0.046±0.016
	70%	0.038±0.027	0.055±0.026	0.16±0.03	0.027±0.019
m2	30%	0.045±0.026	0.047±0.025	0.082±0.025	0.0061±0.025
	50%	0.022±0.024	0.046±0.024	0.072±0.025	0.019±0.023
	70%	0.048±0.028	0.095±0.028	0.098±0.031	0.067±0.028
m3	30%	0.0079±0.024	0.027±0.024	0.052±0.022	0.014±0.015
	50%	0.032±0.022	0.057±0.022	0.094±0.022	0.047±0.014
	70%	0.040±0.026	0.079±0.026	0.11±0.029	0.013±0.018
m4	30%	0.020±0.025	0.059±0.024	0.031±0.023	0.010±0.015
	50%	0.023±0.025	0.052±0.024	0.098±0.024	0.018±0.016
	70%	0.021±0.03	0.081±0.029	0.14±0.032	0.039±0.002
m5	30%	-0.033±0.029	0.0042±0.027	-0.013±0.025	-0.063±0.015
	50%	0.014±0.025	0.037±0.024	0.078±0.024	-0.021±0.014
	70%	-0.00033±0.028	0.042±0.027	0.080±0.03	-0.00094±0.017
m6	30%	-0.0079±0.023	0.0075±0.022	0.037±0.022	0.023±0.015
	50%	0.043±0.023	0.063±0.022	0.011±0.023	0.033±0.015
	70%	0.053±0.028	0.088±0.028	0.012±0.031	0.063±0.019

172

Figure 7.1 Plots of $\chi_{1(23)}$ vs $(\phi_2\chi_{12}+\phi_3\chi_{13})$ for the 50:50 LDPE/LLDPE-a1 blends at four

elevated temperatures. (a) T=170 °C; (b) T=190 °C; (c) T=210 °C; (d) T=230 °C

$$\chi_{1(23)} = 0.9612(\phi_2\chi_{12}+\phi_3\chi_{13}) - 0.0021$$
$$R^2 = 0.9916$$

(a)

$$\chi_{1(23)} = 1.0014(\phi_2\chi_{12}+\phi_3\chi_{13}) - 0.0077$$
$$R^2 = 0.9816$$

(b)

$$\chi_{1(23)} = 1.0777(\phi_2\chi_{12}+\phi_3\chi_{13}) - 0.0196$$
$$R^2 = 0.9612$$

(c)

$$\chi_{1(23)} = 0.9755(\phi_2\chi_{12}+\phi_3\chi_{13}) + 0.0015$$
$$R^2 = 0.9815$$

(d)

173
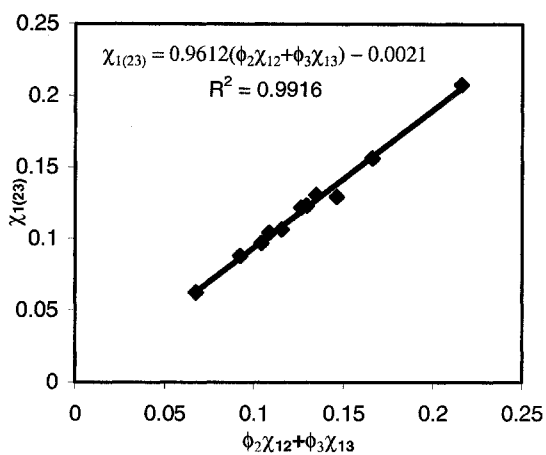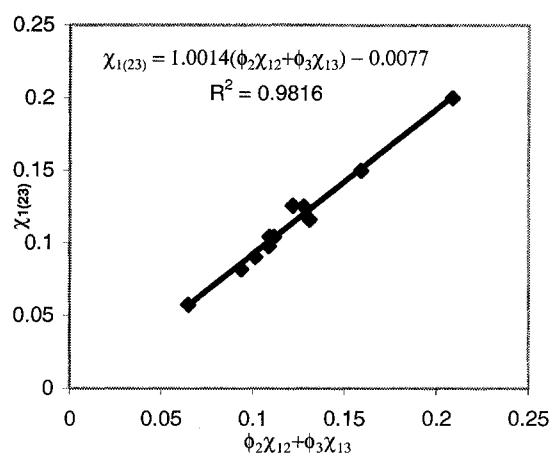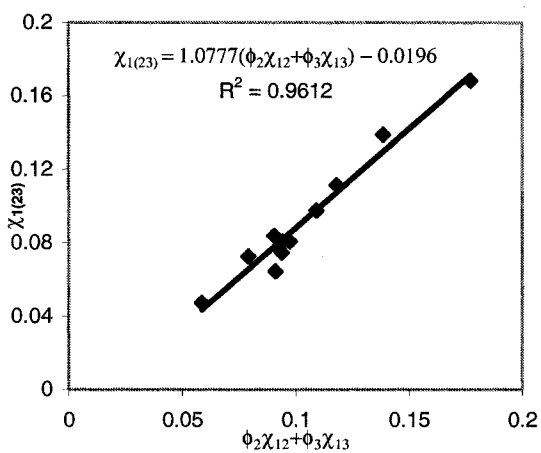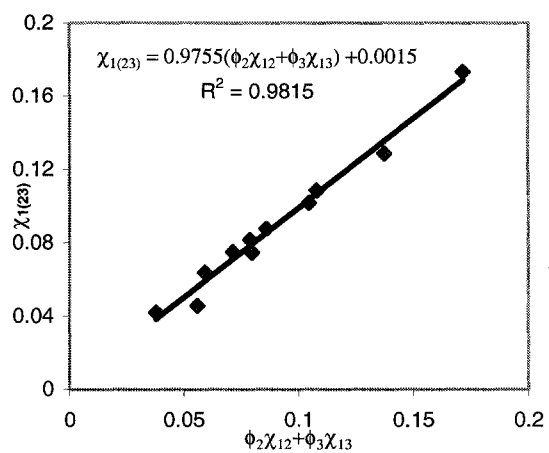
Figure 7.2 Plots of $\chi_{1(23)}$ vs $(\phi_2\chi_{12}+\phi_3\chi_{13})$ for the 50:50 HDPE/LLDPE-m1 blends at four elevated temperatures. (a) T=170 °C; (b) T=190 °C; (c) T=210 °C; (d) T=230 °C

(a)

(b)

(c)

(d)

174
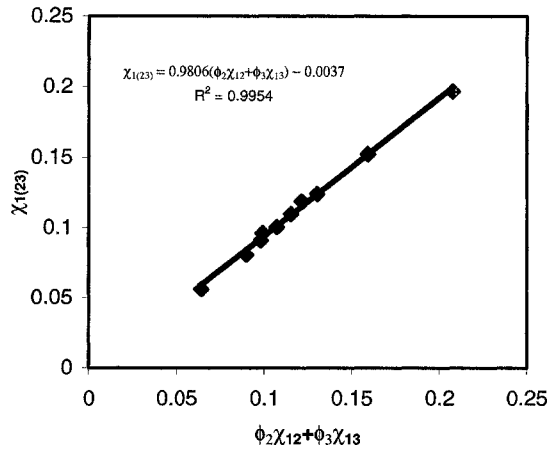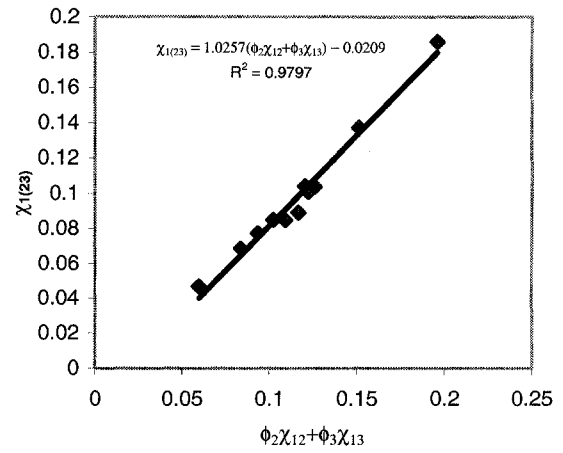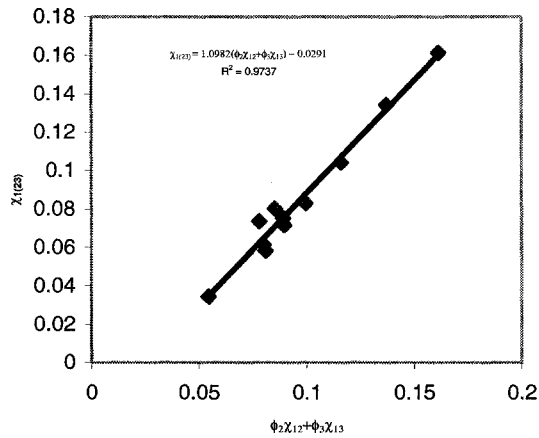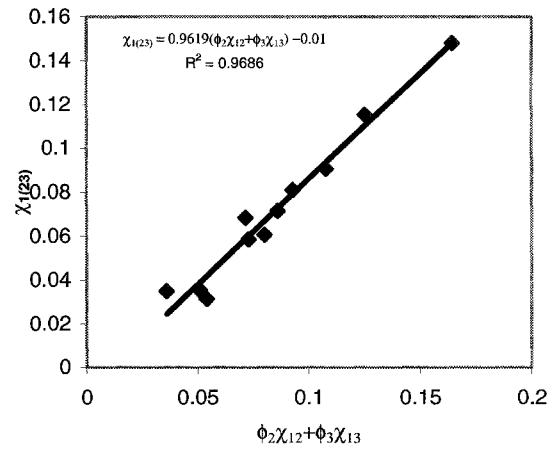
Figure 7.3 Composition dependence of χ_{23} of the LDPE/LLDPE-a1 blends at various temperatures
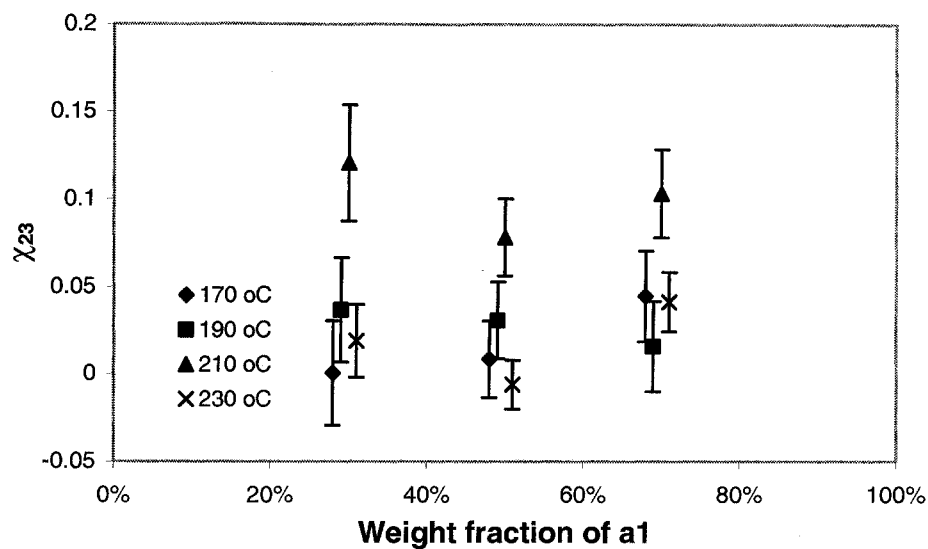
Figure 7.4 Composition dependence of χ_{23} of the LDPE/LLDPE-a2 blends at various temperatures

175
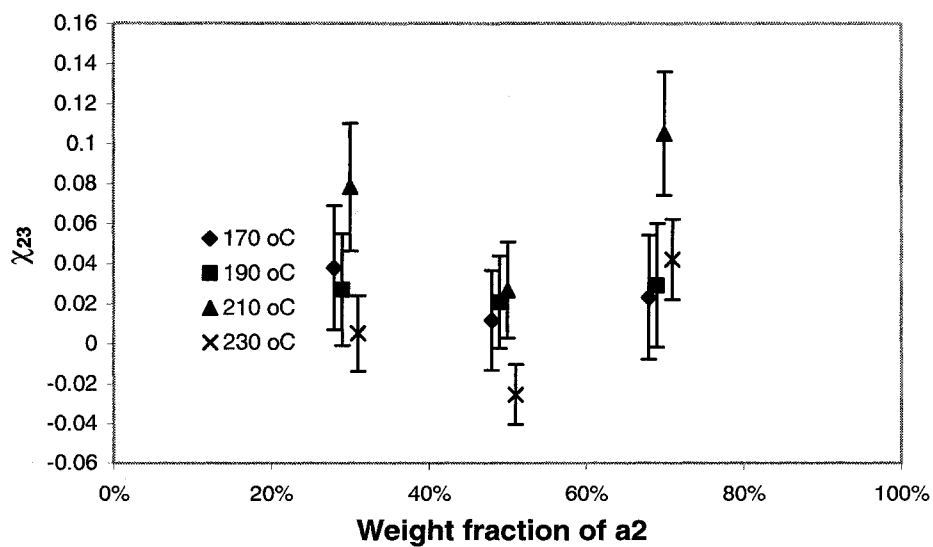
Figure 7.5 Composition dependence of χ_{23} of the LDPE/LLDPE-a3 blends at various temperatures
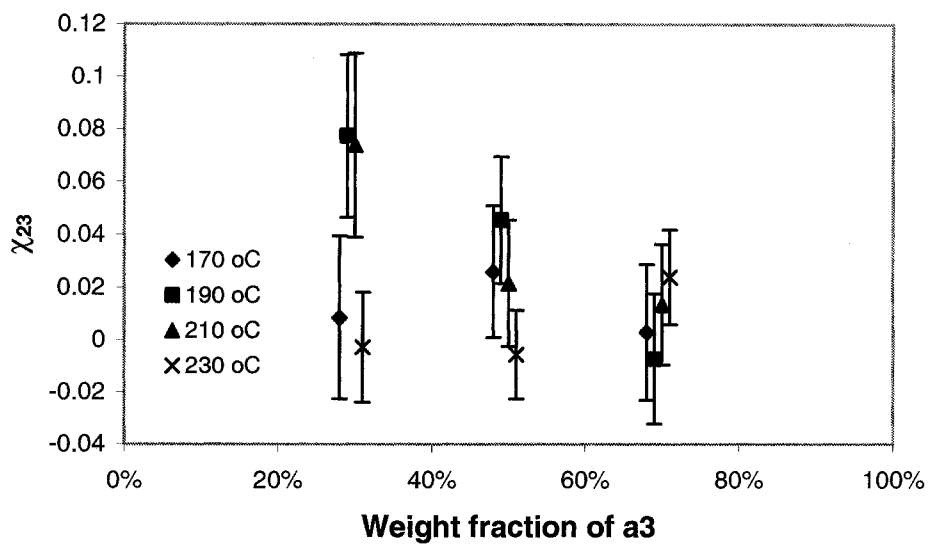
Figure 7.6 Composition dependence of χ_{23} of the LDPE/LLDPE-a4 blends at various temperatures

176
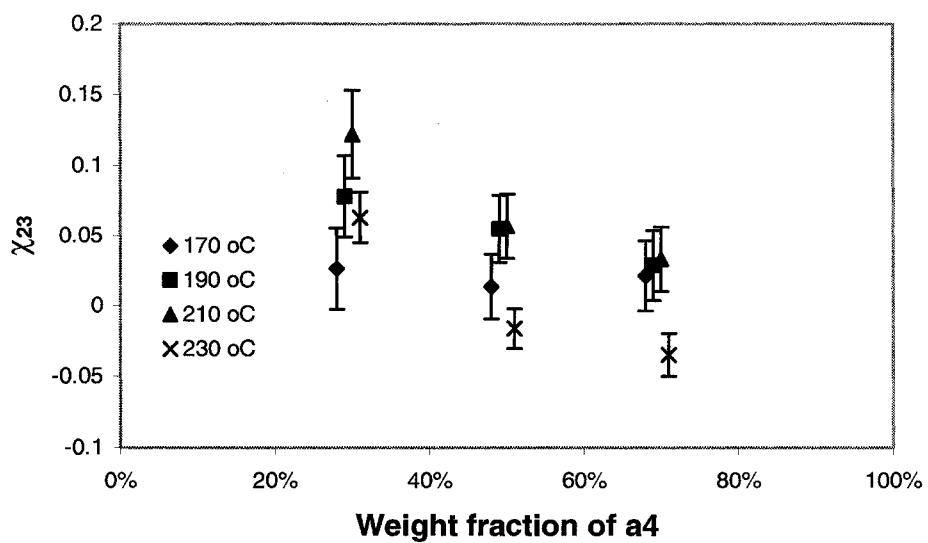
Figure 7.7 Composition dependence of χ_{23} of the LDPE/LLDPE-a5 blends at various temperatures
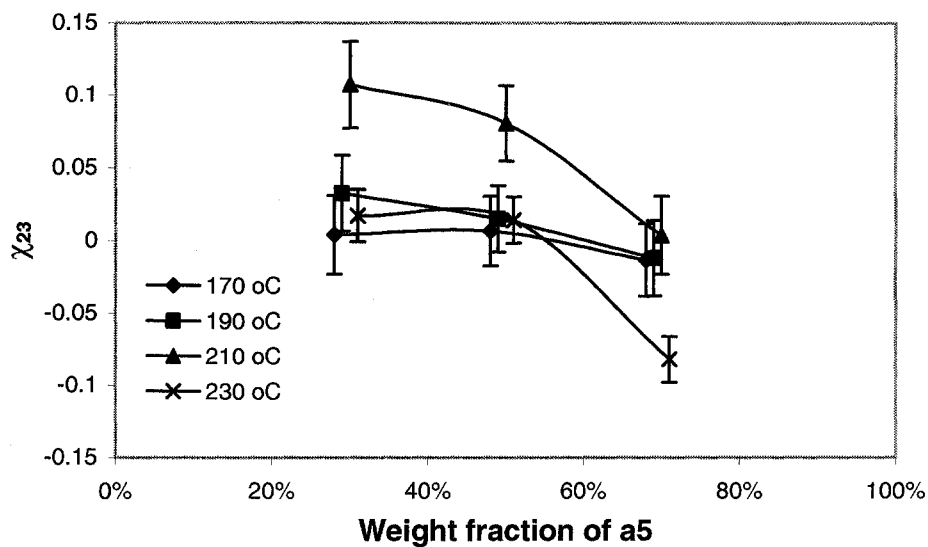
Figure 7.8 Composition dependence of χ_{23} of the LDPE/LLDPE-a6 blends at various temperatures

177
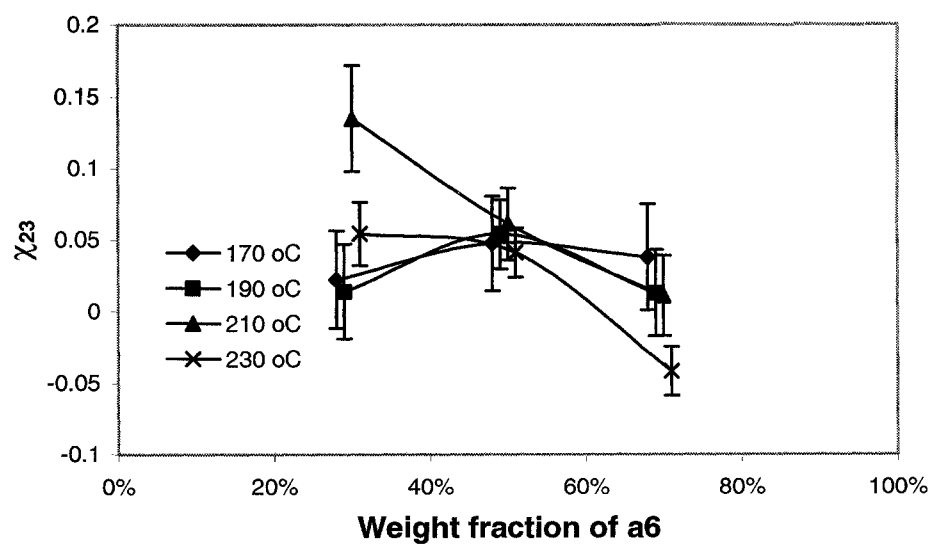
Figure 7.9 Composition dependence of χ_{23} of the LDPE/LLDPE-m1 blends at various temperatures
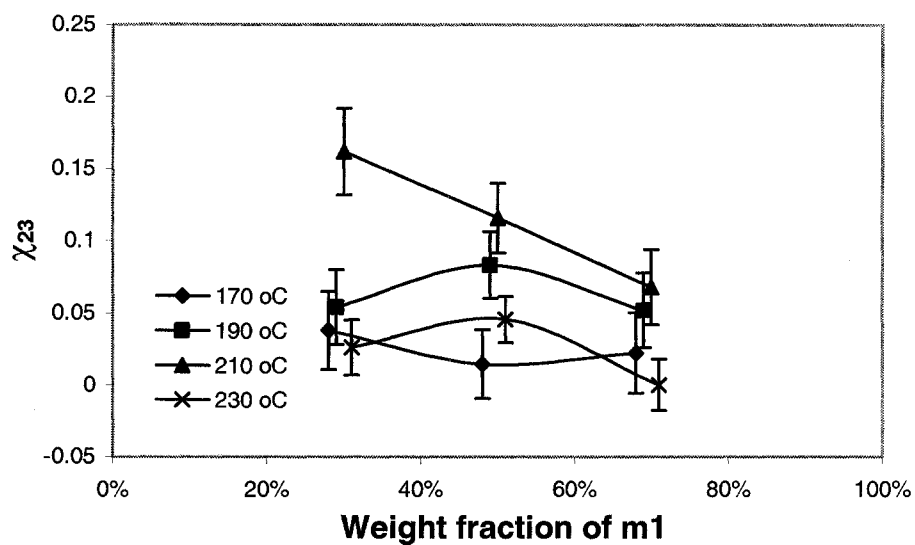
Figure 7.10 Composition dependence of χ_{23} of the LDPE/LLDPE-m2 blends at various temperatures

178
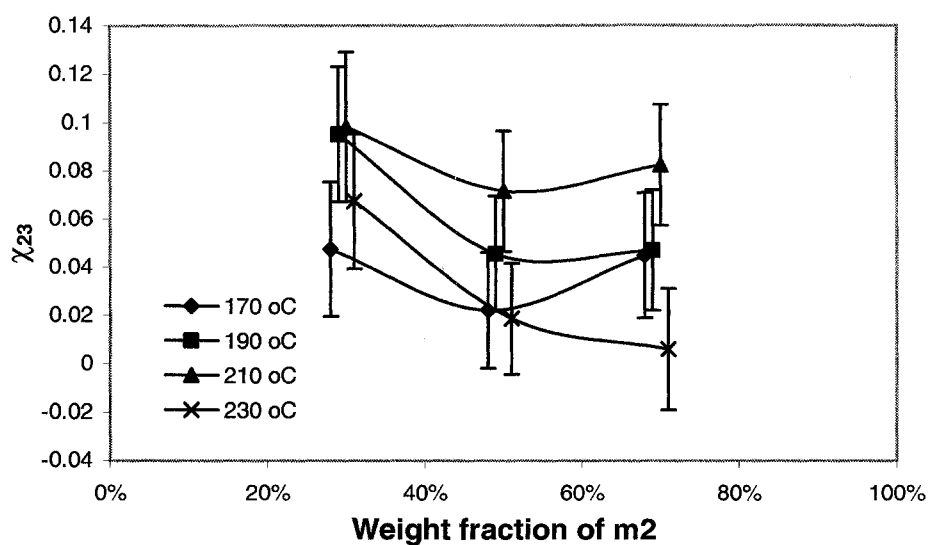
Figure 7.11 Composition dependence of χ_{23} of the LDPE/LLDPE-m3 blends at various
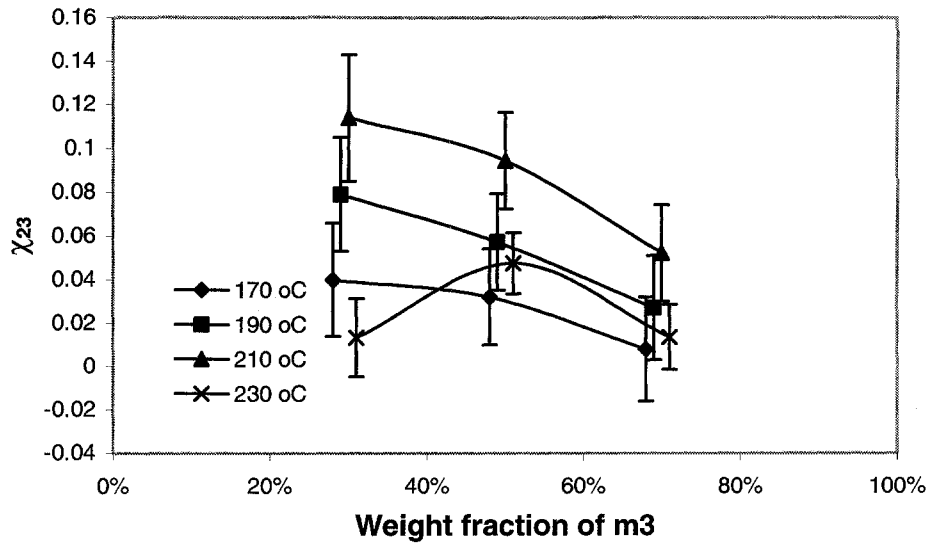
temperatures

Figure 7.12 Composition dependence of χ_{23} of the LDPE/LLDPE-m4 blends at various

temperatures

179
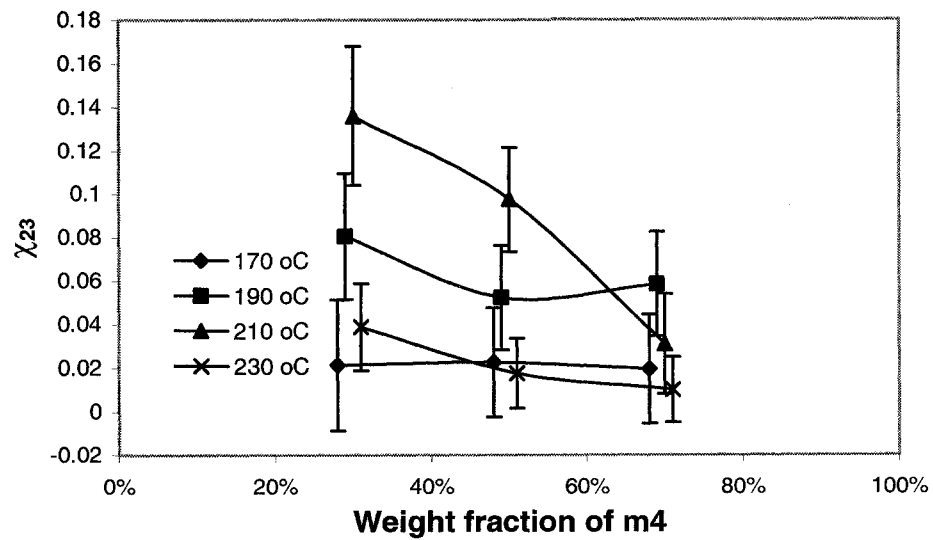
Figure 7.13 Composition dependence of χ_{23} of the LDPE/LLDPE-m5 blends at various temperatures
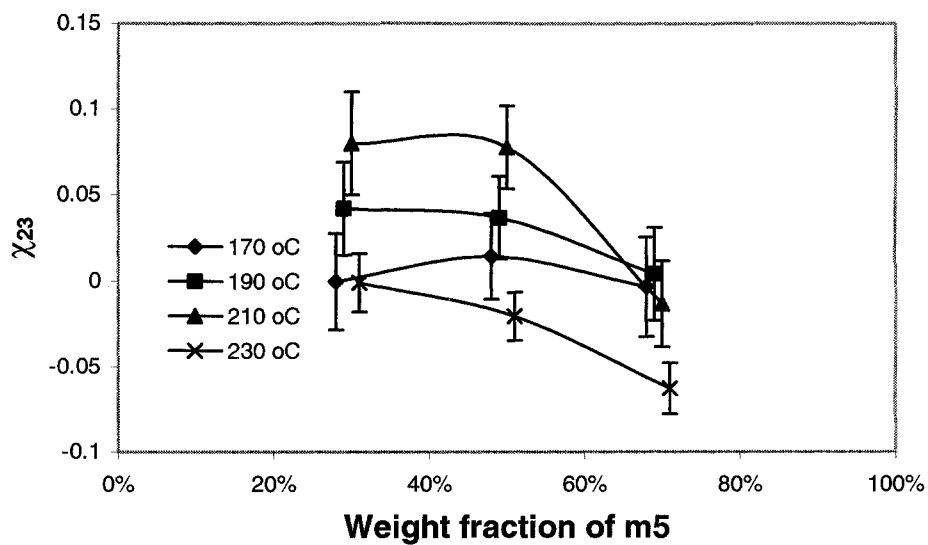
Figure 7.14 Composition dependence of χ_{23} of the LDPE/LLDPE-m6 blends at various temperatures

180
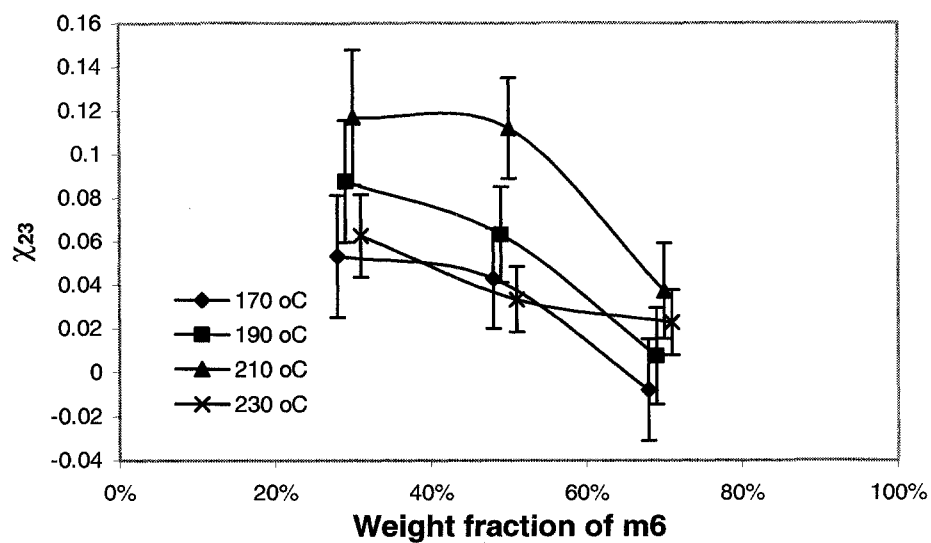
Figure 7.15 Temperature dependence of χ_{23} of the LDPE/LLDPE-a1 blends at various
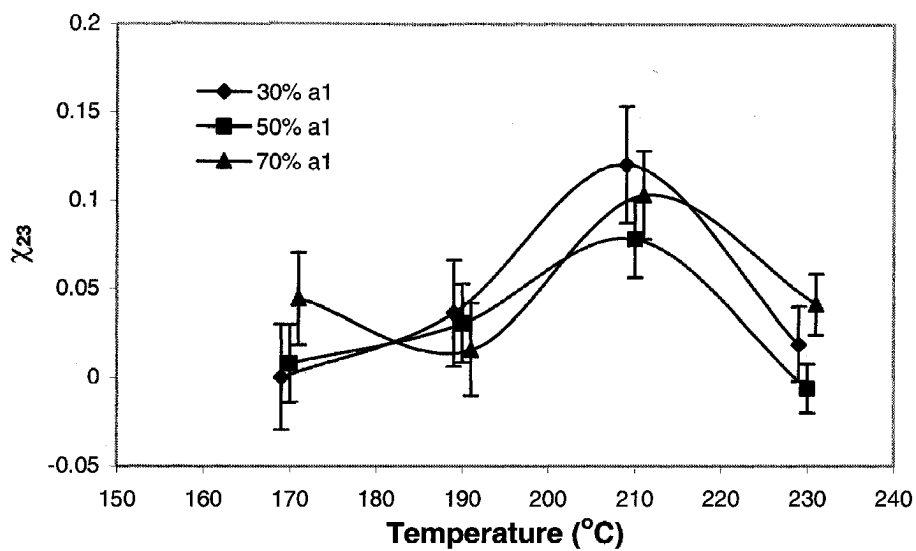
compositions

Figure 7.16 Temperature dependence of χ_{23} of the LDPE/LLDPE-a2 blends at various

compositions

181
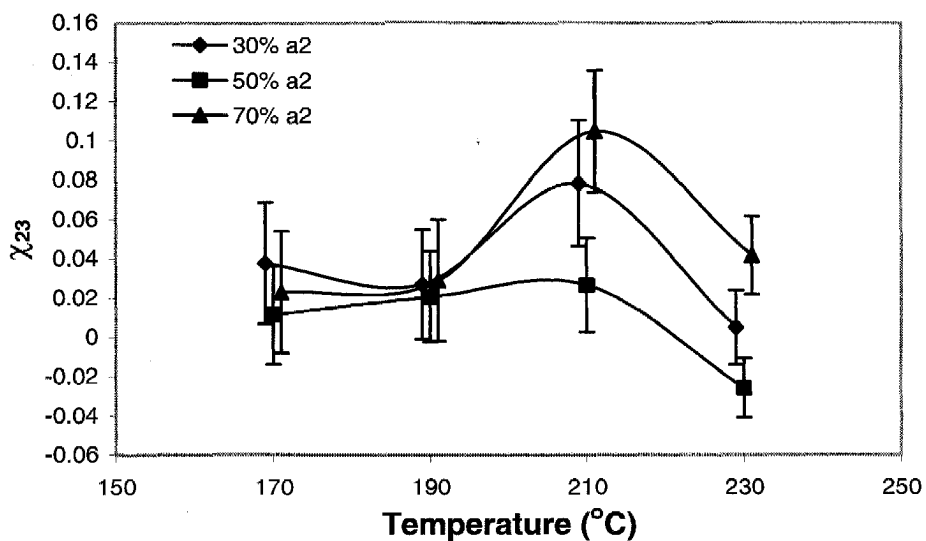
Figure 7.17 Temperature dependence of χ_{23} of the LDPE/LLDPE-a3 blends at various
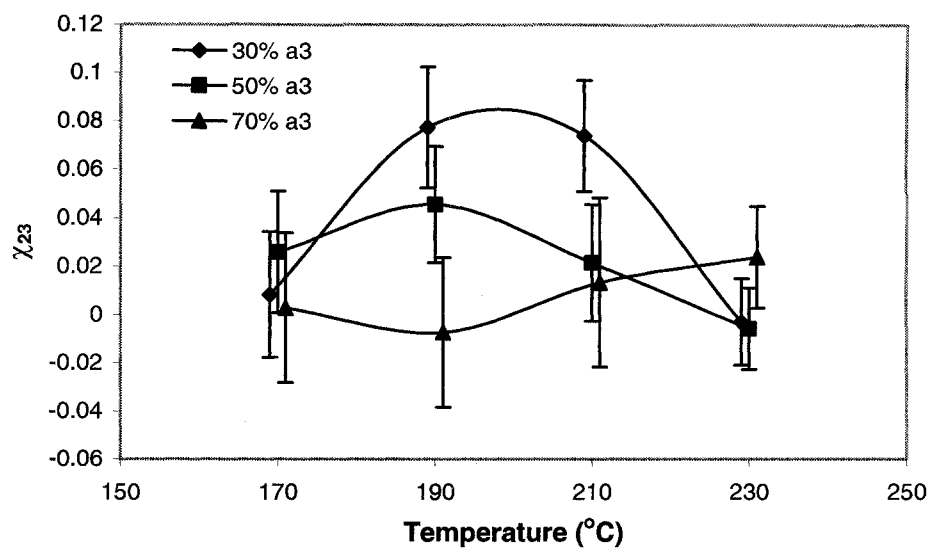
compositions

Figure 7.18 Temperature dependence of χ_{23} of the LDPE/LLDPE-a4 blends at various

compositions

182
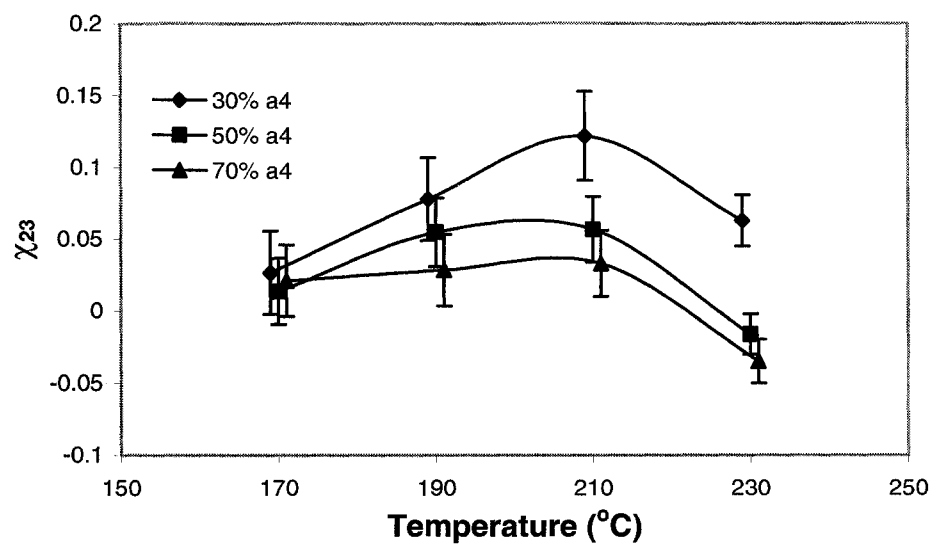
Figure 7.19 Temperature dependence of χ_{23} of the LDPE/LLDPE-a5 blends at various compositions
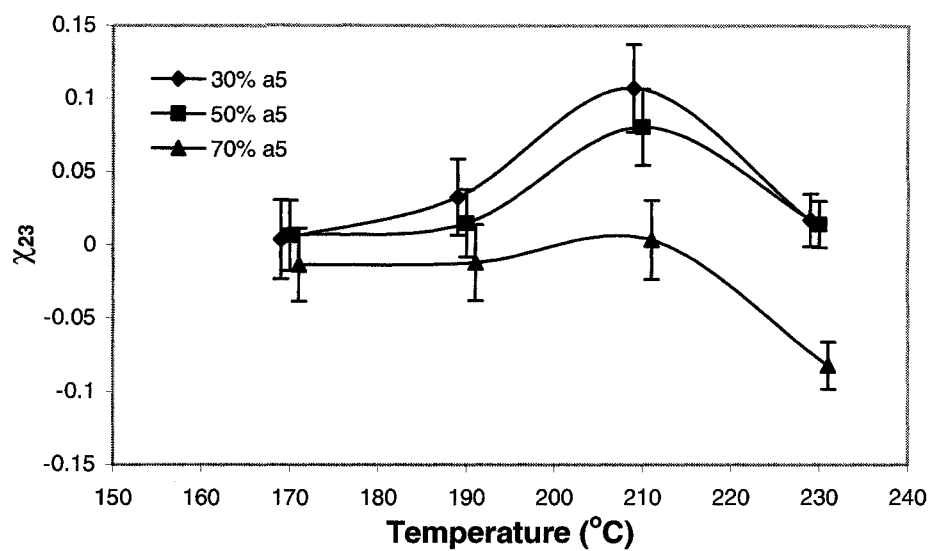
Figure 7.20 Temperature dependence of χ_{23} of the LDPE/LLDPE-a6 blends at various compositions

183
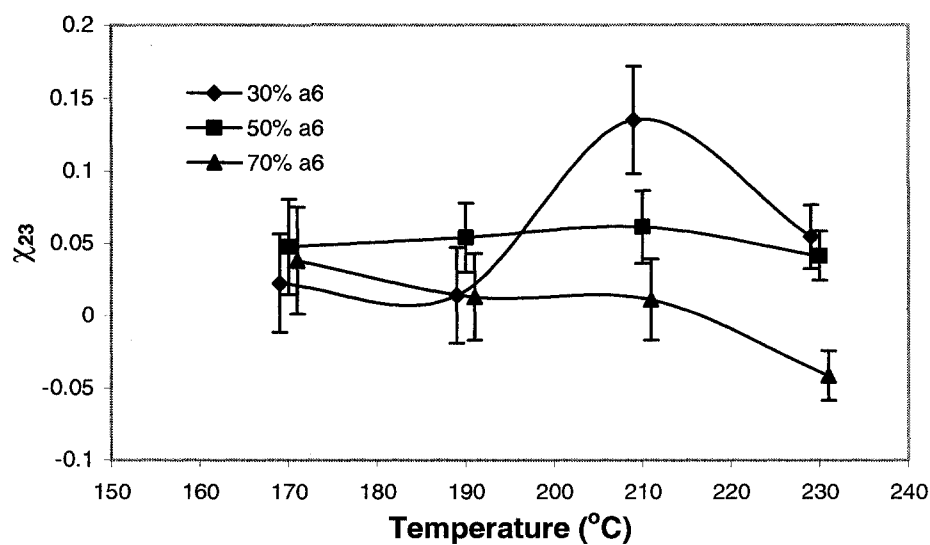
Figure 7.21 Temperature dependence of χ_{23} of the LDPE/LLDPE-m1 blends at various compositions
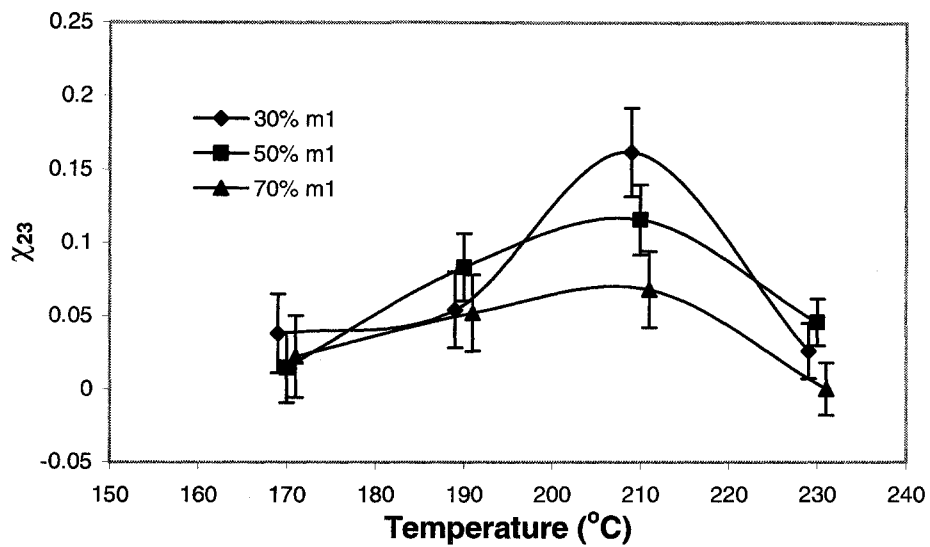
Figure 7.22 Temperature dependence of χ_{23} of the LDPE/LLDPE-m2 blends at various compositions

184
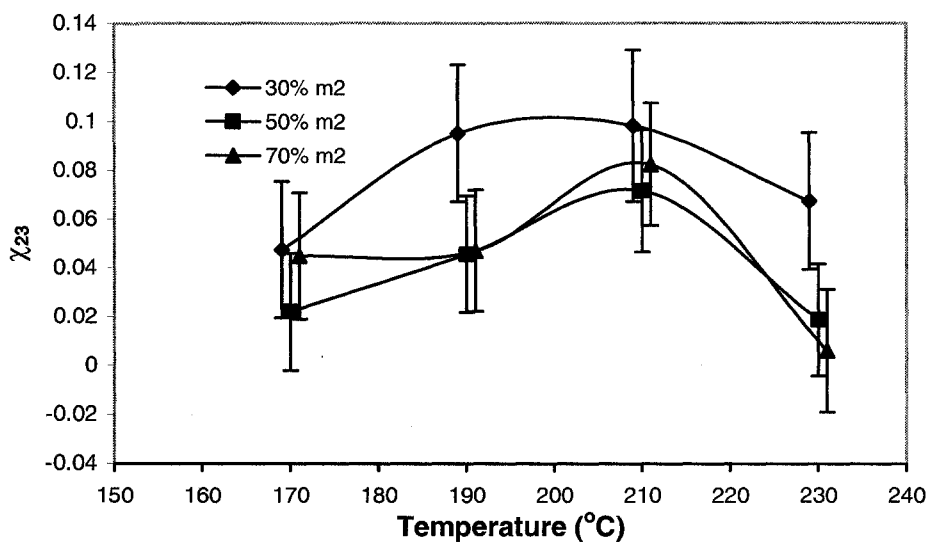
Figure 7.23 Temperature dependence of χ_{23} of the LDPE/LLDPE-m3 blends at various
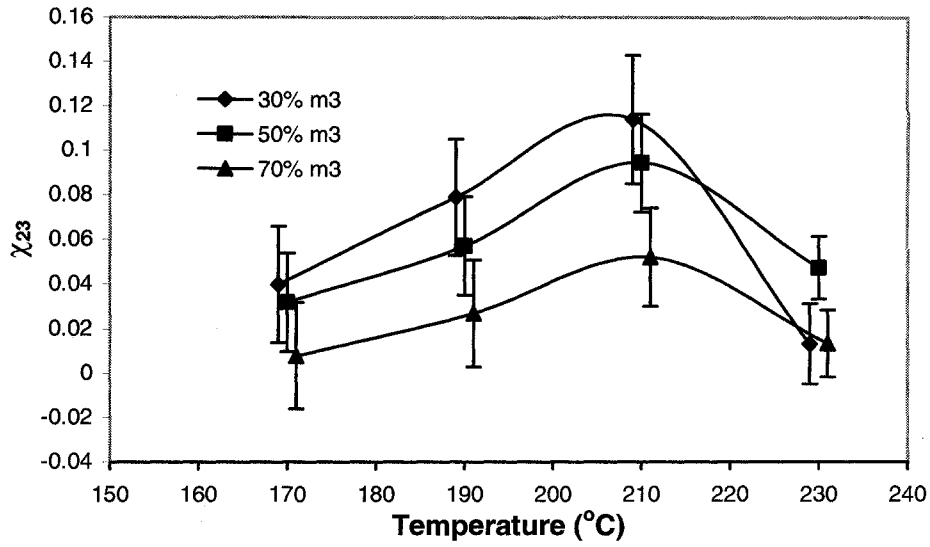
compositions

Figure 7.24 Temperature dependence of χ_{23} of the LDPE/LLDPE-m4 blends at various

compositions

185
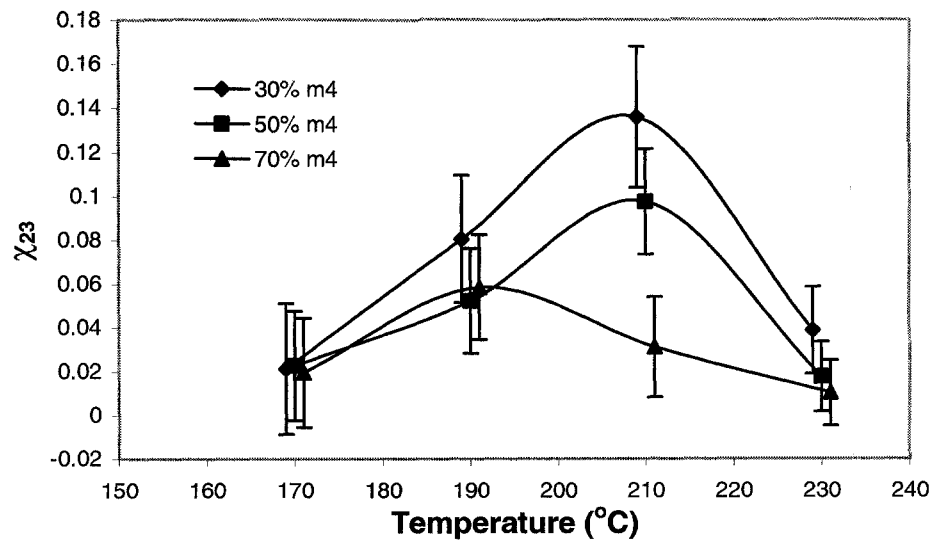
Figure 7.25 Temperature dependence of χ_{23} of the LDPE/LLDPE-m5 blends at various compositions
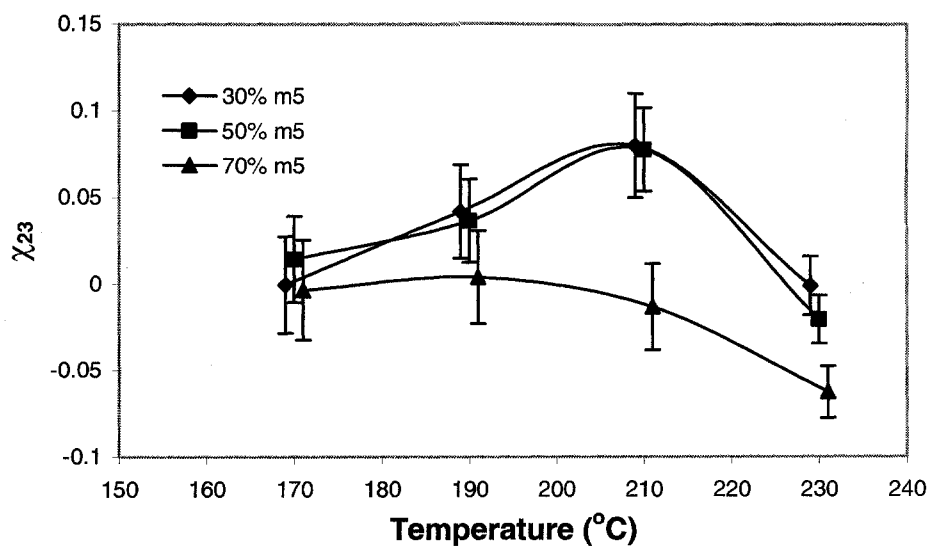
Figure 7.26 Temperature dependence of χ_{23} of the LDPE/LLDPE-m6 blends at various compositions

186
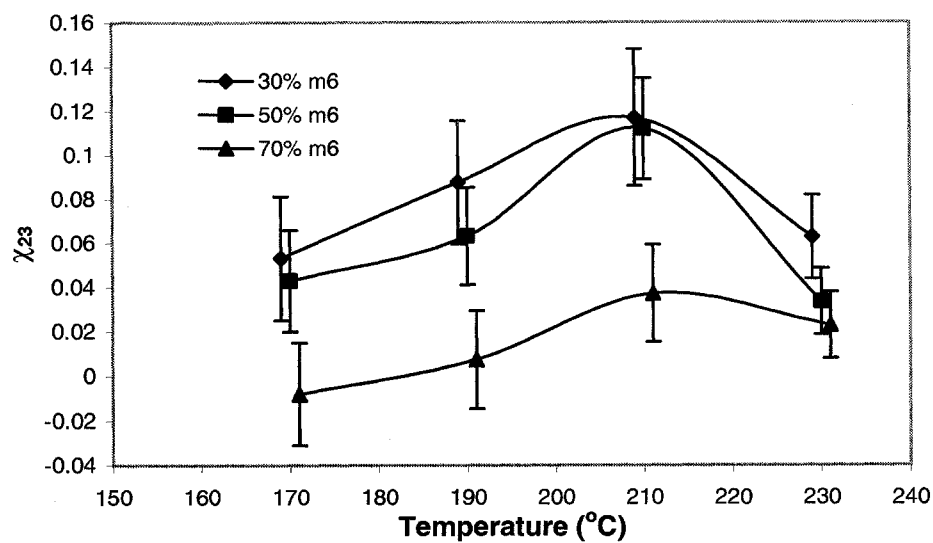
Chapter 8

Conclusions and future work

8.1 Solvent independent polymer-polymer interaction parameters

A new inverse gas chromatography data analysis approach has been developed to measure solvent independent polymer-polymer interaction parameters based on the Flory-Huggins lattice theory. In this approach, a common reference volume has been suggested to use to define the size of a lattice site when a set of solvents are used in IGC. The experimental errors and the reliability of this IGC approach have also been analyzed.

To justify the validity of the proposed approach, it was applied to different polyolefin blends including the HDPE/LDPE, HDPE/LLDPE, HDPE/PS, and HDPE/i-PP blends. All these blends were investigated at three compositions and four elevated temperatures ranging from 170 to 230 °C.

For the HDPE/LDPE blends, the experimental data were found to be well described by the equations proposed in Chapter 3. The measured χ_{23} depended on both temperature and concentration, as expected. For the 30/70 and 50/50 HDPE/LDPE blends, χ_{23} did not show a strong dependence on temperature. However, for the blend containing 70% HDPE, with the consideration of the errors, χ_{23} at 210 °C was much larger than those at other temperatures indicating that the blend is immiscible at 210 °C. For the composition dependence, it was found that χ_{23} at 210 °C increased with increasing concentration of HDPE in the blend. These results were in qualitative

187

agreement with those obtained by molecular dynamics simulations. Quantitatively speaking, χ values obtained in the current work were about one to two orders of magnitude larger than those obtained from MD simulations and SANS. In order to further verify the validity of my approach, I studied the HDPE/i-PP and HDPE/PS blends.

For the HDPE/i-PP and HDPE/PS blends, it was found that the measured interaction parameters were fairly comparable to those obtained from neutron reflectivity measurements. However, they were all about one order of magnitude larger than those obtained from SANS. It is unclear whether neutron reflectivity or SANS yields more reliable χ. Nonetheless, the agreement between the neutron reflectivity and IGC results definitely lent support to the data analysis approach that I proposed. In terms of the composition and temperature dependence, I found that for the 70/30 HDPE/i-PP and 70/30 HDPE/PS blends, χ increased with increasing temperature indicating that they are LCST blends. For blends of HDPE/i-PP at 210 and 230 $^{\circ}$C and of HDPE/PS at 230 $^{\circ}$C, χ decreased with increasing the composition of i-PP from 30% to 50% and did not vary much from 50% to 70% due to the non-random packing of two components. At other temperatures and compositions, no obvious trends were identified considering the large errors associated with the measured χ values.

Su and Patterson (1977) proposed that the nonrandom partitioning of the probe molecules in the components of the blend caused the solvent dependence problem in IGC measurements. By reexamining this argument, I suggested that the probe dependence problem was attributed to two factors. One was the misuse of reference volume and the other was the non-random partitioning. In this work, the first factor could be eliminated by using a common reference volume. Based on my results of the HDPE/PS system, I

188

found that the data analysis approach I proposed was able to obtain the solvent independent interaction parameter even though the systems did not meet the zero $\Delta\chi$ criterion. This implied that the second factor was negligible and the probe dependence problem commonly observed in IGC measurements was mainly attributed to the improper use of the reference volume.

The IGC method has also been applied to HDPE and LLDPE system to study the effect of the branch content of LLDPE on its miscibility with HDPE. It was found that increasing the branch content of LLDPE reduced miscibility and based on the results, the cut-off value of branch content for inducing immiscibility was about 50 branches per 1,000 backbone carbons. This result was consistent with other researcher's findings. For the temperature and composition dependence of χ, it was found that for the same pair of HDPE and LLDPE blend at different compositions, the 50/50 blends showed lower χ values than those at other compositions. The effect of temperature on miscibility depends on the composition of the blends and the branch content of LLDPE studied. It is worth noting that it was not understood in my result that the values of interaction parameters between HDPE and LLDPE containing low levels of the number of branches were negative. LLDPE molecules with low branch contents should be similar to HDPE molecules. Therefore, it is expected that the interaction parameters should be positive and very close to zero.

The miscibility of LLDPE/LDPE blends was studied using the same IGC technique. Twelve different LLDPEs with different molecular characteristics were used to investigate the effect of the molecular characteristics of LLDPE on its miscibility with LDPE at three various compositions and four elevated temperatures. Based on my results,

189

LLDPE/LDPE blends were likely to be miscible at 170 °C and 230 °C, but not at 210 °C. In terms of the composition effect, at 210 °C, χ_{23} decreased with increasing concentration of LLDPE in the blend. These results were also in good agreement with other researchers' findings. At other temperatures, no obvious trends could be obtained owing to the large errors of χ_{23}. It was found that χ values for all LLDPE/LDPE blends were in the same order of magnitude and no obvious trends were obtained. This is because ranges of the variation of the characteristics I studied were narrow.

8.2 Recommendations for future work

It has been pointed out in the previous chapters that reducing errors of χ_{23} is necessary in order to obtain more reliable composition and temperature dependence of χ_{23}, in particular, for polyolefin blends, which exhibited small χ_{23} values. In addition, for the LLDPE/LDPE blends, the effect of the different characteristics of LLDPE on χ_{23} was not elucidated successfully in this thesis owing to the small variation of each characteristic I intended to investigate. For the future study, LLDPE samples with broader ranges of the characteristics are recommended to use.

From a theoretical point of view, it is well known that the Flory-Huggins theory is only suitable to the linear polymers, not to the branched polymers. However, most commercial polyethylenes of interest contain certain amount of branches. I expect that by using a theory that is more suitable to the branched polymers, such as the Lattice Fluid Theory for IGC data analysis, one can obtain more reliable interaction parameters.

190

Additionally, modifications to the theory are needed since the Flory-Huggins lattice theory overestimates the entropy change on mixing.

In the long run, I need to correlate the miscibility of polyethylene blends with their processasibility and physical properties.

8.3 References

Su C. S. and Patterson D., (1977) Determination by Gas-Liquid Chromatography of the Polystyrene-Poly(vinyl methyl ether) Interaction, *Macromolecules*, 10, 708-711.

Appendix A

Estimation of the Flory-Huggins interaction

parameters based on IGC data

A.1 Sample calculations of χ_{12}, χ_{13} and $\chi_{1(23)}$

Let LLDPE-a1 be polymer 2 and LDPE be polymer 3 and 1-hexene be the solvent used.

The following summarizes the characteristics of the LLDPE-a1 column at 170 °C:

Mass of polymer in the column: w=0.060 g (Appendix E)

Flowrate of carrier gas: F=21.54 mL/min (Table C35)

Inlet pressure of column: P_i=248 kPa (Table C35)

Outlet pressure of column: P_o=96 kPa

Retention time for 1-Hexene: t_R=0.17 min (Table C35)

Retention time for Methane: t_o=0.138 min (Table C35)

Net retention time: t_n=t_R-t_o=0.032 min

James-Martin correction factor (equation 3-2):

$$J = \frac{3}{2}\frac{\left(\dfrac{P_i}{P_o}\right)^2 - 1}{\left(\dfrac{P_i}{P_o}\right)^3 - 1} = 0.525$$

192

Specific retention volume for 1-Hexene (equation 3-1):

$$V_g^0 = \frac{273.15 \; t_n \; F \; J}{wT} = 3.72 \; \text{cm}^3/\text{g}$$

The polymer specific volume at 170 °C: (equation 3-5)

$$v = 1.282 + 9.0 \times 10^{-4}(T - 150) = 1.3 \; \text{cm}^3/\text{g}$$

Vapor pressure of 1-Hexene calculated from Antoine equation (equation 3-9):

$$\ln(P_1^0) = A - \frac{B}{(T + C)} = 11.91 \; \text{atm}$$

Second virial coefficient of 1-Hexene using the following equations (equations 3-10, 11, and 12):

$$\frac{B_{11}P_c}{RT_c} = f^0 + \omega f^1$$

with

$$f^0 = 0.1445 - \frac{0.330}{T_r} - \frac{0.1385}{T_r^2} - \frac{0.0121}{T_r^3} - \frac{0.000607}{T_r^8}$$

$$f^1 = 0.0637 + \frac{0.331}{T_r^2} - \frac{0.423}{T_r^3} - \frac{0.008}{T_r^8}$$

for 1-Hexene: ω=0.285, T_c=504 K, P_c=31.7 bar, substituting the parameters into the above equations:

f^0=-0.429 ; f^1= -0.153

and B_{11}=-0.625 L/mol

Liquid density of 1-Hexene can be obtained from the Rackett equation:

$$\rho = A \times B^{-(1-T_r)^{2/7}} = 0.494 \; \text{g/mL}$$

193

for 1-Hexene, $A=0.242$, $B=0.27$

molar volume can be calculated by:

$$V_1 = \rho/M = 170.3 \text{ mL/mol} = 0.17 \text{ L/mol}$$

and M is the molecular weight of 1-Hexene.

Finally, the interaction parameter between LLDPE-a1 and 1-Hexene can be calculated by the following equation (equation 3-26):

$$\chi_{12} = \frac{V_0}{V_1}\left(\ln\frac{273.15R\upsilon_2}{V_g^0 V_1 P_1^0} - 1 + \frac{V_1}{M_2\upsilon_2} - \frac{(B_{11}-V_1)}{RT}P_1^0\right) = 0.129$$

Similiarly, interaction parameter between LDPE and 1-Hexene χ_{13} can be obtained:

χ_{13}=0.14

and for 50/50 blends of LDPE and LLDPE (equation 3-7),

$\chi_{1(23)}$=0.13

A.2 Sample calculations of χ_{23}

Having calcualted χ_{12}, χ_{13}, and $\chi_{1(23)}$ for all the solvents used, one can calculate the interaction parameter between polymer 2 and polymer 3 from the intercept of the plot based on the following equation (equation 3-28):

$$\chi_{1(23)} = \phi_2\chi_{12} + \phi_3\chi_{13} - \phi_2\phi_3\chi_{23}$$

194

The chart shows a linear plot with:
- Y-axis labeled $\chi_{1(23)}$ with values 0, 0.05, 0.1, 0.15, 0.2, 0.25
- X-axis labeled $\phi_2\chi_{12}+\phi_3\chi_{13}$ with values 0, 0.05, 0.1, 0.15, 0.2, 0.25
- Equation: $\chi_{1(23)} = 0.9612(\phi_2\chi_{12}+\phi_3\chi_{13}) - 0.0021$
- $R^2 = 0.9916$
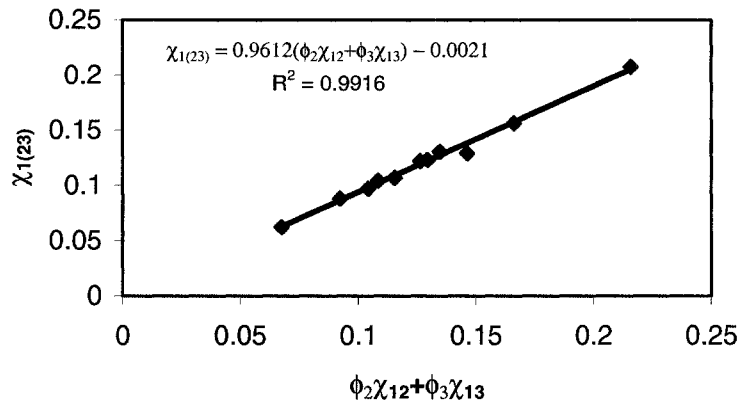
so χ_{23}=0.0021/0.5/0.5=0.0084

195

Appendix B

Error analysis

The procedure of error analysis is listed as follows.

B.1 Experimental errors

There are three major sources of experimental errors. They are the mass of polymer in the column (w), flowrate of the carrier gas (F) and retention times of solvents (t) and the marker. The precision of the mass of polymer in the column depends on the balance used and also the ashing process described in Chapter 3. The accuracy of the balance is ±0.0001g. When I burned the samples to determine the loading of polymer, three samples were used and the average was considered as the loading. Combining of all these factors together, the absolute error for the mass of polymer in the column was about 0.001g. The flowrate of the carrier gas was also obtained from the average of three time measurements and the absolute error was about 0.01 mL/min. The retention time was also obtained from the average of three time measurements and the absolute error was about 0.001 min.

B.2 Error propagation

Let us suppose χ_{12} be a function of w, F and t_n:

$$\chi_{12} = f(w, F, t_n)$$ (B-1)

The deviation of χ_{12} can be expressed as the following:

$$\Delta\chi_{12} = \frac{\partial f}{\partial w}\Delta w + \frac{\partial f}{\partial F}\Delta F + \frac{\partial f}{\partial t_n}\Delta t_n$$ (B-2)

Here, $\Delta\chi_{12}$ is the deviation of χ_{12}; Δw, ΔF, and Δt_n are the deviations of w, F, and t_n, respectively.

It is worth pointing out that all other parameters used in the equations for the calculations of χ_{12}, χ_{13}, and $\chi_{1(23)}$ were obtained from the literature and I did not incorporate their uncertainties into account.

Substituting equation 3-26 into equation B-2,

$$\Delta\chi_{12} = \frac{V_0}{V_1}(\frac{1}{w}\Delta w + \frac{1}{F}\Delta F + \frac{1}{t_n}\Delta t_n)$$ (B-3)

From equation B-3, the deviation of χ_{12} can be obtained. Similarly, the deviation of χ_{13} and $\chi_{1(23)}$ can be estimated using the same equation.

In terms of the standard deviation, the following equation can be used:

$$S_\chi = \frac{V_0}{V_1}\sqrt{\left(\frac{\partial f}{\partial w}\Delta w\right)^2 + \left(\frac{\partial f}{\partial F}\Delta F\right)^2 + \left(\frac{\partial f}{\partial t_n}\Delta t_n\right)^2}$$ (B-4)

197

or

$$S_\chi = \frac{V_0}{V_1} \sqrt{\left(\frac{1}{w}\Delta w\right)^2 + \left(\frac{1}{F}\Delta F\right)^2 + \left(\frac{1}{t_n}\Delta t_n\right)^2} \qquad \text{(B-5)}$$

B.3 The standard deviation of χ_{23}

In this work, χ_{23} was calculated from the intercept of the plot between $\phi_2\chi_{12} + \phi_3\chi_{13}$ and $\chi_{1(23)}$. The deviation of the calculated χ_{23} was caused by the deviation from both x-axis and y-axis. It can be estimated by the following expression:

$$S_{\chi_{23}} = \frac{1}{\phi_2\phi_3} \sqrt{\frac{\sum \dfrac{x^2}{\Delta x^2 + \Delta y^2}}{\sum \dfrac{1}{\Delta x^2 + \Delta y^2} \sum \dfrac{x^2}{\Delta x^2 + \Delta y^2} - \left(\sum \dfrac{x}{\Delta x^2 + \Delta y^2}\right)^2}} \qquad \text{(B-6)}$$

Here, x stands for $\phi_2\chi_{12} + \phi_3\chi_{13}$ and y is $\chi_{1(23)}$. Δx is the standard deviation from x-axis; Δy is the standard deviation from y-axis.

I omitted the derivation of this equation and any readers who are interested in the detailed derivation can refer to the literature of error analysis (Henrici, 1963).

198

B.4 Sample calculations of the standard deviation of χ_{23}

The polymer blend and the solvent I used here are the same as those described in Appendix A. The characteristics of the column have been shown in Appendix A. $\Delta w = 0.001$ g, $\Delta F = 0.01$ mL/min, and $\Delta t_n = 0.001$ min, as introduced in section B.1. From equation B-5:

$$S_{\chi_{12}} = \frac{V_0}{V_1} \sqrt{\left(\frac{1}{w}\Delta w\right)^2 + \left(\frac{1}{F}\Delta F\right)^2 + \left(\frac{1}{t_n}\Delta t_n\right)^2}$$

$$= \frac{36}{170.3} \sqrt{\left(\frac{1}{0.06}0.001\right)^2 + \left(\frac{1}{21.54}0.01\right)^2 + \left(\frac{1}{0.032}0.001\right)^2}$$

$$= 0.0037$$

Similarly, $S_{\chi_{13}} = 0.0046$, and $S_{\chi_{1(23)}} = 0.0039$

The standard deviations of χ_{12}, χ_{13}, and $\chi_{1(23)}$ for all the solvents can be calculated using the above equations and shown in the following table.

Here, for 1-hexene,

$$\Delta x = \phi_2 S_{\chi_{12}} + \phi_3 S_{\chi_{13}}$$

$$= 0.5 \times 0.0037 + 0.5 \times 0.0046$$

$$= 0.0042$$

199

Solvent	$S_{\chi_{12}}$	$S_{\chi_{13}}$	$S_{\chi_{1(23)}}$	$\dfrac{x}{\Delta x^2 + \Delta y^2}$	$\dfrac{1}{\Delta x^2 + \Delta y^2}$	$\dfrac{x^2}{\Delta x^2 + \Delta y^2}$
1 - hexene	0.0037	0.0046	0.0039	4215.2	31294.7	567.8
1-octene	0.0032	0.0040	0.0033	4636.4	42786.5	502.4
benzene	0.0057	0.0071	0.0059	2931.9	13582.8	632.9
cyclohexane	0.0046	0.0057	0.0048	2648.8	20478.4	342.6
hexanes	0.0036	0.0044	0.0037	4288.1	33963.4	541.4
n-dodecane	0.0022	0.0028	0.0023	5959.9	88269.9	402.4
n-heptane	0.0033	0.0041	0.0035	4533.2	39317.7	522.7
n-nonane	0.0028	0.0035	0.0029	5142.9	55773.4	474.2
octane	0.0031	0.0038	0.0032	4865.5	46763.6	506.2
toluene	0.0048	0.0060	0.0049	3185.4	19182.0	529.0
xylenes	0.0042	0.0052	0.0043	3728.8	25511.0	545.0
Σ				46136.2	416923.3	5566.6

Therefore, $S_{\chi_{23}} = \dfrac{1}{0.5 \times 0.5} \sqrt{\dfrac{5566.6}{416923.3 \times 5566.6 - (46136.2)^2}} = 0.022$

B.5 Reference

Henrici, P. (1963) Error propagation for difference methods, Wiley, New York

200

Appendix C

Retention times of different solvents and the marker, flowrate of the carrier gas, and the inlet pressure of the columns used in the thesis

Table C.1 Flowrate of the carrier gas, inlet pressure and measured retention times of the selected probes for the column packed with pure HDPE at 170, 190, 210 and 230 °C.

T (°C)	170	190	210	230
F (mL/min)	19.80	19.85	19.95	19.98
P_i (kPa)	208	214	219	226
PROBE	RETENTION TIME (min)			
Methane	0.143	0.141	0.140	0.136
1 – Hexene	0.169	0.162	0.157	0.151
1-Octene	0.217	0.198	0.181	0.17
Benzene	0.193	0.182	0.171	0.163
Cyclohexane	0.195	0.183	0.173	0.163
n-Hexane	0.171	0.164	0.158	0.152
n-Dodecane	0.754	0.513	0.383	0.298
n-Heptane	0.191	0.177	0.171	0.16
n-Nonane	0.272	0.23	0.211	0.19
n-Octane	0.222	0.201	0.185	0.171
Toluene	0.23	0.205	0.193	0.176
Xylenes	0.293	0.249	0.224	0.197

Table C.2 Flowrate of the carrier gas, inlet pressure and measured retention times of the selected probes for the column packed with 50% HDPE and 50% LDPE at 170, 190, 210 and 230 °C.

T (°C)	170	190	210	230
F (mL/min)	19.88	19.93	20.15	19.93
P_i (kPa)	203	211	216	221
PROBE	RETENTION TIME (min)			
Methane	0.136	0.134	0.133	0.130
1 – Hexene	0.163	0.155	0.149	0.144
1-Octene	0.213	0.19	0.175	0.163
Benzene	0.187	0.173	0.164	0.156
Cyclohexane	0.189	0.174	0.165	0.156
n-Hexane	0.164	0.156	0.151	0.146
n-Dodecane	0.756	0.51	0.374	0.296
n-Heptane	0.185	0.171	0.162	0.154
n-Nonane	0.272	0.23	0.203	0.183
n-Octane	0.218	0.194	0.178	0.165
Toluene	0.226	0.201	0.184	0.172
Xylenes	0.287	0.244	0.214	0.192

Table C.3 Flowrate of the carrier gas, inlet pressure and measured retention times of the selected probes for the column packed with 30% HDPE and 70% LDPE at 170, 190, 210 and 230 °C.

T (°C)	170	190	210	230
F (mL/min)	20.00	19.93	19.85	20.00
P_i (kPa)	216	221	228	236
PROBE	RETENTION TIME (min)			
Methane	0.133	0.133	0.133	0.130
1 – Hexene	0.163	0.156	0.151	0.145
1-Octene	0.217	0.194	0.179	0.166
Benzene	0.19	0.175	0.168	0.158
Cyclohexane	0.192	0.177	0.17	0.158
n-Hexane	0.164	0.158	0.152	0.146
n-Dodecane	0.807	0.55	0.409	0.319
n-Heptane	0.189	0.173	0.163	0.155
n-Nonane	0.284	0.239	0.207	0.187
n-Octane	0.223	0.196	0.179	0.169
Toluene	0.229	0.206	0.187	0.172
Xylenes	0.299	0.252	0.22	0.199

202

Table C.4 Flowrate of the carrier gas, inlet pressure and measured retention times of the selected probes for the column packed with 70% HDPE and 30% LDPE at 170, 190, 210 and 230 °C.

T (°C)	170	190	210	230
F (mL/min)	20.30	19.93	20.30	19.71
P_i (kPa)	219	226	234 -	238
PROBE	RETENTION TIME (min)			
Methane	0.148	0.146	0.145	0.142
1 – Hexene	0.169	0.163	0.158	0.154
1-Octene	0.214	0.192	0.181	0.17
Benzene	0.191	0.178	0.17	0.164
Cyclohexane	0.193	0.18	0.172	0.164
n-Hexane	0.172	0.164	0.159	0.154
n-Dodecane	0.672	0.479	0.367	0.295
n-Heptane	0.187	0.178	0.17	0.162
n-Nonane	0.265	0.23	0.205	0.188
n-Octane	0.216	0.194	0.182	0.172
Toluene	0.22	0.203	0.188	0.177
Xylenes	0.277	0.239	0.215	0.197

Table C.5 Flowrate of the carrier gas, inlet pressure and measured retention times of the selected probes for the column packed with pure i-PP at 170, 190, 210 and 230 °C.

T (°C)	170	190	210	230
F (mL/min)	22.41	22.59	22.41	22.50
P_i (kPa)	171	176	180	185
PROBE	RETENTION TIME (min)			
Methane	0.111	0.108	0.108	0.104
1 – Hexene	0.133	0.127	0.121	0.116
1-Octene	0.173	0.156	0.143	0.13
Benzene	0.149	0.138	0.131	0.123
Cyclohexane	0.153	0.142	0.132	0.125
n-Hexane	0.135	0.128	0.123	0.117
n-Dodecane	0.62	0.438	0.332	0.252
n-Heptane	0.152	0.141	0.131	0.124
n-Nonane	0.225	0.19	0.166	0.148
n-Octane	0.18	0.16	0.145	0.132
Toluene	0.178	0.16	0.147	0.135
Xylenes	0.222	0.192	0.17	0.151

Table C.6 Flowrate of the carrier gas, inlet pressure and measured retention times of the selected probes for the column packed with pure HDPE at 170, 190, 210 and 230 °C.

T (°C)	170	190	210	230
F (mL/min)	23.58	23.58	23.58	23.58
P_i (kPa)	183	188	193	199
PROBE	RETENTION TIME (min)			
Methane	0.115	0.114	0.112	0.11
1 – Hexene	0.14	0.134	0.123	0.119
1-Octene	0.187	0.166	0.146	0.136
Benzene	0.162	0.149	0.135	0.127
Cyclohexane	0.164	0.152	0.136	0.127
n-Hexane	0.142	0.135	0.124	0.119
n-Dodecane	0.708	0.487	0.353	0.268
n-Heptane	0.162	0.148	0.132	0.126
n-Nonane	0.245	0.204	0.172	0.153
n-Octane	0.193	0.17	0.149	0.138
Toluene	0.198	0.176	0.154	0.143
Xylenes	0.259	0.217	0.183	0.16

203

Table C.7 Flowrate of the carrier gas, inlet pressure and measured retention times of the selected probes for the column packed with 70% HDPE and 30% i-PP at 170, 190, 210 and 230 °C.

T (°C)	170	190	210	230
F (mL/min)	22.50	22.69	22.22	22.31
P_i (kPa)	186	192	199	206
PROBE	RETENTION TIME (min)			
Methane	0.119	0.116	0.114	0.112
1 – Hexene	0.141	0.135	0.129	0.126
1-Octene	0.182	0.163	0.153	0.141
Benzene	0.159	0.148	0.14	0.131
Cyclohexane	0.161	0.15	0.141	0.135
n-Hexane	0.143	0.136	0.129	0.125
n-Dodecane	0.62	0.434	0.358	0.272
n-Heptane	0.159	0.147	0.14	0.133
n-Nonane	0.233	0.196	0.178	0.16
n-Octane	0.187	0.166	0.155	0.144
Toluene	0.191	0.17	0.158	0.147
Xylenes	0.241	0.204	0.186	0.166

Table C.8 Flowrate of the carrier gas, inlet pressure and measured retention times of the selected probes for the column packed with 50% HDPE and 50% i-PP at 170, 190, 210 and 230 °C.

T (°C)	170	190	210	230
F (mL/min)	22.50	22.69	22.78	22.50
P_i (kPa)	181	197	191	198
PROBE	RETENTION TIME (min)			
Methane	0.116	0.114	0.110	0.108
1 – Hexene	0.143	0.134	0.128	0.123
1-Octene	0.191	0.168	0.152	0.142
Benzene	0.163	0.149	0.14	0.133
Cyclohexane	0.167	0.152	0.142	0.134
n-Hexane	0.144	0.136	0.128	0.124
n-Dodecane	0.714	0.48	0.354	0.287
n-Heptane	0.164	0.149	0.139	0.132
n-Nonane	0.251	0.204	0.179	0.162
n-Octane	0.197	0.171	0.155	0.144
Toluene	0.198	0.174	0.158	0.147
Xylenes	0.257	0.212	0.186	0.167

Table C.9 Flowrate of the carrier gas, inlet pressure and measured retention times of the selected probes for the column packed with 30% HDPE and 70% i-PP at 170, 190, 210 and 230 °C.

T (°C)	170	190	210	230
F (mL/min)	22.22	22.41	22.31	22.31
P_i (kPa)	174	178	184	188
PROBE	RETENTION TIME (min)			
Methane	0.114	0.111	0.107	0.105
1 – Hexene	0.134	0.128	0.12	0.118
1-Octene	0.17	0.152	0.138	0.131
Benzene	0.146	0.136	0.128	0.124
Cyclohexane	0.151	0.14	0.13	0.125
n-Hexane	0.135	0.128	0.123	0.119
n-Dodecane	0.557	0.385	0.293	0.242
n-Heptane	0.15	0.138	0.129	0.123
n-Nonane	0.214	0.181	0.159	0.147
n-Octane	0.174	0.155	0.142	0.132
Toluene	0.173	0.157	0.143	0.135
Xylenes	0.215	0.186	0.165	0.15

204

Table C.10 Flowrate of the carrier gas, inlet pressure and measured retention times of the selected probes for the column packed with pure PS at 170, 190, 210 and 230 °C.

T (°C)	170	190	210	230
F (mL/min)	21.60	20.61	21.21	21.32
Pᵢ (kPa)	206	211	216	223
PROBE	RETENTION TIME (min)			
Methane	0.139	0.138	0.136	0.134
1 – Hexene	0.154	0.15	0.147	0.143
1-Octene	0.183	0.173	0.162	0.156
Benzene	0.183	0.173	0.163	0.156
Cyclohexane	0.171	0.164	0.157	0.152
n-Hexane	0.155	0.15	0.147	0.143
n-Dodecane	0.431	0.347	0.291	0.242
n-Heptane	0.165	0.158	0.154	0.147
n-Nonane	0.209	0.187	0.179	0.161
n-Octane	0.183	0.17	0.164	0.153
Toluene	0.214	0.19	0.18	0.165
Xylenes	0.262	0.223	0.203	0.18

Table C.11 Flowrate of the carrier gas, inlet pressure and measured retention times of the selected probes for the column packed with 70% HDPE and 30% PS at 170, 190, 210 and 230 °C.

T (°C)	170	190	210	230
F (mL/min)	22.50	22.59	22.50	22.31
Pᵢ (kPa)	186	196	201	206
PROBE	RETENTION TIME (min)			
Methane	0.115	0.117	0.112	0.111
1 – Hexene	0.138	0.131	0.127	0.123
1-Octene	0.176	0.159	0.147	0.139
Benzene	0.16	0.149	0.139	0.134
Cyclohexane	0.158	0.147	0.139	0.133
n-Hexane	0.139	0.133	0.127	0.124
n-Dodecane	0.575	0.405	0.313	0.263
n-Heptane	0.154	0.143	0.136	0.13
n-Nonane	0.219	0.187	0.168	0.154
n-Octane	0.179	0.16	0.149	0.14
Toluene	0.192	0.17	0.156	0.146
Xylenes	0.244	0.206	0.182	0.166

Table C.12 Flowrate of the carrier gas, inlet pressure and measured retention times of the selected probes for the column packed with 50% HDPE and 50% PS at 170, 190, 210 and 230 °C.

T (°C)	170	190	210	230
F (mL/min)	20.77	19.93	19.90	20.06
Pᵢ (kPa)	199	206	210	214
PROBE	RETENTION TIME (min)			
Methane	0.134	0.131	0.13	0.129
1 – Hexene	0.153	0.147	0.144	0.14
1-Octene	0.187	0.172	0.163	0.156
Benzene	0.177	0.165	0.158	0.152
Cyclohexane	0.171	0.16	0.156	0.149
n-Hexane	0.153	0.147	0.145	0.141
n-Dodecane	0.535	0.399	0.329	0.275
n-Heptane	0.169	0.157	0.152	0.147
n-Nonane	0.226	0.197	0.182	0.171
n-Octane	0.19	0.173	0.164	0.155
Toluene	0.209	0.188	0.176	0.164
Xylenes	0.259	0.223	0.201	0.183

205

Table C.13 Flowrate of the carrier gas, inlet pressure and measured retention times of the selected probes for the column packed with 30% HDPE and 70% PS at 170, 190, 210 and 230 °C.

T (°C)	170	190	210	230
F (mL/min)	22.31	22.41	22.41	22.41
P_i (kPa)	186	196	201	206
PROBE	RETENTION TIME (min)			
Methane	0.122	0.119	0.116	0.115
1 – Hexene	0.138	0.133	0.126	0.123
1-Octene	0.17	0.156	0.144	0.137
Benzene	0.163	0.152	0.14	0.134
Cyclohexane	0.156	0.147	0.137	0.131
n-Hexane	0.139	0.133	0.127	0.123
n-Dodecane	0.477	0.354	0.283	0.244
n-Heptane	0.151	0.142	0.134	0.129
n-Nonane	0.202	0.178	0.16	0.15
n-Octane	0.17	0.156	0.144	0.137
Toluene	0.193	0.174	0.156	0.147
Xylenes	0.241	0.207	0.179	0.164

Table C.14 Flowrate of the carrier gas, inlet pressure and measured retention times of the selected probes for the column packed with pure LLDPE-1 at 170, 190, 210 and 230 °C.

T (°C)	170	190	210	230
F (mL/min)	23.48	23.48	23.48	23.48
P_i (kPa)	181	186	191	196
PROBE	RETENTION TIME (min)			
Methane	0.112	0.111	0.109	0.107
1 – Hexene	0.135	0.129	0.124	0.119
1-Octene	0.179	0.161	0.148	0.135
Benzene	0.155	0.144	0.135	0.129
Cyclohexane	0.157	0.145	0.136	0.129
n-Hexane	0.137	0.131	0.125	0.12
n-Dodecane	0.655	0.458	0.376	0.26
n-Heptane	0.154	0.143	0.133	0.126
n-Nonane	0.231	0.195	0.171	0.151
n-Octane	0.183	0.163	0.15	0.136
Toluene	0.188	0.168	0.154	0.14
Xylenes	0.244	0.207	0.182	0.159

Table C.15 Flowrate of the carrier gas, inlet pressure and measured retention times of the selected probes for the column packed with pure HDPE at 170, 190, 210 and 230 °C.

T (°C)	170	190	210	230
F (mL/min)	23.58	23.58	23.58	23.58
P_i (kPa)	183	188	193	199
PROBE	RETENTION TIME (min)			
Methane	0.115	0.114	0.112	0.11
1 – Hexene	0.14	0.134	0.123	0.119
1-Octene	0.187	0.166	0.146	0.136
Benzene	0.162	0.149	0.135	0.127
Cyclohexane	0.164	0.152	0.136	0.127
n-Hexane	0.142	0.135	0.124	0.119
n-Dodecane	0.708	0.487	0.353	0.268
n-Heptane	0.162	0.148	0.132	0.126
n-Nonane	0.245	0.204	0.172	0.153
n-Octane	0.193	0.17	0.149	0.138
Toluene	0.198	0.176	0.154	0.143
Xylenes	0.259	0.217	0.183	0.16

Table C.16 Flowrate of the carrier gas, inlet pressure and measured retention times of the selected probes for the column packed with 70% HDPE and 30% LLDPE-1 at 170, 190, 210 and 230 °C.

T (°C)	170	190	210	230
F (mL/min)	23.48	23.48	23.28	23.48
P_i (kPa)	206	210	214	219
PROBE	RETENTION TIME (min)			
Methane	0.124	0.12	0.118	0.117
1 – Hexene	0.151	0.143	0.137	0.131
1-Octene	0.203	0.182	0.165	0.152
Benzene	0.176	0.162	0.151	0.144
Cyclohexane	0.179	0.164	0.152	0.144
n-Hexane	0.154	0.145	0.138	0.133
n-Dodecane	0.794	0.544	0.406	0.302
n-Heptane	0.174	0.16	0.149	0.141
n-Nonane	0.268	0.223	0.195	0.173
n-Octane	0.209	0.184	0.167	0.154
Toluene	0.215	0.19	0.173	0.16
Xylenes	0.283	0.237	0.208	0.183

Table C.17 Flowrate of the carrier gas, inlet pressure and measured retention times of the selected probes for the column packed with 50% HDPE and 50% LLDPE-1 at 170, 190, 210 and 230 °C.

T (°C)	170	190	210	230
F (mL/min)	23.48	23.48	23.48	23.48
P_i (kPa)	186	193	199	206
PROBE	RETENTION TIME (min)			
Methane	0.113	0.111	0.110	0.107
1 – Hexene	0.138	0.132	0.127	0.121
1-Octene	0.184	0.164	0.15	0.139
Benzene	0.159	0.148	0.139	0.131
Cyclohexane	0.161	0.149	0.14	0.132
n-Hexane	0.14	0.134	0.128	0.121
n-Dodecane	0.697	0.484	0.368	0.271
n-Heptane	0.159	0.146	0.138	0.129
n-Nonane	0.242	0.203	0.178	0.157
n-Octane	0.19	0.168	0.153	0.14
Toluene	0.197	0.173	0.158	0.145
Xylenes	0.257	0.214	0.188	0.166

Table C.18 Flowrate of the carrier gas, inlet pressure and measured retention times of the selected probes for the column packed with 30% HDPE and 70% LLDPE-1 at 170, 190, 210 and 230 °C.

T (°C)	170	190	210	230
F (mL/min)	23.48	23.48	23.68	23.48
P_i (kPa)	188	196	208	216
PROBE	RETENTION TIME (min)			
Methane	0.116	0.113	0.112	0.111
1 – Hexene	0.145	0.136	0.131	0.127
1-Octene	0.199	0.174	0.159	0.147
Benzene	0.171	0.156	0.146	0.14
Cyclohexane	0.172	0.157	0.147	0.138
n-Hexane	0.147	0.138	0.132	0.127
n-Dodecane	0.793	0.537	0.399	0.298
n-Heptane	0.169	0.154	0.143	0.135
n-Nonane	0.264	0.218	0.188	0.166
n-Octane	0.205	0.179	0.162	0.148
Toluene	0.21	0.185	0.168	0.154
Xylenes	0.281	0.232	0.202	0.178

207

Table C.19 Flowrate of the carrier gas, inlet pressure and measured retention times of the selected probes for the column packed with pure LLDPE-2 at 170, 190, 210 and 230 °C.

T (°C)	170	190	210	230
F (mL/min)	23.58	23.79	23.58	23.38
P_i (kPa)	201	206	211	216
PROBE	RETENTION TIME (min)			
Methane	0.119	0.118	0.117	0.115
1 – Hexene	0.141	0.136	0.132	0.126
1-Octene	0.18	0.165	0.153	0.14
Benzene	0.158	0.151	0.143	0.135
Cyclohexane	0.159	0.151	0.143	0.136
n-Hexane	0.142	0.137	0.132	0.127
n-Dodecane	0.605	0.435	0.331	0.253
n-Heptane	0.158	0.148	0.14	0.132
n-Nonane	0.225	0.194	0.17	0.154
n-Octane	0.184	0.167	0.152	0.142
Toluene	0.188	0.171	0.156	0.145
Xylenes	0.236	0.205	0.179	0.161

Table C.20 Flowrate of the carrier gas, inlet pressure and measured retention times of the selected probes for the column packed with 70% HDPE and 30% LLDPE-2 at 170, 190, 210 and 230 °C.

T (°C)	170	190	210	230
F (mL/min)	23.48	23.48	23.28	23.48
P_i (kPa)	211	217	224	231
PROBE	RETENTION TIME (min)			
Methane	0.123	0.122	0.12	0.119
1 – Hexene	0.148	0.143	0.138	0.133
1-Octene	0.196	0.178	0.163	0.152
Benzene	0.169	0.159	0.151	0.143
Cyclohexane	0.173	0.162	0.152	0.144
n-Hexane	0.151	0.144	0.14	0.134
n-Dodecane	0.726	0.518	0.398	0.303
n-Heptane	0.17	0.158	0.149	0.142
n-Nonane	0.255	0.215	0.192	0.172
n-Octane	0.203	0.18	0.166	0.154
Toluene	0.209	0.187	0.171	0.159
Xylenes	0.271	0.231	0.203	0.182

Table C.21 Flowrate of the carrier gas, inlet pressure and measured retention times of the selected probes for the column packed with 50% HDPE and 50% LLDPE-2 at 170, 190, 210 and 230 °C.

T (°C)	170	190	210	230
F (mL/min)	23.79	23.79	23.79	23.79
P_i (kPa)	186	193	198	204
PROBE	RETENTION TIME (min)			
Methane	0.113	0.112	0.11	0.107
1 – Hexene	0.143	0.135	0.13	0.123
1-Octene	0.199	0.175	0.157	0.143
Benzene	0.169	0.154	0.145	0.136
Cyclohexane	0.172	0.156	0.146	0.136
n-Hexane	0.145	0.137	0.131	0.124
n-Dodecane	0.826	0.559	0.413	0.304
n-Heptane	0.167	0.153	0.144	0.133
n-Nonane	0.266	0.22	0.193	0.167
n-Octane	0.207	0.177	0.163	0.147
Toluene	0.214	0.184	0.169	0.153
Xylenes	0.287	0.232	0.206	0.178

208

Table C.22 Flowrate of the carrier gas, inlet pressure and measured retention times of the selected probes for the column packed with 30% HDPE and 70% LLDPE-2 at 170, 190, 210 and 230 °C.

T (°C)	170	190	210	230
F (mL/min)	23.48	23.48	23.48	23.58
P_i (kPa)	193	199	205	211
PROBE	RETENTION TIME (min)			
Methane	0.115	0.114	0.113	0.111
1 – Hexene	0.14	0.134	0.129	0.123
1-Octene	0.186	0.168	0.154	0.142
Benzene	0.161	0.151	0.144	0.134
Cyclohexane	0.164	0.153	0.144	0.135
n-Hexane	0.142	0.136	0.132	0.125
n-Dodecane	0.7	0.489	0.376	0.281
n-Heptane	0.16	0.149	0.143	0.133
n-Nonane	0.242	0.206	0.185	0.162
n-Octane	0.191	0.173	0.156	0.144
Toluene	0.196	0.176	0.162	0.149
Xylenes	0.256	0.218	0.193	0.171

Table C.23 Flowrate of the carrier gas, inlet pressure and measured retention times of the selected probes for the column packed with pure LLDPE-3 at 170, 190, 210 and 230 °C.

T (°C)	170	190	210	230
F (mL/min)	23.28	23.58	23.58	23.79
P_i (kPa)	186	191	196	203
PROBE	RETENTION TIME (min)			
Methane	0.111	0.111	0.11	0.107
1 – Hexene	0.141	0.133	0.127	0.122
1-Octene	0.197	0.174	0.155	0.142
Benzene	0.167	0.154	0.142	0.134
Cyclohexane	0.17	0.154	0.143	0.134
n-Hexane	0.143	0.136	0.129	0.124
n-Dodecane	0.814	0.553	0.406	0.295
n-Heptane	0.166	0.153	0.141	0.131
n-Nonane	0.266	0.22	0.187	0.164
n-Octane	0.205	0.179	0.159	0.145
Toluene	0.211	0.185	0.164	0.15
Xylenes	0.281	0.234	0.199	0.173

Table C.24 Flowrate of the carrier gas, inlet pressure and measured retention times of the selected probes for the column packed with 70% HDPE and 30% LLDPE-3 at 170, 190, 210 and 230 °C.

T (°C)	170	190	210	230
F (mL/min)	23.48	23.48	23.68	23.48
P_i (kPa)	205	210	215	219
PROBE	RETENTION TIME (min)			
Methane	0.119	0.118	0.117	0.115
1 – Hexene	0.149	0.142	0.137	0.131
1-Octene	0.206	0.183	0.167	0.153
Benzene	0.176	0.163	0.154	0.145
Cyclohexane	0.178	0.164	0.155	0.145
n-Hexane	0.151	0.144	0.139	0.133
n-Dodecane	0.836	0.571	0.427	0.321
n-Heptane	0.175	0.161	0.151	0.143
n-Nonane	0.276	0.229	0.201	0.178
n-Octane	0.213	0.187	0.171	0.157
Toluene	0.22	0.193	0.177	0.163
Xylenes	0.293	0.243	0.213	0.189

209

Table C.25 Flowrate of the carrier gas, inlet pressure and measured retention times of the selected probes for the column packed with 50% HDPE and 50% LLDPE-3 at 170, 190, 210 and 230 °C.

T (°C)	170	190	210	230
F (mL/min)	23.38	23.58	23.28	23.68
P_i (kPa)	194	199	206	211
PROBE	RETENTION TIME (min)			
Methane	0.119	0.118	0.117	0.113
1 – Hexene	0.143	0.139	0.133	0.126
1-Octene	0.19	0.169	0.158	0.144
Benzene	0.165	0.154	0.147	0.137
Cyclohexane	0.165	0.156	0.148	0.138
n-Hexane	0.145	0.141	0.135	0.127
n-Dodecane	0.692	0.487	0.372	0.278
n-Heptane	0.164	0.154	0.145	0.135
n-Nonane	0.247	0.211	0.186	0.164
n-Octane	0.196	0.177	0.161	0.148
Toluene	0.202	0.183	0.166	0.152
Xylenes	0.256	0.216	0.195	0.174

Table C.26 Flowrate of the carrier gas, inlet pressure and measured retention times of the selected probes for the column packed with 30% HDPE and 70% LLDPE-3 at 170, 190, 210 and 230 °C.

T (°C)	170	190	210	230
F (mL/min)	23.38	23.79	23.48	23.48
P_i (kPa)	191	201	206	210
PROBE	RETENTION TIME (min)			
Methane	0.114	0.113	0.112	0.11
1 – Hexene	0.141	0.135	0.13	0.125
1-Octene	0.192	0.172	0.157	0.144
Benzene	0.166	0.153	0.146	0.138
Cyclohexane	0.167	0.154	0.146	0.138
n-Hexane	0.144	0.137	0.131	0.126
n-Dodecane	0.754	0.517	0.397	0.295
n-Heptane	0.164	0.151	0.143	0.133
n-Nonane	0.254	0.212	0.187	0.164
n-Octane	0.198	0.175	0.16	0.147
Toluene	0.203	0.181	0.165	0.151
Xylenes	0.268	0.226	0.198	0.174

Table C.27 Flowrate of the carrier gas, inlet pressure and measured retention times of the selected probes for the column packed with pure LLDPE-4 at 170, 190, 210 and 230 °C.

T (°C)	170	190	210	230
F (mL/min)	23.48	23.79	23.48	23.68
P_i (kPa)	181	186	191	196
PROBE	RETENTION TIME (min)			
Methane	0.110	0.108	0.107	0.106
1 – Hexene	0.135	0.129	0.123	0.118
1-Octene	0.18	0.16	0.146	0.136
Benzene	0.155	0.144	0.135	0.128
Cyclohexane	0.158	0.146	0.137	0.129
n-Hexane	0.138	0.13	0.124	0.119
n-Dodecane	0.688	0.465	0.357	0.264
n-Heptane	0.154	0.143	0.134	0.127
n-Nonane	0.236	0.196	0.173	0.152
n-Octane	0.185	0.164	0.149	0.137
Toluene	0.188	0.168	0.153	0.141
Xylenes	0.244	0.207	0.182	0.161

210

Table C.28 Flowrate of the carrier gas, inlet pressure and measured retention times of the selected probes for the column packed with 70% HDPE and 30% LLDPE-4 at 170, 190, 210 and 230 °C.

T (°C)	170	190	210	230
F (mL/min)	23.48	23.68	23.48	23.58
P_i (kPa)	191	196	201	206
PROBE	RETENTION TIME (min)			
Methane	0.112	0.111	0.109	0.107
1 – Hexene	0.141	0.134	0.128	0.123
1-Octene	0.194	0.172	0.156	0.144
Benzene	0.165	0.152	0.143	0.136
Cyclohexane	0.168	0.153	0.145	0.136
n-Hexane	0.144	0.135	0.13	0.125
n-Dodecane	0.783	0.536	0.404	0.298
n-Heptane	0.165	0.151	0.141	0.133
n-Nonane	0.256	0.215	0.186	0.165
n-Octane	0.199	0.176	0.159	0.146
Toluene	0.204	0.181	0.165	0.15
Xylenes	0.271	0.227	0.199	0.174

Table C.29 Flowrate of the carrier gas, inlet pressure and measured retention times of the selected probes for the column packed with 50% HDPE and 50% LLDPE-4 at 170, 190, 210 and 230 °C.

T (°C)	170	190	210	230
F (mL/min)	23.48	23.58	23.58	23.78
P_i (kPa)	191	199	204	209
PROBE	RETENTION TIME (min)			
Methane	0.118	0.114	0.113	0.111
1 – Hexene	0.144	0.136	0.131	0.125
1-Octene	0.194	0.17	0.158	0.145
Benzene	0.166	0.153	0.146	0.137
Cyclohexane	0.167	0.155	0.147	0.137
n-Hexane	0.145	0.137	0.132	0.127
n-Dodecane	0.754	0.524	0.39	0.289
n-Heptane	0.164	0.152	0.144	0.135
n-Nonane	0.253	0.211	0.188	0.161
n-Octane	0.198	0.175	0.161	0.147
Toluene	0.205	0.182	0.167	0.151
Xylenes	0.268	0.227	0.2	0.173

Table C.30 Flowrate of the carrier gas, inlet pressure and measured retention times of the selected probes for the column packed with 30% HDPE and 70% LLDPE-4 at 170, 190, 210 and 230 °C.

T (°C)	170	190	210	230
F (mL/min)	23.48	23.48	23.68	23.68
P_o (kPa)	185	190	194	199
PROBE	RETENTION TIME (min)			
Methane	0.110	0.109	0.107	0.106
1 – Hexene	0.136	0.13	0.124	0.12
1-Octene	0.185	0.164	0.151	0.137
Benzene	0.157	0.146	0.139	0.13
Cyclohexane	0.16	0.148	0.141	0.131
n-Hexane	0.138	0.131	0.126	0.121
n-Dodecane	0.711	0.491	0.37	0.28
n-Heptane	0.157	0.145	0.137	0.129
n-Nonane	0.24	0.204	0.178	0.158
n-Octane	0.189	0.168	0.153	0.141
Toluene	0.194	0.174	0.157	0.146
Xylenes	0.254	0.216	0.187	0.168

Table C.31 Flowrate of the carrier gas, inlet pressure and measured retention times of the selected probes for the column packed with pure LLDPE-5 at 170, 190, 210 and 230 °C.

T (°C)	170	190	210	230
F (mL/min)	23.48	23.48	23.48	23.58
P_i (kPa)	199	206	211	216
PROBE	RETENTION TIME (min)			
Methane	0.119	0.119	0.117	0.115
1 – Hexene	0.146	0.14	0.136	0.129
1-Octene	0.194	0.175	0.16	0.147
Benzene	0.167	0.157	0.147	0.14
Cyclohexane	0.17	0.159	0.149	0.141
n-Hexane	0.147	0.141	0.136	0.131
n-Dodecane	0.735	0.508	0.387	0.295
n-Heptane	0.168	0.156	0.146	0.138
n-Nonane	0.253	0.213	0.189	0.168
n-Octane	0.2	0.178	0.164	0.15
Toluene	0.205	0.183	0.169	0.154
Xylenes	0.266	0.226	0.201	0.177

Table C.32 Flowrate of the carrier gas, inlet pressure and measured retention times of the selected probes for the column packed with 70% HDPE and 30% LLDPE-5 at 170, 190, 210 and 230 °C.

T (°C)	170	190	210	230
F (mL/min)	23.48	23.48	23.48	23.68
P_i (kPa)	184	189	199	204
PROBE	RETENTION TIME (min)			
Methane	0.111	0.110	0.108	0.107
1 – Hexene	0.138	0.131	0.126	0.12
1-Octene	0.188	0.167	0.152	0.139
Benzene	0.16	0.1475	0.139	0.129
Cyclohexane	0.163	0.15	0.14	0.132
n-Hexane	0.14	0.133	0.127	0.121
n-Dodecane	0.744	0.506	0.382	0.281
n-Heptane	0.16	0.147	0.138	0.128
n-Nonane	0.25	0.207	0.182	0.157
n-Octane	0.194	0.17	0.156	0.141
Toluene	0.2	0.175	0.16	0.145
Xylenes	0.265	0.219	0.193	0.167

Table C.33 Flowrate of the carrier gas, inlet pressure and measured retention times of the selected probes for the column packed with 50% HDPE and 50% LLDPE-5 at 170, 190, 210 and 230 °C.

T (°C)	170	190	210	230
F (mL/min)	23.58	23.58	23.58	23.89
P_i (kPa)	169	174	178	185
PROBE	RETENTION TIME (min)			
Methane	0.107	0.107	0.105	0.103
1 – Hexene	0.129	0.123	0.118	0.114
1-Octene	0.169	0.152	0.14	0.129
Benzene	0.147	0.138	0.129	0.123
Cyclohexane	0.148	0.14	0.131	0.124
n-Hexane	0.131	0.125	0.12	0.115
n-Dodecane	0.614	0.428	0.328	0.247
n-Heptane	0.145	0.137	0.129	0.121
n-Nonane	0.216	0.187	0.16	0.144
n-Octane	0.173	0.157	0.141	0.13
Toluene	0.178	0.162	0.145	0.133
Xylenes	0.226	0.197	0.17	0.152

212

Table C.34 Flowrate of the carrier gas, inlet pressure and measured retention times of the selected probes for the column packed with 30% HDPE and 70% LLDPE-5 at 170, 190, 210 and 230 °C.

T (°C)	170	190	210	230
F (mL/min)	23.58	23.48	23.68	23.48
P_i (kPa)	191	198	203	208
PROBE	RETENTION TIME (min)			
Methane	0.114	0.113	0.111	0.108
1 – Hexene	0.143	0.136	0.13	0.124
1-Octene	0.197	0.174	0.158	0.145
Benzene	0.166	0.153	0.142	0.134
Cyclohexane	0.17	0.157	0.146	0.137
n-Hexane	0.145	0.137	0.132	0.125
n-Dodecane	0.796	0.544	0.405	0.302
n-Heptane	0.167	0.153	0.143	0.134
n-Nonane	0.263	0.217	0.19	0.167
n-Octane	0.203	0.178	0.163	0.147
Toluene	0.209	0.184	0.168	0.152
Xylenes	0.279	0.231	0.202	0.176

Table C.35 Flowrate of the carrier gas, inlet pressure and measured retention times of the selected probes for the column packed with pure LLDPE-a1 at 170, 190, 210 and 230 °C.

T (°C)	170	190	210	230
F (mL/min)	21.54	21.51	21.51	21.49
P_i (kPa)	152	160	168	175
PROBE	RETENTION TIME (min)			
Methane	0.138	0.137	0.137	0.135
1 – Hexene	0.17	0.164	0.158	0.153
1-Octene	0.229	0.207	0.191	0.177
Benzene	0.199	0.185	0.176	0.167
Cyclohexane	0.2	0.187	0.177	0.167
n-Hexane	0.172	0.167	0.159	0.153
n-Dodecane	0.901	0.626	0.47	0.361
n-Heptane	0.197	0.184	0.172	0.164
n-Nonane	0.307	0.247	0.227	0.202
n-Octane	0.238	0.209	0.194	0.176
Toluene	0.246	0.218	0.201	0.181
Xylenes	0.307	0.271	0.238	0.212

Table C.36 Flowrate of the carrier gas, inlet pressure and measured retention times of the selected probes for the column packed with 70% LDPE and 30% LLDPE-a1 at 170, 190, 210 and 230 °C.

T (°C)	170	190	210	230
F (mL/min)	21.23	21.15	21.12	21.51
P_1 (kPa)	171	176	181	186
PROBE	RETENTION TIME (min)			
Methane	0.121	0.119	0.117	0.115
1 – Hexene	0.139	0.134	0.128	0.125
1-Octene	0.177	0.158	0.147	0.139
Benzene	0.157	0.147	0.138	0.133
Cyclohexane	0.158	0.148	0.139	0.133
n-Hexane	0.141	0.135	0.129	0.125
n-Dodecane	0.565	0.398	0.312	0.245
n-Heptane	0.155	0.146	0.137	0.131
n-Nonane	0.213	0.188	0.167	0.153
n-Octane	0.178	0.161	0.149	0.139
Toluene	0.182	0.166	0.154	0.142
Xylenes	0.226	0.195	0.176	0.157

213

Table C.37 Flowrate of the carrier gas, inlet pressure and measured retention times of the selected probes for the column packed with 50% LDPE and 50% LLDPE-a1 at 170, 190, 210 and 230 °C.

T (°C)	170	190	210	230
F (mL/min)	21.57	21.34	21.34	21.34
P_i (kPa)	188	194	198	204
PROBE	RETENTION TIME (min)			
Methane	0.124	0.123	0.120	0.119
1 – Hexene	0.15	0.143	0.139	0.133
1-Octene	0.2	0.178	0.166	0.152
Benzene	0.174	0.162	0.153	0.144
Cyclohexane	0.176	0.164	0.154	0.145
n-Hexane	0.152	0.146	0.141	0.133
n-Dodecane	0.745	0.514	0.386	0.298
n-Heptane	0.173	0.161	0.151	0.142
n-Nonane	0.261	0.221	0.193	0.171
n-Octane	0.206	0.184	0.166	0.155
Toluene	0.213	0.19	0.172	0.16
Xylenes	0.276	0.232	0.203	0.181

Table C.38 Flowrate of the carrier gas, inlet pressure and measured retention times of the selected probes for the column packed with 30% LDPE and 70% LLDPE-a1 at 170, 190, 210 and 230 °C.

T (°C)	170	190	210	230
F (mL/min)	21.37	21.51	21.51	21.68
P_i (kPa)	186	194	198	204
PROBE	RETENTION TIME (min)			
Methane	0.128	0.126	0.124	0.121
1 – Hexene	0.153	0.145	0.14	0.134
1-Octene	0.201	0.177	0.165	0.152
Benzene	0.175	0.162	0.153	0.145
Cyclohexane	0.177	0.162	0.154	0.145
n-Hexane	0.155	0.146	0.142	0.135
n-Dodecane	0.725	0.496	0.38	0.293
n-Heptane	0.175	0.16	0.152	0.143
n-Nonane	0.259	0.216	0.191	0.171
n-Octane	0.207	0.181	0.165	0.154
Toluene	0.212	0.188	0.171	0.158
Xylenes	0.271	0.227	0.198	0.179

Table C.39 Flowrate of the carrier gas, inlet pressure and measured retention times of the selected probes for the column packed with pure LLDPE-a2 at 170, 190, 210 and 230 °C.

T (°C)	170	190	210	230
F (mL/min)	21.98	21.01	21.23	21.26
P_i (kPa)	254	261	268	272
PROBE	RETENTION TIME (min)			
Methane	0.142	0.141	0.139	0.138
1 – Hexene	0.164	0.161	0.156	0.152
1-Octene	0.208	0.195	0.181	0.17
Benzene	0.185	0.176	0.168	0.161
Cyclohexane	0.187	0.178	0.17	0.162
n-Hexane	0.166	0.162	0.158	0.153
n-Dodecane	0.688	0.507	0.403	0.312
n-Heptane	0.185	0.174	0.167	0.161
n-Nonane	0.258	0.231	0.208	0.191
n-Octane	0.212	0.197	0.181	0.172
Toluene	0.219	0.201	0.188	0.176
Xylenes	0.262	0.238	0.215	0.196

214

Table C.40 Flowrate of the carrier gas, inlet pressure and measured retention times of the selected probes for the column packed with 70% LDPE and 30% LLDPE-a2 at 170, 190, 210 and 230 °C.

T (°C)	170	190	210	230
F (mL/min)	20.90	21.34	21.34	21.77
P_i (kPa)	196	201	206	214
PROBE	RETENTION TIME (min)			
Methane	0.132	0.129	0.127	0.123
1 – Hexene	0.154	0.148	0.143	0.136
1-Octene	0.198	0.181	0.168	0.153
Benzene	0.174	0.165	0.156	0.146
Cyclohexane	0.176	0.166	0.157	0.147
n-Hexane	0.155	0.15	0.144	0.137
n-Dodecane	0.699	0.495	0.382	0.287
n-Heptane	0.174	0.163	0.153	0.145
n-Nonane	0.254	0.218	0.192	0.172
n-Octane	0.204	0.184	0.169	0.155
Toluene	0.21	0.19	0.174	0.159
Xylenes	0.266	0.23	0.201	0.179

Table C.41 Flowrate of the carrier gas, inlet pressure and measured retention times of the selected probes for the column packed with 50% LDPE and 50% LLDPE-a2 at 170, 190, 210 and 230 °C.

T (°C)	170	190	210	230
F (mL/min)	21.57	21.92	21.77	21.51
P_i (kPa)	199	206	210	216
PROBE	RETENTION TIME (min)			
Methane	0.131	0.130	0.127	0.125
1 – Hexene	0.156	0.15	0.145	0.139
1-Octene	0.205	0.185	0.171	0.159
Benzene	0.18	0.167	0.159	0.151
Cyclohexane	0.182	0.169	0.16	0.151
n-Hexane	0.159	0.151	0.146	0.14
n-Dodecane	0.756	0.522	0.398	0.315
n-Heptane	0.179	0.166	0.157	0.149
n-Nonane	0.268	0.224	0.199	0.18
n-Octane	0.213	0.188	0.173	0.162
Toluene	0.219	0.194	0.179	0.166
Xylenes	0.28	0.235	0.209	0.188

Table C.42 Flowrate of the carrier gas, inlet pressure and measured retention times of the selected probes for the column packed with 30% LDPE and 70% LLDPE-a2 at 170, 190, 210 and 230 °C.

T (°C)	170	190	210	230
F (mL/min)	21.66	21.74	21.69	21.68
P_i (kPa)	184	191	196	204
PROBE	RETENTION TIME (min)			
Methane	0.126	0.124	0.122	0.120
1 – Hexene	0.148	0.141	0.135	0.131
1-Octene	0.188	0.17	0.157	0.148
Benzene	0.167	0.156	0.146	0.141
Cyclohexane	0.168	0.157	0.147	0.141
n-Hexane	0.15	0.143	0.137	0.132
n-Dodecane	0.63	0.442	0.339	0.281
n-Heptane	0.166	0.154	0.145	0.14
n-Nonane	0.237	0.201	0.179	0.165
n-Octane	0.192	0.172	0.159	0.149
Toluene	0.197	0.177	0.163	0.152
Xylenes	0.247	0.211	0.187	0.169

215

Table C.43 Flowrate of the carrier gas, inlet pressure and measured retention times of the selected probes for the column packed with pure LLDPE-a3 at 170, 190, 210 and 230 °C.

T (°C)	170	190	210	230
F (mL/min)	20.85	20.93	20.98	21.04
P_i (kPa)	191	196	201	206
PROBE	RETENTION TIME (min)			
Methane	0.129	0.127	0.126	0.124
1 – Hexene	0.153	0.145	0.143	0.136
1-Octene	0.198	0.178	0.168	0.155
Benzene	0.174	0.162	0.155	0.147
Cyclohexane	0.176	0.164	0.156	0.147
n-Hexane	0.155	0.148	0.144	0.138
n-Dodecane	0.697	0.487	0.379	0.29
n-Heptane	0.173	0.161	0.154	0.145
n-Nonane	0.253	0.216	0.194	0.173
n-Octane	0.204	0.183	0.17	0.155
Toluene	0.211	0.189	0.174	0.16
Xylenes	0.268	0.23	0.204	0.18

Table C.44 Flowrate of the carrier gas, inlet pressure and measured retention times of the selected probes for the column packed with 70% LDPE and 30% LLDPE-a3 at 170, 190, 210 and 230 °C.

T (°C)	170	190	210	230
F (mL/min)	20.37	20.38	20.38	20.29
P_i (kPa)	181	188	194	198
PROBE	RETENTION TIME (min)			
Methane	0.124	0.123	0.120	0.117
1 – Hexene	0.144	0.139	0.132	0.128
1-Octene	0.182	0.165	0.15	0.144
Benzene	0.162	0.151	0.142	0.138
Cyclohexane	0.164	0.152	0.143	0.139
n-Hexane	0.146	0.14	0.133	0.131
n-Dodecane	0.58	0.406	0.311	0.252
n-Heptane	0.161	0.151	0.141	0.134
n-Nonane	0.227	0.195	0.169	0.155
n-Octane	0.189	0.169	0.152	0.142
Toluene	0.193	0.171	0.156	0.147
Xylenes	0.237	0.203	0.178	0.163

Table C.45 Flowrate of the carrier gas, inlet pressure and measured retention times of the selected probes for the column packed with 50% LDPE and 50% LLDPE-a3 at 170, 190, 210 and 230 °C.

T (°C)	170	190	210	230
F (mL/min)	21.26	20.93	20.93	21.51
P_i (kPa)	179	186	191	194
PROBE	RETENTION TIME (min)			
Methane	0.127	0.124	0.122	0.120
1 – Hexene	0.149	0.141	0.136	0.131
1-Octene	0.188	0.17	0.159	0.147
Benzene	0.167	0.155	0.148	0.14
Cyclohexane	0.168	0.157	0.149	0.141
n-Hexane	0.149	0.143	0.138	0.131
n-Dodecane	0.644	0.451	0.347	0.265
n-Heptane	0.167	0.154	0.145	0.138
n-Nonane	0.24	0.201	0.176	0.163
n-Octane	0.195	0.174	0.16	0.148
Toluene	0.2	0.177	0.165	0.153
Xylenes	0.251	0.212	0.188	0.169

Table C.46 Flowrate of the carrier gas, inlet pressure and measured retention times of the selected probes for the column packed with 30% LDPE and 70% LLDPE-a3 at 170, 190, 210 and 230 °C.

T (°C)	170	190	210	230
F (mL/min)	21.34	20.61	21.09	20.85
P_i (kPa)	205	209	216	220
PROBE	RETENTION TIME (min)			
Methane	0.137	0.135	0.134	0.132
1 – Hexene	0.169	0.16	0.155	0.148
1-Octene	0.229	0.202	0.186	0.171
Benzene	0.197	0.181	0.171	0.16
Cyclohexane	0.199	0.182	0.172	0.162
n-Hexane	0.171	0.16	0.155	0.149
n-Dodecane	0.878	0.594	0.448	0.338
n-Heptane	0.193	0.178	0.169	0.158
n-Nonane	0.298	0.249	0.219	0.193
n-Octane	0.234	0.207	0.187	0.174
Toluene	0.242	0.214	0.194	0.179
Xylenes	0.317	0.264	0.23	0.204

Table C.47 Flowrate of the carrier gas, inlet pressure and measured retention times of the selected probes for the column packed with pure LLDPE-a4 at 170, 190, 210 and 230 °C.

T (°C)	170	190	210	230
F (mL/min)	21.23	21.57	21.18	20.93
P_i (kPa)	246	254	264	268
PROBE	RETENTION TIME (min)			
Methane	0.143	0.141	0.139	0.138
1 – Hexene	0.171	0.165	0.159	0.155
1-Octene	0.227	0.206	0.191	0.177
Benzene	0.198	0.187	0.174	0.166
Cyclohexane	0.198	0.188	0.176	0.168
n-Hexane	0.173	0.167	0.16	0.156
n-Dodecane	0.838	0.593	0.458	0.348
n-Heptane	0.195	0.183	0.172	0.165
n-Nonane	0.295	0.249	0.221	0.199
n-Octane	0.232	0.21	0.192	0.179
Toluene	0.239	0.217	0.199	0.182
Xylenes	0.31	0.263	0.235	0.21

Table C.48 Flowrate of the carrier gas, inlet pressure and measured retention times of the selected probes for the column packed with 70% LDPE and 30% LLDPE-a4 at 170, 190, 210 and 230 °C.

T (°C)	170	190	210	230
F (mL/min)	21.20	21.07	21.26	21.34
P_i (kPa)	186	192	198	205
PROBE	RETENTION TIME (min)			
Methane	0.129	0.128	0.126	0.123
1 – Hexene	0.151	0.147	0.142	0.136
1-Octene	0.195	0.177	0.165	0.154
Benzene	0.173	0.162	0.154	0.146
Cyclohexane	0.174	0.164	0.154	0.147
n-Hexane	0.154	0.147	0.143	0.138
n-Dodecane	0.671	0.477	0.368	0.289
n-Heptane	0.172	0.161	0.152	0.145
n-Nonane	0.249	0.214	0.19	0.172
n-Octane	0.203	0.181	0.167	0.156
Toluene	0.206	0.186	0.171	0.159
Xylenes	0.26	0.223	0.198	0.179

217

Table C.49 Flowrate of the carrier gas, inlet pressure and measured retention times of the selected probes for the column packed with 50% LDPE and 50% LLDPE-a4 at 170, 190, 210 and 230 °C.

T (°C)	170	190	210	230
F (mL/min)	21.15	20.77	20.66	21.18
P_i (kPa)	179	185	189	194
PROBE	RETENTION TIME (min)			
Methane	0.125	0.124	0.121	0.119
1 – Hexene	0.149	0.142	0.136	0.132
1-Octene	0.195	0.175	0.162	0.149
Benzene	0.171	0.159	0.15	0.142
Cyclohexane	0.173	0.16	0.152	0.142
n-Hexane	0.152	0.145	0.139	0.133
n-Dodecane	0.694	0.483	0.37	0.288
n-Heptane	0.17	0.159	0.149	0.138
n-Nonane	0.251	0.211	0.187	0.167
n-Octane	0.2	0.179	0.164	0.15
Toluene	0.206	0.184	0.168	0.155
Xylenes	0.26	0.224	0.195	0.174

Table C.50 Flowrate of the carrier gas, inlet pressure and measured retention times of the selected probes for the column packed with 30% LDPE and 70% LLDPE-a4 at 170, 190, 210 and 230 °C.

T (°C)	170	190	210	230
F (mL/min)	21.15	21.34	21.43	21.18
P_i (kPa)	181	186	189	194
PROBE	RETENTION TIME (min)			
Methane	0.125	0.122	0.120	0.119
1 – Hexene	0.154	0.146	0.139	0.133
1-Octene	0.208	0.185	0.166	0.154
Benzene	0.179	0.166	0.153	0.145
Cyclohexane	0.182	0.167	0.154	0.145
n-Hexane	0.156	0.149	0.141	0.135
n-Dodecane	0.794	0.547	0.403	0.304
n-Heptane	0.178	0.161	0.152	0.143
n-Nonane	0.274	0.228	0.195	0.175
n-Octane	0.214	0.186	0.168	0.156
Toluene	0.22	0.193	0.176	0.161
Xylenes	0.286	0.236	0.207	0.186

Table C.51 Flowrate of the carrier gas, inlet pressure and measured retention times of the selected probes for the column packed with pure LLDPE-a5 at 170, 190, 210 and 230 °C.

T (°C)	170	190	210	230
F (mL/min)	21.29	21.34	21.26	21.26
P_i (kPa)	244	254	261	268
PROBE	RETENTION TIME (min)			
Methane	0.148	0.148	0.146	0.145
1 – Hexene	0.183	0.175	0.168	0.163
1-Octene	0.246	0.22	0.202	0.188
Benzene	0.211	0.197	0.187	0.177
Cyclohexane	0.214	0.198	0.188	0.178
n-Hexane	0.184	0.176	0.17	0.164
n-Dodecane	0.938	0.649	0.49	0.376
n-Heptane	0.209	0.194	0.184	0.174
n-Nonane	0.321	0.269	0.237	0.212
n-Octane	0.252	0.221	0.205	0.19
Toluene	0.259	0.23	0.212	0.196
Xylenes	0.337	0.284	0.25	0.223

218

Table C.52 Flowrate of the carrier gas, inlet pressure and measured retention times of the selected probes for the column packed with 70% LDPE and 30% LLDPE-a5 at 170, 190, 210 and 230 °C.

T (°C)	170	190	210	230
F (mL/min)	21.43	21.60	21.51	21.60
P_i (kPa)	206	209	215	219
PROBE	RETENTION TIME (min)			
Methane	0.135	0.134	0.132	0.130
1 – Hexene	0.164	0.158	0.152	0.146
1-Octene	0.219	0.198	0.181	0.167
Benzene	0.19	0.178	0.167	0.158
Cyclohexane	0.191	0.18	0.168	0.159
n-Hexane	0.166	0.16	0.153	0.147
n-Dodecane	0.814	0.565	0.42	0.32
n-Heptane	0.189	0.175	0.164	0.156
n-Nonane	0.286	0.241	0.212	0.188
n-Octane	0.226	0.201	0.183	0.168
Toluene	0.232	0.208	0.189	0.174
Xylenes	0.302	0.254	0.222	0.197

Table C.53 Flowrate of the carrier gas, inlet pressure and measured retention times of the selected probes for the column packed with 50% LDPE and 50% LLDPE-a5 at 170, 190, 210 and 230 °C.

T (°C)	170	190	210	230
F (mL/min)	21.34	21.26	20.85	21.01
P_i (kPa)	191	196	201	206
PROBE	RETENTION TIME (min)			
Methane	0.130	0.128	0.126	0.125
1 – Hexene	0.154	0.148	0.141	0.138
1-Octene	0.199	0.18	0.166	0.156
Benzene	0.175	0.164	0.154	0.148
Cyclohexane	0.177	0.165	0.155	0.149
n-Hexane	0.157	0.15	0.144	0.139
n-Dodecane	0.688	0.474	0.366	0.289
n-Heptane	0.175	0.162	0.153	0.146
n-Nonane	0.253	0.214	0.192	0.174
n-Octane	0.204	0.183	0.168	0.158
Toluene	0.209	0.187	0.173	0.161
Xylenes	0.265	0.227	0.2	0.181

Table C.54 Flowrate of the carrier gas, inlet pressure and measured retention times of the selected probes for the column packed with 30% LDPE and 70% LLDPE-a5 at 170, 190, 210 and 230 °C.

T (°C)	170	190	210	230
F (mL/min)	21.26	21.34	20.77	21.26
P_i (kPa)	186	191	196	201
PROBE	RETENTION TIME (min)			
Methane	0.130	0.129	0.128	0.127
1 – Hexene	0.16	0.147	0.144	0.14
1-Octene	0.216	0.181	0.17	0.159
Benzene	0.186	0.165	0.158	0.152
Cyclohexane	0.187	0.167	0.158	0.152
n-Hexane	0.162	0.15	0.146	0.142
n-Dodecane	0.826	0.501	0.383	0.293
n-Heptane	0.184	0.164	0.156	0.149
n-Nonane	0.283	0.221	0.197	0.178
n-Octane	0.222	0.186	0.172	0.162
Toluene	0.229	0.191	0.177	0.166
Xylenes	0.299	0.231	0.206	0.189

219

Table C.55 Flowrate of the carrier gas, inlet pressure and measured retention times of the selected probes for the column packed with pure LLDPE-a6 at 170, 190, 210 and 230 °C.

T (°C)	170	190	210	230
F (mL/min)	21.26	20.77	21.32	21.18
P_i (kPa)	206	211	218	225
PROBE	RETENTION TIME (min)			
Methane	0.129	0.128	0.127	0.126
1 – Hexene	0.148	0.145	0.14	0.137
1-Octene	0.185	0.173	0.161	0.15
Benzene	0.167	0.158	0.152	0.145
Cyclohexane	0.168	0.16	0.152	0.146
n-Hexane	0.15	0.146	0.142	0.136
n-Dodecane	0.597	0.431	0.346	0.27
n-Heptane	0.164	0.157	0.151	0.143
n-Nonane	0.233	0.202	0.184	0.166
n-Octane	0.189	0.174	0.164	0.152
Toluene	0.195	0.178	0.167	0.157
Xylenes	0.241	0.211	0.19	0.172

Table C.56 Flowrate of the carrier gas, inlet pressure and measured retention times of the selected probes for the column packed with 70% LDPE and 30% LLDPE-a6 at 170, 190, 210 and 230 °C.

T (°C)	170	190	210	230
F (mL/min)	21.09	20.93	20.83	20.77
P_i (kPa)	196	204	208	214
PROBE	RETENTION TIME (min)			
Methane	0.137	0.136	0.135	0.131
1 – Hexene	0.157	0.152	0.149	0.142
1-Octene	0.197	0.18	0.169	0.158
Benzene	0.176	0.167	0.159	0.151
Cyclohexane	0.177	0.167	0.16	0.152
n-Hexane	0.16	0.153	0.149	0.143
n-Dodecane	0.603	0.428	0.355	0.275
n-Heptane	0.174	0.166	0.157	0.15
n-Nonane	0.24	0.211	0.192	0.174
n-Octane	0.201	0.183	0.172	0.16
Toluene	0.204	0.188	0.176	0.163
Xylenes	0.252	0.22	0.201	0.181

Table C.57 Flowrate of the carrier gas, inlet pressure and measured retention times of the selected probes for the column packed with 50% LDPE and 50% LLDPE-a6 at 170, 190, 210 and 230 °C.

T (°C)	170	190	210	230
F (mL/min)	21.18	21.43	21.51	21.26
P_i (kPa)	191	196	204	208
PROBE	RETENTION TIME (min)			
Methane	0.134	0.131	0.128	0.125
1 – Hexene	0.162	0.163	0.146	0.14
1-Octene	0.217	0.204	0.17	0.159
Benzene	0.186	0.183	0.159	0.151
Cyclohexane	0.188	0.184	0.16	0.152
n-Hexane	0.164	0.165	0.146	0.142
n-Dodecane	0.783	0.567	0.396	0.302
n-Heptane	0.184	0.182	0.158	0.149
n-Nonane	0.277	0.247	0.201	0.179
n-Octane	0.22	0.208	0.174	0.16
Toluene	0.225	0.213	0.18	0.165
Xylenes	0.289	0.26	0.21	0.186

220

Table C.58 Flowrate of the carrier gas, inlet pressure and measured retention times of the selected probes for the column packed with 30% LDPE and 70% LLDPE-a6 at 170, 190, 210 and 230 °C.

T (°C)	170	190	210	230
F (mL/min)	21.60	21.34	20.77	21.26
P (kPa)	186	191	196	201
PROBE	RETENTION TIME (min)			
Methane	0.131	0.129	0.128	0.127
1 – Hexene	0.155	0.147	0.144	0.14
1-Octene	0.203	0.181	0.17	0.159
Benzene	0.178	0.165	0.158	0.152
Cyclohexane	0.18	0.167	0.158	0.152
n-Hexane	0.158	0.15	0.146	0.142
n-Dodecane	0.723	0.501	0.383	0.293
n-Heptane	0.178	0.164	0.156	0.149
n-Nonane	0.262	0.221	0.197	0.178
n-Octane	0.209	0.186	0.172	0.162
Toluene	0.215	0.191	0.177	0.166
Xylenes	0.274	0.231	0.206	0.189

Table C.59 Flowrate of the carrier gas, inlet pressure and measured retention times of the selected probes for the column packed with pure LLDPE-m1 at 170, 190, 210 and 230 °C.

T (°C)	170	190	210	230
F (mL/min)	23.58	23.79	23.58	23.38
P_i (kPa)	201	206	211	216
PROBE	RETENTION TIME (min)			
Methane	0.120	0.119	0.117	0.115
1 – Hexene	0.141	0.136	0.132	0.126
1-Octene	0.18	0.165	0.153	0.14
Benzene	0.158	0.151	0.143	0.135
Cyclohexane	0.159	0.151	0.143	0.136
n-Hexane	0.142	0.137	0.132	0.127
n-Dodecane	0.605	0.435	0.331	0.253
n-Heptane	0.158	0.148	0.14	0.132
n-Nonane	0.225	0.194	0.17	0.154
n-Octane	0.184	0.167	0.152	0.142
Toluene	0.188	0.171	0.156	0.145
Xylenes	0.236	0.205	0.179	0.161

Table C.60 Flowrate of the carrier gas, inlet pressure and measured retention times of the selected probes for the column packed with 70% LDPE and 30% LLDPE-m1 at 170, 190, 210 and 230 °C.

T (°C)	170	190	210	230
F (mL/min)	23.38	23.52	23.79	23.52
P_i (kPa)	206	211	216	223
PROBE	RETENTION TIME (min)			
Methane	0.121	0.120	0.119	0.118
1 – Hexene	0.149	0.143	0.138	0.132
1-Octene	0.2	0.178	0.161	0.15
Benzene	0.172	0.161	0.15	0.142
Cyclohexane	0.173	0.162	0.152	0.142
n-Hexane	0.15	0.145	0.138	0.132
n-Dodecane	0.762	0.53	0.402	0.298
n-Heptane	0.172	0.16	0.148	0.14
n-Nonane	0.263	0.218	0.19	0.169
n-Octane	0.207	0.181	0.163	0.15
Toluene	0.211	0.186	0.169	0.155
Xylenes	0.276	0.231	0.2	0.176

221

Table C.61 Flowrate of the carrier gas, inlet pressure and measured retention times of the selected probes for the column packed with 50% LDPE and 50% LLDPE-m1 at 170, 190, 210 and 230 °C.

T (°C)	170	190	210	230
F (mL/min)	23.38	23.68	23.68	23.79
P_i (kPa)	203	208	214	219
PROBE	RETENTION TIME (min)			
Methane	0.120	0.118	0.117	0.116
1 – Hexene	0.145	0.138	0.134	0.129
1-Octene	0.192	0.172	0.158	0.148
Benzene	0.167	0.154	0.147	0.14
Cyclohexane	0.168	0.156	0.149	0.141
n-Hexane	0.147	0.14	0.136	0.131
n-Dodecane	0.71	0.492	0.378	0.292
n-Heptane	0.166	0.154	0.146	0.139
n-Nonane	0.25	0.212	0.188	0.167
n-Octane	0.197	0.176	0.16	0.149
Toluene	0.202	0.18	0.164	0.154
Xylenes	0.261	0.223	0.193	0.175

Table C.62 Flowrate of the carrier gas, inlet pressure and measured retention times of the selected probes for the column packed with 30% LDPE and 70% LLDPE-m1 at 170, 190, 210 and 230 °C.

T (°C)	170	190	210	230
F (mL/min)	23.18	23.38	22.98	23.08
P_i (kPa)	206	214	219	224
PROBE	RETENTION TIME (min)			
Methane	0.124	0.123	0.121	0.119
1 – Hexene	0.149	0.142	0.137	0.132
1-Octene	0.196	0.175	0.162	0.15
Benzene	0.17	0.159	0.15	0.143
Cyclohexane	0.172	0.16	0.151	0.143
n-Hexane	0.151	0.144	0.139	0.133
n-Dodecane	0.702	0.492	0.378	0.285
n-Heptane	0.17	0.158	0.149	0.14
n-Nonane	0.253	0.214	0.188	0.168
n-Octane	0.201	0.18	0.165	0.151
Toluene	0.207	0.185	0.169	0.156
Xylenes	0.265	0.227	0.198	0.177

Table C.63 Flowrate of the carrier gas, inlet pressure and measured retention times of the selected probes for the column packed with pure LLDPE-m2 at 170, 190, 210 and 230 °C.

T (°C)	170	190	210	230
F (mL/min)	23.48	23.48	23.58	23.58
P_i (kPa)	216	221	226	231
PROBE	RETENTION TIME (min)			
Methane	0.123	0.122	0.121	0.119
1 – Hexene	0.155	0.147	0.141	0.135
1-Octene	0.212	0.188	0.17	0.157
Benzene	0.181	0.168	0.157	0.148
Cyclohexane	0.184	0.171	0.159	0.149
n-Hexane	0.157	0.15	0.143	0.137
n-Dodecane	0.845	0.582	0.43	0.322
n-Heptane	0.18	0.168	0.156	0.145
n-Nonane	0.278	0.234	0.204	0.176
n-Octane	0.218	0.191	0.174	0.159
Toluene	0.223	0.198	0.18	0.164
Xylenes	0.295	0.248	0.216	0.19

222

Table C.64 Flowrate of the carrier gas, inlet pressure and measured retention times of the selected probes for the column packed with 70% LDPE and 30% LLDPE-m2 at 170, 190, 210 and 230 °C.

T (°C)	170	190	210	230
F (mL/min)	23.79	23.79	23.79	23.48
P_i (kPa)	201	206	211	216
PROBE	RETENTION TIME (min)			
Methane	0.124	0.122	0.121	0.118
1 – Hexene	0.149	0.143	0.137	0.132
1-Octene	0.197	0.177	0.161	0.15
Benzene	0.171	0.159	0.151	0.142
Cyclohexane	0.173	0.161	0.152	0.142
n-Hexane	0.151	0.144	0.139	0.133
n-Dodecane	0.719	0.502	0.38	0.291
n-Heptane	0.171	0.159	0.148	0.14
n-Nonane	0.256	0.216	0.187	0.169
n-Octane	0.203	0.18	0.163	0.152
Toluene	0.209	0.185	0.168	0.156
Xylenes	0.269	0.225	0.198	0.175

Table C.65 Flowrate of the carrier gas, inlet pressure and measured retention times of the selected probes for the column packed with 50% LDPE and 50% LLDPE-m2 at 170, 190, 210 and 230 °C.

T (°C)	170	190	210	230
F (mL/min)	23.48	23.48	23.79	23.79
P_i (kPa)	201	207	213	221
PROBE	RETENTION TIME (min)			
Methane	0.120	0.118	0.117	0.115
1 – Hexene	0.146	0.14	0.135	0.129
1-Octene	0.194	0.174	0.161	0.146
Benzene	0.169	0.157	0.149	0.14
Cyclohexane	0.171	0.159	0.15	0.141
n-Hexane	0.148	0.141	0.136	0.13
n-Dodecane	0.74	0.515	0.387	0.29
n-Heptane	0.168	0.155	0.147	0.137
n-Nonane	0.254	0.215	0.19	0.165
n-Octane	0.201	0.178	0.164	0.149
Toluene	0.206	0.184	0.169	0.154
Xylenes	0.269	0.227	0.2	0.175

Table C.66 Flowrate of the carrier gas, inlet pressure and measured retention times of the selected probes for the column packed with 30% LDPE and 70% LLDPE-m2 at 170, 190, 210 and 230 °C.

T (°C)	170	190	210	230
F (mL/min)	24.32	24.32	23.68	23.68
P_i (kPa)	188	193	199	204
PROBE	RETENTION TIME (min)			
Methane	0.113	0.111	0.11	0.107
1 – Hexene	0.14	0.133	0.128	0.12
1-Octene	0.19	0.166	0.152	0.139
Benzene	0.162	0.148	0.139	0.131
Cyclohexane	0.164	0.15	0.14	0.133
n-Hexane	0.142	0.133	0.128	0.121
n-Dodecane	0.727	0.493	0.366	0.278
n-Heptane	0.162	0.148	0.138	0.129
n-Nonane	0.25	0.202	0.177	0.158
n-Octane	0.196	0.169	0.152	0.141
Toluene	0.201	0.176	0.157	0.146
Xylenes	0.261	0.216	0.185	0.166

Table C.67 Flowrate of the carrier gas, inlet pressure and measured retention times of the selected probes for the column packed with pure LLDPE-m3 at 170, 190, 210 and 230 °C.

T (°C)	170	190	210	230
F (mL/min)	23.48	23.79	23.79	23.79
P_i (kPa)	199	206	211	216
PROBE	RETENTION TIME (min)			
Methane	0.120	0.119	0.117	0.114
1 – Hexene	0.145	0.139	0.133	0.128
1-Octene	0.193	0.173	0.157	0.146
Benzene	0.166	0.156	0.146	0.138
Cyclohexane	0.168	0.158	0.147	0.139
n-Hexane	0.146	0.141	0.134	0.129
n-Dodecane	0.721	0.495	0.375	0.282
n-Heptane	0.164	0.154	0.145	0.137
n-Nonane	0.249	0.207	0.184	0.165
n-Octane	0.198	0.174	0.16	0.148
Toluene	0.203	0.18	0.166	0.153
Xylenes	0.263	0.22	0.194	0.173

Table C.68 Flowrate of the carrier gas, inlet pressure and measured retention times of the selected probes for the column packed with 70% LDPE and 30% LLDPE-m3 at 170, 190, 210 and 230 °C.

T (°C)	170	190	210	230
F (mL/min)	23.68	23.89	23.79	23.79
P_i (kPa)	206	214	219	226
PROBE	RETENTION TIME (min)			
Methane	0.124	0.123	0.121	0.120
1 – Hexene	0.153	0.145	0.14	0.135
1-Octene	0.205	0.183	0.168	0.156
Benzene	0.176	0.164	0.155	0.148
Cyclohexane	0.179	0.166	0.156	0.148
n-Hexane	0.155	0.147	0.141	0.137
n-Dodecane	0.778	0.539	0.407	0.303
n-Heptane	0.175	0.163	0.152	0.145
n-Nonane	0.267	0.226	0.202	0.178
n-Octane	0.21	0.187	0.171	0.158
Toluene	0.216	0.192	0.177	0.163
Xylenes	0.282	0.237	0.211	0.187

Table C.69 Flowrate of the carrier gas, inlet pressure and measured retention times of the selected probes for the column packed with 50% LDPE and 50% LLDPE-m3 at 170, 190, 210 and 230 °C.

T (°C)	170	190	210	230
F (mL/min)	23.58	23.79	23.58	23.48
P_i (kPa)	206	214	219	226
PROBE	RETENTION TIME (min)			
Methane	0.123	0.121	0.120	0.118
1 – Hexene	0.15	0.144	0.139	0.134
1-Octene	0.203	0.181	0.167	0.154
Benzene	0.174	0.162	0.153	0.145
Cyclohexane	0.177	0.164	0.154	0.146
n-Hexane	0.152	0.146	0.14	0.135
n-Dodecane	0.78	0.537	0.41	0.31
n-Heptane	0.174	0.16	0.151	0.144
n-Nonane	0.267	0.224	0.198	0.176
n-Octane	0.209	0.185	0.17	0.156
Toluene	0.215	0.191	0.175	0.161
Xylenes	0.282	0.236	0.208	0.184

224

Table C.70 Flowrate of the carrier gas, inlet pressure and measured retention times of the selected probes for the column packed with 30% LDPE and 70% LLDPE-m3 at 170, 190, 210 and 230 °C.

T (°C)	170	190	210	230
F (mL/min)	23.38	23.48	23.38	23.38
P_i (kPa)	206	211	216	221
PROBE	RETENTION TIME (min)			
Methane	0.124	0.122	0.120	0.118
1 – Hexene	0.153	0.147	0.14	0.134
1-Octene	0.206	0.185	0.168	0.154
Benzene	0.177	0.166	0.155	0.146
Cyclohexane	0.179	0.167	0.156	0.146
n-Hexane	0.154	0.148	0.141	0.135
n-Dodecane	0.79	0.548	0.414	0.308
n-Heptane	0.176	0.164	0.152	0.144
n-Nonane	0.271	0.228	0.198	0.177
n-Octane	0.212	0.188	0.17	0.156
Toluene	0.218	0.195	0.175	0.161
Xylenes	0.284	0.24	0.209	0.186

Table C.71 Flowrate of the carrier gas, inlet pressure and measured retention times of the selected probes for the column packed with pure LLDPE-m4 at 170, 190, 210 and 230 °C.

T (°C)	170	190	210	230
F (mL/min)	23.68	23.28	23.48	23.79
P_i (kPa)	199	206	211	216
PROBE	RETENTION TIME (min)			
Methane	0.120	0.119	0.117	0.115
1 – Hexene	0.144	0.138	0.132	0.128
1-Octene	0.189	0.171	0.158	0.147
Benzene	0.165	0.155	0.145	0.138
Cyclohexane	0.167	0.155	0.146	0.139
n-Hexane	0.146	0.14	0.134	0.13
n-Dodecane	0.687	0.48	0.364	0.283
n-Heptane	0.164	0.153	0.143	0.136
n-Nonane	0.243	0.208	0.183	0.159
n-Octane	0.194	0.174	0.16	0.147
Toluene	0.199	0.179	0.164	0.153
Xylenes	0.256	0.218	0.192	0.17

Table C.72 Flowrate of the carrier gas, inlet pressure and measured retention times of the selected probes for the column packed with 70% LDPE and 30% LLDPE-m4 at 170, 190, 210 and 230 °C.

T (°C)	170	190	210	230
F (mL/min)	23.38	23.79	23.58	23.58
P_1 (kPa)	191	199	204	209
PROBE	RETENTION TIME (min)			
Methane	0.119	0.118	0.116	0.115
1 – Hexene	0.141	0.136	0.131	0.127
1-Octene	0.181	0.163	0.152	0.143
Benzene	0.16	0.149	0.142	0.136
Cyclohexane	0.162	0.15	0.143	0.136
n-Hexane	0.143	0.137	0.132	0.127
n-Dodecane	0.611	0.434	0.342	0.263
n-Heptane	0.158	0.148	0.141	0.134
n-Nonane	0.23	0.196	0.175	0.158
n-Octane	0.184	0.166	0.154	0.143
Toluene	0.189	0.171	0.159	0.147
Xylenes	0.235	0.205	0.184	0.166

225

Table C.73 Flowrate of the carrier gas, inlet pressure and measured retention times of the selected probes for the column packed with 50% LDPE and 50% LLDPE-m4 at 170, 190, 210 and 230 °C.

T (°C)	170	190	210	230
F (mL/min)	23.68	23.68	23.68	23.79
P$_i$ (kPa)	201	206	211	216
PROBE	RETENTION TIME (min)			
Methane	0.121	0.120	0.119	0.117
1 – Hexene	0.144	0.139	0.134	0.13
1-Octene	0.185	0.169	0.158	0.146
Benzene	0.164	0.154	0.146	0.14
Cyclohexane	0.165	0.155	0.146	0.14
n-Hexane	0.147	0.14	0.135	0.13
n-Dodecane	0.673	0.463	0.361	0.272
n-Heptane	0.163	0.152	0.144	0.137
n-Nonane	0.235	0.204	0.182	0.162
n-Octane	0.19	0.172	0.159	0.147
Toluene	0.195	0.176	0.162	0.151
Xylenes	0.248	0.214	0.19	0.171

Table C.74 Flowrate of the carrier gas, inlet pressure and measured retention times of the selected probes for the column packed with 30% LDPE and 70% LLDPE-m4 at 170, 190, 210 and 230 °C.

T (°C)	170	190	210	230
F (mL/min)	21.38	21.79	21.79	21.79
P$_i$ (kPa)	191	198	203	208
PROBE	RETENTION TIME (min)			
Methane	0.117	0.116	0.115	0.114
1 – Hexene	0.145	0.138	0.132	0.128
1-Octene	0.196	0.175	0.159	0.147
Benzene	0.169	0.156	0.147	0.139
Cyclohexane	0.171	0.158	0.148	0.141
n-Hexane	0.147	0.14	0.134	0.129
n-Dodecane	0.758	0.521	0.386	0.294
n-Heptane	0.168	0.155	0.145	0.137
n-Nonane	0.258	0.217	0.189	0.169
n-Octane	0.202	0.178	0.162	0.15
Toluene	0.207	0.184	0.169	0.155
Xylenes	0.271	0.228	0.202	0.178

Table C.75 Flowrate of the carrier gas, inlet pressure and measured retention times of the selected probes for the column packed with pure LLDPE-m5 at 170, 190, 210 and 230 °C.

T (°C)	170	190	210	230
F (mL/min)	21.07	21.01	21.09	21.60
P$_i$ (kPa)	196	201	206	211
PROBE	RETENTION TIME (min)			
Methane	0.132	0.131	0.128	0.126
1 – Hexene	0.154	0.149	0.143	0.139
1-Octene	0.195	0.179	0.165	0.155
Benzene	0.174	0.164	0.155	0.148
Cyclohexane	0.175	0.165	0.156	0.149
n-Hexane	0.157	0.151	0.145	0.141
n-Dodecane	0.652	0.469	0.36	0.277
n-Heptane	0.173	0.163	0.154	0.147
n-Nonane	0.247	0.213	0.192	0.173
n-Octane	0.201	0.182	0.167	0.157
Toluene	0.206	0.187	0.172	0.159
Xylenes	0.259	0.224	0.198	0.177

Table C.76 Flowrate of the carrier gas, inlet pressure and measured retention times of the selected probes for the column packed with 70% LDPE and 30% LLDPE-m5 at 170, 190, 210 and 230 °C.

T (°C)	170	190	210	230
F (mL/min)	21.01	20.61	20.77	20.77
P_1 (kPa)	199	205	209	214
PROBE	RETENTION TIME (min)			
Methane	0.134	0.133	0.131	0.128
1 – Hexene	0.163	0.156	0.15	0.144
1-Octene	0.216	0.198	0.179	0.165
Benzene	0.188	0.176	0.166	0.156
Cyclohexane	0.189	0.177	0.167	0.157
n-Hexane	0.164	0.158	0.152	0.145
n-Dodecane	0.786	0.566	0.42	0.313
n-Heptane	0.186	0.174	0.163	0.153
n-Nonane	0.279	0.237	0.21	0.184
n-Octane	0.223	0.199	0.181	0.166
Toluene	0.228	0.206	0.187	0.17
Xylenes	0.293	0.254	0.221	0.194

Table C.77 Flowrate of the carrier gas, inlet pressure and measured retention times of the selected probes for the column packed with 50% LDPE and 50% LLDPE-m5 at 170, 190, 210 and 230 °C.

T (°C)	170	190	210	230
F (mL/min)	20.45	20.77	20.77	20.69
P_1 (kPa)	196	201	206	213
PROBE	RETENTION TIME (min)			
Methane	0.137	0.137	0.134	0.132
1 – Hexene	0.163	0.159	0.153	0.146
1-Octene	0.212	0.195	0.178	0.165
Benzene	0.187	0.176	0.166	0.157
Cyclohexane	0.189	0.178	0.167	0.158
n-Hexane	0.166	0.16	0.154	0.147
n-Dodecane	0.757	0.532	0.4	0.309
n-Heptane	0.187	0.174	0.165	0.157
n-Nonane	0.276	0.234	0.205	0.187
n-Octane	0.221	0.198	0.18	0.169
Toluene	0.226	0.204	0.185	0.174
Xylenes	0.289	0.247	0.216	0.194

Table C.78 Flowrate of the carrier gas, inlet pressure and measured retention times of the selected probes for the column packed with 30% LDPE and 70% LLDPE-m5 at 170, 190, 210 and 230 °C.

T (°C)	170	190	210	230
F (mL/min)	21.63	22.13	21.86	21.34
P_1 (kPa)	201	206	211	216
PROBE	RETENTION TIME (min)			
Methane	0.129	0.127	0.126	0.123
1 – Hexene	0.157	0.149	0.143	0.138
1-Octene	0.211	0.186	0.171	0.157
Benzene	0.182	0.168	0.159	0.15
Cyclohexane	0.184	0.169	0.16	0.15
n-Hexane	0.159	0.151	0.145	0.14
n-Dodecane	0.778	0.534	0.401	0.3
n-Heptane	0.18	0.166	0.157	0.147
n-Nonane	0.274	0.228	0.199	0.178
n-Octane	0.214	0.191	0.173	0.159
Toluene	0.22	0.196	0.177	0.164
Xylenes	0.286	0.241	0.211	0.187

227

Table C.79 Flowrate of the carrier gas, inlet pressure and measured retention times of the selected probes for the column packed with pure LLDPE-m6 at 170, 190, 210 and 230 °C.

T (°C)	170	190	210	230
F (mL/min)	23.89	23.89	23.68	23.89
P_i (kPa)	179	184	189	194
PROBE	RETENTION TIME (min)			
Methane	0.109	0.107	0.105	0.103
1 – Hexene	0.132	0.126	0.121	0.116
1-Octene	0.176	0.158	0.145	0.134
Benzene	0.152	0.142	0.134	0.126
Cyclohexane	0.154	0.143	0.135	0.127
n-Hexane	0.134	0.127	0.123	0.117
n-Dodecane	0.661	0.458	0.348	0.262
n-Heptane	0.151	0.14	0.133	0.123
n-Nonane	0.23	0.195	0.171	0.149
n-Octane	0.18	0.161	0.147	0.134
Toluene	0.187	0.166	0.152	0.139
Xylenes	0.242	0.205	0.18	0.159

Table C.80 Flowrate of the carrier gas, inlet pressure and measured retention times of the selected probes for the column packed with 70% LDPE and 30% LLDPE-m6 at 170, 190, 210 and 230 °C.

T (°C)	170	190	210	230
F (mL/min)	23.48	23.58	23.48	23.48
P_1 (kPa)	176	183	188	193
PROBE	RETENTION TIME (min)			
Methane	0.111	0.110	0.109	0.106
1 – Hexene	0.135	0.128	0.124	0.119
1-Octene	0.176	0.156	0.146	0.134
Benzene	0.153	0.142	0.136	0.128
Cyclohexane	0.155	0.144	0.136	0.129
n-Hexane	0.136	0.129	0.125	0.12
n-Dodecane	0.64	0.442	0.34	0.258
n-Heptane	0.153	0.141	0.134	0.126
n-Nonane	0.223	0.191	0.17	0.148
n-Octane	0.179	0.161	0.148	0.135
Toluene	0.183	0.165	0.152	0.14
Xylenes	0.236	0.202	0.179	0.156

Table C.81 Flowrate of the carrier gas, inlet pressure and measured retention times of the selected probes for the column packed with 50% LDPE and 50% LLDPE-m6 at 170, 190, 210 and 230 °C.

T (°C)	170	190	210	230
F (mL/min)	23.27	23.48	23.38	23.48
P_1 (kPa)	186	191	196	204
PROBE	RETENTION TIME (min)			
Methane	0.114	0.112	0.110	0.109
1 – Hexene	0.138	0.132	0.126	0.121
1-Octene	0.184	0.164	0.15	0.138
Benzene	0.158	0.147	0.138	0.131
Cyclohexane	0.16	0.149	0.14	0.132
n-Hexane	0.14	0.133	0.128	0.123
n-Dodecane	0.677	0.471	0.356	0.264
n-Heptane	0.158	0.146	0.138	0.13
n-Nonane	0.239	0.201	0.177	0.157
n-Octane	0.189	0.168	0.153	0.141
Toluene	0.194	0.172	0.157	0.144
Xylenes	0.251	0.212	0.187	0.165

228

Table C.82 Flowrate of the carrier gas, inlet pressure and measured retention times of the selected probes for the column packed with 30% LDPE and 70% LLDPE-m6 at 170, 190, 210 and 230 °C.

T (°C)	170	190	210	230
F (mL/min)	23.48	23.79	23.58	23.48
P_i (kPa)	193	199	205	211
PROBE	RETENTION TIME (min)			
Methane	0.118	0.116	0.114	0.112
1 — Hexene	0.147	0.14	0.134	0.128
1-Octene	0.201	0.178	0.162	0.148
Benzene	0.173	0.159	0.149	0.14
Cyclohexane	0.174	0.16	0.15	0.141
n-Hexane	0.149	0.141	0.135	0.13
n-Dodecane	0.802	0.548	0.413	0.304
n-Heptane	0.171	0.157	0.147	0.138
n-Nonane	0.268	0.218	0.194	0.171
n-Octane	0.208	0.181	0.164	0.15
Toluene	0.214	0.188	0.171	0.155
Xylenes	0.284	0.235	0.205	0.179

229

Appendix D

Measured Flory-Huggins interaction parameters

between the selected solvents and different pure

polymers (blends) used in the thesis

Table D.1 Measured Flory-Huggins interaction parameters between the selected solvents and 30/70 HDPE/LDPE blend at 170, 190, 210 and 230 °C.

T (°C)	170	190	210	230
PROBE	$\chi_{1(23)}$			
1 – Hexene	0.12	0.11	0.10	0.04
1-Octene	0.10	0.10	0.09	0.09
Benzene	0.21	0.20	0.17	0.16
Cyclohexane	0.11	0.11	0.10	0.10
n-Hexane	0.12	0.10	0.10	0.05
n-Dodecane	0.06	0.06	0.05	0.05
n-Heptane	0.10	0.10	0.10	0.08
n-Nonane	0.08	0.08	0.08	0.07
n-Octane	0.09	0.10	0.10	0.07
Toluene	0.16	0.14	0.15	0.14
Xylenes	0.13	0.12	0.12	0.10

Table D.2 Measured Flory-Huggins interaction parameters between the selected solvents and 70/30 HDPE/LDPE blend at 170, 190, 210 and 230 °C.

T (°C)	170	190	210	230
PROBE	$\chi_{1(23)}$			
1 – Hexene	0.13	0.12	0.11	0.04
1-Octene	0.10	0.10	0.09	0.09
Benzene	0.21	0.20	0.19	0.18
Cyclohexane	0.11	0.12	0.11	0.10
n-Hexane	0.11	0.12	0.10	0.06
n-Dodecane	0.06	0.06	0.05	0.04
n-Heptane	0.11	0.09	0.08	0.08
n-Nonane	0.08	0.08	0.07	0.07
n-Octane	0.10	0.10	0.09	0.08
Toluene	0.16	0.14	0.14	0.12
Xylenes	0.12	0.12	0.11	0.10

Table D.3 Measured Flory-Huggins interaction parameters between the selected solvents and pure i-PP at 170, 190, 210 and 230 °C.

T (°C)	170	190	210	230
PROBE	χ_{13}			
1 – Hexene	0.08	0.06	0.07	0.01
1-Octene	0.07	0.06	0.06	0.06
Benzene	0.17	0.16	0.15	0.13
Cyclohexane	0.07	0.06	0.08	0.05
n-Hexane	0.07	0.06	0.05	0.01
n-Dodecane	0.04	0.03	0.02	0.02
n-Heptane	0.06	0.05	0.06	0.04
n-Nonane	0.05	0.04	0.04	0.04
n-Octane	0.06	0.05	0.05	0.05
Toluene	0.12	0.11	0.10	0.09
Xylenes	0.11	0.09	0.08	0.07

Table D.4 Measured Flory-Huggins interaction parameters between the selected solvents and 30/70 HDPE/i-PP blend at 170, 190, 210 and 230 °C.

T (°C)	170	190	210	230
PROBE	$\chi_{1(23)}$			
1 – Hexene	0.09	0.06	0.06	-0.01
1-Octene	0.08	0.07	0.07	0.05
Benzene	0.21	0.19	0.16	0.12
Cyclohexane	0.10	0.08	0.08	0.06
n-Hexane	0.09	0.07	0.03	0.00
n-Dodecane	0.05	0.04	0.03	0.02
n-Heptane	0.08	0.07	0.06	0.05
n-Nonane	0.07	0.06	0.05	0.03
n-Octane	0.07	0.06	0.05	0.05
Toluene	0.15	0.12	0.11	0.09
xylenes	0.12	0.10	0.08	0.07

231

Table D.5 Measured Flory-Huggins interaction parameters between the selected solvents and 50/50 HDPE/i-PP blend at 170, 190, 210 and 230 °C.

T (°C)	170	190	210	230
PROBE	$\chi_{1(23)}$			
1 – Hexene	0.08	0.08	0.04	0.003
1-Octene	0.07	0.07	0.05	0.05
Benzene	0.16	0.16	0.12	0.11
Cyclohexane	0.07	0.07	0.05	0.05
n-Hexane	0.08	0.07	0.05	0.01
n-Dodecane	0.04	0.04	0.03	0.02
n-Heptane	0.07	0.07	0.05	0.04
n-Nonane	0.05	0.06	0.04	0.03
n-Octane	0.06	0.06	0.04	0.04
Toluene	0.12	0.11	0.09	0.08
Xylenes	0.09	0.09	0.07	0.07

Table D.6 Measured Flory-Huggins interaction parameters between the selected solvents and 70/30 HDPE/i-PP blend at 170, 190, 210 and 230 °C.

T (°C)	170	190	210	230
PROBE	$\chi_{1(23)}$			
1 – Hexene	0.10	0.07	0.06	0.01
1-Octene	0.08	0.07	0.06	0.06
Benzene	0.18	0.16	0.14	0.17
Cyclohexane	0.10	0.08	0.08	0.06
n-Hexane	0.09	0.07	0.07	0.04
n-Dodecane	0.05	0.04	0.02	0.02
n-Heptane	0.09	0.07	0.06	0.05
n-Nonane	0.07	0.06	0.04	0.04
n-Octane	0.07	0.07	0.05	0.04
Toluene	0.13	0.12	0.10	0.09
Xylenes	0.11	0.09	0.07	0.07

Table D.7 Measured Flory-Huggins interaction parameters between the selected solvents and 30/70 HDPE/PS blend at 170, 190, 210 and 230 °C.

T (°C)	170	190	210	230
PROBE	$\chi_{1(23)}$			
1 – Hexene	0.19	0.15	0.16	0.04
1-Octene	0.15	0.14	0.13	0.09
Benzene	0.20	0.18	0.20	0.13
Cyclohexane	0.18	0.16	0.16	0.11
n-Hexane	0.18	0.16	0.14	0.06
n-Dodecane	0.11	0.09	0.08	0.05
n-Heptane	0.16	0.15	0.14	0.09
n-Nonane	0.14	0.13	0.12	0.08
n-Octane	0.15	0.14	0.13	0.09
Toluene	0.16	0.14	0.15	0.10
Xylenes	0.14	0.12	0.12	0.09

Table D.8 Measured Flory-Huggins interaction parameters between the selected solvents and 70/30 HDPE/PS blend at 170, 190, 210 and 230 °C.

T (°C)	170	190	210	230
PROBE	$\chi_{1(23)}$			
1 – Hexene	0.14	0.14	0.09	0.04
1-Octene	0.12	0.11	0.10	0.08
Benzene	0.20	0.19	0.17	0.14
Cyclohexane	0.14	0.13	0.11	0.09
n-Hexane	0.14	0.12	0.09	0.05
n-Dodecane	0.08	0.07	0.06	0.04
n-Heptane	0.13	0.12	0.09	0.08
n-Nonane	0.11	0.10	0.08	0.07
n-Octane	0.12	0.11	0.09	0.08
Toluene	0.16	0.15	0.13	0.12
Xylenes	0.13	0.12	0.11	0.09

232

Table D.9 Measured Flory-Huggins interaction parameters between the selected solvents and 30/70 HDPE/LLDPE-1 blend at 170, 190, 210 and 230 °C.

T (°C)	170	190	210	230
PROBE	$\chi_{1(23)}$			
1 – Hexene	0.11	0.10	0.07	0.02
1-Octene	0.09	0.08	0.07	0.07
Benzene	0.17	0.16	0.15	0.13
Cyclohexane	0.10	0.09	0.09	0.09
n-Hexane	0.10	0.09	0.07	0.04
n-Dodecane	0.05	0.04	0.04	0.04
n-Heptane	0.09	0.08	0.08	0.07
n-Nonane	0.07	0.07	0.06	0.06
n-Octane	0.08	0.07	0.07	0.07
Toluene	0.14	0.13	0.11	0.11
Xylenes	0.11	0.10	0.09	0.09

Table D.10 Measured Flory-Huggins interaction parameters between the selected solvents and 70/30 HDPE/LLDPE-1 blend at 170, 190, 210 and 230 °C.

T (°C)	170	190	210	230
PROBE	$\chi_{1(23)}$			
1 – Hexene	0.15	0.12	0.09	0.05
1-Octene	0.12	0.10	0.10	0.09
Benzene	0.23	0.21	0.20	0.18
Cyclohexane	0.14	0.12	0.12	0.11
n-Hexane	0.13	0.11	0.09	0.06
n-Dodecane	0.07	0.06	0.05	0.05
n-Heptane	0.12	0.11	0.10	0.09
n-Nonane	0.10	0.09	0.08	0.08
n-Octane	0.11	0.10	0.09	0.08
Toluene	0.18	0.16	0.15	0.14
Xylenes	0.15	0.13	0.12	0.11

Table D.11 Measured Flory-Huggins interaction parameters between the selected solvents and pure LLDPE-2 at 170, 190, 210 and 230 °C.

T (°C)	170	190	210	230
PROBE	χ_{13}			
1 – Hexene	0.12	0.10	0.09	0.04
1-Octene	0.10	0.10	0.09	0.09
Benzene	0.20	0.20	0.19	0.19
Cyclohexane	0.11	0.11	0.11	0.13
n-Hexane	0.11	0.10	0.08	0.06
n-Dodecane	0.06	0.05	0.05	0.05
n-Heptane	0.10	0.10	0.10	0.09
n-Nonane	0.08	0.08	0.07	0.07
n-Octane	0.09	0.09	0.08	0.08
Toluene	0.15	0.14	0.14	0.13
Xylenes	0.12	0.11	0.11	0.12

Table D.12 Measured Flory-Huggins interaction parameters between the selected solvents and 30/70 HDPE/LLDPE-2 blend at 170, 190, 210 and 230 °C.

T (°C)	170	190	210	230
PROBE	$\chi_{1(23)}$			
1 – Hexene	0.14	0.13	0.11	0.07
1-Octene	0.12	0.11	0.11	0.10
Benzene	0.24	0.22	0.19	0.20
Cyclohexane	0.15	0.13	0.13	0.12
n-Hexane	0.13	0.12	0.09	0.07
n-Dodecane	0.07	0.06	0.05	0.05
n-Heptane	0.13	0.12	0.09	0.09
n-Nonane	0.10	0.09	0.08	0.08
n-Octane	0.11	0.10	0.10	0.09
Toluene	0.19	0.18	0.16	0.15
Xylenes	0.15	0.14	0.13	0.12

233

Table D.13 Measured Flory-Huggins interaction parameters between the selected solvents and 50/50 HDPE/LLDPE-2 blend at 170, 190, 210 and 230 °C.

T (°C)	170	190	210	230
PROBE	$\chi_{1(23)}$			
1 – Hexene	0.15	0.14	0.11	0.05
1-Octene	0.12	0.12	0.12	0.11
Benzene	0.24	0.24	0.22	0.19
Cyclohexane	0.15	0.15	0.14	0.13
n-Hexane	0.14	0.13	0.10	0.07
n-Dodecane	0.07	0.07	0.06	0.06
n-Heptane	0.13	0.12	0.10	0.10
n-Nonane	0.11	0.10	0.09	0.09
n-Octane	0.11	0.12	0.10	0.09
Toluene	0.18	0.19	0.16	0.15
Xylenes	0.15	0.15	0.13	0.13

Table D.14 Measured Flory-Huggins interaction parameters between the selected solvents and 70/30 HDPE/LLDPE-2 blend at 170, 190, 210 and 230 °C.

T (°C)	170	190	210	230
PROBE	$\chi_{1(23)}$			
1 – Hexene	0.17	0.14	0.11	0.06
1-Octene	0.14	0.12	0.12	0.11
Benzene	0.28	0.26	0.23	0.23
Cyclohexane	0.17	0.16	0.15	0.14
n-Hexane	0.15	0.14	0.10	0.07
n-Dodecane	0.09	0.07	0.06	0.06
n-Heptane	0.14	0.13	0.12	0.11
n-Nonane	0.12	0.11	0.10	0.09
n-Octane	0.13	0.12	0.11	0.10
Toluene	0.21	0.19	0.18	0.17
Xylenes	0.17	0.16	0.15	0.14

Table D.15 Measured Flory-Huggins interaction parameters between the selected solvents and pure LLDPE-3 at 170, 190, 210 and 230 °C.

T (°C)	170	190	210	230
PROBE	χ_{13}			
1 – Hexene	0.11	0.11	0.10	0.04
1-Octene	0.09	0.09	0.09	0.08
Benzene	0.19	0.18	0.19	0.16
Cyclohexane	0.10	0.11	0.11	0.10
n-Hexane	0.11	0.09	0.09	0.04
n-Dodecane	0.05	0.05	0.04	0.04
n-Heptane	0.09	0.08	0.09	0.08
n-Nonane	0.08	0.07	0.07	0.06
n-Octane	0.08	0.08	0.08	0.07
Toluene	0.14	0.13	0.14	0.12
Xylenes	0.11	0.10	0.10	0.10

Table D.16 Measured Flory-Huggins interaction parameters between the selected solvents and 30/70 HDPE/LLDPE-3 blend at 170, 190, 210 and 230 °C.

T (°C)	170	190	210	230
PROBE	$\chi_{1(23)}$			
1 – Hexene	0.11	0.09	0.08	0.03
1-Octene	0.09	0.08	0.08	0.07
Benzene	0.18	0.17	0.15	0.13
Cyclohexane	0.11	0.10	0.09	0.07
n-Hexane	0.10	0.08	0.07	0.04
n-Dodecane	0.05	0.05	0.03	0.03
n-Heptane	0.09	0.09	0.07	0.07
n-Nonane	0.08	0.07	0.06	0.06
n-Octane	0.08	0.08	0.07	0.06
Toluene	0.14	0.13	0.12	0.12
Xylenes	0.11	0.10	0.09	0.09

234

Table D.17 Measured Flory-Huggins interaction parameters between the selected solvents and 50/50 HDPE/LLDPE-3 blend at 170, 190, 210 and 230 °C.

T (°C)	170	190	210	230
PROBE	$\chi_{1(23)}$			
1 – Hexene	0.14	0.10	0.10	0.04
1-Octene	0.11	0.11	0.09	0.09
Benzene	0.22	0.20	0.18	0.17
Cyclohexane	0.14	0.12	0.11	0.09
n-Hexane	0.13	0.09	0.08	0.05
n-Dodecane	0.07	0.06	0.05	0.05
n-Heptane	0.11	0.09	0.09	0.08
n-Nonane	0.09	0.08	0.07	0.07
n-Octane	0.10	0.08	0.08	0.07
Toluene	0.16	0.14	0.14	0.12
Xylenes	0.14	0.13	0.11	0.10

Table D.18 Measured Flory-Huggins interaction parameters between the selected solvents and 70/30 HDPE/LLDPE-3 blend at 170, 190, 210 and 230 °C.

T (°C)	170	190	210	230
PROBE	$\chi_{1(23)}$			
1 – Hexene	0.12	0.11	0.08	0.04
1-Octene	0.10	0.09	0.08	0.08
Benzene	0.20	0.18	0.16	0.14
Cyclohexane	0.12	0.11	0.09	0.09
n-Hexane	0.12	0.10	0.07	0.04
n-Dodecane	0.06	0.05	0.04	0.04
n-Heptane	0.10	0.09	0.08	0.06
n-Nonane	0.08	0.08	0.06	0.06
n-Octane	0.09	0.08	0.07	0.06
Toluene	0.15	0.14	0.12	0.11
Xylenes	0.12	0.11	0.10	0.09

Table D.19 Measured Flory-Huggins interaction parameters between the selected solvents and pure LLDPE-4 at 170, 190, 210 and 230 °C.

T (°C)	170	190	210	230
PROBE	χ_{13}			
1 – Hexene	0.14	0.11	0.11	0.06
1-Octene	0.12	0.11	0.11	0.10
Benzene	0.24	0.22	0.22	0.21
Cyclohexane	0.15	0.13	0.13	0.13
n-Hexane	0.12	0.11	0.10	0.07
n-Dodecane	0.07	0.07	0.06	0.06
n-Heptane	0.13	0.11	0.11	0.09
n-Nonane	0.10	0.10	0.09	0.09
n-Octane	0.11	0.10	0.10	0.10
Toluene	0.19	0.17	0.17	0.17
Xylenes	0.16	0.14	0.13	0.13

Table D.20 Measured Flory-Huggins interaction parameters between the selected solvents and 30/70 HDPE/LLDPE-4 blend at 170, 190, 210 and 230 °C.

T (°C)	170	190	210	230
PROBE	$\chi_{1(23)}$			
1 – Hexene	0.12	0.12	0.08	0.03
1-Octene	0.10	0.10	0.08	0.09
Benzene	0.22	0.21	0.16	0.17
Cyclohexane	0.12	0.12	0.08	0.10
n-Hexane	0.11	0.11	0.07	0.05
n-Dodecane	0.06	0.05	0.04	0.04
n-Heptane	0.11	0.10	0.08	0.07
n-Nonane	0.09	0.08	0.07	0.07
n-Octane	0.10	0.09	0.07	0.07
Toluene	0.16	0.15	0.13	0.12
Xylenes	0.13	0.12	0.11	0.09

235

Table D.21 Measured Flory-Huggins interaction parameters between the selected solvents and 50/50 HDPE/LLDPE-4 blend at 170, 190, 210 and 230 °C.

T (°C)	170	190	210	230
PROBE	$\chi_{1(23)}$			
1 – Hexene	0.12	0.10	0.08	0.03
1-Octene	0.09	0.09	0.08	0.07
Benzene	0.20	0.18	0.15	0.14
Cyclohexane	0.13	0.10	0.08	0.09
n-Hexane	0.12	0.09	0.07	0.04
n-Dodecane	0.05	0.04	0.04	0.04
n-Heptane	0.11	0.09	0.07	0.06
n-Nonane	0.08	0.07	0.06	0.07
n-Octane	0.09	0.08	0.07	0.06
Toluene	0.15	0.13	0.11	0.12
Xylenes	0.12	0.10	0.09	0.09

Table D.22 Measured Flory-Huggins interaction parameters between the selected solvents and 70/30 HDPE/LLDPE-4 blend at 170, 190, 210 and 230 °C.

T (°C)	170	190	210	230
PROBE	$\chi_{1(23)}$			
1 – Hexene	0.11	0.10	0.08	0.03
1-Octene	0.10	0.09	0.08	0.07
Benzene	0.20	0.19	0.17	0.13
Cyclohexane	0.11	0.11	0.09	0.08
n-Hexane	0.10	0.10	0.07	0.03
n-Dodecane	0.06	0.05	0.04	0.04
n-Heptane	0.10	0.09	0.08	0.06
n-Nonane	0.09	0.07	0.07	0.06
n-Octane	0.09	0.08	0.07	0.06
Toluene	0.16	0.14	0.12	0.12
Xylenes	0.13	0.11	0.10	0.09

Table D.23 Measured Flory-Huggins interaction parameters between the selected solvents and pure LLDPE-5 at 170, 190, 210 and 230 °C.

T (°C)	170	190	210	230
PROBE	χ_{13}			
1 – Hexene	0.13	0.12	0.08	0.04
1-Octene	0.11	0.11	0.10	0.10
Benzene	0.23	0.21	0.20	0.18
Cyclohexane	0.13	0.13	0.12	0.10
n-Hexane	0.13	0.12	0.09	0.05
n-Dodecane	0.07	0.06	0.05	0.05
n-Heptane	0.11	0.11	0.10	0.08
n-Nonane	0.10	0.09	0.08	0.07
n-Octane	0.10	0.10	0.08	0.08
Toluene	0.17	0.17	0.14	0.14
Xylenes	0.14	0.13	0.11	0.11

Table D.24 Measured Flory-Huggins interaction parameters between the selected solvents and 30/70 HDPE/LLDPE-5 blend at 170, 190, 210 and 230 °C.

T (°C)	170	190	210	230
PROBE	$\chi_{1(23)}$			
1 – Hexene	0.13	0.12	0.10	0.04
1-Octene	0.11	0.11	0.10	0.09
Benzene	0.24	0.23	0.23	0.20
Cyclohexane	0.14	0.13	0.12	0.11
n-Hexane	0.13	0.12	0.09	0.05
n-Dodecane	0.07	0.06	0.05	0.05
n-Heptane	0.12	0.11	0.10	0.08
n-Nonane	0.10	0.09	0.08	0.07
n-Octane	0.11	0.10	0.08	0.08
Toluene	0.17	0.17	0.15	0.14
Xylenes	0.14	0.14	0.12	0.12

236

Table D.25 Measured Flory-Huggins interaction parameters between the selected solvents and 50/50 HDPE/LLDPE-5 blend at 170, 190, 210 and 230 °C.

T (°C)	170	190	210	230
PROBE	$\chi_{1(23)}$			
1 – Hexene	0.11	0.11	0.09	0.03
1-Octene	0.09	0.09	0.08	0.08
Benzene	0.19	0.18	0.17	0.15
Cyclohexane	0.11	0.09	0.09	0.08
n-Hexane	0.09	0.09	0.07	0.04
n-Dodecane	0.05	0.04	0.03	0.03
n-Heptane	0.10	0.09	0.07	0.07
n-Nonane	0.08	0.07	0.07	0.06
n-Octane	0.08	0.07	0.07	0.07
Toluene	0.14	0.12	0.13	0.13
Xylenes	0.12	0.10	0.10	0.09

Table D.26 Measured Flory-Huggins interaction parameters between the selected solvents and 70/30 HDPE/LLDPE-5 blend at 170, 190, 210 and 230 °C.

T (°C)	170	190	210	230
PROBE	$\chi_{1(23)}$			
1 – Hexene	0.12	0.11	0.09	0.05
1-Octene	0.10	0.09	0.09	0.09
Benzene	0.21	0.20	0.19	0.20
Cyclohexane	0.12	0.11	0.11	0.10
n-Hexane	0.11	0.10	0.08	0.06
n-Dodecane	0.06	0.05	0.04	0.04
n-Heptane	0.10	0.10	0.09	0.09
n-Nonane	0.08	0.08	0.07	0.07
n-Octane	0.09	0.09	0.08	0.08
Toluene	0.15	0.15	0.14	0.14
Xylenes	0.12	0.12	0.11	0.11

Table D.27 Measured Flory-Huggins interaction parameters between the selected solvents and 30/70 LLDPE-a1/LDPE blend at 170, 190, 210 and 230 °C.

T (°C)	170	190	210	230
PROBE	$\chi_{1(23)}$			
1 – Hexene	0.11	0.11	0.07	0.03
1-Octene	0.09	0.10	0.07	0.08
Benzene	0.19	0.19	0.15	0.15
Cyclohexane	0.11	0.12	0.08	0.09
n-Hexane	0.11	0.11	0.06	0.04
n-Dodecane	0.05	0.05	0.03	0.03
n-Heptane	0.09	0.10	0.07	0.07
n-Nonane	0.08	0.08	0.06	0.06
n-Octane	0.08	0.09	0.07	0.07
Toluene	0.14	0.14	0.12	0.12
Xylenes	0.12	0.11	0.10	0.09

Table D.28 Measured Flory-Huggins interaction parameters between the selected solvents and 70/30 LLDPE-a1/LDPE blend at 170, 190, 210 and 230 °C.

T (°C)	170	190	210	230
PROBE	$\chi_{1(23)}$			
1 – Hexene	0.13	0.11	0.08	0.04
1-Octene	0.09	0.10	0.08	0.08
Benzene	0.20	0.19	0.17	0.16
Cyclohexane	0.12	0.11	0.09	0.10
n-Hexane	0.12	0.10	0.07	0.06
n-Dodecane	0.06	0.05	0.04	0.04
n-Heptane	0.11	0.09	0.08	0.08
n-Nonane	0.09	0.08	0.07	0.06
n-Octane	0.10	0.09	0.07	0.08
Toluene	0.16	0.15	0.12	0.14
Xylenes	0.13	0.12	0.10	0.11

237

Table D.29 Measured Flory-Huggins interaction parameters between the selected solvents and pure LLDPE-a2 at 170, 190, 210 and 230 °C.

T (°C)	170	190	210	230
PROBE	χ_{13}			
1 – Hexene	0.12	0.10	0.05	0.01
1-Octene	0.09	0.08	0.06	0.06
Benzene	0.18	0.18	0.14	0.13
Cyclohexane	0.10	0.10	0.06	0.07
n-Hexane	0.11	0.10	0.04	0.02
n-Dodecane	0.05	0.04	0.02	0.02
n-Heptane	0.09	0.09	0.06	0.04
n-Nonane	0.07	0.06	0.05	0.04
n-Octane	0.08	0.07	0.06	0.05
Toluene	0.13	0.13	0.09	0.09
Xylenes	0.13	0.10	0.08	0.07

Table D.30 Measured Flory-Huggins interaction parameters between the selected solvents and 30/70 LLDPE-a2/LDPE blend at 170, 190, 210 and 230 °C.

T (°C)	170	190	210	230
PROBE	$\chi_{1(23)}$			
1 – Hexene	0.11	0.10	0.09	0.04
1-Octene	0.09	0.08	0.08	0.07
Benzene	0.18	0.17	0.18	0.14
Cyclohexane	0.10	0.10	0.10	0.08
n-Hexane	0.10	0.08	0.07	0.04
n-Dodecane	0.05	0.05	0.04	0.02
n-Heptane	0.09	0.09	0.08	0.06
n-Nonane	0.08	0.07	0.07	0.05
n-Octane	0.08	0.08	0.07	0.06
Toluene	0.14	0.13	0.12	0.12
Xylenes	0.12	0.11	0.10	0.10

Table D.31 Measured Flory-Huggins interaction parameters between the selected solvents and 50/50 LLDPE-a2/LDPE blend at 170, 190, 210 and 230 °C.

T (°C)	170	190	210	230
PROBE	$\chi_{1(23)}$			
1 – Hexene	0.13	0.11	0.07	0.04
1-Octene	0.10	0.09	0.08	0.08
Benzene	0.20	0.20	0.16	0.15
Cyclohexane	0.12	0.11	0.09	0.09
n-Hexane	0.11	0.11	0.07	0.05
n-Dodecane	0.06	0.05	0.04	0.03
n-Heptane	0.10	0.10	0.08	0.07
n-Nonane	0.08	0.08	0.07	0.06
n-Octane	0.09	0.09	0.07	0.06
Toluene	0.15	0.15	0.12	0.12
Xylenes	0.12	0.12	0.10	0.09

Table D.32 Measured Flory-Huggins interaction parameters between the selected solvents and 70/30 LLDPE-a2/LDPE blend at 170, 190, 210 and 230 °C.

T (°C)	170	190	210	230
PROBE	$\chi_{1(23)}$			
1 – Hexene	0.15	0.11	0.08	0.03
1-Octene	0.11	0.09	0.08	0.08
Benzene	0.23	0.18	0.17	0.16
Cyclohexane	0.14	0.11	0.10	0.09
n-Hexane	0.14	0.10	0.08	0.04
n-Dodecane	0.06	0.05	0.04	0.04
n-Heptane	0.12	0.09	0.09	0.07
n-Nonane	0.09	0.08	0.07	0.06
n-Octane	0.10	0.09	0.08	0.07
Toluene	0.17	0.14	0.13	0.13
Xylenes	0.14	0.11	0.11	0.10

238

Table D.33 Measured Flory-Huggins interaction parameters between the selected solvents and pure LLDPE-a3 at 170, 190, 210 and 230 °C.

T (°C)	170	190	210	230
PROBE	χ_{13}			
1 – Hexene	0.13	0.12	0.09	0.05
1-Octene	0.11	0.10	0.08	0.08
Benzene	0.21	0.20	0.18	0.16
Cyclohexane	0.12	0.11	0.11	0.10
n-Hexane	0.12	0.10	0.08	0.05
n-Dodecane	0.06	0.05	0.04	0.04
n-Heptane	0.11	0.10	0.08	0.08
n-Nonane	0.09	0.08	0.07	0.07
n-Octane	0.10	0.08	0.08	0.08
Toluene	0.15	0.14	0.13	0.13
Xylenes	0.13	0.11	0.10	0.10

Table D.34 Measured Flory-Huggins interaction parameters between the selected solvents and 30/70 LLDPE-a3/LDPE blend at 170, 190, 210 and 230 °C.

T (°C)	170	190	210	230
PROBE	$\chi_{1(23)}$			
1 – Hexene	0.11	0.11	0.08	0.04
1-Octene	0.09	0.09	0.08	0.08
Benzene	0.19	0.19	0.17	0.18
Cyclohexane	0.11	0.12	0.10	0.10
n-Hexane	0.11	0.12	0.09	0.06
n-Dodecane	0.06	0.06	0.04	0.04
n-Heptane	0.11	0.10	0.08	0.08
n-Nonane	0.08	0.08	0.07	0.07
n-Octane	0.09	0.09	0.08	0.07
Toluene	0.15	0.14	0.14	0.13
Xylenes	0.12	0.12	0.11	0.10

Table D.35 Measured Flory-Huggins interaction parameters between the selected solvents and 50/50 LLDPE-a3/LDPE blend at 170, 190, 210 and 230 °C.

T (°C)	170	190	210	230
PROBE	$\chi_{1(23)}$			
1 – Hexene	0.12	0.12	0.10	0.04
1-Octene	0.11	0.10	0.09	0.08
Benzene	0.21	0.21	0.18	0.17
Cyclohexane	0.13	0.12	0.11	0.10
n-Hexane	0.13	0.10	0.08	0.07
n-Dodecane	0.06	0.05	0.04	0.04
n-Heptane	0.11	0.11	0.10	0.08
n-Nonane	0.09	0.09	0.09	0.07
n-Octane	0.09	0.09	0.08	0.08
Toluene	0.15	0.16	0.14	0.12
Xylenes	0.13	0.13	0.12	0.11

Table D.36 Measured Flory-Huggins interaction parameters between the selected solvents and 70/30 LLDPE-a3/LDPE blend at 170, 190, 210 and 230 °C.

T (°C)	170	190	210	230
PROBE	$\chi_{1(23)}$			
1 – Hexene	0.12	0.11	0.10	0.03
1-Octene	0.10	0.10	0.10	0.07
Benzene	0.20	0.21	0.20	0.14
Cyclohexane	0.11	0.13	0.12	0.07
n-Hexane	0.11	0.10	0.10	0.02
n-Dodecane	0.06	0.06	0.05	0.04
n-Heptane	0.10	0.10	0.10	0.08
n-Nonane	0.09	0.08	0.09	0.08
n-Octane	0.08	0.09	0.09	0.08
Toluene	0.14	0.16	0.16	0.13
Xylenes	0.13	0.13	0.13	0.11

239

Table D.37 Measured Flory-Huggins interaction parameters between the selected solvents and pure LLDPE-a4 at 170, 190, 210 and 230 °C.

T (°C)	170	190	210	230
PROBE	χ_{13}			
1 – Hexene	0.12	0.09	0.08	0.02
1-Octene	0.09	0.08	0.07	0.07
Benzene	0.19	0.15	0.17	0.16
Cyclohexane	0.12	0.09	0.09	0.08
n-Hexane	0.12	0.09	0.07	0.04
n-Dodecane	0.05	0.04	0.03	0.03
n-Heptane	0.10	0.08	0.08	0.06
n-Nonane	0.08	0.07	0.06	0.06
n-Octane	0.09	0.07	0.07	0.06
Toluene	0.15	0.12	0.11	0.12
Xylenes	0.12	0.10	0.09	0.09

Table D.38 Measured Flory-Huggins interaction parameters between the selected solvents and 30/70 LLDPE-a4/LDPE blend at 170, 190, 210 and 230 °C.

T (°C)	170	190	210	230
PROBE	$\chi_{1(23)}$			
1 – Hexene	0.11	0.09	0.07	0.04
1-Octene	0.09	0.08	0.08	0.08
Benzene	0.19	0.16	0.17	0.16
Cyclohexane	0.11	0.09	0.10	0.10
n-Hexane	0.11	0.07	0.06	0.04
n-Dodecane	0.06	0.05	0.04	0.04
n-Heptane	0.10	0.09	0.07	0.08
n-Nonane	0.08	0.07	0.07	0.06
n-Octane	0.09	0.08	0.08	0.07
Toluene	0.15	0.13	0.12	0.12
Xylenes	0.12	0.11	0.10	0.09

Table D.39 Measured Flory-Huggins interaction parameters between the selected solvents and 50/50 LLDPE-a4/LDPE blend at 170, 190, 210 and 230 °C.

T (°C)	170	190	210	230
PROBE	$\chi_{1(23)}$			
1 – Hexene	0.12	0.12	0.09	0.03
1-Octene	0.10	0.10	0.08	0.08
Benzene	0.20	0.20	0.16	0.16
Cyclohexane	0.11	0.12	0.09	0.10
n-Hexane	0.11	0.10	0.06	0.04
n-Dodecane	0.06	0.05	0.04	0.04
n-Heptane	0.10	0.09	0.07	0.09
n-Nonane	0.08	0.08	0.07	0.07
n-Octane	0.09	0.09	0.07	0.08
Toluene	0.15	0.15	0.13	0.13
Xylenes	0.13	0.12	0.11	0.11

Table D.40 Measured Flory-Huggins interaction parameters between the selected solvents and 70/30 LLDPE-a4/LDPE blend at 170, 190, 210 and 230 °C.

T (°C)	170	190	210	230
PROBE	$\chi_{1(23)}$			
1 – Hexene	0.12	0.09	0.07	0.02
1-Octene	0.09	0.09	0.07	0.06
Benzene	0.18	0.18	0.15	0.14
Cyclohexane	0.11	0.10	0.09	0.07
n-Hexane	0.10	0.10	0.06	0.02
n-Dodecane	0.05	0.04	0.03	0.03
n-Heptane	0.09	0.09	0.07	0.05
n-Nonane	0.08	0.07	0.06	0.05
n-Octane	0.08	0.08	0.07	0.05
Toluene	0.14	0.13	0.12	0.11
Xylenes	0.12	0.11	0.09	0.08

240

Table D.41 Measured Flory-Huggins interaction parameters between the selected solvents and pure LLDPE-a5 at 170, 190, 210 and 230 °C.

T (°C)	170	190	210	230
PROBE	χ_{13}			
1 – Hexene	0.08	0.08	0.06	0.02
1-Octene	0.07	0.07	0.06	0.06
Benzene	0.15	0.14	0.12	0.12
Cyclohexane	0.08	0.08	0.06	0.06
n-Hexane	0.08	0.08	0.05	0.03
n-Dodecane	0.04	0.03	0.02	0.02
n-Heptane	0.08	0.07	0.06	0.05
n-Nonane	0.06	0.06	0.05	0.05
n-Octane	0.07	0.07	0.05	0.05
Toluene	0.11	0.11	0.09	0.09
Xylenes	0.09	0.08	0.07	0.07

Table D.42 Measured Flory-Huggins interaction parameters between the selected solvents and 30/70 LLDPE-a5/LDPE blend at 170, 190, 210 and 230 °C.

T (°C)	170	190	210	230
PROBE	$\chi_{1(23)}$			
1 – Hexene	0.11	0.15	0.12	0.05
1-Octene	0.09	0.12	0.11	0.10
Benzene	0.18	0.23	0.21	0.18
Cyclohexane	0.11	0.14	0.14	0.12
n-Hexane	0.10	0.12	0.10	0.06
n-Dodecane	0.05	0.07	0.06	0.06
n-Heptane	0.09	0.12	0.11	0.09
n-Nonane	0.08	0.09	0.09	0.08
n-Octane	0.08	0.10	0.10	0.08
Toluene	0.14	0.18	0.17	0.15
Xylenes	0.11	0.14	0.14	0.11

Table D.43 Measured Flory-Huggins interaction parameters between the selected solvents and 50/50 LLDPE-a5/LDPE blend at 170, 190, 210 and 230 °C.

T (°C)	170	190	210	230
PROBE	$\chi_{1(23)}$			
1 – Hexene	0.12	0.09	0.09	0.03
1-Octene	0.09	0.08	0.08	0.07
Benzene	0.19	0.17	0.18	0.15
Cyclohexane	0.11	0.10	0.10	0.08
n-Hexane	0.10	0.08	0.07	0.04
n-Dodecane	0.06	0.05	0.04	0.04
n-Heptane	0.09	0.09	0.08	0.07
n-Nonane	0.08	0.08	0.07	0.06
n-Octane	0.09	0.08	0.08	0.06
Toluene	0.15	0.14	0.13	0.12
Xylenes	0.12	0.11	0.11	0.10

Table D.44 Measured Flory-Huggins interaction parameters between the selected solvents and 70/30 LLDPE-a5/LDPE blend at 170, 190, 210 and 230 °C.

T (°C)	170	190	210	230
PROBE	$\chi_{1(23)}$			
1 – Hexene	0.12	0.10	0.07	0.03
1-Octene	0.10	0.08	0.08	0.07
Benzene	0.20	0.17	0.16	0.15
Cyclohexane	0.12	0.10	0.09	0.08
n-Hexane	0.11	0.09	0.07	0.04
n-Dodecane	0.06	0.05	0.04	0.04
n-Heptane	0.10	0.09	0.08	0.07
n-Nonane	0.08	0.07	0.07	0.06
n-Octane	0.09	0.08	0.07	0.07
Toluene	0.15	0.13	0.13	0.12
Xylenes	0.12	0.11	0.10	0.10

241

Table D.45 Measured Flory-Huggins interaction parameters between the selected solvents and pure LLDPE-a6 at 170, 190, 210 and 230 °C.

T (°C)	170	190	210	230
PROBE	χ_{13}			
1 – Hexene	0.11	0.08	0.07	0.02
1-Octene	0.09	0.07	0.06	0.08
Benzene	0.17	0.16	0.13	0.14
Cyclohexane	0.09	0.08	0.07	0.07
n-Hexane	0.10	0.08	0.05	0.02
n-Dodecane	0.05	0.04	0.02	0.02
n-Heptane	0.10	0.08	0.05	0.07
n-Nonane	0.07	0.06	0.05	0.05
n-Octane	0.08	0.07	0.05	0.06
Toluene	0.13	0.12	0.10	0.10
Xylenes	0.11	0.10	0.08	0.09

Table D.46 Measured Flory-Huggins interaction parameters between the selected solvents and 30/70 LLDPE-a6/LDPE blend at 170, 190, 210 and 230 °C.

T (°C)	170	190	210	230
PROBE	$\chi_{1(23)}$			
1 – Hexene	0.12	0.12	0.09	0.04
1-Octene	0.09	0.09	0.08	0.07
Benzene	0.19	0.19	0.17	0.14
Cyclohexane	0.11	0.10	0.11	0.08
n-Hexane	0.11	0.10	0.08	0.04
n-Dodecane	0.05	0.05	0.04	0.04
n-Heptane	0.09	0.09	0.08	0.07
n-Nonane	0.08	0.07	0.07	0.06
n-Octane	0.08	0.08	0.08	0.06
Toluene	0.14	0.14	0.13	0.11
Xylenes	0.12	0.11	0.10	0.08

Table D.47 Measured Flory-Huggins interaction parameters between the selected solvents and 50/50 LLDPE-a6/LDPE blend at 170, 190, 210 and 230 °C.

T (°C)	170	190	210	230
PROBE	$\chi_{1(23)}$			
1 – Hexene	0.12	0.09	0.07	0.02
1-Octene	0.08	0.06	0.08	0.07
Benzene	0.19	0.15	0.16	0.14
Cyclohexane	0.11	0.08	0.09	0.07
n-Hexane	0.11	0.08	0.08	0.02
n-Dodecane	0.05	0.03	0.04	0.04
n-Heptane	0.10	0.07	0.07	0.06
n-Nonane	0.07	0.05	0.06	0.06
n-Octane	0.08	0.06	0.07	0.07
Toluene	0.14	0.10	0.12	0.11
Xylenes	0.11	0.08	0.09	0.09

Table D.48 Measured Flory-Huggins interaction parameters between the selected solvents and 70/30 LLDPE-a6/LDPE blend at 170, 190, 210 and 230 °C.

T (°C)	170	190	210	230
PROBE	$\chi_{1(23)}$			
1 – Hexene	0.11	0.10	0.07	0.03
1-Octene	0.08	0.08	0.07	0.06
Benzene	0.17	0.16	0.16	0.14
Cyclohexane	0.10	0.10	0.09	0.07
n-Hexane	0.09	0.09	0.07	0.04
n-Dodecane	0.05	0.05	0.03	0.03
n-Heptane	0.09	0.08	0.08	0.06
n-Nonane	0.08	0.07	0.06	0.05
n-Octane	0.08	0.07	0.06	0.05
Toluene	0.14	0.12	0.11	0.10
Xylenes	0.11	0.10	0.08	0.08

242

Table D.49 Measured Flory-Huggins interaction parameters between the selected solvents and pure LLDPE-m1 at 170, 190, 210 and 230 °C.

T (°C)	170	190	210	230
PROBE	χ_{13}			
1 – Hexene	0.10	0.11	0.06	0.03
1-Octene	0.09	0.08	0.07	0.08
Benzene	0.19	0.17	0.15	0.15
Cyclohexane	0.11	0.10	0.09	0.08
n-Hexane	0.10	0.10	0.07	0.04
n-Dodecane	0.06	0.04	0.04	0.04
n-Heptane	0.09	0.09	0.08	0.08
n-Nonane	0.08	0.07	0.08	0.07
n-Octane	0.09	0.08	0.08	0.07
Toluene	0.14	0.14	0.13	0.13
Xylenes	0.12	0.11	0.11	0.10

Table D.50 Measured Flory-Huggins interaction parameters between the selected solvents and 30/70 LLDPE-m1/LDPE blend at 170, 190, 210 and 230 °C.

T (°C)	170	190	210	230
PROBE	$\chi_{1(23)}$			
1 – Hexene	0.14	0.13	0.11	0.07
1-Octene	0.12	0.11	0.11	0.10
Benzene	0.24	0.22	0.19	0.20
Cyclohexane	0.15	0.13	0.13	0.12
n-Hexane	0.13	0.12	0.09	0.07
n-Dodecane	0.07	0.06	0.05	0.05
n-Heptane	0.13	0.12	0.09	0.09
n-Nonane	0.10	0.09	0.08	0.08
n-Octane	0.11	0.10	0.10	0.09
Toluene	0.19	0.18	0.16	0.15
Xylenes	0.15	0.14	0.13	0.12

Table D.51 Measured Flory-Huggins interaction parameters between the selected solvents and 50/50 LLDPE-m1/LDPE blend at 170, 190, 210 and 230 °C.

T (°C)	170	190	210	230
PROBE	$\chi_{1(23)}$			
1 – Hexene	0.15	0.14	0.11	0.05
1-Octene	0.12	0.12	0.12	0.11
Benzene	0.24	0.24	0.22	0.19
Cyclohexane	0.15	0.15	0.14	0.13
n-Hexane	0.14	0.13	0.10	0.07
n-Dodecane	0.07	0.07	0.06	0.06
n-Heptane	0.13	0.12	0.10	0.10
n-Nonane	0.11	0.10	0.09	0.09
n-Octane	0.11	0.12	0.10	0.09
Toluene	0.18	0.19	0.16	0.15
Xylenes	0.15	0.15	0.13	0.13

Table D.52 Measured Flory-Huggins interaction parameters between the selected solvents and 70/30 LLDPE-m1/LDPE blend at 170, 190, 210 and 230 °C.

T (°C)	170	190	210	230
PROBE	$\chi_{1(23)}$			
1 – Hexene	0.17	0.14	0.11	0.06
1-Octene	0.14	0.12	0.12	0.11
Benzene	0.28	0.26	0.23	0.23
Cyclohexane	0.17	0.16	0.15	0.14
n-Hexane	0.15	0.14	0.10	0.07
n-Dodecane	0.09	0.07	0.06	0.06
n-Heptane	0.14	0.13	0.12	0.11
n-Nonane	0.12	0.11	0.10	0.09
n-Octane	0.13	0.12	0.11	0.10
Toluene	0.21	0.19	0.18	0.17
Xylenes	0.17	0.16	0.15	0.14

243

Table D.53 Measured Flory-Huggins interaction parameters between the selected solvents and pure LLDPE-m2 at 170, 190, 210 and 230 °C.

T (°C)	170	190	210	230
PROBE	χ_{13}			
1 – Hexene	0.11	0.10	0.09	0.04
1-Octene	0.10	0.09	0.09	0.08
Benzene	0.20	0.18	0.17	0.16
Cyclohexane	0.11	0.10	0.10	0.09
n-Hexane	0.11	0.09	0.08	0.04
n-Dodecane	0.06	0.05	0.04	0.04
n-Heptane	0.10	0.08	0.08	0.08
n-Nonane	0.09	0.08	0.07	0.08
n-Octane	0.09	0.09	0.08	0.07
Toluene	0.16	0.15	0.13	0.13
Xylenes	0.13	0.12	0.10	0.10

Table D.54 Measured Flory-Huggins interaction parameters between the selected solvents and 30/70 LLDPE-m2/LDPE blend at 170, 190, 210 and 230 °C.

T (°C)	170	190	210	230
PROBE	$\chi_{1(23)}$			
1 – Hexene	0.10	0.08	0.07	0.04
1-Octene	0.08	0.08	0.08	0.08
Benzene	0.18	0.18	0.18	0.16
Cyclohexane	0.10	0.10	0.11	0.08
n-Hexane	0.09	0.09	0.08	0.05
n-Dodecane	0.05	0.05	0.04	0.04
n-Heptane	0.09	0.08	0.08	0.07
n-Nonane	0.07	0.08	0.07	0.06
n-Octane	0.08	0.08	0.09	0.07
Toluene	0.13	0.13	0.14	0.12
Xylenes	0.11	0.11	0.12	0.10

Table D.55 Measured Flory-Huggins interaction parameters between the selected solvents and 50/50 LLDPE-m2/LDPE blend at 170, 190, 210 and 230 °C.

T (°C)	170	190	210	230
PROBE	$\chi_{1(23)}$			
1 – Hexene	0.11	0.09	0.07	0.03
1-Octene	0.09	0.08	0.07	0.08
Benzene	0.19	0.17	0.15	0.15
Cyclohexane	0.11	0.09	0.08	0.08
n-Hexane	0.11	0.09	0.07	0.04
n-Dodecane	0.05	0.04	0.03	0.04
n-Heptane	0.10	0.09	0.07	0.07
n-Nonane	0.08	0.07	0.06	0.07
n-Octane	0.09	0.08	0.06	0.07
Toluene	0.14	0.13	0.11	0.12
Xylenes	0.12	0.10	0.09	0.10

Table D.56 Measured Flory-Huggins interaction parameters between the selected solvents and 70/30 LLDPE-m2/LDPE blend at 170, 190, 210 and 230 °C.

T (°C)	170	190	210	230
PROBE	$\chi_{1(23)}$			
1 – Hexene	0.11	0.09	0.08	0.02
1-Octene	0.09	0.08	0.08	0.07
Benzene	0.18	0.17	0.15	0.15
Cyclohexane	0.10	0.09	0.08	0.09
n-Hexane	0.10	0.08	0.07	0.03
n-Dodecane	0.05	0.04	0.03	0.03
n-Heptane	0.09	0.08	0.08	0.07
n-Nonane	0.07	0.06	0.07	0.06
n-Octane	0.08	0.07	0.07	0.06
Toluene	0.13	0.13	0.13	0.11
Xylenes	0.11	0.10	0.09	0.10

244

Table D.57 Measured Flory-Huggins interaction parameters between the selected solvents and pure LLDPE-m3 at 170, 190, 210 and 230 °C.

T (°C)	170	190	210	230
PROBE	χ_{13}			
1 – Hexene	0.11	0.10	0.08	0.02
1-Octene	0.09	0.08	0.08	0.07
Benzene	0.19	0.17	0.16	0.14
Cyclohexane	0.11	0.09	0.09	0.07
n-Hexane	0.11	0.08	0.08	0.03
n-Dodecane	0.05	0.04	0.03	0.04
n-Heptane	0.10	0.08	0.07	0.06
n-Nonane	0.08	0.07	0.06	0.05
n-Octane	0.08	0.08	0.07	0.06
Toluene	0.14	0.13	0.11	0.10
Xylenes	0.11	0.11	0.09	0.08

Table D.58 Measured Flory-Huggins interaction parameters between the selected solvents and 30/70 LLDPE-m3/LDPE blend at 170, 190, 210 and 230 °C.

T (°C)	170	190	210	230
PROBE	$\chi_{1(23)}$			
1 – Hexene	0.11	0.08	0.06	0.02
1-Octene	0.09	0.08	0.07	0.07
Benzene	0.19	0.15	0.15	0.13
Cyclohexane	0.11	0.09	0.08	0.08
n-Hexane	0.11	0.08	0.06	0.03
n-Dodecane	0.05	0.04	0.03	0.04
n-Heptane	0.10	0.08	0.07	0.06
n-Nonane	0.08	0.07	0.06	0.05
n-Octane	0.08	0.07	0.07	0.06
Toluene	0.14	0.12	0.12	0.11
Xylenes	0.12	0.10	0.09	0.08

Table D.59 Measured Flory-Huggins interaction parameters between the selected solvents and 50/50 LLDPE-m3/LDPE blend at 170, 190, 210 and 230 °C.

T (°C)	170	190	210	230
PROBE	$\chi_{1(23)}$			
1 – Hexene	0.12	0.09	0.07	0.02
1-Octene	0.09	0.08	0.07	0.07
Benzene	0.19	0.17	0.16	0.14
Cyclohexane	0.11	0.09	0.09	0.08
n-Hexane	0.11	0.08	0.07	0.03
n-Dodecane	0.05	0.04	0.03	0.03
n-Heptane	0.09	0.08	0.08	0.06
n-Nonane	0.07	0.07	0.06	0.05
n-Octane	0.08	0.07	0.06	0.06
Toluene	0.14	0.13	0.11	0.11
Xylenes	0.11	0.10	0.09	0.09

Table D.60 Measured Flory-Huggins interaction parameters between the selected solvents and 70/30 LLDPE-m3/LDPE blend at 170, 190, 210 and 230 °C.

T (°C)	170	190	210	230
PROBE	$\chi_{1(23)}$			
1 – Hexene	0.10	0.10	0.07	0.03
1-Octene	0.09	0.08	0.07	0.07
Benzene	0.18	0.17	0.15	0.13
Cyclohexane	0.10	0.09	0.08	0.08
n-Hexane	0.09	0.09	0.07	0.03
n-Dodecane	0.05	0.04	0.03	0.04
n-Heptane	0.09	0.08	0.07	0.06
n-Nonane	0.08	0.07	0.05	0.05
n-Octane	0.08	0.07	0.06	0.06
Toluene	0.14	0.13	0.11	0.11
Xylenes	0.11	0.10	0.08	0.08

245

Table D.61 Measured Flory-Huggins interaction parameters between the selected solvents and pure LLDPE-m4 at 170, 190, 210 and 230 °C.

T (°C)	170	190	210	230
PROBE	χ_{13}			
1 – Hexene	0.11	0.10	0.09	0.03
1-Octene	0.09	0.08	0.07	0.06
Benzene	0.18	0.17	0.16	0.14
Cyclohexane	0.10	0.10	0.09	0.07
n-Hexane	0.10	0.09	0.07	0.03
n-Dodecane	0.05	0.05	0.03	0.03
n-Heptane	0.09	0.09	0.08	0.06
n-Nonane	0.07	0.07	0.06	0.07
n-Octane	0.08	0.08	0.06	0.06
Toluene	0.14	0.13	0.12	0.10
Xylenes	0.11	0.11	0.09	0.09

Table D.62 Measured Flory-Huggins interaction parameters between the selected solvents and 30/70 LLDPE-m4/LDPE blend at 170, 190, 210 and 230 °C.

T (°C)	170	190	210	230
PROBE	$\chi_{1(23)}$			
1 – Hexene	0.10	0.09	0.08	0.03
1-Octene	0.08	0.07	0.07	0.07
Benzene	0.17	0.16	0.15	0.14
Cyclohexane	0.09	0.08	0.08	0.07
n-Hexane	0.09	0.08	0.07	0.04
n-Dodecane	0.05	0.04	0.03	0.03
n-Heptane	0.08	0.07	0.07	0.06
n-Nonane	0.07	0.06	0.05	0.05
n-Octane	0.08	0.07	0.06	0.06
Toluene	0.13	0.12	0.10	0.10
Xylenes	0.11	0.09	0.08	0.08

Table D.63 Measured Flory-Huggins interaction parameters between the selected solvents and 50/50 LLDPE-m4/LDPE blend at 170, 190, 210 and 230 °C.

T (°C)	170	190	210	230
PROBE	$\chi_{1(23)}$			
1 – Hexene	0.10	0.08	0.07	0.01
1-Octene	0.09	0.07	0.06	0.06
Benzene	0.17	0.15	0.14	0.11
Cyclohexane	0.10	0.08	0.08	0.06
n-Hexane	0.08	0.08	0.06	0.03
n-Dodecane	0.04	0.04	0.02	0.03
n-Heptane	0.08	0.08	0.07	0.06
n-Nonane	0.07	0.06	0.05	0.05
n-Octane	0.08	0.07	0.06	0.06
Toluene	0.13	0.12	0.11	0.10
Xylenes	0.11	0.09	0.08	0.07

Table D.64 Measured Flory-Huggins interaction parameters between the selected solvents and 70/30 LLDPE-m4/LDPE blend at 170, 190, 210 and 230 °C.

T (°C)	170	190	210	230
PROBE	$\chi_{1(23)}$			
1 – Hexene	0.10	0.08	0.06	0.02
1-Octene	0.08	0.08	0.06	0.06
Benzene	0.17	0.16	0.14	0.12
Cyclohexane	0.09	0.09	0.07	0.07
n-Hexane	0.09	0.07	0.05	0.04
n-Dodecane	0.05	0.04	0.02	0.03
n-Heptane	0.09	0.08	0.06	0.06
n-Nonane	0.07	0.06	0.05	0.05
n-Octane	0.08	0.07	0.06	0.06
Toluene	0.13	0.12	0.10	0.10
Xylenes	0.11	0.10	0.08	0.07

246

Table D.65 Measured Flory-Huggins interaction parameters between the selected solvents and pure LLDPE-m5 at 170, 190, 210 and 230 °C.

T (°C)	170	190	210	230
PROBE	χ_{13}			
1 – Hexene	0.10	0.09	0.06	0.01
1-Octene	0.09	0.08	0.07	0.06
Benzene	0.17	0.16	0.14	0.11
Cyclohexane	0.10	0.09	0.07	0.05
n-Hexane	0.09	0.07	0.05	0.01
n-Dodecane	0.05	0.04	0.03	0.03
n-Heptane	0.09	0.07	0.06	0.04
n-Nonane	0.07	0.06	0.05	0.04
n-Octane	0.08	0.07	0.06	0.05
Toluene	0.13	0.12	0.10	0.10
Xylenes	0.10	0.09	0.08	0.08

Table D.66 Measured Flory-Huggins interaction parameters between the selected solvents and 30/70 LLDPE-m5/LDPE blend at 170, 190, 210 and 230 °C.

T (°C)	170	190	210	230
PROBE	$\chi_{1(23)}$			
1 – Hexene	0.12	0.10	0.09	0.03
1-Octene	0.09	0.09	0.08	0.09
Benzene	0.19	0.18	0.17	0.16
Cyclohexane	0.11	0.10	0.10	0.10
n-Hexane	0.11	0.09	0.08	0.04
n-Dodecane	0.06	0.05	0.04	0.05
n-Heptane	0.10	0.09	0.08	0.08
n-Nonane	0.08	0.07	0.07	0.07
n-Octane	0.09	0.08	0.08	0.08
Toluene	0.16	0.14	0.14	0.13
Xylenes	0.13	0.11	0.10	0.10

Table D.67 Measured Flory-Huggins interaction parameters between the selected solvents and 50/50 LLDPE-m5/LDPE blend at 170, 190, 210 and 230 °C.

T (°C)	170	190	210	230
PROBE	$\chi_{1(23)}$			
1 – Hexene	0.12	0.09	0.06	0.04
1-Octene	0.10	0.08	0.08	0.08
Benzene	0.20	0.18	0.16	0.16
Cyclohexane	0.11	0.10	0.09	0.09
n-Hexane	0.11	0.09	0.06	0.05
n-Dodecane	0.06	0.05	0.04	0.04
n-Heptane	0.10	0.09	0.07	0.06
n-Nonane	0.08	0.07	0.07	0.06
n-Octane	0.09	0.08	0.07	0.06
Toluene	0.15	0.13	0.13	0.11
Xylenes	0.12	0.11	0.179	0.10

Table D.68 Measured Flory-Huggins interaction parameters between the selected solvents and 70/30 LLDPE-m5/LDPE blend at 170, 190, 210 and 230 °C.

T (°C)	170	190	210	230
PROBE	$\chi_{1(23)}$			
1 – Hexene	0.11	0.11	0.08	0.03
1-Octene	0.10	0.08	0.08	0.07
Benzene	0.19	0.18	0.16	0.15
Cyclohexane	0.12	0.11	0.09	0.08
n-Hexane	0.11	0.10	0.07	0.04
n-Dodecane	0.06	0.05	0.04	0.04
n-Heptane	0.10	0.09	0.08	0.07
n-Nonane	0.08	0.08	0.06	0.07
n-Octane	0.09	0.08	0.07	0.07
Toluene	0.15	0.14	0.13	0.13
Xylenes	0.13	0.11	0.10	0.10

247

Table D.69 Measured Flory-Huggins interaction parameters between the selected solvents and pure LLDPE-m6 at 170, 190, 210 and 230 °C.

T (°C)	170	190	210	230
PROBE	χ_{13}			
1 – Hexene	0.11	0.09	0.07	0.02
1-Octene	0.09	0.08	0.07	0.06
Benzene	0.19	0.17	0.14	0.13
Cyclohexane	0.11	0.09	0.08	0.07
n-Hexane	0.10	0.09	0.06	0.03
n-Dodecane	0.05	0.04	0.03	0.03
n-Heptane	0.10	0.08	0.06	0.07
n-Nonane	0.07	0.06	0.06	0.06
n-Octane	0.09	0.07	0.06	0.06
Toluene	0.14	0.12	0.11	0.11
Xylenes	0.11	0.10	0.09	0.08

Table D.70 Measured Flory-Huggins interaction parameters between the selected solvents and 30/70 LLDPE-m6/LDPE blend at 170, 190, 210 and 230 °C.

T (°C)	170	190	210	230
PROBE	$\chi_{1(23)}$			
1 – Hexene	0.12	0.09	0.07	0.03
1-Octene	0.10	0.09	0.08	0.08
Benzene	0.19	0.18	0.16	0.15
Cyclohexane	0.12	0.11	0.09	0.09
n-Hexane	0.11	0.09	0.07	0.03
n-Dodecane	0.06	0.05	0.04	0.04
n-Heptane	0.10	0.09	0.08	0.07
n-Nonane	0.08	0.08	0.07	0.06
n-Octane	0.09	0.08	0.08	0.07
Toluene	0.15	0.14	0.13	0.13
Xylenes	0.12	0.11	0.10	0.10

Table D.71 Measured Flory-Huggins interaction parameters between the selected solvents and 50/50 LLDPE-m6/LDPE blend at 170, 190, 210 and 230 °C.

T (°C)	170	190	210	230
PROBE	$\chi_{1(23)}$			
1 – Hexene	0.11	0.08	0.07	0.04
1-Octene	0.08	0.08	0.07	0.08
Benzene	0.19	0.17	0.16	0.15
Cyclohexane	0.11	0.09	0.08	0.08
n-Hexane	0.10	0.08	0.06	0.04
n-Dodecane	0.05	0.04	0.03	0.04
n-Heptane	0.09	0.08	0.06	0.06
n-Nonane	0.07	0.06	0.05	0.06
n-Octane	0.08	0.07	0.06	0.06
Toluene	0.13	0.12	0.11	0.12
Xylenes	0.11	0.10	0.08	0.09

Table D.72 Measured Flory-Huggins interaction parameters between the selected solvents and 70/30 LLDPE-m6/LDPE blend at 170, 190, 210 and 230 °C.

T (°C)	170	190	210	230
PROBE	$\chi_{1(23)}$			
1 – Hexene	0.08	0.08	0.06	0.01
1-Octene	0.08	0.08	0.07	0.06
Benzene	0.17	0.16	0.14	0.12
Cyclohexane	0.09	0.08	0.08	0.06
n-Hexane	0.08	0.08	0.06	0.02
n-Dodecane	0.04	0.04	0.03	0.03
n-Heptane	0.08	0.08	0.06	0.05
n-Nonane	0.07	0.06	0.05	0.06
n-Octane	0.08	0.07	0.06	0.06
Toluene	0.13	0.12	0.11	0.10
Xylenes	0.10	0.09	0.08	0.09

248